ISOTOPIC LABELLING APPLIED TO THE INFRARED SPECTRA OF METAL COMPLEXES

A thesis submitted to the

UNIVERSITY OF CAPE TOWN

in fulfilment of the requirements for the degree of

DOCTOR OF PHILOSOPHY

by

MARGARET LILIAN NIVEN B.Sc. (Hons.) (Cape Town)

Department of Inorganic Chemistry
University of Cape Town
Rondebosch
Cape
South Africa

February 1980

to the memory of my father

ACKNOWLEDGEMENTS

The author wishes to extend her sincere thanks to

her supervisors, the late Dr G.C. Percy and Professor D.A. Thornton for their excellent advice and guidance in the direction of this study;

Professor L.R. Nassimbeni for his assistance in the x-ray crystallographic sections;

Professor J. Shamir for the determination of the Raman spectra;

her colleagues, Drs C. Engelter and J.B. Hodgson, for their assistance and useful discussion;

Mr W.R.T. Hemsted for his efficiency in carrying out microanalyses;

A E C I Limited for the award of a Postgraduate Fellowship (1977);

The University of Cape Town and the Council for Scientific and Industrial Research for financial assistance (1978 - 1980);

Mrs G. Rootman for the typing of this thesis;

Mr Marco Celotti for his assistance in the proof-reading of the manuscript and also for his immeasureable encouragement and understanding;

and finally her mother for her unfailing support.

SUMMARY

An ir investigation of a series of 2-aminomethylpyridine complexes of first transition metal(II) perchlorates, tetrafluoroborates, halides and thiocyanates is reported. Comparisons with the spectra of related complexes of 2,2'-bipyridine and ethylenediamine together with metal-ion substitution, deuteration and ^{15}N isotopic labelling of the amino group in 2-aminomethylpyridine enable reliable band assignments to be made. The study shows that in complexes of the type $M(amp)_nX_2$, metal-to-amino-nitrogen stretches occur at frequencies greater than 350 cm^{-1}, while the metal-to-pyridine-nitrogen stretches are generally below 300 cm^{-1}, the assignment of the latter being generally complicated by the presence of metal-to-halogen vibrations. In addition to an x-ray crystallographic investigation of the complex $[Ni(amp)_3](BF_4)_2$, considerable structural information about these complexes is obtained from correlations between the number of M-L vibrations observed in the far ir and those predicted for localized molecular point symmetries on a group theoretical basis.

A subsequent examination of *bis*- and *mono*{2-(2-aminoethyl)-pyridine} complexes of Cu(II) and Zn(II) perchlorates, tetrafluoroborates, halides and isothiocyanates reveals that the spectra of these species show a marked similarity to those of the 2-aminomethylpyridine complexes; this facilitates the assignment of both ligand and metal-ligand modes allowing

significant structural comparisons and assignments to be made.

The ir spectra of quinoline, quinoline-d_7 and their metal complexes are examined in order to determine the ratio ν^D/ν^H for bands assigned to the C-H(D) and ring modes of the heterocyclic ring. Practically without exception, ν^D/ν^H falls within the ranges 0.76 ± 0.08 (C-H(D) modes) and 0.92 ± 0.08 (ring modes). The potential usefulness of the results is discussed. Assignments of the M-N and M-halide vibrations are based on the results of the deuteration studies and the metal ion and halide substitutions. A number of structural conclusions in accordance with the selection rules for the various localized point symmetries are also drawn. The results support only some of the earlier publications on these complexes.

An attempt to clarify various earlier contradictory reports on band assignments in the ir spectra of metal acetylacetonates is carried out by the examination of the spectrum of $Zn(acac)_2.H_2O$ in conjunction with the shift data obtained for its ^{18}O (acetylacetonate) and $^{64,68}Zn$ analogues. An investigation of the complexes $M(acac)_2B$ and $Na[M(acac)_3]$ where M = Co(II), Ni(II) or Zn(II), and B = 2,2'-bipyridine, 2-aminomethylpyridine and ethylenediamine is also discussed. Complete band assignments are made on a comparative basis with the effects of ligand and metal ion substitution being considered. Assignments for ir bands in the spectra of quinoline adducts of a series of metal(II) acetylacetonates are proposed on the basis of the effects of quinoline deuteration and metal ion substitution. The structural

aspects of the spectra are discussed.

Complete band assignments in the ir spectra (4000 - 150 cm^{-1}) of a number of M(II) and M(III) complexes of glycine have been carried out using the technique of multiple isotopic labelling. In most cases the spectra of the complexes with each of the glycinate atoms independently isotopically substituted are presented, and in the spectrum of $Zn(gly)_2.H_2O$, the inclusion of $^{64,68}Zn$ labelling facilitates the identification of metal-ligand modes. In most cases, the N-H, C-H, C=O, C-C and C-N stretching vibrations and the NH_2 scissoring and rocking modes are vibrationally pure, but all other bands exhibit coupling to a greater or lesser extent. The assignments proposed yield a νM-L series consistent with cfse expectations.

An x-ray crystallographic investigation of the *hexakis*(urea) chromium(III) chloride trihydrate has been carried out. The information obtained here is used in an attempted vibrational analysis of the complex involving both ir and Raman spectroscopy in addition to shift data obtained for the ^{18}O-, ^{15}N- and ^{13}C-isotopically substituted analogues of the complex. Multiple isotopic labelling of the urea molecules in complexes of that ligand with Pt(II) and Pd(II) is also discussed in relation to an examination of their ir spectra.

PUBLICATIONS

1. Infrared spectra of some metal(II) complexes of 2-aminomethylpyridine. M.L. Niven and G.C. Percy. *Spectroscopy Letters 10* (1977) 519.

2. The infrared spectra (3500 - 140 cm^{-1}) of the 2,2'-bipyridine, 2-aminomethylpyridine and ethylenediamine adducts and the sodium *tris*-compounds of cobalt(II), nickel(II) and zinc(II) acetylacetonates. M.L. Niven and G.C. Percy. *Transition Metal Chemistry 3* (1978) 267.

3. Band assignments in the infrared spectrum of cadmium glycinate monohydrate by multiple isotopic labelling. M.L. Niven and D.A. Thornton. *Inorganica Chimica Acta 32* (1979) 205.

4. The infrared spectra of quinoline complexes of metal(II) halides and isothiocyanates: assignments by isotopic labelling and structural aspects of the spectra. M.L. Niven and D.A. Thornton. *Journal of Molecular Structure 53* (1979) 157.

5. Examination of the ratio ν^D/ν^H for infrared bands assigned to the C-H(D) and ring vibrations in metal complexes of quinoline, pyridine, aniline and their fully-deuterated analogues. G.A. Foulds, J.B. Hodgson, A.T. Hutton, M.L. Niven, G.C. Percy, P.E. Rutherford and D.A. Thornton. *Spectroscopy Letters 12* (1) (1979) 25.

6. The infrared spectra of quinoline adducts of transition metal(II) acetylacetonates. M.L. Niven and D.A. Thornton. *South African Journal of Chemistry 32* (3) (1979) 135.

7. The infrared spectra of *trans*-bis(glycinato)zinc(II) monohydrate and its isotopically-substituted analogues: assignments, structure and bonding. M.L. Niven and D.A. Thornton. *Journal of Molecular Structure 55* (1979) 1.

8. The crystal and molecular structure of the complex *tris*-(2-aminomethylpyridine)nickel(II) tetrafluoroborate $[Ni(C_6H_8N_2)_3](BF_4)_2$. L.R. Nassimbeni and M.L. Niven. *Crystal Structure Communications* (1980) in press.

9. Band assignments in the infrared spectrum of zinc acetylacetonate monohydrate by ^{18}O-, ^{68}Zn- and ^{64}Zn-labelling. M.L. Niven and D.A. Thornton. *Spectroscopy Letters* (1980) submitted.

10. The infrared spectrum of 2-aminomethylpyridine complexes of metal(II) ions. M.L. Niven, G.C. Percy and D.A. Thornton. *Journal of Molecular Structure* (1980) submitted.

11. The crystal and molecular structure of the complex *hexakis*(urea)chromium(III) chloride trihydrate $[Cr(OCN_2H_4)_6]Cl_3.3H_2O$. L.R. Nassimbeni and M.L. Niven. *Crystal Structure Communications* (1980) submitted.

CONFERENCE PROCEEDINGS

1. Infrared Spectra of some metal(II) complexes of 2-aminomethylpyridine. M.L. Niven and G.C. Percy 25th Convention of the South African Chemical Institute, Johannesburg. 1977.

2. Infrared studies of metal complexes of glycine illustrating the use of ligand atom isotopic substitution. M.L. Niven and D.A. Thornton. 26th Convention of the South African Chemical Institute. Port Elizabeth. 1979.

ABBREVIATIONS

aa	acetylacetonate anion
aep	2-(2-aminoethyl)pyridine
amp	2-aminomethylpyridine
B	generalized base
bipy	2,2'-bipyridine
cfse	crystal field stablization energy
en	ethylenediamine (1,2-diaminoethane)
gly	glycinate anion
i.p.	in-plane
ir	infrared
L	generalized ligand
M	generalized metal ion
o.o.p.	out-of-plane
py	pyridine
quin	quinoline
X	generalized anion
ur	urea
ν	stretching mode of vibration
δ	bending mode of vibration

STRUCTURAL FORMULAE OF LIGANDS APPEARING IN THE TEXT

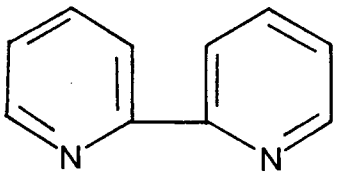

2,2'-bipyridine
(bipy)

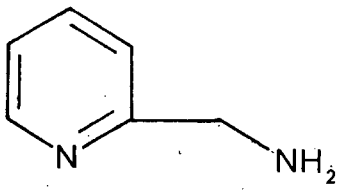

2-aminomethylpyridine
(amp)

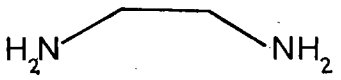

ethylenediamine
(en)

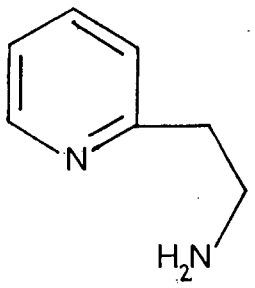

2-(2-aminoethyl)pyridine
(aep)

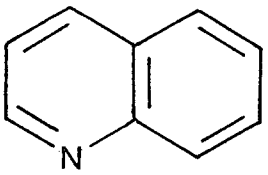

quinoline
(quin)

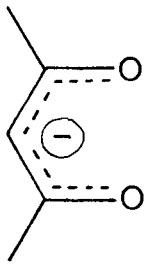

acetylacetonate anion
(acac)

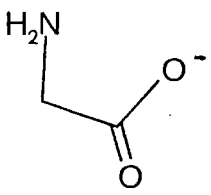

glycinate anion
(gly)

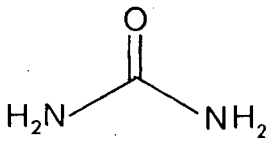

urea
(ur)

CONTENTS

SECTION 3 - RESULTS AND DISCUSSION

SECTION 1 - INTRODUCTION

1. INTRODUCTION

1.1 METHODS USED FOR BAND ASSIGNMENT IN THE VIBRATIONAL SPECTRA OF METAL COMPLEXES

The precise assignment of bands in the ir spectra of metal complexes to vibrations of specific atoms is of value in determining direct information regarding many structural and bonding features. However such a task applied to systems as many-bodied as those studied in this work is most certainly non-trivial since the interpretation of the spectra is complicated by intermolecular interactions, lowering of symmetry and extensive vibrational coupling. An analysis of metal-ligand modes is of particular interest with regard to the nature of the co-ordination within the metal complex. However, owing to the high mass of the metal ion and the relatively weak nature of the metal-ligand bond, these vibrations occur below 600 cm^{-1} where further complications may arise from the appearance of lattice modes [1]. Various methods are employed to assign (a) internal ligand vibrations, (b) metal-ligand vibrations.

(a) Internal Ligand Vibrations

(1) The best known theoretical approach to a study of vibrational spectra is analysis *via* a normal coordinate treatment of the molecule [2-7]. This involves an experimental observation of the vibrational frequencies and their subsequent assignment to normal modes. An expression of force constants as total energy functions can then be

obtained directly from the vibrational frequencies. A determinantal or secular equation may be set up

$$|GF - E\lambda| = 0$$

where F represents a matrix of force constants and potential energy terms, and

G represents a matrix of masses and kinetic energy terms

$$\lambda = 4\pi^2 c^2 \omega^2$$

Ultimately the matrices are used in refinement procedures to best reproduce the observed frequencies.

However this method of normal coordinate treatment has in the past led to the publication of force constants differing sometimes by more than a factor of 3 [6]. Difficulties arise since the number of independent force constants is in general larger than the number of vibrational frequencies (of a single molecule without considering isotopic substitution); hence it is problematical to calculate a unique set of physically reasonable force constants. In fact, certain earlier assignments based on normal coordinate treatments have had to be withdrawn or revised by the original authors [2].

(2) A more practically-oriented solution to the problem of band assignments lies in the substitution of metal ions and ligand atoms by stable isotopes. The physical results can be interpreted with confidence in an analysis of the spectra. Isotopic labelling of a particular atom in a metal complex results in an infrared spectrum which differs distinctly from that of the unlabelled compound. Bands

shifted by labelling may be assigned to vibrations involving the labelled atoms. It can be assumed that the force constants of the bonds are unaltered by isotopic substitution and hence the observed shifts in the spectra depend on the ratio of the masses of the labelled to the unlabelled atoms. The larger the relative mass difference, the greater the isotopic shifts of the respective bands. The biggest shifts are observed for tritiated and deuterated molecules: up to 1300 and 1000 cm^{-1}, respectively [8]. With other labelled atoms, where the relative mass difference is much smaller, shifts are considerably less, but may yet be as large as 40 cm^{-1}, for example, in an ^{18}O-labelled molecule [8].

To a first approximation, the expected isotopic shifts may be estimated [8] by assuming the labelled atom to behave as part of a diatomic simple harmonic oscillator, for which

$$\nu = 1/(2\pi c)(f/\mu)^{\frac{1}{2}}$$

where ν = vibrational frequency (wavenumber)

f = harmonic force constant

μ = reduced mass of the diatomic species

c = velocity of light.

Hence, the isotopic shifts may be calculated from

$$\nu_i/\nu = (\mu/\mu_i)^{\frac{1}{2}}$$

where the subscript i refers to the labelled molecule. This expression appears to hold for the vibration of two atoms in a many-bodied system provided that the vibration of these two atoms is not significantly affected by the

1. INTRODUCTION

1.1 METHODS USED FOR BAND ASSIGNMENT IN THE VIBRATIONAL SPECTRA OF METAL COMPLEXES

The precise assignment of bands in the ir spectra of metal complexes to vibrations of specific atoms is of value in determining direct information regarding many structural and bonding features. However such a task applied to systems as many-bodied as those studied in this work is most certainly non-trivial since the interpretation of the spectra is complicated by intermolecular interactions, lowering of symmetry and extensive vibrational coupling. An analysis of metal-ligand modes is of particular interest with regard to the nature of the coordination within the metal complex. However, owing to the high mass of the metal ion and the relatively weak nature of the metal-ligand bond, these vibrations occur below 600 cm^{-1} where further complications may arise from the appearance of lattice modes [1]. Various methods are employed to assign (a) internal ligand vibrations, (b) metal-ligand vibrations.

(a) Internal Ligand Vibrations

(1) The best known theoretical approach to a study of vibrational spectra is analysis *via* a normal coordinate treatment of the molecule [2-7]. This involves an experimental observation of the vibrational frequencies and their subsequent assignment to normal modes. An expression of force constants as total energy functions can then be

obtained directly from the vibrational frequencies. A determinantal or secular equation may be set up

$$|GF - E\lambda| = 0$$

where F represents a matrix of force constants and potential energy terms, and

G represents a matrix of masses and kinetic energy terms

$$\lambda = 4\pi^2 c^2 \omega^2$$

Ultimately the matrices are used in refinement procedures to best reproduce the observed frequencies.

However this method of normal coordinate treatment has in the past led to the publication of force constants differing sometimes by more than a factor of 3 [6]. Difficulties arise since the number of independent force constants is in general larger than the number of vibrational frequencies (of a single molecule without considering isotopic substitution); hence it is problematical to calculate a unique set of physically reasonable force constants. In fact, certain earlier assignments based on normal coordinate treatments have had to be withdrawn or revised by the original authors [2].

(2) A more practically-oriented solution to the problem of band assignments lies in the substitution of metal ions and ligand atoms by stable isotopes. The physical results can be interpreted with confidence in an analysis of the spectra. Isotopic labelling of a particular atom in a metal complex results in an infrared spectrum which differs distinctly from that of the unlabelled compound. Bands

shifted by labelling may be assigned to vibrations involving the labelled atoms. It can be assumed that the force constants of the bonds are unaltered by isotopic substitution and hence the observed shifts in the spectra depend on the ratio of the masses of the labelled to the unlabelled atoms. The larger the relative mass difference, the greater the isotopic shifts of the respective bands. The biggest shifts are observed for tritiated and deuterated molecules: up to 1300 and 1000 cm^{-1}, respectively [8]. With other labelled atoms, where the relative mass difference is much smaller, shifts are considerably less, but may yet be as large as 40 cm^{-1}, for example, in an ^{18}O-labelled molecule [8].

To a first approximation, the expected isotopic shifts may be estimated [8] by assuming the labelled atom to behave as part of a diatomic simple harmonic oscillator, for which

$$\nu = 1/(2\pi c)(f/\mu)^{\frac{1}{2}}$$

where ν = vibrational frequency (wavenumber)

f = harmonic force constant

μ = reduced mass of the diatomic species

c = velocity of light.

Hence, the isotopic shifts may be calculated from

$$\nu_i/\nu = (\mu/\mu_i)^{\frac{1}{2}}$$

where the subscript i refers to the labelled molecule. This expression appears to hold for the vibration of two atoms in a many-bodied system provided that the vibration of these two atoms is not significantly affected by the

remainder of the molecule.

This means that factors such as hydrogen bonding and vibrational coupling must not influence the specific atoms concerned to any great extent. However for the case of vibrationally pure modes, that the calculated shifts agree well with those observed experimentally has been demonstrated previously [8] and in the present work.

(3) Clearly, a combination of both theoretical considerations and detailed practical data is desirable in the solution of the assignment problem. Even a relatively simplistic group theoretical study of an isolated molecule of the species under consideration is of value in interpretations of isotopic shift data.

Group theory [9-13] is, in essence, a piece of abstract mathematics whose development is independent of any particular physical model. In chemistry, symmetry is of fundamental importance in studies of molecular structure, and using the mathematics of groups, elegant symmetry arguments may be used to work out molecular problems.

The application of group theory to many chemical problems can be summarised in three rules:

(a) Use an appropriate basis to generate a reducible representation of the point group of the molecule.

(b) Reduce this representation to its constituent irreducible representations.

(c) Interpret the results.

In order to perform a vibrational analysis on an N-atom molecule, which gives the number and symmetries of

stretching and bending modes and their Raman/ir activities, the procedure is as follows:

Label each atom of the molecule with the three Cartesian coordinates which represent unit displacement vectors, the overall displacement being given as their vector sum. The Cartesian displacement vectors are used as the basis to generate a reducible representation of the point group. On performing the symmetry operations of the molecular point group, the new vector positions can be related to the original ones by $3N \times 3N$ matrices. The characters (sum of diagonal elements) of each matrix may then be used as a reducible representation of the point group. To determine the symmetry species of all the possible molecular motions, the reducible representation must be expressed in terms of its constituent irreducible representations, and the following reduction formula is used:

$$n_i = \frac{1}{h} \sum_{\substack{\text{over all} \\ \text{classes}}} \chi_R \chi_I N$$

where n_i = the number of times each irreducible representation appears in the reducible representation

h = the order of the point group

N = the number of symmetry operations in the particular class of the point group

χ_R = the character of the reducible representation

χ_I = the character of the irreducible representation

For a particular point group, the characters of the irreducible representations and their symmetries are listed in the relevant character table. In addition,

character tables list which of the irreducible representationstransform under the symmetry operations as Cartesian coordinates, x, y, z, as their squares and binary products x^2, y^2, z^2, xy, xz, and yz, and as rotation vectors R_x, R_y and R_z. Removal of those irreducible representations relating to translation and rotation leaves the representations responsible for vibrations.

Infrared and Raman activities of vibrational modes are associated with accompanying changes in the bonds concerning respectively, dipole moments and polarizabilities. It may subsequently be shown that a fundamental will be ir active if the normal mode which is excited belongs to the same representation as any one or several of the Cartesian coordinates; while a fundamental mode will be Raman active if the normal mode involved belongs to the same representation as squares and binary products of the Cartesian coordinates. Clearly this information may be read directly from the relevant character table.

Finally, information about the nature of the vibrations in terms of the stretching or bending of the bonds may be obtained by using internal displacement vectors as a new basis, again generating a reducible representation by performing the symmetry operations of the point group, and reducing this representation to its constituent irreducible representations as previously described.

The vibrations of a molecule in the gaseous phase are governed only by the restrictions of its own point symmetry [9]. These are the conditions described above. To be precise, when a molecule occupies a site in a crystal,

it cannot be regarded as an isolated unit, since the solid environment imposes its own symmetry restrictions. These additional effects can split degenerate vibrations, change the activities of various modes, and generate lattice modes which arise from translatory and rotatory motions of the molecule within the solid. For a rigorous vibrational analysis, the entire array of molecules should be considered, and there are two frequently used approximations: site group [14] and factor group analyses [15-16].

In the site group analysis by Halford [14] the surrounding of a molecule is treated as static, but its symmetry is imposed on the molecule. The site symmetry, which is generally lower than the molecular symmetry, may be found if the space group, the number of molecules per unit cell and the point group of the isolated molecule are known. Halford derived tables listing the possible site symmetries and the number of equivalent sites for the 230 space groups.

Factor group analysis [15-16] is more complete in that it accounts for lattice modes and solid state splittings of the nondegenerate vibrations of the free molecule. The information necessary for the analysis is a full x-ray crystal structure determination with atomic coordinates in terms of Wykoff notation. Adams and Newton [17] have published tables of reduced representations which readily facilitate the vibrational analysis of solids belonging to any of the 230 space groups.

(b) Metal-Ligand Vibrations

While all of the above approaches may also be used in a study of metal-ligand modes, certain other techniques, though somewhat empirical, are of particular interest and value.

(1) Comparison of the spectrum of the free ligand with that of its complex; bands in the spectrum of the complex which are absent from that of the ligand, may be assigned to M-L modes. However, this method is prone to yield erroneous assignments because some ligand vibrations, activated by complex formation, may appear in the same region as the M-L vibrations [18].

(2) For complexes of identical metal ions with a series of similarly-substituted ligands, M-L vibrations are expected to appear within a relatively narrow frequency range. This method has been used to assign νCu-N in the compounds CuX_2L_2 [19] (X = Cl, Br; L = substituted pyridine), νNi-O in substituted pyridine adducts of Ni(II) acetylacetonate [20] and νM-O in metal β-ketoenolates [21].

(3) The M-L vibrations of a series of isostructural complexes are metal-sensitive and shift according to the properties of the metals. For a series of transition metal complexes with a constant ligand combination, it has been shown that there is a direct correlation between cfse and various thermodynamic properties, such as lattice energies, heats of ligation and M-L bond distances [22-24]. Since the variation in cfse influences the M-L bond strength and hence the M-L force constants, it can be expected that

in the absence of significant mass effects, the M-L stretching frequencies of such a series of complexes will vary in parallel with their cfse's.

This has been shown to be the case by Thornton and coworkers [25-38] for several transition metal complex systems. Variations of νM-O have been found to correlate with the relative cfse values for β-ketoenolates of trivalent first transition series metal ions [25]. Similar correlations have been obtained for νM-L in several series of metal(II) and metal(III) tropolonate complexes [26], in divalent metal acetylacetonates and their nitrogenous base adducts [27], metal(II) 2,2'-bipyridine and 1,10-phenanthroline complexes [28], 2-thenoyltrifluoroacetonates [29], metal(II) anthranilates [30], di- and trivalent γ-substituted actylacetonates [31], and others [32]. Studies have been extended to the second transition series metal acetylacetonates [33], the *tris*- and *tetrakis*-lanthanide(III) tropolonate complexes [34,35], and more recently to metal(II) salicylaldimine complexes [36-38].

(4) If the aforementioned assignment technique of isotopic substitution is applied specifically to studies of metal-ligand modes, two distinct approaches may be undertaken, independently or in conjunction with one another: the metal ion and/or the ligand donor atom may be replaced with isotopically-labelled species.

The use of isotopic substitution of the metal ion in the assignment of metal-ligand vibrations has been extensively reviewed [39]. Metal labelling has been applied to a number of coordination compounds such as phosphines,

α-diimines, acetylacetonates, triarylphosphine complexes of nickel and palladium, *tris*(bipyridine) complexes of first transition series metal(II) ions, amine complexes of zinc iodide and pyridine complexes of zinc(II) and tin(IV) halides. Nakamoto has used the technique extensively, and Lever and co-workers [40,41] have applied metal labelling to ir studies of complexes of amino acids and diamines while Hutchinson [42] has carried out related studies on metal complexes of tropolone. Isotopic substitution of the metal ion is advantageous in that it results in wavenumber shifts of the metal-ligand vibrations only, hence facilitating unambiguous assignments of νM-L. However, disadvantages lie in the fact that not only may the isotopic shifts be very small (owing to an unfavourable mass ratio between the unlabelled and labelled metal ion), but also the method does not differentiate between different types of metal-ligand vibrations which arise in complexes with different donor atoms, *e.g.* between νM-N and νM-Cl in $M(py)_2Cl_2$ complexes. In addition, suitable stable metal isotopes are of limited availability and extremely costly.

The alternative technique of labelling the ligand donor atom is generally of greater applicability because the mass ratio of unlabelled to labelled species is more favourable for the stable and relatively available isotopes such as ^{2}H, ^{18}O, ^{15}N and ^{13}C, and their cost is somewhat less prohibitive. However, a disadvantage of the ligand labelling technique is that relatively low wavenumber bands originating from ligand vibrations involving the donor atom

but not the metal ion may be erroneously assigned to metal-ligand modes. Labelling of the ligand donor atom has been used successfully in a wide variety of studies [30,36,38,43-47] for example, to assign νM-L in salicylaldimine, tropolonate, acetylacetonate, and anthranilate complexes. Similar studies have been carried out for *trans*-nitro-bis(acetylacetonato)mono(amine) cobalt(III) complexes [47,48] and a wide variety of amino acid complexes [49-55].

1.2 METAL(II) CHELATES OF 2-AMINOMETHYLPYRIDINE

2-Aminomethylpyridine is a chelating agent which is a structural intermediate of 1,2-diaminoethane and 2,2'-bipyridine; undoubtedly, the initial interest in 2-aminomethylpyridine came from its similarities to these two better known ligands. Considering the structure of 2-aminomethylpyridine, it is easy to see that stable five-membered ring systems can be formed on chelation to metal cations; complexes with metal:ligand ratios 1:1, 1:2 and 1:3 can be formed. Various workers [56-58] have found that the electronic absorption spectra of 2-aminomethylpyridine metal(II) chelates have similarities to those of 1,2-diaminoethane and 2,2'-bipyridine metal(II) chelates of corresponding structure, with the spectra of the 2-aminomethylpyridine complexes showing greater similarity to those of the 1,2-diaminoethane complexes. In addition, magnetic and conductance measurements [56-58] have allowed detailed structural information to be derived. Further studies of this nature [59-62], on metal(II) complexes of 2-aminomethylpyridine have been somewhat limited, but Michelson has reported [63,64] a number of spectral investigations of the metal(III) complexes. A number of studies [65-70] concerning the stability of the metal complexes has also been carried out.

To date, the application of far ir spectroscopy to studies of the structure and bonding of 2-aminomethylpyridine chelates has been minimal. Noji, Kidani and Koike [71] synthesized $M(amp)_2X_2$ where M = Cu(II), Ni(II), Co(II) and Zn(II); X = Cl^-, Br^-, I^-, and measured their magnetic moments and diffuse reflectance spectra. Consequent structural proposals were

used to analyse the far ir spectra of the chelates. However, that some of their assignments are incorrect is shown in this work.

The use of x-ray techniques in structural determinations of metal complexes of 2-aminomethylpyridine has also been limited. X-ray powder photographs [64], have shown isomorphism to exist between various octahedral bis(2-aminomethylpyridine) complexes of chromium(III). Single crystal work on the *tris*-(2-aminomethylpyridine) nickel(II) perchlorate [72], gave an approximate structure of the complex: From Weissenberg and precession x-ray photographs the crystal was found to be cubic with space group $P\bar{4}3n$ (*hkl*, no conditions; *hhl*, $l = 2n$; and cyclicly). The cell constant was found to be a = 16.95(1) Å, at 19°C. Considering the symmetry of the ligand and assuming that the complex cation is not disordered, the following conclusions were drawn: the nickel(II) ions are at Wyckoff positions 8(*e*) on the three-fold axes; the complexed nickel(II) ions contain a molecular three-fold axis and each of the three pyridine rings must be *cis* to the other two. It was felt that the coordination configuration is nearer to trigonal antiprismatic (pseudo-octahedral) than to trigonal prismatic. The only complete crystallographic investigation of a metal complex of 2-aminomethylpyridine has been carried out by Helis *et al* [73]: *mono*(2-aminomethylpyridine) copper(II) bromide was found to consist of infinite dibromo-bridged chains, with a distorted octahedral geometry around each copper centre.

1.3 METAL(II) CHELATES OF 2-(2-AMINOETHYL)PYRIDINE

The ligand 2-(2-aminoethyl)pyridine is structurally similar to 2-aminomethylpyridine in that coordination to a metal ion can occur through an aromatic nitrogen and an amine group; however the additional methylene group in the amino side chain of 2-(2-aminoethyl)pyridine results in the formation of six-membered rings on chelation as opposed to five-membered chelate rings in metal complexes of 2-aminomethylpyridine; the chelating tendency of 2-(2-aminoethyl)pyridine may therefore be expected to be comparatively low. Stability constant measurements of Lacoste and Martell [67] have clearly illustrated this fact. The 2-(2-aminoethyl)pyridine complexes of Ni(II), Cu(II) and Zn(II) are more stable than those of other metal(II) ions and this is verified by the relative ease with which the Cu(II) and Zn(II) complexes crystallize from solution.

Uhlig and Masser [74,75] reported the isolation of several solid Cu(II), Ni(II), Co(II), Zn(II) and Ag(II) complexes of 2-(2-aminoethyl)pyridine but did not use any physical measurements that could have led to the elucidation of their structure. In later studies by Uhlig, Bergmann and Schneider [76] and Sutton and Nicholson [58] magnetic, conductance and spectral measurements have been presented. A number [77-82] of x-ray crystal structure determinations of various *mono*- and *bis*-2-(2-aminoethyl)pyridine complexes has also been reported. only one far ir investigation [83] of the complexes has been carried out; assignments of metal-ligand stretching frequencies reported there appear to have been made on a largely empirical basis.

1.4 THE INFRARED SPECTRA OF QUINOLINE AND ITS METAL COMPLEXES

Band assignments of ligand modes in the ir spectra of pyridine and aniline and their ring-deuterated analogues have previously been made [84]. It has been shown that there are two ratios between frequencies of corresponding bands (deuterated: undeuterated); the (essentially) ring modes yield a higher ratio while, as expected, vibrations involving C-H modes are more sensitive to deuterium substitution and yield a lower ratio. Precisely similar ratios have been observed for their deuterated and undeuterated metal complexes. McClellan and Pimental [85] have reported a complete vibrational assignment of naphthalene and naphthalene-d_8. Although presented slightly differently, their data show that again two ratios for corresponding bands in the deuterated and undeuterated species exist: in general, the ratio for skeletal modes lies within the range 0.92 ± 0.05, while that for the C-H modes lies within the range 0.79 ± 0.05. A vibrational assignment of ligand modes for quinoline, based predominantly upon this naphthalene study, has been reported [86]; the ir spectra of monodeuterated quinolines have also been studied [87] but no correlation with quinoline-d_7 appears yet to have been made.

Previous assignments [19,88-91] of metal-quinoline vibrations in the complexes $M(quin)_2(halide)_2$ which are tetrahedral or polymeric have largely been based upon halide substitution. However structural differences between the complexes and solid state splittings of degenerate vibrations often give rise to ambiguities, and make such assignments not totally conclusive. In previous reports of bis-(quinoline) metal(II) isothiocyanates

[92-94] elucidation of the type of bonding and structure and assignments of metal-ligand vibrations have been based upon the characteristic absorptions of the SCN^- anion. Owing to the fact that most of these are obscured by quinoline modes, clarification of the situation appears to be necessary. Since shifts of metal-nitrogen vibrations on $-d_5$ labelling of pyridine have been shown [95] to yield reliable assignments in pyridine complexes of metal halides as have [96] $-^{15}N$ shifts in pyridine ^{15}NCS complexes, analogous studies with quinoline complexes are feasible.

1.5 METAL(II) ACETYLACETONATES AND THEIR BASE ADDUCTS

Acetylacetone was first employed as a chelating agent by Werner [97] in 1901. Since then, M(II) and M(III) complexes of the ligand have received considerable attention and the literature contains a number of reviews [98,99] on the subject.

While the early ir studies were directed to the mid-ir region, the more recent research has been in the region below 700 cm^{-1} where the metal-ligand modes are expected to occur. However the ir spectra of metal complexes of acetylacetone are still a subject of controversy. For $Cr(acac)_3$ alone, a number of conflicting assignments for the metal-ligand modes based upon independent normal coordinate treatments or isotopic labelling studies, can be found in the literature [45,100-105]. Reports [106-109] on the infrared spectra of other metal complexes of acetylacetonate are no less confusing.

The ability of various aromatic and aliphatic nitrogeneous bases to form stable adducts with metal(II) β-ketoenolates has been well established [110-113]. Those formed by reaction between monodentate bases (B) such as imidazole and pyridine and metal(II) acetylacetonates are generally [114,115] six-coordinate and of the nature *trans*- $M(acac)_2B_2$; bases such as pyrazine and pyrimidine have the capacity to form neutral polymers in which each of the two nitrogen donors is bonded to discrete planar $M(acac)_2$ units and formulated $[M(acac)_2B]_n$ (2,16,17). Quinoline forms both 1:1 and 2:1 complexes with metal(II) acetylacetonates [98]: for M = Mn(II),

Co(II), Ni(II), the six-coordinate species *trans*-$M(acac)_2(quin)_2$;for M = Cu(II), Zn(II), the five-coordinate species $M(acac)_2quin$. The crystal structure [116] of $Cu(acac)_2quin$ has shown the pentacoordination of the copper ion to be square based pyramidal; the zinc complex is most likely similar to this. Certain bidentate bases such as 1,10-phenanthroline, have also been shown [117] to form six-coordinate complexes of the type *cis*-$M(acac)_2B$ and similarly the alkali metal *tris*(acetylacetonate) metal(II) complexes such as $Na[M(acac)_3]$. Recent work in this laboratory [118-119] has included the application of isotopic labelling and metal ion substitution to complexes of this type.

1.6 THE INFRARED SPECTRA OF METAL COMPLEXES OF GLYCINE

The manner in which metal ions bind to amino acids has long been of interest in studies of biological systems. Vibrational spectroscopy can provide useful information not only about the ligands themselves but also about the extent and nature of the metal-ligand interaction. However, there exists in the literature some measure of disagreement on the assignment of the ir bands in the spectra of glycinate and other amino acid complexes [120-123]. One view assumes low covalency in the M-O bonds [121,122] with essentially monodentate M-N coordination of the amino acid while another [120,123] considers the M-O bonds to be highly covalent. Independent normal coordinate analyses [120,121] have not succeeded in unambiguously resolving the problem, the two sets of assignments showing considerable differences.

Isotopic labelling of the ligand atoms has led to reliable band assignments in the ir spectra of glycine [124-126] and its Ni(II) and Cu(II) complexes [53,54]. An independant study [129] involving ^{65}Cu-substitution has also been carried out for *cis*- $Cu(gly)_2H_2O$. To date, the most comprehensive investigations of the assignment problem in amino acid complexes have involved the isotopic labelling of most of the ligand atoms present in the system [127-130]. This technique is adopted in the present work for elucidating the assignments in five metal glycinate complexes.

1.7 METAL COMPLEXES OF UREA

While the literature contains considerable information on the chemistry of thiourea, comparatively little work has been published on the related diamide urea and its metal complexes. Metal complexes with up to six molecules of urea coordinated are known [131-135]; however, except by crystallographic means, [136-140] attempts to establish whether coordination occurs through one or both of the nitrogen atoms or through the oxygen atom have not been totally conclusive.

The Raman and ir spectra of urea itself have been observed by several investigators [141,142]. A normal vibration calculation was initially published by Kellner [143]. However after the planarity of the ligand had been established [144, 145], Yamaguchi *et al* [146] carried out a normal coordinate treatment for urea and urea-d_4. Further information about the vibrations of urea was obtained in a more recent ^{18}O-substitution study [147].

To date no infrared investigations below 300 cm^{-1} have been carried out. Since this is the region where a number of metal-ligand modes might be expected to occur, studies of this nature are merited and are made in this work.

SECTION 2 - EXPERIMENTAL

2. EXPERIMENTAL

2.1 PHYSICAL METHODS

2.1.1 Infrared Spectra

The ir spectra of the solid state ligands and metal complexes studied were determined as nujol mulls in the regions 2000 - 1500 cm^{-1} and 1300 - 80 cm^{-1} and as hexachlorobutadiene mulls in the regions 4000 - 2000 cm^{-1} and 1500 - 1300 cm^{-1}. The ir spectra of liquid ligands were determined as thin films. In all cases samples were observed through plates made of the following window materials: caesium bromide (4000 - 300 cm^{-1}) caesium iodide (4000 - 200 cm^{-1}) and high density polyethylene (300 - 80 cm^{-1}). Instruments used were a Beckman IR-12 spectrophotometer (4000 - 200 cm^{-1}), a Perkin-Elmer 180 spectrophotometer (4000 - 140 cm^{-1}) and a Digilab FTS-16 B/D interferometer (450 - 80 cm^{-1}), each of which was calibrated against carbon dioxide, water vapour and polystyrene. Spectral determinations of labelled compounds and their unlabelled analogues were repeated at least three times. Reproducibility of quoted frequencies is generally better than 0.5 cm^{-1}.

2.1.2 Raman Spectra

The Raman spectra reported in this work were determined in the Department of Inorganic and Analytical Chemistry of the Hebrew University, Jerusalem. A PHi Coderg machine was used; the exciting line was of wavelength 5145 Å (the green line of an Ar^{+} laser). All spectra were recorded using the rotating disc technique to prevent decomposition by the heat

of the laser beam. The reproducibility of reported frequencies is better than 3 cm^{-1}.

2.1.3 *General Experimental and Computational Procedures used in the Crystallographic Analyses*

For each of the complexes studied crystallographically in this work, the preliminary space group determinations and data collections for the crystals were essentially the same and are hence outlined together. The required crystals were prepared from various recrystallizations and their densities determined by flotation in suitable solvents as described in the relevant sections (3.2.3 and 3.7.1). Selected crystals were suitably mounted at the tips of thin glass fibres, and a two-circle goniometer was used for alignment. Preliminary crystallographic information was obtained from oscillation, Weissenberg, precession and Laue photographs, taken using a Stöe (Heidelberg) goniometer. Cu-K_α radiation (λ = 1.5418 Å) was obtained from a copper target in conjunction with a nickel filter using Philips PW 1120 and PW 1008 x-ray generators operated at 20 mA and 40 kV. The oscillation camera radius was 28.65 mm. The x-ray films (Ilford Industrial G) were processed in the usual way with Kodak x-ray developer and fixer solutions. Suitable crystals were cut to roughly cubic dimensions and sent to the National Physical Research Laboratory, C.S.I.R. (Pretoria) for intensity data collection on a Philips PW 1100 computer-controlled four-circle diffractometer. A Philips PW 1130 3 kW x-ray generator operating at 50 kV and 20 mA provided the source of radiation. Molybdenum-K_α radiation (λ = 0.7107 Å) was obtained with the aid of a

graphite monochromator. Lattice constants were obtained by a least-squares fit of the χ, ϕ and 2θ angles of 25 reflections accurately centred on the diffractometer. The $\omega - 2\theta$ scan mode [148] was used for all data collections. For any one crystal, the intensities of three suitable reference reflections were monitored after every 68 measured reflections to indicate crystal and instrument stability during the data collection. The standard error $\sigma(I_{rel})$ in the relative integrated intensity I_{rel} was calculated by:

$$\sigma(I_{rel}) = [(0.02\ N_o)^2 + k^2 N_b + N_o]^{\frac{1}{2}}$$

where N_o is the gross peak count for the reflection, N_b the background count (measured on each side of the peak) and k the ratio of scan to background times. The criteria for reflections being considered "observed" varied for each complex and are given separately in the relevant sections (3.2.3 and 3.7.1). Lorentz-polarization corrections were applied to all reflection data in Pretoria immediately after data collection but absorption effects were not taken into account. All calculations were performed on a Univac 1181 computer at the Computer Centre, University of Cape Town. The program SHELX [149] was used for data reduction and structure determination, and PLUTO [150] was used to obtain molecular illustrations. In all cases, the agreement between observed (F_o) and calculated (F_c) structure factors is expressed by the conventional residual factors defined by:

$$R = \frac{\Sigma||F_o|-|F_c||}{\Sigma|F_o|} = \frac{\Sigma|\Delta|}{\Sigma|F_o|}$$

and $R_w = \Sigma w^{\frac{1}{2}} \frac{||F_o|-|F_c||}{\Sigma w^{\frac{1}{2}}|F_o|}$ where $w = \frac{1}{[\sigma^2(F)+gF^2]}$

The value of g was taken as 0.0 or chosen to give the smallest variation of $w\Delta^2$ with the magnitude of F_c. An analysis of variance computed after each of the final cycles showed whether the weighting schemes were satisfactory. Thermal parameters are of the form:

$$\exp[-2\pi^2(U_{11}h^2a^{*2} + U_{22}k^2b^{*2} + U_{33}l^2c^{*2} + 2U_{12}hka^*b^* + 2U_{13}hla^*c^* + 2U_{23}klb^*c^*) \times 10^3]$$

where U_{ij} are the anisotropic temperature factors referred to in the subsequent text. Scattering factors for all elements considered in the refinement procedures were those of Cromer and Mann [151].

Further information pertaining to the solution of any one of the crystal structures is given in the relevant sections of the work.

2.1.4 Microanalyses

Microanalyses were performed on an Heraeus Universal Combustion Analyser Model CHN-Micro, by Mr W.R.T. Hemsted of the Department of Organic Chemistry, University of Cape Town. For isotopically-labelled species, the calculated values are based on the assumption that the effect of the mass change (due to the labelling) on the heat conductivity of nitrogen or water vapour is negligible.

2.2 PREPARATION OF COMPOUNDS

The isotopically-labelled substances used in this study, together with their commercial sources and isotopic purities, are listed in Table 1.

Table 1.

Isotopically-labelled substance	Isotopic purity (atom %)	Commercial source
deuterium oxide	99.7	Merck, Sharp & Dohme (Canada) Ltd.
2-aminomethylpyridine-^{15}N	97.2	BOC Prochem Ltd.
potassiumthiocyanate- ^{15}N	97.0	Merck, Sharp & Dohme (Canada) Ltd.
quinoline-d_7	98.0	Merck, Sharp & Dohme (Canada) Ltd.
acetylacetonate-^{18}O	72.0	BOC Prochem Ltd.
glycine-^{18}O	78.0	BOC Prochem Ltd.
glycine-^{15}N	97.0	BOC Prochem Ltd.
glycine-1-^{13}C	91.0	BOC Prochem Ltd.
glycine-2-^{13}C	91.0	BOC Prochem Ltd.
glycine-2,2-d_2	97.0	Merck, Sharp & Dohme (Canada) Ltd.
urea-^{18}O	99.0	BOC Prochem Ltd.
urea-^{15}N	96.5	BOC Prochem Ltd.
urea-^{13}C	90.5	BOC Prochem Ltd.
zinc sulphate-^{68}Zn	97.6	BOC Prochem Ltd.
zinc sulphate-^{64}Zn	98.6	BOC Prochem Ltd.

2.2.1 *The tris-2,2'-bipyridine, 2-aminomethylpyridine and ethylenediamine complexes of metal(II) perchlorates*

The complexes $[M(bipy)_3](ClO_4)_2$ were prepared as previously reported [152] by adding a hot aqueous solution of the metal(II) sulphate to a hot aqueous solution of the ligand in the molar ratio 1:3. Addition of an excess of aqueous $KClO_4$ precipitated the product which was collected, washed with water and dried over silica gel at room temperature and 0.1 mm Hg pressure. Preparations of the *tris*(2-aminomethylpyridine) complexes of Co(II) and Ni(II) are known [56,152]. However the following general procedure for the preparation of complexes $[M(amp)_3](ClO_4)_2$ was employed. An aqueous solution of the hydrated metal(II) perchlorate (.017 mmole) was added to an aqueous solution of 2-aminomethylpyridine (.05 mmole). Precipitated crystals were washed with ethanol and dried overnight over silica gel at room temperature and 0.1 mm Hg pressure. The *tris*(ethylenediamine) complexes were prepared by adding the ligand to a methanolic solution of the metal(II) perchlorate in the molar ratio 3:1. The precipitates formed were filtered off and dried over silica gel at room temperature and 0.1 mm Hg pressure. These complexes have previously [153] been prepared.

2.2.2 *The tris(2-aminomethylpyridine) complexes of metal(II) tetrafluoroborates*

These complexes were prepared from the metal(II) tetrafluoroborates in a manner similar to that used for their perchlorate analogues. Crystals of the complex $[Ni(amp)_3](BF_4)_2$ suitable for the x-ray analysis were obtained by slow

recrystallization of the complex from an aqueous/ethanolic solution.

2.2.3 The bis complexes $M(amp)_2X_2$: $X = Cl^-, Br^-, I^-, SCN^-, ClO_4^-, BF_4^-$

The halide, perchlorate and tetrafluoroborate complexes were obtained by the methods of Sutton [56] and Noji *et al* [71]. In general, hot aqueous or ethanolic solutions of the ligand and metal salts were mixed in the ratio 2:1. The precipitated products were sometimes only obtained on continuous stirring for two to three hours. The complexes were filtered, washed and dried over silica gel at 0.1 mm Hg pressure. In most of the cases where an hydrated product was formed, the anhydrous analogue was prepared by heating *in vacuo* to 100°C.
The complexes $M(amp)_2(SCN)_2$ were prepared by the method reported [154] for bis(aniline) and bis(*p*-toluidine) metal(II) isothiocyanate complexes.

2.2.4 The mono complexes $M(amp)X_2$: $X = Cl^-, Br^-, I^-, SCN^-$.

Most of these halides were prepared from the metal salts by methods reported previously [57,155]. The complex $Pt(amp)Cl_2$ was prepared by adding an aqueous solution of 2-aminomethylpyridine (2 mmole) to aqueous K_2PtCl_4 (2 mmol) and stirring. The analogous $Pt(amp)Br_2$ was similarly obtained from K_2PtBr_4 which was prepared by the oxalate reduction of a fresh sample of K_2PtBr_6 ($H_2PtBr_6.9H_2O$ + excess KBr). The $Pt(amp)(SCN)_2$ complex was formed by adding aqueous 2-aminomethylpyridine to a hot aqueous solution of K_2PtCl_4 and excess NaSCN.

The amp-^{15}N and -^{15}NCS complexes were obtained by methods identical to those used for the unlabelled complexes. The amino-deuterated species amp-*N,N*-d_2 were obtained using deuterium oxide and deuterated ethanol as solvents in the preparations. All amp-*N,N*-d_2 complexes were stored under high vacuum to prevent deuterium/hydrogen exchange.

2.2.5 *2-(2-Aminoethyl)pyridine complexes of metal(II) perchlorates, tetrafluoroborates, halides and pseudohalides*

The bis{2-(2-aminoethyl)pyridine} complexes of Cu(II) and Zn(II) perchlorate, iodide and isothiocyanate were prepared by the methods of Uhlig and Masser [74]. The preparations reported by these workers for the *bis* $Cu(aep)_2Br_2$ complex and the various *mono* Cu(II) and Zn(II) complexes could not be repeated. However the methods of Hodgson *et al* [77,79,81] yielded the desired Cu(II) halide complexes. $Cu(aep)_2(BF_4)_2$ was precipitated in a manner similar to that used for the analogous perchlorate. The *mono*{2-(2-aminoethyl)pyridine} zinc(II) chloride, bromide and iodide complexes were formed by warming stoichiometric quantities (1:1) of the ligand and metal halide in methanolic solution and allowing slow cooling to room temperature. The precipitated products were filtered off, washed with methanol and ether and dried over silica gel at 0.1 mm Hg pressure.

2.2.6 *Quinoline complexes of metal(II) halides and pseudohalides*

Complexes of the form $M(quin)_2(halide)_2$ were prepared using syntheses of metal-quinoline complexes similar to those

reported in the literature [156-157]. The newly prepared zinc iodide complex was precipitated by adding an aqueous solution of excess KI to an ethanolic solution of stoichiometric amounts of zinc acetate and quinoline. The product was washed with ethanol and ether and dried at room temperature over silica gel at 0.1 mm Hg pressure. Deuterated analogues of all these complexes were similarly obtained from the commercially prepared quinoline-d_7. The $Cu(quin)_2(NCS)_2$ and $Zn(quin)_2(NCS)_2$ complexes were both prepared by a method reported [92] for $Cu(quin)_2(NCS)_2$ as were their quinoline-d_7 and -^{15}NCS analogues.

2.2.7 *Zinc(II) acetylacetonate monohydrate*

This complex was prepared from the metal(II) sulphate as described in the literature [158]. Two successive recrystallizations from hot ethylacetate and acetylacetone were required to obtain a product of the desired purity. The isotopically substituted analogues were similarly obtained using the commercially prepared starting materials.

2.2.8 *Base adducts and sodium tris complexes of metal(II) acetylacetonates.*

The 2,2'-bipyridine, 2-aminomethylpyridine and ethylenediamine adducts and sodium *tris* complexes of Co(II), Ni(II) and Zn(II) acetylacetonates were prepared according to previously published methods [159,160]. The quinoline and quinoline-d_7 adducts of the metal(II) acetylactonates were

prepared by reaction of the *bis*(acetylacetonate) metal(II) complex with the base directly, or on warming with toluene, washed with ethanol and ether and dried under reduced pressure. The quinoline adduct of Cu(II) acetylacetonate was prepared and maintained under nitrogen, since on exposure to air, it reverts to *bis*(acetylacetonato)copper(II) [116].

2.2.9 *The complexes* $[Cd(gly)_2].H_2O$, $[Zn(gly)_2].H_2O$ *and* $Cd(gly)_2$, *and their isotopically substituted analogues*

The hydrated complexes were prepared according to the method of Low *et al* [161]. Glycine (2 mmole) was added to the metal oxide (1 mmole) and boiled in 3 ml water for a few minutes. The resulting solution was quickly filtered, and the filtrate evaporated down to about 1 ml. Crystals of the desired complexes separated out within twelve hours, were filtered off, washed with a small volume of ethanol and dried over silica gel under reduced pressure. Preparations of the isotopically-substituted analogues were similarly performed except that quantities of reagents were scaled down so that only 0.1 g of each labelled glycine was used. The anhydrous complex $Cd(gly)_2$ was prepared by heating the hydrate to 150°C *in vacuo* for four hours.

2.2.10 *The complexes* $Cr(gly)_3$ *and* $Co(gly)_3.2H_2O$

A method of preparation of *cis-cis*- $Cr(gly)_3$ has previously been reported [162]. However owing to the fact that a yield of the desired complex no better than that quoted

(50%) could be obtained, a new procedure was devised. On addition of stoichiometric amounts of Cr(III) acetate to glycine and warming to 95°C in dimethyl sulphoxide, a red precipitate of $Cr(gly)_3$ was obtained with a yield of 85%. The complex was filtered off and dried over silica gel at reduced pressure. The complex *cis-cis*-$[Co(gly)_3].2H_2O$ was obtained using the method of Mori *et al* [163]. An aqueous solution containing stoichiometric amounts of hexamminecobalt-(III) chloride, glycine and potassium hydroxide was introduced into a round bottom flask fitted with an air condenser and heated for two hours. On cooling, the desired crystals were filtered off, recrystallized from water and dried over silica gel at reduced pressure.

The isotopically substituted analogues of these complexes were similarly obtained using the commercially-labelled samples of glycine.

2.2.11 Metal complexes of urea

Crystals of hexakis(urea)chromium(III) chloride trihydrate were prepared according to a previously published method [164] with slight modifications. An aqueous solution of chromium-(III) chloride was boiled with urea (molar ratio 1:6) and the whole was evaporated almost to dryness. The green paste thus formed was taken up in methanol and after 48 hours, green needle-shaped crystals began to separate. They were filtered off, washed with a small amount of methanol, and dried over silica gel under reduced pressure. Samples of $Pt(ur)_2Cl_2$ and $Pd(ur)_2Cl_2$ were prepared using K_2PtCl_4 and $PdCl_2$

respectively as starting materials. Stoichiometric amounts of urea and the metal salts were boiled in an aqueous solution, and the heat was removed after all the starting materials had dissolved. On stirring for 1 hour, the required complexes separated out, were filtered off and dried over silica gel under reduced pressure.

SECTION 3 - RESULTS AND DISCUSSION

3. RESULTS AND DISCUSSION

3.1 MICROANALYSES OF COMPOUNDS

Table 2. Microanalytical data for the *tris*-complexes $[ML_3]X_2$ where L = amp, bipy, en; X = ClO_4^-, BF_4^-.

Complex	Calculated			Found		
	%C	%H	%N	%C	%H	%N
$[Mn(amp)_3](ClO_4)_2$	37.4	4.2	14.5	37.5	4.2	14.5
$[Fe(amp)_3](ClO_4)_2$	37.3	4.2	14.5	37.4	4.2	14.3
$[Co(amp)_3](ClO_4)_2$	37.1	4.2	14.4	37.1	4.2	14.4
$[Ni(amp)_3](ClO_4)_2$	37.1	4.2	14.4	37.3	4.2	14.4
$[Zn(amp)_3](ClO_4)_2$	36.7	4.1	14.3	36.9	4.2	14.3
$[Co(bipy)_3](ClO_4)_2$	49.6	3.3	11.6	49.4	3.4	11.5
$[Ni(bipy)_3](ClO_4)_2$	49.6	3.3	11.6	49.8	3.4	11.6
$[Zn(bipy)_3](ClO_4)_2$	49.2	3.3	11.5	49.4	3.4	11.6
$[Co(en)_3](ClO_4)_2$	16.5	5.2	19.2	16.2	5.5	18.7
$[Ni(en)_3](ClO_4)_2$	16.5	5.5	19.2	16.3	5.6	18.8
$[Zn(en)_3](ClO_4)_2$	16.2	5.4	18.9	16.2	5.6	18.9
$[Co(amp)_3](BF_4)_2$	38.8	4.3	15.1	38.8	4.4	15.1
$[Ni(amp)_3](BF_4)_2$	38.8	4.3	15.0	38.8	4.3	15.0
$[Zn(amp)_3](BF_4)_2$	38.4	4.3	14.9	38.4	4.4	14.9

Table 3. Microanalytical data for the *bis*-complexes $M(amp)_2X_2$, where X = ClO_4^-, BF_4^-, Cl^-, Br^- and I^-.

Complex	Calculated			Found		
	%C	%H	%N	%C	%H	%N
$Cu(amp)_2(ClO_4)_2$	30.1	3.4	11.7	30.5	3.5	11.8
$Cu(amp)_2(BF_4)_2$	31.8	3.6	12.4	31.7	3.6	12.4
$Ni(amp)_2Cl_2.2H_2O$	37.7	5.3	14.7	37.6	5.2	14.8
$Ni(amp)_2Cl_2$	41.1	4.8	16.1	41.7	4.7	16.2
$Cu(amp)_2Cl_2.2H_2O$	37.3	5.2	14.5	37.2	5.2	14.5
$Cu(amp)_2Cl_2$	41.0	4.5	15.9	40.9	4.6	16.0
$Zn(amp)_2Cl_2.1\frac{1}{2}H_2O$	38.0	5.0	14.8	38.1	4.3	14.9
$Mn(amp)_2Br_2$	33.4	3.7	13.0	33.2	3.8	12.8
$Ni(amp)_2Br_2.2H_2O$	30.6	4.3	11.9	30.5	4.3	11.8
$Ni(amp)_2Br_2$	33.1	3.7	12.9	33.0	3.7	12.9
$Cu(amp)_2Br_2$ [a]	32.8	3.7	12.7	32.5	3.7	12.6
$Cu(amp)_2Br_2$ [b]	32.8	3.7	12.7	32.3	3.6	12.5
$Zn(amp)_2Br_2$	32.6	3.7	12.8	32.4	3.6	12.5
$Ni(amp)_2I_2.2H_2O$	25.5	3.6	9.9	25.1	3.6	9.9
$Ni(amp)_2I_2.H_2O$	26.4	3.3	10.3	26.4	3.1	10.3
$Cu(amp)_2I_2$	27.0	3.0	10.5	27.0	3.0	10.4
$Zn(amp)_2I_2$	26.9	3.0	10.5	26.8	3.0	10.3
$Mn(amp)_2(SCN)_2$	43.4	4.2	21.7	43.8	4.1	21.3
$Co(amp)_2(SCN)_2$	43.0	4.1	21.5	42.5	4.1	20.8
$Ni(amp)_2(SCN)_2$	43.0	4.1	21.5	42.7	4.1	21.0
$Cu(amp)_2(SCN)_2$	42.5	4.1	21.2	42.3	4.1	21.0

a - prepared in ethanol
b - prepared in water

Table 4. Microanalytical data for the *mono*-complexes $M(amp)X_2$, where $X = Cl^-, Br^-, SCN^-$.

Complex	Calculated			Found		
	%C	%H	%N	%C	%H	%N
$Ni(amp)Cl_2.H_2O$	28.2	3.9	11.0	28.0	3.9	11.0
$Ni(amp)Cl_2$	30.3	3.4	11.8	28.8	3.8	11.2
$Cu(amp)Cl_2$	29.7	3.3	11.6	29.7	3.4	11.4
$Zn(amp)Cl_2$	29.5	3.3	11.5	29.7	3.3	11.5
$Pt(amp)Cl_2$	19.3	2.2	7.5	19.5	2.2	7.6
$Cu(amp)Br_2$	21.7	2.4	8.5	22.0	2.5	8.4
$Zn(amp)Br_2$	21.6	2.4	8.4	21.8	2.5	8.4
$Pt(amp)Br_2$	15.6	1.7	6.0	15.9	1.8	6.0
$Pt(amp)(SCN)_2$	22.9	1.9	13.4	23.2	1.9	13.3

Table 5. Microanalytical data for the complexes *bis* $M(aep)_2X_2$ and *mono* $M(aep)X_2$, where $X = ClO_4^-, BF_4^-, Cl^-, Br^-, I^-$ and SCN^-.

Complex	Calculated			Found		
	%C	%H	%N	%C	%H	%N
$Cu(aep)_2(ClO_4)_2$	33.2	4.0	11.1	33.2	4.0	11.0
$Cu(aep)_2(BF_4)_2$	34.9	4.2	11.6	35.0	4.2	11.6
$Cu(aep)_2(NCS)_2$	45.3	4.8	19.9	45.5	4.6	19.7
$Cu(aep)_2Br_2$	36.0	4.3	12.0	35.5	4.3	11.7
$Cu(aep)_2I_2$	29.9	3.6	10.0	29.7	3.6	9.6
$Zn(aep)_2(ClO_4)_2$	33.0	4.0	11.0	32.7	4.0	10.7
$Cu(aep)Cl_2$	32.8	3.9	10.9	33.1	4.0	10.9
$Cu(aep)Br_2$	24.3	2.9	8.1	24.1	3.0	7.9
$Zn(aep)Cl_2$	32.5	3.9	10.8	32.8	4.0	10.6
$Zn(aep)Br_2$	24.2	2.9	8.1	24.6	3.0	7.9
$Zn(aep)I_2$	19.1	2.3	6.4	19.3	2.3	6.4

Table 6. Microanalytical data for the complexes $M(quin)_2X_2$, where X = Cl^-, Br^-, I^-, SCN^-.[a]

Complex	Calculated %C	%H	%N	Found %C	%H	%N
$Co(quin)_2Cl_2$	55.7	3.6	7.2	55.7	3.6	7.2
$Co(quin\text{-}d_7)_2Cl_2$	53.7	3.5	7.0	53.4	3.5	6.9
$Co(quin)_2Br_2$	45.3	3.0	5.9	45.0	3.0	5.8
$Co(quin\text{-}d_7)_2Br_2$	44.0	2.9	5.7	43.5	2.9	5.6
$Ni(quin)_2Br_2$	45.3	3.0	5.9	45.2	2.9	5.9
$Ni(quin\text{-}d_7)_2Br_2$	44.0	2.9	5.7	43.6	2.7	5.5
$Cu(quin)_2Cl_2$	55.0	3.6	7.1	54.8	3.6	7.0
$Cu(quin\text{-}d_7)_2Cl_2$	53.1	3.4	6.9	52.8	3.5	6.4
$Cu(quin)_2Br_2$	44.9	2.9	5.8	44.5	2.9	5.8
$Cu(quin\text{-}d_7)_2Br_2$	43.6	2.8	5.7	43.1	2.9	5.5
$Zn(quin)_2Cl_2$	54.8	3.6	7.1	54.3	3.6	7.0
$Zn(quin\text{-}d_7)_2Cl_2$	52.9	3.5	6.9	52.8	3.5	6.9
$Zn(quin)_2Br_2$	44.7	2.9	5.8	44.3	3.0	5.6
$Zn(quin\text{-}d_7)_2Br_2$	43.4	2.9	5.6	43.3	2.9	5.6
$Zn(quin)_2I_2$	37.4	2.4	4.9	37.2	2.5	4.8
$Zn(quin\text{-}d_7)_2I_2$	36.5	2.4	4.7	36.7	2.4	4.8
$Cu(quin)_2(NCS)_2$	54.8	3.2	12.8	53.9	3.2	12.6
$Cu(quin)_2(^{15}NCS)_2$	54.7	3.2	13.2	53.8	3.1	12.8
$Cu(quin\text{-}d_7)_2(NCS)_2$	53.1	3.1	12.4	52.1	3.0	12.2
$Zn(quin)_2(NCS)_2$	54.6	3.2	12.7	53.8	3.2	12.7
$Zn(quin)_2(^{15}NCS)_2$	54.4	3.2	13.1	53.9	3.1	12.8
$Zn(quin\text{-}d_7)_2(NCS)_2$	52.9	3.1	12.3	51.8	3.1	12.4

a - %*d* for the quinoline-d_7 complexes has been determined and reported as %H

Table 7. Microanalytical data for the complexes $Zn(acac)_2H_2O$, $Na[M(acac)_3]$, and $M(acac)_2B_n$, where M = Mn, Co, Ni, Cu, Zn; B = bipy, amp, en, quin; n = 1,2.

Complex	Calculated			Found		
	%C	%H	%N	%C	%H	%N
$Zn(acac)_2H_2O$	42.7	5.7	-	42.4	5.7	-
$^{68}Zn(acac)_2H_2O$	42.3	5.7	-	42.1	5.6	-
$^{64}Zn(acac)_2H_2O$	42.9	5.8	-	42.4	5.7	-
$Zn(acac\text{-}^{18}O)_2H_2O$	41.5	5.6	-	40.3	5.6	-
$Na[Co(acac)_3].H_2O$	45.4	5.8	-	45.4	5.5	-
$Na[Ni(acac)_3]$	47.5	5.6	-	46.7	5.6	-
$Na[Zn(acac)_3]$	46.7	5.5	-	46.1	5.4	-
$Co(acac)_2bipy$	58.1	5.4	6.8	58.0	5.4	6.6
$Ni(acac)_2bipy$	58.2	5.4	6.8	58.0	5.4	6.9
$Zn(acac)_2bipy$	57.2	5.3	6.7	56.6	5.1	6.8
$Co(acac)_2amp$	52.6	6.0	7.7	52.5	6.0	7.9
$Ni(acac)_2amp$	52.6	6.1	7.7	52.2	5.9	7.9
$Zn(acac)_2amp$	51.7	6.0	7.5	51.3	5.9	7.7
$Co(acac)_2en$	45.4	7.0	8.8	44.5	6.9	9.3
$Ni(acac)_2en$	45.5	7.0	8.8	45.5	7.0	8.9
$Zn(acac)_2en$	44.5	6.9	8.7	44.0	6.8	8.5
$Mn(acac)_2(quin)_2$	65.8	5.5	5.5	65.8	5.5	5.5
$Mn(acac)_2(quin\text{-}d_7)_2$	64.0	5.4	5.3	63.6	5.4	5.3
$Co(acac)_2(quin)_2$	65.2	5.5	5.4	65.0	5.4	5.5
$Co(acac)_2(quin\text{-}d_7)_2$	63.5	5.3	5.3	63.3	5.4	5.3
$Ni(acac)_2(quin)_2$	65.3	5.5	5.4	65.3	5.5	5.6
$Ni(acac)_2(quin\text{-}d_7)_2$	63.5	5.3	5.3	63.6	5.5	5.4
$Cu(acac)_2(quin)$	58.4	5.4	3.6	58.2	5.4	3.6
$Cu(acac)_2(quin\text{-}d_7)$	57.3	5.3	3.5	57.2	5.4	3.6
$Zn(acac)_2(quin)$	58.1	5.4	3.6	57.5	5.4	3.7
$Zn(acac)_2(quin\text{-}d_7)$	57.1	5.3	3.5	56.8	5.4	3.5

Table 8. Microanalytical data on the complex *trans*-$[Zn(gly)_2].H_2O$ and its isotopically-labelled analogues.

Complex	Calculated			Found		
	%C	%H	%N	%C	%H	%N
trans-$[Zn(gly)_2].H_2O$	20.8	4.4	12.1	20.8	4.4	12.1
trans-$[^{68}Zn(gly)_2].H_2O$	20.5	4.3	12.0	20.6	4.3	12.0
trans-$[^{64}Zn(gly)_2].H_2O$	20.9	4.4	12.2	21.0	4.4	12.2
trans-$[Zn(^{18}O\text{-gly})_2].H_2O$	20.1	4.2	11.7	20.1	4.2	11.9
trans-$[Zn(^{15}N\text{-gly})_2].H_2O$	20.6	4.3	12.8	20.7	4.4	12.9
trans-$[Zn(1\text{-}^{13}C\text{-gly})_2].H_2O$	22.3	4.3	12.0	21.9	4.3	12.0
trans-$[Zn(2\text{-}^{13}C\text{-gly})_2].H_2O$	22.3	4.3	12.0	22.1	4.3	12.0
trans-$[Zn(2,2\text{-}d_2\text{-gly})_2].H_2O$	20.4	4.3	11.9	20.7	4.4	11.8
trans-$[Zn(N,N\text{-}d_2\text{-gly})_2].H_2O$	20.3	4.2	11.8	20.5	4.3	11.7

Table 9. Microanalytical data on the complexes *trans*-$[Cd(gly)_2].H_2O$ and *trans*-$Cd(gly)_2$ and their isotopically-labelled analogues.

Complex	Calculated			Found		
	%C	%H	%N	%C	%H	%N
trans-$[Cd(gly)_2].H_2O$	17.3	3.6	10.1	17.4	3.7	10.1
trans-$[Cd(^{18}O\text{-gly})_2].H_2O$	16.8	3.5	9.8	17.4	3.7	10.0
trans-$[Cd(^{15}N\text{-gly})_2].H_2O$	17.1	3.6	10.7	17.3	3.6	10.6
trans-$[Cd(1\text{-}^{13}C\text{-gly})_2].H_2O$	17.8	3.6	10.0	17.4	3.7	10.2
trans-$[Cd(2\text{-}^{13}C\text{-gly})_2].H_2O$	17.8	3.6	10.0	17.2	3.6	10.1
trans-$[Cd(2,2\text{-}d_2\text{-gly})_2].H_2O$	16.8	3.5	9.8	17.4	3.7	10.0
trans-$[Cd(N,N\text{-}d_2\text{-gly})_2].H_2O$	16.8	3.5	9.8	17.2	3.6	10.0
trans-$Cd(gly)_2$	18.4	3.1	10.8	18.5	3.1	10.7
trans-$Cd(^{18}O\text{-gly})_2$	17.9	3.0	10.4	18.0	3.1	10.3
trans-$Cd(^{15}N\text{-gly})_2$	18.3	3.1	11.4	18.3	3.0	11.3
trans-$Cd(1\text{-}^{13}C\text{-gly})_2$	19.1	3.1	10.7	19.1	3.1	10.6
trans-$Cd(2\text{-}^{13}C\text{-gly})_2$	19.1	3.1	10.7	19.0	3.0	10.7

Table 10. Microanalytical data for the complexes $[Cr(gly)_3]Cl_3$ and $[Co(gly)_3]Cl_3.2H_2O$, and their isotopically-labelled analogues

Complex	Calculated			Found		
	%C	%H	%N	%C	%H	%N
$Cr(gly)_3$	26.3	4.4	15.3	26.4	4.3	15.4
$Cr(^{18}O\text{-}gly)_3$	25.2	4.2	14.7	25.3	4.3	14.9
$Cr(^{15}N\text{-}gly)_3$	26.0	4.4	16.2	26.1	4.3	16.3
$Cr(1\text{-}^{13}C\text{-}gly)_3$	27.1	4.4	15.2	27.1	4.4	15.4
$Cr(2\text{-}^{13}C\text{-}gly)_3$	27.1	4.4	15.2	27.0	4.4	15.3
$Co(gly)_3.2H_2O$	22.7	5.1	13.3	22.6	5.2	13.3
$Co(^{18}O\text{-}gly)_3.2H_2O$	21.9	4.9	12.8	21.8	4.7	12.6
$Co(^{15}N\text{-}gly)_3.2H_2O$	22.5	5.0	14.1	22.6	5.1	14.2
$Co(1\text{-}^{13}C\text{-}gly)_3.2H_2O$	23.4	5.0	13.1	23.5	5.0	13.1
$Co(2\text{-}^{13}C\text{-}gly)_3.2H_2O$	23.4	5.0	13.1	23.4	5.1	13.2

Table 11. Microanalytical data for the complexes $Pt(ur)_2Cl_2$, $Pd(ur)_2Cl_2$ and $[Cr(ur)_6]Cl_3.3H_2O$.

Complex	Calculated			Found		
	%C	%H	%N	%C	%H	%N
$Pt(ur)_2Cl_2$	6.2	2.1	14.5	6.3	2.1	14.4
$Pt(^{18}O\text{-}ur)_2Cl_2$	6.2	2.1	14.4	6.2	2.2	13.9
$Pt(^{15}N\text{-}ur)_2Cl_2$	6.2	2.1	15.4	6.1	2.2	14.4
$Pt(^{13}C\text{-}ur)_2Cl_2$	6.7	2.1	14.4	6.5	2.2	13.8
$Pd(ur)_2Cl_2$	8.1	2.7	18.9	8.2	2.8	18.7
$Pd(^{18}O\text{-}ur)_2Cl_2$	8.0	2.7	18.6	8.1	2.7	18.5
$Pd(^{15}N\text{-}ur)_2Cl_2$	8.0	2.7	19.9	8.0	2.6	19.6
$Pd(^{13}C\text{-}ur)_2Cl_2$	8.7	2.7	18.7	8.5	2.7	18.5
$Cr(ur)_6Cl_3.3H_2O$	12.6	5.3	29.3	12.9	5.1	29.8
$Cr(^{18}O\text{-}ur)_6Cl_3.3H_2O$	12.3	5.2	28.7	12.6	5.0	29.0
$Cr(^{15}N\text{-}ur)_6Cl_3.3H_2O$	12.3	5.2	30.8	12.7	5.0	31.1
$Cr(^{13}C\text{-}ur)_6Cl_3.3H_2O$	13.5	5.2	29.0	13.9	5.1	29.7

3.2 METAL(II) COMPLEXES OF 2-AMINOMETHYLPYRIDINE

3.2.1 An examination of the ir spectra of the ligand 2-aminomethylpyridine and of the perchlorates of the tris metal(II) complexes of 2,2'-bipyridine, 2-aminomethylpyridine and ethylenediamine

An initial attempt to establish which vibrations occur and are observable in the ir spectra of metal(II) complexes of 2-aminomethylpyridine was carried out by examining the spectrum of the free ligand in conjunction with a comparison of the spectra obtained for the Co(II), Ni(II) and Zn(II) *tris*(2-aminomethylpyridine) perchlorates and the analogous 2,2'-bipyridine and ethylenediamine complexes.

The ir spectrum, frequencies (4000 - 200 cm^{-1}) and band assignments for the ligand are given in Table 12 and a list of frequencies (4000 - 200 cm^{-1}) and band assignments for the *tris* complexes is given in Table 13. The regions of the spectra below 700 cm^{-1} are depicted in Fig. 1. Relatively comprehensive vibrational studies of 2,2'-bipyridine [165] and ethylenediamine [166] have reported assignments for many of the ligand modes of these two bases. Much information regarding metal-ligand vibrations in their complexes [167-169] has also been accumulated. Direct correlations with the ir spectra of 2-aminomethylpyridine and its complexes can subsequently be attempted if cogniscance of the following is taken:

(a) Bands found in the ir spectra of only the bipy and amp complexes must be associated with the aryl ring vibrations or with metal-heterocycle (M-py) vibrations.

(b) Bands found in the ir spectra of only the amp and en complexes must be associated with methylene or amine

Table 12. Ir spectrum, frequencies and assignments for the ligand 2-aminomethylpyridine

amp	assignments
3365	νN-H
3291	
3192	
3058	νC-H
3008	
2918	νC-H
2851	
1592	ν ring + NH_2 scissor
1569	
1475	Ring H-bend
1435	δNH_2
1383	
1346	
1300	
1150	δC-H + νC-N
1095	
1075	
1048	
995	δNH_2
961	δC-H + δC-C
901	
763	
730	NH_2 rock.
629	
600	i.p. δ py
475	δCCN
405	o.o.p. δpy

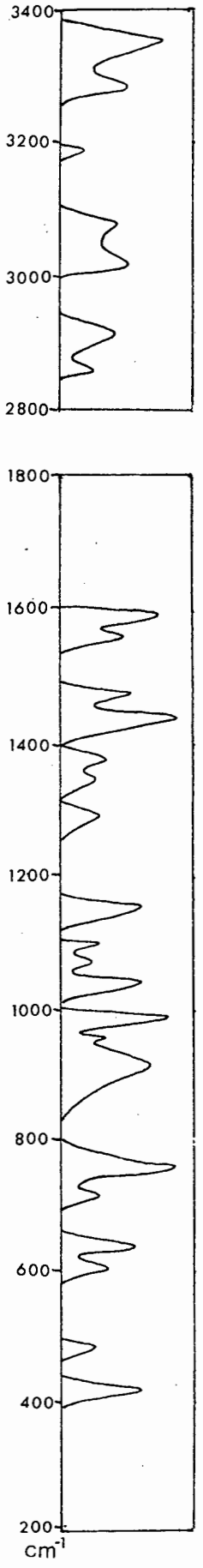

Table 13. Ir frequencies (4000 - 200 cm^{-1}) and band assignments for the complexes $[M(N\text{-}N)_3](ClO_4)_2$: M = Co(II), Ni(II), Zn(II); N-N = 2,2'-bipyridine, 2-aminomethylpyridine, ethylenediamine.

$[M(bipy)_3](ClO_4)_2$			$[M(amp)_3](ClO_4)_2$			$[M(en)_3](ClO_4)_2$			Assignments
Co	Ni	Zn	Co	Ni	Zn	Co	Ni	Zn	
			3361	3357	3365	3347	3351	3354	
			3308	3296	3304	3298	3300	3303	νN-H
			3177	3173	3171	3162	3187	3176	
2954	2951	2950	2950	2950	2950	2950	2948	2950	
2923	2924	2922	2920	2922	2922	2923	2920	2923	νC-H
2858	2851	2852	2865	2854	2852	2855	2851	2854	
1602	1601	1600	1609	1609	1608				νC⎓C + νC⎓N
1573	1571	1575	1595	1588	1593	1580	1579	1578	ν ring + NH_2
1563	1562	1562	1568	1569	1570				scissor
1494	1496	1494	1484	1482	1483				
1473	1473	1474							ring H-bend
1443	1441	1439	1443	1447	1445	1468	1469	1468	
			1437	1436	1438	1401	1401	1399	
			1389	1389	1388	1371	1370	1374	NH_2 wag
			1331	1331	1332	1327	1328	1328	
1315	1315	1316							ν inter-ring
			1286	1287	1287	1282	1281	1278	NH_2 twist
1245	1245	1248	1251	1251	1251				
1218	1218	1219	1226	1226	1224				
1172	1170	1170							ring H-bend
1158	1156	1157	1158	1160	1159				
∿1086	∿1082	∿1083	∿1100	∿1100	∿1100	∿1081	∿1081	∿1081	νClO_4^-
1018	1020	1016	1018	1017	1015	1011	1010	1025	
963	960	962	969	968	969	967	970	960	
928	928	927	935	935	935				
			925	926	924	930	930	927	
890	889	890	887	886	887	874	878	871	
811	813	812	815	817	815	776	770	780	δC-H + δC-C
764	765	765	763	762	762				
735	735	735	733	734	734	724	721	720	
652	651	650	660	676	658				NH_2 rock
632	635	633	644	644	641	641	649	640	δClO_4^-
620	620	620	625	620	623				ip δpy
			582	590	580	620	621	620	NH_2 rock
433	441	428	478	480	480	494	504	491	skeletal δCCN
			438	445	435	470	479	465	$\nu M\text{-}NH_2$
413	414	413	418	421	416				oop δpy
			373	381	365	408	409	406	$\nu M\text{-}NH_2$
						287	302	282	$\delta NH_2\text{-}M\text{-}NH_2$
264	294	234	258	274	240				
232	270		236	237	217				νM-py

Fig. 1. The ir spectra (700 - 200 cm^{-1}) of the complexes $[M(N\text{-}N)_3](ClO_4)_2$

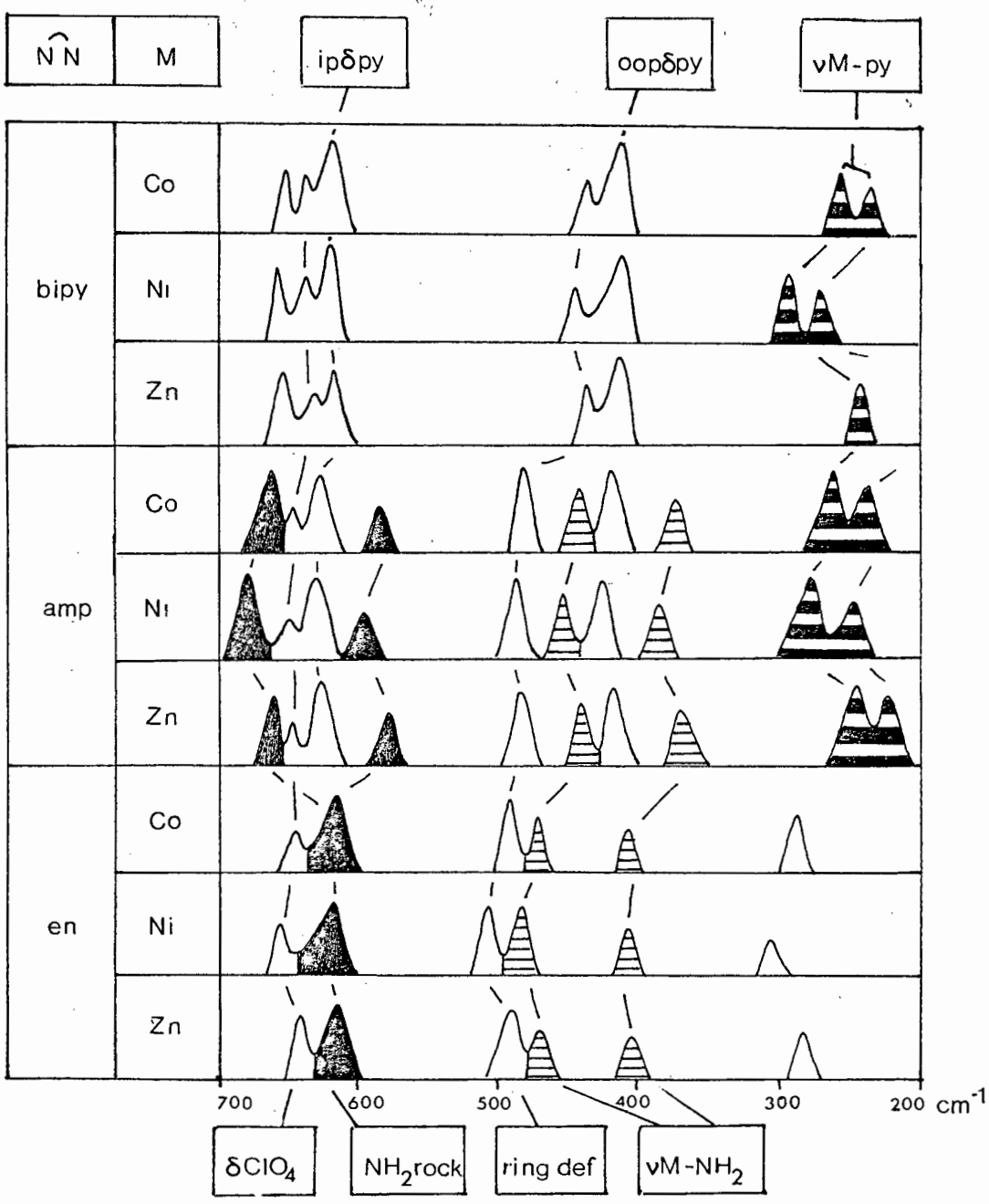

vibrations (including the vibration of the C-N bond linking these two groups), or with metal-amine ($M-NH_2$) vibrations. However it is appreciated that the greater asymmetry of 2-aminomethylpyridine as compared with that of 2,2'-bipyridine and ethylenediamine may complicate such an approach.

The 4000 - 700 cm^{-1} region of the spectra

Bands associated with the C-H group are expected and observed in all the spectra investigated. Stretching vibrations are discernable near 2900 cm^{-1}, while the various bending modes may be identified throughout the region 1500 - 700 cm^{-1}, and assigned accordingly [165-166]. Expected [18] in the spectra of all the complexes but not in the spectrum of the uncoordinated 2-aminomethylpyridine is an absorption associated with the perchlorate anion ClO_4^-. Such a band is observed as a broad and intense peak centred near 1080 cm^{-1} and spanning $\sim$150 cm^{-1}. A number of ligand modes are partially or totally obscured by this band, and hence their assignment is somewhat tentative at this stage. Remaining bands are systematically absent from the spectra of all the complexes of at least one ligand type which facilitates their assignment in accordance with the previously published [165,166] data. Finally a comparison of the spectra of free and coordinated 2-aminomethylpyridine indicates that not only do many of the vibrations become ir active only on complexation but also bands in the free ligand spectrum are shifted to higher wavenumber in the coordinated species.

The 700 - 200 cm^{-1} region of the spectra

This spectral region is of primary interest as the metal ligand modes are expected here.

The uncoordinated 2-aminomethylpyridine exhibits only four bands below 700 cm^{-1}: at 629, 600, 475 and 405 cm^{-1}. By analogy with 2,2'-bipyridine [165] and pyridine [88], the bands at 600 and 405 cm^{-1} are in-plane and out-of-plane aryl ring deformation modes, respectively. The band at 475 cm^{-1} is possibly a ligand skeletal mode (CCN bend) in accordance with related studies of ethylenediamine [167]. The remaining absorption at 629 cm^{-1} is assigned as an NH_2 rocking mode expected in that region. These assignments are confirmed by the examination of the spectra of the *tris*-(2,2'-bipyridine), -(2-aminomethylpyridine) and -(ethylenediamine) chelates. Additional bands found only in the spectra of the 2-aminomethylpyridine and ethylenediamine complexes, are presumably associated with M-NH_2 vibrations and further NH_2 rocking modes, while bands attributable to M-py vibrations are observed only in the spectra of the 2,2'-bipyridine and 2-aminomethylpyridine chelates. A final remaining band near 640 cm^{-1} in the spectra of all the chelates is assigned to an expected [18] ClO_4^- bending mode.

Possibly one of the most interesting points established at this stage is that, of the two types of metal-nitrogen vibrations, the metal-amino modes occur at a higher frequency than the metal-pyridine nitrogen modes. This is in agreement with previously published [84,95] related works.

All of the above assignments in the *tris*(2-aminomethylpyridine)complexes are now confirmed.

3.2.2 Band assignments in the ir spectra (4000 - 150 cm^{-1}) of the complexes $[M(amp)_3]X_2$; M = Mn(II), Fe(II), Co(II), Ni(II), Zn(II); X = ClO_4^-, BF_4^-.

The ir spectra (700 - 150 cm^{-1}) of all the *tris* complexes investigated are depicted in Fig. 2. A list of frequencies (4000 - 150 cm^{-1}), shifts induced by deuteration of the amino group in $[Ni(amp)_3](ClO_4)_2$ and $[Zn(amp)_3](BF_4)_2$, and assignments is given in Table 14.

In the region 4000 - 700 cm^{-1}, ligand modes are observed at remarkably similar frequencies in all of the complexes. Assignments (presented in Section 3.2.1) of certain of these bands to NH_2 vibrations are confirmed by the isotopic shift data obtained in the deuteration studies. No further discussion of this region is given since it is only below 700 cm^{-1} that the metal-ligand modes and subsequent structural information are expected to arise.

The spectra of the perchlorate complexes (700 - 150 cm^{-1})

The band-for-band correspondence in the spectra strongly suggests that they are isostructural. It is therefore proposed that they all have a structure similar to that suggested [72] for the Ni(II) complex in which each amino donor group is *cis* to each of the other two, in a pseudo-octahedral configuration. All bands in the spectra, with the exception of the pyridine in-plane ring deformation mode near 620 cm^{-1} and the ligand skeletal mode near 470 cm^{-1}, exhibit a metal ion dependence which is in the sequence of the cfse's calculated on the assumption that all the complexes have high-spin configurations; *i.e.* Mn < Co < Ni > Zn. The assignment of

Table 14. Ir frequencies (4000 - 150 cm^{-1}) and assignments for the complexes $[M(amp)_3]X_2$: M = Mn(II), Fe(II), Co(II), Ni(II), Zn(II); X = ClO_4^-, BF_4^-

X	ClO_4^-					BF_4^-			Assignments
M	Mn	Fe	Co	Ni	Zn	Co	Ni	Zn	
	3361	3356	3361	3357(849)[a]	3365	3374	3375	3387(864)	
	3304	3297	3308	3296(843)	3304	3323	3325	3323(844)	νN-H
	3170	3176	3177	3173(743)	3171	3191	3198	3193(749)	
	3072	3072	3075	3072	3073	3079	3081	3081	
	2954	2956	2958	2958	2959	2957	2963	2962	
	2927	2929	2932	2932	2932	2929	2932	2938	νC-H
	2860	2860	2860	2857	2860	2860	2862	2861	
	1607	1607	1609	1609	1608	1610	1611	1609	
	1589	1590	1595	1588(158)	1593	1600	1604	1596(143)	NH_2 scissor
	1568	1568	1568	1569	1570	1569	1570	1573	
	1484	1481	1484	1482	1483	1487	1485	1486	
	1444	1444	1443	1447(60)	1445	1447	1448	1445(51)	
	1439	1439	1437	1436(56)	1438	1435	1440	1442(56)	
	1388	1387	1389	1389(110)	1388	1381	1389	1389(108)	δNH_2
	1329	1328	1331	1331(142)	1332	1331	1331	1333(137)	
	1283	1283	1286	1287	1287	1287	1288	1287	
	1250	1250	1251	1251	1251	1249	1251	1253	
	1225	1227	1226	1226	1224	1224	1226	1226	
	1157	1157	1158	1160	1159	1160	1151	1157	
	~1100	~1100	~1100	~1100	~1100	1097	1090	1089	
						1062	1065	1060	
						1030	1034	1030	
	1014	1015	1018	1017(14)	1015	1018	1021	1017(19)	δNH_2
	968	968	969	968	969	969	968	970	
	933	934	935	935	935				
	922	924	925	926(34)	924	924	926	924(37)	
	886	886	887	886(84)	887	887	887	887(88)	δNH_2
	812	814	815	817(33)	815	817	818	815(29)	
	763	763	763	762	762	767	767	765	
	733	733	733	734	734	732	732	733	
	637	650	660	676(45)	658	661	676	657(44)	NH_2 rock
			644	644	641				δClO_4^-
	625	625	625	620	623	644	645	641	ip δpy
	563	571	582	590(61)	580	579	590	579(22)	NH_2 rock
						558	585	547(12)	
						522	522	522	δBF_4^-
	478	478	478	480	480	477	479	478	skeletal δCCN
	426	434	438	445(25)	435	439	447	436(29)	$\nu M\text{-}NH_2$
	412	415	418	421	416	417	422	415	oop δpy + νM-py
	359	363	373	381(22)	365	372	382	374(14)	$\nu M\text{-}NH_2$
						352	355	353(6)	
	249	260	258	274	240	258	278	245	νM-py
	216	226	236	237	217	224	227	222	
	188	191	199	201(14)	179	184	212	183(5)	δL-M-L
	174	177	186	158	155		197		

a - Figures in parentheses indicate negative shift experienced on deuteration of the amino group

Fig. 2. The ir spectra (700 - 150 cm^{-1}) of the complexes $[M(amp)_3]X_2$

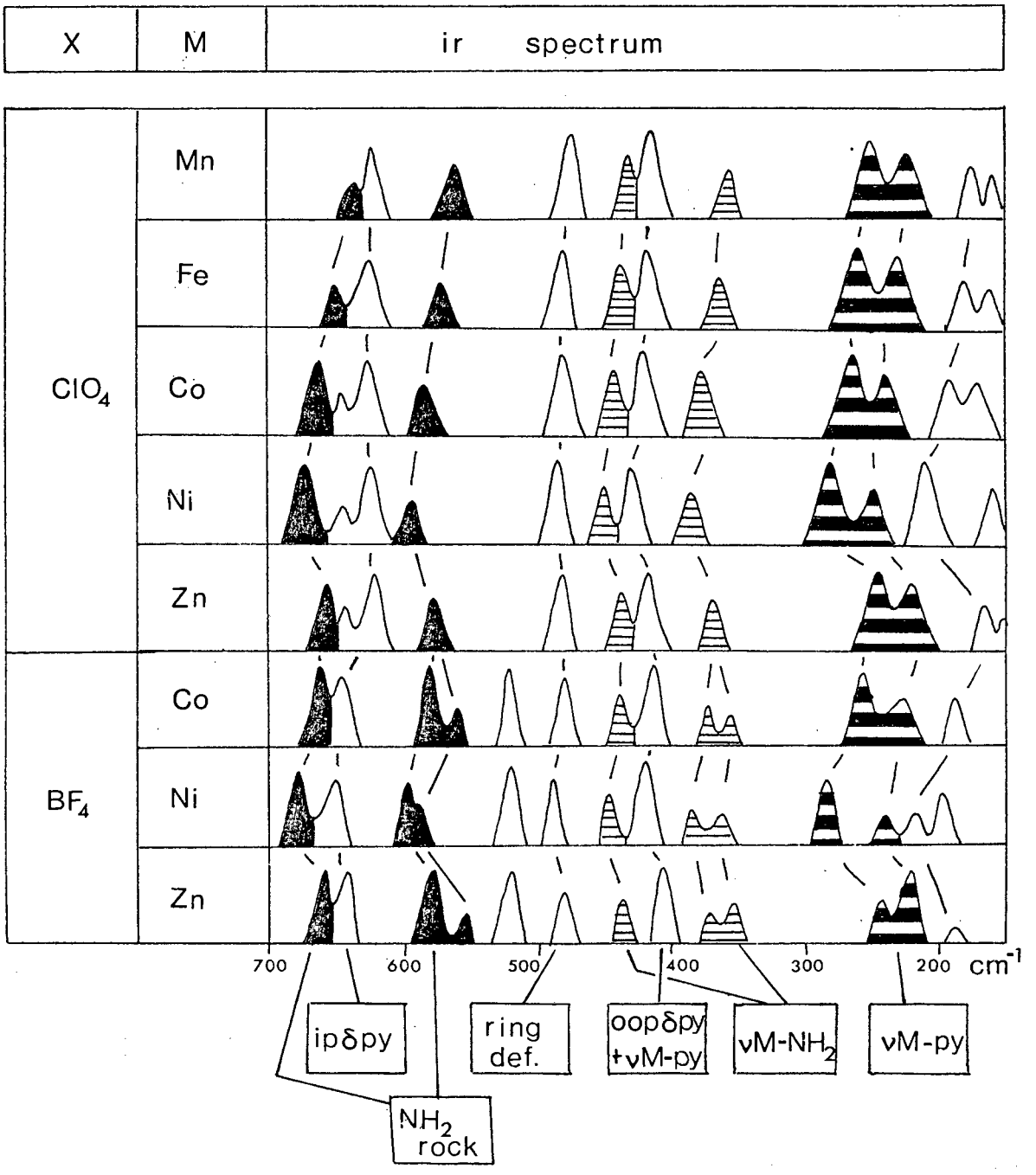

the absorptions near 650 and 590 cm^{-1} to NH_2 rocking modes is confirmed by the fact that they exhibit the extreme metal-ion dependence previously observed [32] for these vibrations in related complexes.

Further confirmation of these assignments is provided by the fact that deuteration of the amino group in the $[Ni(amp)_3](ClO_4)_2$ complex shifts these bands by -45 and -61 cm^{-1} respectively. It may be noted that in the spectra of the Mn(II) and Fe(II) complexes, the expected [18] δClO_4^- mode is obscured by the NH_2 rocking modes at 637 and 650 cm^{-1} respectively; only as the amino vibrations move to higher wavenumber with change in metal ion is the δClO_4^- band revealed. The assignment of bands at *ca.* 435 and 370 cm^{-1} to metal-amino nitrogen stretches ($\nu M\text{-}NH_2$) is confirmed by their metal-sensitivity and shifts experienced on deuterium exchange in the Ni(II) complex, while the insensitivity to deuteration of the first two bands below 300 cm^{-1} substantiates their assignment to $\nu M\text{-}py$ modes. The absorption near 400 cm^{-1}, which has been assigned as the out-of-plane aryl ring deformation mode in the ligand spectrum not only moves to slightly higher frequency in the spectra of the complexes, but has a small metal-sensitivity in the order expected from the calculated cfse values.
Previous suggestions [95] are therefore followed; the band is considered to arise from the out-of-plane aryl ring deformation mode coupled to the metal-pyridine-nitrogen stretch, $\nu M\text{-}py$. The low frequency band at *ca.* 200 cm^{-1} undergoes a shift of -14 cm^{-1} on amino deuteration of $[Ni(amp)_3](ClO_4)_2$. This fact together with its small metal-ion sensitivity allows the assignment of this band to a $\delta NH_2\text{-}M\text{-}NH_2$, which

is supported by the fact that it occurs at about half the frequency of the M-NH_2 stretches.

It is noteworthy that the observation of four metal ligand stretches is consistent with the group theoretical expectations for the C_{3v} point symmetry of the coordination around the central metal ion.

The spectra of the tetrafluoroborate complexes (700 - 150 cm^{-1})

The spectra of the complexes $[M(amp)_3](BF_4)_2$; M = Co(II), Ni(II) and Zn(II), show sufficient differences from their perchlorate analogues to warrant their separate discussion.

A new band, insensitive to both metal-ion and -*N,N*-d_2-substitutions, is found at 522 cm^{-1} and is most likely an expected [18] δBF_4 mode, occurring at *ca.* 100 cm^{-1} lower than the analogous δClO_4. By comparison with the ligand modes reported and assigned earlier, the band at *ca.* 640 cm^{-1} is the in-plane aryl ring deformation, while that at *ca.* 480 cm^{-1} is a δCCN skeletal ring deformation.

All other bands in this region of the spectra are shifted by metal-ion substitution in the order of the calculated cfse's, *i.e.* Co < Ni > Zn. The three bands at *ca.* 660, 580 and 550 cm^{-1} show additional sensitivity to deuteration of the amino group in $[Zn(amp)_3](BF_4)_2$; they are therefore most logically assigned as NH_2 rocking modes. Three lower frequency bands at *ca.* 440, 370 and 350 cm^{-1} also undergo shifts on N,N-d_2-substitution and are therefore νM-NH_2 vibrations, while bands at *ca.* 250 and 225 cm^{-1} may be assigned to νM-py, owing to their N,N-d_2 insensitivity. The small shift on metal-ion substitution of the out-of-plane aryl ring deformation mode

near 420 cm^{-1} indicates that it is coupled to these νM-py vibrations. The remaining low frequency bands near 200 cm^{-1} may probably be assigned to δNH_2-M-NH_2 or δNH_2-M-py vibrations.

While assignment of bands in the ir spectra of the complexes $[M(amp)_3](BF_4)_2$ is therefore relatively straightforward, the variation in the number of metal-ligand vibrations observed in these complexes as compared with their perchlorate analogues, precludes the derivation of any structural information, *i.e.* whether the *all cis (facial)* arrangement of the ligands is maintained in the tetrafluroborates or whether a *cis-trans (meridional)* configuration obtains. For this reason, an x-ray crystallographic determination of the complex $[Ni(amp)_3](BF_4)_2$ was carried out.

3.2.3 *The crystal and molecular structure of the complex tris(2-aminomethylpyridine) nickel(II) tetrafluoroborate* $[Ni(amp)_3](BF_4)_2$

Results

Crystal data and experimental details of the data collection are listed in Table 15. The crystals, which were found to be cubic, exhibited only one series of systematic absences, *viz.*

hkl for *l* odd (and cyclicly)

Hence two space groups are possible: $P\bar{4}3n$ (No. 218) or $Pm3n$ (No. 223). The density was measured in an ethanol/ethylene bromide flotation mixture as 1.56 Mg m^{-3}. Using the accurately determined values of the cell parameters $a = b = c$ =1685.9 pm in the expression:

$$ZM = N D_m V$$

where M is the relative molar mass, N is the Avogadro Constant, D_m is the measured density and V is the volume of the unit cell,

Table 15. Crystal data, experimental and refinement parameters for $[Ni(amp)_3](BF_4)_2$

Molecular formula	$[Ni(C_6H_8N_2)_3](BF_4)_2$
M_r	556.75
Space group	$P\bar{4}3n$
a	1685.9(8) pm
Dm	1.56 Mg m^{-3}
Dc	1.54 Mg m^{-3} for $Z = 8$
μ(MoKα)	0.83 mm^{-1}
$F(000)$	2256
Crystal dimensions	0.38 x 0.30 x 0.40 mm
Scan mode	ω-2θ
Scan width	$1.2^{o}\theta$
Scan speed	$0.03^{o}\theta$ s^{-1}
Range scanned (2θ)	$6\text{-}46^{o}$
Stability of standard reflections	1.6 %
Number of reflections collected	728
Number of observed reflections	457 with I(rel)>2σI(rel)
Number of Variables	54
$R = \Sigma\|\|F_o\| - \|F_c\|\|/\Sigma\|F_o\|$	0.093
$R_w = \Sigma w^{\frac{1}{2}}\|\|F_o\| - \|F_c\|\|/\Sigma w^{\frac{1}{2}}\|F_o\|$	0.103
Weighting Scheme w	$(\sigma^2F + 2x10^{-3}F^2)^{-1}$

the number of molecules / unit cell (Z) = 8 (±1%). Examination of the space group tables [170] shows that this requires the Ni(II) ions to be at the (e) positions and that the ligand "groups" have 32 symmetry in $Pm3n$ or 3 symmetry in $P\bar{4}3n$. Either possibility requires an *all cis facial* arrangement of the ligands. The Ni(II) ion was located in a Patterson map. Subsequent weighted difference syntheses yielded the positions of the remaining non-hydrogen atoms of the coordinated species, all of them sitting at the 24 general positions (i). Considerable difficulty was encountered in determining the positions of the BF_4^- anions. However, the 16 B atoms were finally found to occupy the following Wyckoff positions: 2 at a, with which are associated 8 F atoms at the e positions; 8 at e having 24 F atoms at the general position i; and the remaining 6 B atoms were located at the b positions. The fluorine atoms corresponding to these 6 borons showed up in an electron density map (see Figure 3) as smeared peaks, indicating that the tetrafluoroborate anions are not ordered. The multiplicity of the peaks required that statistical disorder be invoked, with 12 of the remaining F atoms placed at h and the final 12 at a general position i but with a site occupancy factor of 0.5

In the final refinement, Ni was treated anisotropically, the other atoms isotropically and hydrogens were not included in the model. The B-F bond lengths were fixed to 140(1) pm. Fractional atomic coordinates and thermal parameters are listed in Table 16. A final listing of Miller indices, observed and calculated structure factors, the real and imaginary parts of the structure factors (A and B), the phase angle

Fig. 3. Electron density map through the section x = 0.5 in the vicinity of the B2 atom, with contours drawn at values of 0.5 e / $\mathring{A}^3$

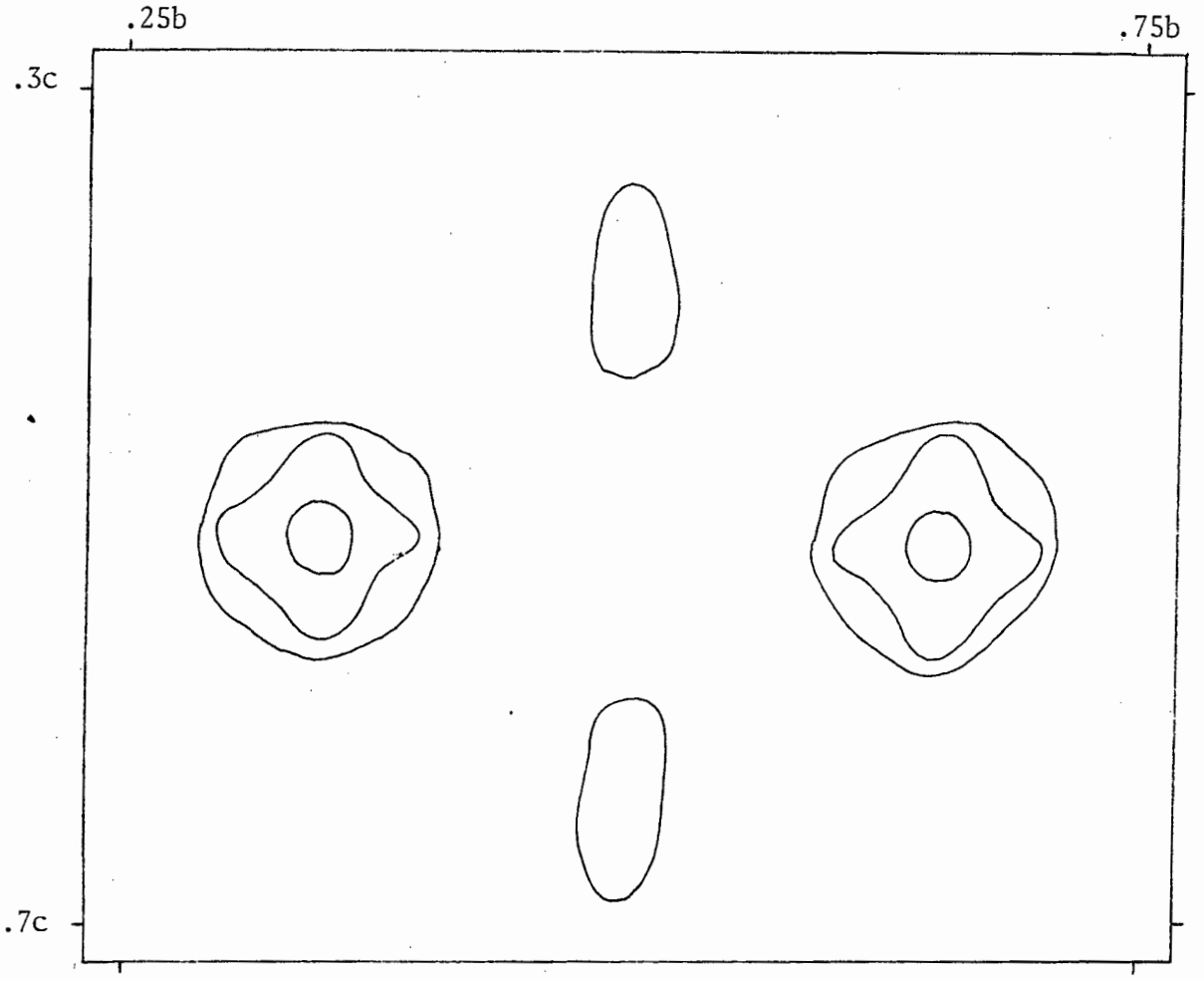

Table 16. Fractional atomic coordinates ($x10^3$) and thermal parameters (pm^2x10^{-1}) $[Ni(amp)_3](BF_4)_2$

Atom	x	y	z	U_{11}	U_{22}	U_{33}	U_{23}	U_{13}	U_{12}
Ni	341(0)	341(0)	341(0)	36(1)	36(1)	36(1)	-3(1)	-3(1)	-3(1)
N1	296(1)	433(1)	416(1)	60(4)					
N2	256(1)	392(1)	269(1)	40(3)					
C1	210(1)	450(1)	299(1)	49(4)					
C2	161(1)	498(1)	255(1)	67(5)					
C3	159(2)	489(1)	178(1)	71(6)					
C4	202(1)	420(1)	139(2)	78(7)					
C5	249(1)	379(1)	184(1)	61(5)					
C6	220(1)	461(1)	386(1)	57(5)					
B1	151(1)	151(1)	151(1)	34(6)					
B2	0.0(0)	500(0)	500(0)	85(15)					
B3	0.0(0)	0.0(0)	0.0(0)	46(16)					
F1	199(1)	199(1)	199(1)	118(9)					
F11	191(1)	79(1)	141(1)	97(5)					
F2	0.0(0)	500(0)	417(1)	252(16)					
F22	57(2)	438(2)	499(3)	145(12)					
F3	47(0)	47(0)	47(0)	197(17)					

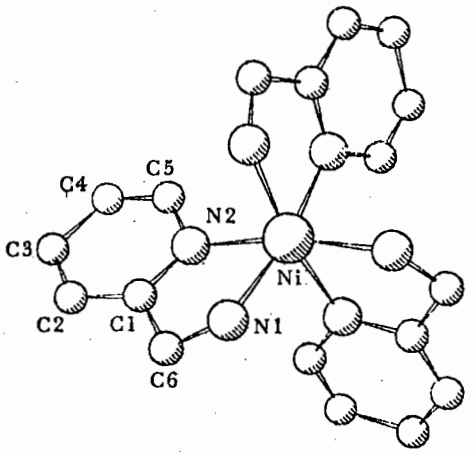

Fig. 4. Cation viewed down 3-fold axis

in degrees, the difference $F_o - F_c$, and the weighting for each reflection is given in Table 18.

Discussion

As mentioned earlier, the space group symmetry requires the orientation of the ligands about the Ni(II) ion to be *all cis* in a *facial* configuration (Fig. 4) similar to the perchlorate analogue [72]. The greater complexity of the ir spectrum of $[Ni(amp)_3](BF_4)_2$ is therefore attributed to additional distortions within the ligands or the disorder in the BF_4 anions. Bond lengths and angles are given in Table 17. The variations in some C⋯C bond lengths are attributed to the poor data resulting from disorder of the anions, and are not regarded as significant. Published data for the related *tris* perchlorate complex is incomplete and hence could give no direct comparison of molecular parameters. However the bond lengths and angles obtained in this work for the complexed 2-aminomethylpyridine are similar to those reported [73] for *mono*(2-aminomethylpyridine) copper(II) bromide.

Table 17. Interatomic distances (pm) and bond angles (deg.) in $[Ni(amp)_3](BF_4)_2$

Ni - N1	213	N1 - Ni - N2	78
Ni - N2	207	Ni - N2 - C1	118
N2 - C1	136	N2 - C1 - C2	124
C1 - C2	137	C1 - C2 - C3	119
C2 - C3	131	C2 - C3 - C4	119
C3 - C4	152	C3 - C4 - C5	116
C4 - C5	129	C4 - C5 - N2	123
C5 - N2	144	C5 - N2 - C1	115
C1 - C6	148	Ni - N1 - C6	110
C6 - N1	145	N1 - C6 - C1	114
B1 - F1	140	C6 - C1 - N2	113
B1 - F11	139	F1 - B1 - F11	107
B2 - F2	140	F2 - B2 - F22	89
B2 - F22	142	N1 - Ni - $N1^{(i)}$	93
B3 - F3	140	N2 - Ni - $N2^{(i)}$	97

(i) = z, x, y

Average σ = 2 pm

Average $\sigma = 2^{o}$

Table 18. Individual reflection data for the crystal $[Ni(amp)_3](BF_4)_2$

H	K	L	FO	FC	A	B	PHI	DEL(F)	SIG*(F)
0	2	2	129.01	122.53	122.52	1.63	.76	6.48	2.99
2	2	2	263.29	261.68	251.19	73.34	16.28	1.62	6.10
0	1	3	186.41	191.29	-191.23	-4.77	181.43	-4.87	4.32
0	2	3	93.64	75.67	75.67	.01	.01	17.96	2.18
1	2	3	77.83	81.62	.40	-81.62	270.28	-3.79	1.81
0	3	3	398.12	375.38	375.28	8.45	1.29	22.74	9.22
2	3	3	112.77	108.46	-108.29	-6.01	183.18	4.30	2.62
0	0	4	6.52	11.47	10.02	-5.58	330.90	-4.95	.61
0	1	4	60.41	61.74	61.74	.03	.02	-1.33	1.41
1	1	4	131.03	113.94	-22.26	111.75	101.27	17.09	3.04
0	2	4	174.66	158.08	158.07	2.42	.88	16.57	4.05
1	2	4	78.27	72.15	45.80	55.75	50.60	6.12	1.82
2	2	4	119.69	107.95	78.33	-74.28	316.52	11.74	2.79
0	3	4	82.61	56.50	-56.50	-.03	180.03	26.11	1.92
1	3	4	103.39	112.30	111.47	-13.68	353.00	-8.91	2.39
2	3	4	82.88	83.01	82.35	10.46	7.24	-.14	1.93
3	3	4	165.24	147.63	-140.34	-45.83	198.08	17.61	3.84
0	4	4	20.98	30.23	30.02	3.56	6.76	-9.24	.56
2	4	4	57.04	51.37	25.91	44.36	59.71	5.67	1.34
4	4	4	241.54	234.75	-158.20	-173.43	227.63	6.79	5.60
0	1	5	11.33	15.20	-15.15	1.23	175.37	-3.87	.51
0	2	5	67.17	76.63	-76.63	-.06	180.04	-9.46	1.56
1	2	5	77.29	68.12	50.33	-45.90	317.64	9.17	1.80
0	3	5	64.42	74.32	-74.29	-2.21	181.71	-9.90	1.50
1	3	5	113.51	112.53	-28.20	108.94	104.51	.98	2.63
2	3	5	54.21	48.75	38.92	-29.36	322.97	5.46	1.28
0	4	5	14.14	17.69	-17.69	-.05	180.16	-3.55	.55
1	4	5	147.86	129.15	-20.13	127.57	98.97	18.71	3.42
2	4	5	38.71	45.21	-41.54	17.84	156.75	-6.49	.92
3	4	5	51.02	55.65	21.49	-51.33	292.72	-4.63	1.21
0	5	5	64.53	63.67	-63.67	.43	179.61	.87	1.50
2	5	5	223.21	180.16	-57.98	170.58	108.77	43.05	5.18
4	5	5	175.30	169.84	34.36	-166.33	281.67	5.46	4.06
0	0	6	142.38	146.90	146.70	7.76	3.03	-4.53	3.30
0	1	6	31.96	25.82	25.82	.02	.04	6.14	.78
1	1	6	47.28	59.77	32.75	-49.99	303.23	-12.48	1.11
1	2	6	34.12	33.88	25.26	22.58	41.80	.24	.83
2	2	6	52.96	51.76	13.82	-49.89	285.48	1.19	1.25
0	3	6	38.52	40.90	40.90	.03	.05	-2.38	.92
1	3	6	78.41	75.13	-67.52	32.95	153.99	3.29	1.83
2	3	6	64.27	64.18	-15.13	62.37	103.64	.09	1.50
3	3	6	198.78	201.95	177.68	-95.98	331.62	-3.17	4.61
0	4	6	120.46	102.45	-102.32	-4.98	182.79	18.02	2.80
1	4	6	39.78	34.25	-32.90	-9.53	196.16	5.52	.95
2	4	6	55.80	48.48	3.41	48.36	85.97	7.32	1.31
3	4	6	51.78	53.11	30.36	43.57	55.13	-1.33	1.23
4	4	6	93.94	112.37	101.10	-49.04	334.12	-18.42	2.19
0	5	6	11.11	4.62	4.62	-.01	359.93	6.49	.71
1	5	6	13.97	9.76	-1.34	9.67	97.90	4.21	.60
2	5	6	8.65	8.09	-7.04	3.99	150.45	.55	.83
3	5	6	54.05	44.97	-29.93	33.57	131.72	9.08	1.28
4	5	6	47.27	42.79	42.71	2.66	3.56	4.48	1.13
5	5	6	68.21	66.96	63.43	-21.44	341.33	1.25	1.60
0	6	6	152.21	173.12	172.99	6.76	2.24	-20.92	3.54
2	6	6	125.16	96.82	-90.35	-34.79	201.06	28.34	2.91
4	6	6	49.38	45.55	-39.08	23.41	149.08	3.83	1.18
6	6	6	72.32	76.58	70.68	-29.47	337.37	-4.26	1.69
0	1	7	7.42	16.45	-16.14	3.17	168.90	-9.03	.83

Table 18 continued/

H	K	L	FO	FC	A	B	PHI	DEL(F)	SIG*(F)
0	2	7	56.15	51.32	51.32	.06	.07	4.83	1.32
1	2	7	63.06	40.49	19.82	35.31	60.70	22.57	1.47
0	3	7	100.74	96.82	-96.65	-5.79	183.43	3.92	2.35
1	3	7	25.57	26.42	26.42	.32	.68	-.85	.69
2	3	7	15.97	9.89	-9.89	-.18	181.03	6.07	.57
1	4	7	64.04	69.97	-44.76	-53.79	230.24	-5.94	1.51
2	4	7	15.60	14.37	5.13	13.42	69.09	1.23	.62
3	4	7	61.30	70.30	70.26	-2.21	358.20	-9.00	1.43
0	5	7	11.31	20.18	20.12	1.57	4.45	-8.87	.71
1	5	7	51.56	50.71	-9.02	49.90	100.25	.84	1.22
2	5	7	91.17	87.65	18.89	-85.59	282.44	3.52	2.12
4	5	7	65.54	55.85	-16.85	53.24	107.56	9.69	1.55
0	6	7	83.41	91.44	-91.44	-.12	180.08	-8.02	1.96
1	6	7	95.37	101.59	95.96	-33.36	340.83	-6.22	2.22
2	6	7	24.48	20.17	4.85	19.58	76.10	4.31	.71
3	6	7	95.87	93.82	-93.74	3.84	177.66	2.04	2.23
4	6	7	12.19	11.69	-6.39	-9.79	236.86	.50	.72
5	6	7	12.68	13.81	-3.27	13.41	103.69	-1.12	.72
0	7	7	69.64	74.95	74.84	4.01	3.07	-5.31	1.64
2	7	7	60.17	49.28	-38.23	31.10	140.87	10.89	1.43
4	7	7	52.99	52.44	-44.82	-27.23	211.28	.55	1.25
6	7	7	53.51	56.16	55.98	-4.44	355.47	-2.64	1.29
0	0	8	75.03	55.66	-55.65	-1.03	181.06	19.37	1.75
1	1	8	109.65	96.53	-62.23	73.80	130.14	13.12	2.55
0	2	8	36.63	28.44	-28.44	.31	179.39	8.19	.91
1	2	8	43.61	53.80	30.03	44.65	56.08	-10.19	1.05
2	2	8	109.72	89.99	.62	89.99	89.60	19.72	2.55
0	3	8	10.03	10.46	10.46	.03	.17	-.43	.84
1	3	8	16.18	21.25	21.25	.10	.28	-5.07	.63
2	3	8	38.33	28.45	25.98	11.60	24.07	9.88	.94
3	3	8	42.95	40.25	-24.23	32.14	127.00	2.70	1.04
0	4	8	36.26	39.05	39.04	.69	1.02	-2.78	.90
1	4	8	14.22	9.49	6.04	7.32	50.50	4.72	.67
2	4	8	108.76	94.09	6.93	-93.83	274.23	14.67	2.53
3	4	8	29.15	33.68	25.61	-21.87	319.51	-4.53	.75
4	4	8	62.86	64.50	-23.98	59.88	111.82	-1.64	1.49
0	5	8	44.46	40.39	-40.39	-.05	180.07	4.07	1.07
1	5	8	155.40	143.21	9.50	-142.89	273.80	12.19	3.61
2	5	8	32.76	35.34	33.54	-11.13	341.64	-2.58	.83
5	5	8	74.58	69.41	-1.33	69.40	91.10	5.17	1.74
0	6	8	28.50	16.17	-16.15	-.80	182.83	12.33	.78
1	6	8	34.00	23.56	-12.46	20.00	121.92	10.44	.85
2	6	8	31.07	35.13	23.79	-25.85	312.62	-4.06	.79
4	6	8	9.91	2.86	-2.82	-.43	188.56	7.06	.91
5	6	8	11.58	13.04	8.64	-9.77	311.46	-1.46	.78
6	6	8	13.02	14.57	5.02	13.68	69.86	-1.55	.79
0	7	8	30.66	34.76	34.76	.03	.05	-4.10	.82
1	7	8	85.28	86.78	15.38	85.41	79.79	-1.50	2.00
2	7	8	33.11	27.28	-16.42	21.78	127.01	5.83	.87
3	7	8	25.91	18.57	15.73	-9.87	327.89	7.34	.73
4	7	8	15.31	12.80	12.06	-4.27	340.49	2.51	.75
5	7	8	63.98	63.80	-1.64	-63.78	268.53	.17	1.51
6	7	8	10.89	10.08	7.24	-7.01	315.93	.81	.92
7	7	8	20.31	18.55	-10.97	14.97	126.23	1.76	.69
0	8	8	38.83	45.78	45.78	-.04	359.95	-6.95	.98
2	8	8	124.37	115.91	-19.01	114.34	99.44	8.46	2.89
4	8	8	90.63	88.94	12.03	-88.12	277.78	1.69	2.11
6	8	8	25.85	28.58	20.08	-20.34	314.62	-2.73	.78

Table 18 continued/

H	K	L	FO	FC	A	B	PHI	DEL(F)	SIG*(F)
8	8	8	48.74	49.15	-6.68	48.69	97.82	-.40	1.19
0	1	9	67.17	81.35	-81.27	-3.57	182.52	-14.18	1.58
0	2	9	62.94	58.18	-58.18	-.05	180.05	4.77	1.49
1	2	9	55.60	55.51	-3.59	55.39	93.71	.09	1.31
0	3	9	172.55	173.16	173.04	6.35	2.10	-.61	4.00
2	3	9	48.41	53.95	-46.91	-26.65	209.60	-5.55	1.15
0	4	9	21.80	15.95	15.95	.00	.00	5.85	.71
1	4	9	86.91	83.81	58.58	-59.93	314.35	3.11	2.03
2	4	9	54.47	54.25	-31.95	-43.84	233.92	.22	1.29
3	4	9	44.25	51.20	-50.09	10.62	168.03	-6.95	1.07
0	5	9	39.59	35.00	-34.96	-1.61	182.63	4.59	.97
1	5	9	24.64	24.95	-2.41	-24.83	264.46	-.31	.71
2	5	9	55.20	51.82	-16.16	-49.24	251.83	3.38	1.32
3	5	9	29.23	28.54	-3.23	-28.36	263.51	.70	.80
4	5	9	44.44	42.38	3.80	42.21	84.86	2.06	1.07
1	6	9	71.91	78.70	-62.57	-47.74	217.34	-6.79	1.68
2	6	9	31.83	30.84	-22.49	21.09	136.84	.99	.84
3	6	9	104.48	112.78	112.55	-7.20	356.34	-8.30	2.43
4	6	9	27.02	26.56	22.18	-14.62	326.61	.46	.75
5	6	9	24.42	26.85	-1.63	-26.80	266.53	-2.43	.76
0	7	9	83.23	79.72	-79.59	-4.49	183.23	3.50	1.95
1	7	9	16.87	12.93	-1.60	12.83	97.09	3.94	.77
2	7	9	32.44	40.47	27.97	29.25	46.28	-8.03	.86
3	7	9	12.85	12.78	-6.15	11.21	118.75	.06	.86
4	7	9	57.86	61.07	44.64	-41.67	316.97	-3.21	1.38
5	7	9	17.42	19.42	10.29	-16.47	301.99	-2.00	.71
6	7	9	66.85	59.51	-59.12	-6.86	186.61	7.34	1.57
1	8	9	31.23	26.58	12.81	23.29	61.18	4.65	.83
2	8	9	15.37	12.52	-9.13	-8.57	223.20	2.84	.75
3	8	9	17.50	23.76	-9.11	21.94	112.56	-6.26	.77
5	8	9	18.78	17.24	.31	-17.24	271.04	1.54	.73
6	8	9	10.57	10.57	4.37	-9.63	294.43	-.00	1.06
7	8	9	21.23	26.58	-7.52	25.49	106.44	-5.35	.76
0	9	9	103.24	114.86	114.76	4.80	2.40	-11.61	2.41
2	9	9	58.64	63.53	-62.65	10.52	170.47	-4.88	1.40
4	9	9	42.50	37.73	-36.92	7.77	168.12	4.78	1.06
6	9	9	58.21	64.25	56.44	30.69	28.53	-6.04	1.39
8	9	9	21.05	20.54	17.87	-10.12	330.47	.52	.76
0	0	10	61.85	69.64	-69.40	-5.86	184.83	-7.79	1.47
0	1	10	29.34	40.76	-40.76	-.05	180.08	-11.43	.80
1	1	10	22.85	14.90	-14.68	2.56	170.10	7.95	.68
0	2	10	37.97	38.53	38.45	2.41	3.58	-.56	.93
1	2	10	39.05	32.07	-27.60	-16.33	210.62	6.98	.96
2	2	10	61.47	59.41	28.23	-52.28	298.37	2.06	1.46
1	3	10	38.23	41.30	31.02	-27.26	318.70	-3.07	.94
2	3	10	26.17	25.82	-10.34	-23.66	246.39	.35	.74
3	3	10	90.71	85.68	-85.52	-5.23	183.50	5.03	2.11
0	4	10	67.06	73.76	73.66	3.70	2.88	-6.70	1.58
1	4	10	37.33	39.84	34.34	-20.20	329.53	-2.51	.92
2	4	10	65.06	62.75	-56.61	27.05	154.46	2.31	1.54
3	4	10	17.03	13.63	1.16	-13.58	274.87	3.40	.70
4	4	10	9.90	9.49	-.69	9.47	94.18	.41	.98
0	5	10	14.29	17.30	17.30	.05	.16	-3.01	.80
1	5	10	38.46	39.51	-11.11	37.91	106.33	-1.04	.94
2	5	10	8.63	6.58	-5.90	-2.90	206.19	2.06	1.05
3	5	10	23.11	26.85	-7.54	25.77	106.32	-3.74	.73
5	5	10	59.93	55.35	28.20	-47.63	300.63	4.57	1.43
0	6	10	107.68	102.05	-101.92	-5.20	182.92	5.62	2.50

Table 18 continued/

H	K	L	FO	FC	A	B	PHI	DEL(F)	SIG*(F)
2	6	10	30.50	31.76	31.29	-5.47	350.09	-1.26	.82
3	6	10	21.49	20.25	-20.11	-2.34	186.64	1.24	.71
4	6	10	71.87	69.72	68.42	-13.40	348.92	2.15	1.70
5	6	10	12.79	9.27	9.27	.04	.25	3.52	.86
6	6	10	62.46	67.17	-64.72	-17.98	195.53	-4.71	1.48
0	7	10	19.80	24.65	24.65	.05	.11	-4.85	.74
1	7	10	57.99	56.29	-30.38	-47.39	237.34	1.70	1.38
3	7	10	78.92	75.00	74.42	-9.33	352.85	3.92	1.86
5	7	10	21.07	19.92	-14.89	13.23	138.39	1.15	.76
7	7	10	25.01	27.72	-26.04	9.53	159.89	-2.72	.77
2	8	10	45.81	40.16	16.68	-36.53	294.55	5.65	1.13
4	8	10	36.58	36.89	.69	36.88	88.93	-.30	.94
6	8	10	26.38	22.24	7.00	21.11	71.65	4.13	.79
7	8	10	12.64	13.28	12.43	4.67	20.60	-.64	1.00
8	8	10	36.23	31.29	13.87	-28.05	296.32	4.94	.97
0	9	10	26.70	14.13	-14.13	-.01	180.02	12.57	.79
1	9	10	36.32	34.39	32.17	12.16	20.70	1.93	.93
2	9	10	11.93	14.94	8.88	12.01	53.50	-3.01	1.00
3	9	10	73.65	73.36	-73.30	-3.05	182.38	.28	1.74
4	9	10	17.70	13.06	-11.47	-6.24	208.53	4.64	.77
5	9	10	35.87	34.44	24.25	24.45	45.23	1.43	.96
7	9	10	37.28	35.24	34.71	-6.09	350.04	2.05	.99
9	9	10	54.37	51.25	-46.11	-22.38	205.89	3.12	1.33
0	10	10	30.94	28.88	28.63	3.83	7.61	2.06	.87
2	10	10	23.15	20.95	20.19	5.60	15.49	2.20	.79
4	10	10	44.69	43.61	-40.11	-17.11	203.11	1.08	1.10
6	10	10	75.88	68.46	68.44	1.59	1.33	7.42	1.79
10	10	10	39.97	39.54	-38.93	-6.90	190.06	.43	1.04
0	1	11	15.99	7.44	-7.44	-.07	180.53	8.56	.69
0	2	11	17.19	19.60	-19.60	-.04	180.12	-2.41	.71
1	2	11	92.16	86.99	27.62	-82.49	288.51	5.17	2.15
1	3	11	17.90	22.20	-13.99	-17.24	230.94	-4.30	.72
2	3	11	24.51	24.08	-23.96	2.35	174.40	.43	.71
0	4	11	22.89	21.55	21.55	.02	.05	1.34	.73
1	4	11	73.27	77.68	-10.90	76.91	98.07	-4.42	1.73
2	4	11	10.94	11.38	-6.39	9.42	124.14	-.45	.92
3	4	11	23.65	21.85	-.35	21.85	90.91	1.80	.74
1	5	11	13.55	14.56	8.16	12.05	55.91	-1.01	.87
2	5	11	79.26	74.48	-24.08	70.49	108.86	4.78	1.86
3	5	11	16.84	19.16	1.71	19.09	84.88	-2.32	.76
4	5	11	52.02	51.14	28.50	-42.47	303.86	.88	1.26
0	6	11	15.69	14.98	14.98	.03	.12	.71	.82
1	6	11	28.81	31.38	7.11	30.56	76.91	-2.57	.79
2	6	11	12.03	18.87	-4.05	18.43	102.39	-6.84	.93
4	6	11	31.06	33.54	-24.77	-22.62	222.41	-2.49	.83
5	6	11	19.52	20.51	-10.97	-17.33	237.68	-.99	.74
0	7	11	20.92	19.72	-19.72	.00	180.00	1.21	.76
1	7	11	16.86	16.88	5.78	15.86	69.98	-.03	.77
2	7	11	51.56	53.62	30.51	-44.09	304.68	-2.06	1.25
4	7	11	34.64	37.38	-4.99	37.05	97.67	-2.74	.90
1	8	11	46.67	46.42	2.69	-46.34	273.32	.26	1.14
2	8	11	18.90	23.63	-23.18	4.55	168.89	-4.73	.79
3	8	11	14.80	14.17	6.63	-12.53	297.89	.63	.81
4	8	11	15.72	11.87	11.66	2.21	10.75	3.85	.82
5	8	11	65.61	65.65	7.44	65.23	83.49	-.04	1.57
6	8	11	19.96	24.82	8.50	23.31	69.96	-4.86	.80
7	8	11	34.76	37.33	2.02	-37.28	273.11	-2.57	.94
1	9	11	25.46	27.71	-13.61	-24.13	240.57	-2.25	.77

Table 18 continued/

H	K	L	FO	FC	A	B	PHI	DEL(F)	SIG*(F)
2	9	11	20.00	20.85	9.82	-18.39	298.10	-.84	.80
4	9	11	12.00	11.68	-11.63	1.07	174.73	.32	1.00
6	9	11	13.71	11.13	9.12	6.39	35.02	2.57	1.01
8	9	11	24.89	27.48	-9.69	-25.71	249.35	-2.59	.82
0	10	11	11.80	11.13	11.13	.02	.08	.67	.99
1	10	11	34.02	32.70	14.88	29.12	62.93	1.31	.93
3	10	11	25.56	23.17	-1.71	-23.11	265.76	2.39	.83
5	10	11	27.37	28.41	1.40	-28.38	272.83	-1.04	.85
7	10	11	15.92	17.20	6.81	15.79	66.66	-1.27	.95
9	10	11	12.64	16.87	-6.41	15.61	112.34	-4.23	1.14
0	11	11	15.83	14.04	-14.03	-.28	181.15	1.80	.89
2	11	11	53.93	57.40	2.59	57.34	87.41	-3.47	1.32
4	11	11	41.06	41.36	6.19	-40.90	278.61	-.30	1.06
6	11	11	14.62	15.61	.81	-15.59	272.97	-.98	1.01
8	11	11	63.16	60.91	-.85	60.90	90.80	2.25	1.52
10	11	11	20.56	22.38	2.71	-22.22	276.94	-1.82	.87
0	0	12	113.29	97.44	97.30	5.12	3.01	15.85	2.65
1	1	12	34.79	33.93	6.03	-33.39	280.24	.85	.90
0	2	12	29.45	30.72	-30.65	-2.04	183.82	-1.27	.80
2	2	12	36.60	36.49	.57	-36.49	270.90	.10	.94
0	3	12	15.88	16.21	-16.21	-.02	180.07	-.33	.75
1	3	12	65.17	61.52	-60.06	-13.34	192.52	3.65	1.54
2	3	12	20.57	17.36	-12.27	12.28	134.98	3.21	.75
3	3	12	100.12	106.64	103.53	25.56	13.87	-6.52	2.34
0	4	12	51.56	56.50	-56.40	-3.32	183.37	-4.94	1.25
1	4	12	11.43	13.59	-11.67	6.96	149.20	-2.16	1.06
2	4	12	61.98	57.53	46.16	34.34	36.64	4.45	1.47
3	4	12	17.22	16.27	-10.72	12.23	131.24	.95	.77
4	4	12	22.56	15.90	15.89	.37	1.34	6.66	.78
0	5	12	18.91	18.92	18.92	.03	.10	-.01	.79
1	5	12	51.26	49.57	19.43	45.60	66.92	1.69	1.24
3	5	12	20.15	19.83	-10.21	-17.00	239.00	.32	.75
0	6	12	98.86	104.99	104.89	4.47	2.44	-6.13	2.31
1	6	12	18.20	14.83	11.92	-8.82	323.50	3.37	.78
2	6	12	18.77	26.14	-26.12	.97	177.86	-7.37	.79
3	6	12	16.86	16.82	-1.61	16.74	95.51	.04	.77
4	6	12	35.15	41.28	-38.20	-15.64	202.27	-6.12	.91
5	6	12	16.33	14.92	11.00	-10.08	317.50	1.41	.82
6	6	12	69.62	69.83	69.83	.77	.63	-.21	1.66
1	7	12	19.11	19.08	18.50	-4.69	345.77	.03	.79
2	7	12	22.35	20.61	-17.75	10.48	149.44	1.74	.78
3	7	12	37.57	42.52	-42.45	2.48	176.65	-4.95	.96
5	7	12	23.28	22.21	7.11	21.04	71.34	1.07	.79
7	7	12	37.50	38.48	26.00	-28.37	312.50	-.98	.99
0	8	12	23.23	27.45	27.45	-.37	359.24	-4.22	.79
2	8	12	11.58	17.85	-6.83	-16.49	247.51	-6.27	1.06
4	8	12	29.12	30.09	11.34	27.88	67.86	-.98	.84
7	8	12	11.68	15.20	-7.51	13.21	119.61	-3.52	1.14
8	8	12	20.82	22.49	-1.46	-22.44	266.28	-1.66	.87
2	9	12	11.80	18.67	12.18	-14.15	310.71	-6.87	1.07
3	9	12	59.95	62.42	59.55	-18.72	342.55	-2.47	1.45
5	9	12	19.06	20.08	-18.97	6.60	160.81	-1.02	.85
7	9	12	40.43	37.33	-36.71	-6.80	190.49	3.10	1.05
9	9	12	47.02	49.07	48.78	5.33	6.24	-2.05	1.18
0	10	12	42.08	45.77	-45.63	-3.48	184.36	-3.69	1.08
1	10	12	17.53	16.19	14.57	7.05	25.83	1.34	.90
2	10	12	20.89	16.85	10.34	13.31	52.17	4.04	.88
3	10	12	18.33	22.33	-20.55	-8.75	203.06	-4.01	.91

Table 18 continued/

H	K	L	FO	FC	A	B	PHI	DEL(F)	SIG*(F)
4	10	12	31.97	31.81	26.49	-17.61	326.38	.17	.89
5	10	12	12.29	13.64	13.63	.54	2.28	-1.35	1.14
6	10	12	37.87	39.92	-39.36	-6.68	189.64	-2.06	1.00
7	10	12	12.13	15.79	-12.87	-9.14	215.37	-3.65	1.21
8	10	12	17.28	18.03	7.93	16.19	63.90	-.75	.97
9	10	12	11.91	4.39	4.02	1.77	23.73	7.52	1.21
0	11	12	16.42	21.28	21.28	.04	.10	-4.86	.96
1	11	12	18.59	18.87	-15.86	10.22	147.22	-.28	.91
3	11	12	27.47	26.18	4.53	25.79	80.04	1.29	.86
5	11	12	27.57	29.43	2.55	-29.32	274.96	-1.86	.86
6	11	12	11.52	10.84	-10.83	.34	178.20	.68	1.21
7	11	12	17.45	18.14	-.72	18.13	92.28	-.69	.97
8	11	12	10.99	10.22	5.62	-8.53	303.37	.78	1.35
0	12	12	55.22	59.55	59.48	2.87	2.77	-4.33	1.35
2	12	12	14.29	17.05	-13.38	10.56	141.72	-2.76	1.08
6	12	12	36.14	35.80	35.76	-1.70	357.27	.34	1.01
0	1	13	43.00	36.38	36.26	2.88	4.54	6.62	1.07
1	2	13	32.95	34.45	-24.32	24.41	134.90	-1.50	.87
0	3	13	100.75	98.63	-98.50	-5.21	183.03	2.12	2.35
2	3	13	33.58	30.35	29.79	-5.83	348.93	3.23	.88
0	4	13	18.01	15.39	15.39	.02	.09	2.62	.78
1	4	13	36.41	38.88	-25.00	-29.77	229.98	-2.47	.93
2	4	13	17.18	17.44	-13.71	-10.77	218.16	-.26	.83
3	4	13	55.07	52.62	52.20	-6.62	352.77	2.45	1.32
0	5	13	25.85	27.65	27.62	1.43	2.96	-1.80	.78
2	5	13	41.41	38.31	31.39	-21.96	325.02	3.10	1.04
4	5	13	37.46	34.88	-33.47	9.81	163.66	2.58	.96
0	6	13	32.47	32.79	-32.79	-.05	180.09	-.32	.90
1	6	13	46.93	44.52	42.91	-11.88	344.53	2.41	1.15
2	6	13	12.09	13.61	13.61	.20	.85	-1.52	1.00
3	6	13	57.13	54.28	-54.22	-2.43	182.56	2.85	1.37
4	6	13	12.50	14.32	9.87	10.38	46.45	-1.83	1.00
5	6	13	18.42	19.35	12.96	14.37	47.97	-.94	.85
0	7	13	36.49	35.13	34.95	3.57	5.83	1.37	.97
1	7	13	17.53	15.68	-4.44	-15.04	253.53	1.85	.84
2	7	13	29.92	32.05	-31.67	4.89	171.22	-2.13	.85
3	7	13	10.26	12.09	-12.05	-.96	184.55	-1.82	1.20
4	7	13	32.11	30.45	-29.88	-5.84	191.07	1.66	.89
6	7	13	50.89	51.91	51.89	1.66	1.83	-1.03	1.26
2	8	13	11.52	11.42	8.97	-7.07	321.79	.10	1.14
3	8	13	12.74	12.62	1.61	12.52	82.66	.12	1.07
5	8	13	26.67	26.02	-8.30	-24.66	251.40	.65	.84
7	8	13	15.12	15.74	1.52	15.67	84.47	-.62	1.02
0	9	13	37.60	37.58	-37.37	-3.96	186.05	.02	.99
2	9	13	27.83	28.09	24.79	13.21	28.05	-.25	.86
4	9	13	35.46	30.95	30.56	4.89	9.08	4.51	.95
5	9	13	11.94	12.41	12.07	-2.90	346.48	-.47	1.21
6	9	13	53.93	50.90	-50.37	-7.29	188.24	3.04	1.32
8	9	13	14.78	12.22	5.05	11.13	65.59	2.56	1.01
1	10	13	31.89	30.50	-29.57	7.47	165.83	1.38	.93
2	10	13	13.59	9.77	8.54	-4.76	330.87	3.81	1.08
3	10	13	51.09	50.99	50.95	2.25	2.53	.10	1.26
4	10	13	12.76	7.26	-7.20	.93	172.66	5.50	1.07
5	10	13	14.07	13.43	-11.28	7.29	147.14	.64	1.08
7	10	13	35.90	35.17	-34.09	-8.64	194.22	.73	1.00
0	11	13	14.26	4.00	4.00	.01	.17	10.26	1.08
2	11	13	26.77	26.38	-3.12	-26.19	263.20	.39	.84
4	11	13	14.73	16.31	10.42	12.55	50.30	-1.59	1.08

Table 18 continued/

H	K	L	FO	FC	A	B	PHI	DEL(F)	SIG*(F)
0	12	13	11.50	15.33	15.33	.03	.10	-3.83	1.35
1	12	13	20.78	25.72	24.25	-8.58	340.50	-4.95	.94
2	12	13	11.90	12.55	5.34	11.36	64.83	-.65	1.21
3	12	13	38.26	37.01	-35.40	-10.80	196.96	1.25	1.05
5	12	13	11.74	14.32	3.76	13.82	74.78	-2.58	1.28
0	13	13	37.02	37.62	37.49	3.19	4.86	-.60	1.02
2	13	13	14.17	15.21	-13.29	7.39	150.93	-1.04	1.15
0	0	14	43.76	33.08	33.06	1.00	1.73	10.68	1.08
1	1	14	56.60	59.98	20.62	56.32	69.89	-3.38	1.35
0	2	14	22.13	12.84	12.83	-.43	358.08	9.30	.77
2	2	14	62.13	66.15	-3.79	66.04	93.29	-4.02	1.50
0	3	14	19.79	22.83	22.83	.03	.09	-3.05	.80
1	3	14	31.20	31.32	-26.65	16.44	148.33	-.11	.87
2	3	14	16.11	13.09	-6.82	-11.17	238.61	3.03	.82
3	3	14	27.78	22.48	15.66	-16.13	314.15	5.29	.81
0	4	14	15.70	21.04	-21.03	-.53	181.44	-5.33	.89
2	4	14	60.74	61.84	22.46	-57.61	291.30	-1.09	1.47
4	4	14	23.96	26.43	9.74	24.57	68.36	-2.47	.80
1	5	14	58.06	59.14	20.01	-55.65	289.78	-1.08	1.41
5	5	14	44.86	43.08	-9.81	41.95	103.16	1.78	1.14
0	6	14	33.62	23.85	23.83	.90	2.17	9.78	.92
5	6	14	10.28	13.10	-9.50	9.02	136.49	-2.82	1.27
6	6	14	21.23	20.32	.11	20.32	89.70	.91	.88
1	7	14	16.83	18.27	-.55	18.26	91.71	-1.44	.83
3	7	14	11.93	15.84	-12.57	9.64	142.49	-3.91	1.07
5	7	14	37.43	38.68	14.87	-35.71	292.61	-1.26	.99
6	7	14	12.41	6.56	-6.13	2.35	159.01	5.85	1.14
7	7	14	38.54	40.22	16.71	36.59	65.46	-1.69	1.05
0	8	14	34.58	34.99	-34.99	-.38	180.63	-.40	.94
1	8	14	16.29	13.01	-8.18	10.12	128.95	3.28	.89
2	8	14	46.03	43.42	13.07	41.40	72.48	2.61	1.16
3	8	14	20.50	18.08	12.54	-13.02	313.93	2.42	.81
4	8	14	34.06	39.21	5.84	-38.77	278.57	-5.15	.93
6	8	14	18.21	17.82	11.66	-13.47	310.90	.39	.91
8	8	14	47.20	41.95	.77	41.95	88.95	5.24	1.19
0	9	14	20.25	14.53	-14.53	-.02	180.07	5.73	.87
1	9	14	21.07	18.64	-7.88	16.89	115.02	2.43	.82
3	9	14	21.83	17.60	14.18	10.44	36.35	4.22	.83
4	9	14	12.51	13.04	-12.92	1.74	172.33	-.53	1.14
8	9	14	10.66	5.87	-2.61	5.26	116.35	4.78	1.35
2	10	14	29.04	27.18	22.20	-15.68	324.77	1.86	.93
4	10	14	22.99	22.20	8.69	20.43	66.95	.79	.84
5	10	14	10.82	3.64	3.58	.65	10.33	7.18	1.28
6	10	14	15.54	16.23	-13.42	9.14	145.75	-.69	1.02
1	11	14	42.63	39.82	8.48	-38.90	282.29	2.82	1.09
5	11	14	45.91	42.70	-6.85	42.15	99.23	3.21	1.16
0	1	15	20.81	20.02	-19.92	-2.00	185.73	.79	.81
0	2	15	11.24	6.76	6.76	.01	.10	4.48	1.13
1	2	15	26.74	24.44	14.87	19.39	52.52	2.30	.84
0	3	15	52.59	56.16	56.05	3.55	3.63	-3.57	1.30
2	3	15	35.74	34.59	-28.92	18.98	146.73	1.14	.96
1	4	15	13.73	16.40	9.82	-13.14	306.76	-2.67	1.01
3	4	15	15.37	16.89	-16.44	-3.87	193.23	-1.52	.88
2	5	15	22.00	22.72	-3.88	-22.39	260.16	-.72	.83
4	5	15	14.10	16.79	7.27	15.13	64.32	-2.69	1.01
1	6	15	21.59	22.50	-22.09	4.26	169.09	-.91	.82
2	6	15	11.11	6.51	5.54	-3.42	328.35	4.60	1.21
3	6	15	37.98	36.74	36.73	-.74	358.85	1.25	1.00

Table 18 continued/

H	K	L	FO	FC	A	B	PHI	DEL(F)	SIG*(F)
5	6	15	20.92	14.46	-11.73	8.45	144.22	6.47	.88
0	7	15	34.45	34.18	-34.08	-2.61	184.37	.27	.93
2	7	15	26.67	26.15	12.92	22.73	60.38	.52	.84
4	7	15	26.48	29.42	25.72	-14.29	330.95	-2.94	.89
6	7	15	22.98	25.31	-25.10	-3.26	187.41	-2.33	.90
1	8	15	26.19	26.69	-10.89	24.37	114.08	-.50	.89
5	8	15	28.33	25.44	8.78	-23.87	290.19	2.89	.87
0	9	15	31.89	26.75	26.63	2.63	5.64	5.13	.93
1	9	15	14.14	15.71	-6.89	14.12	116.00	-1.56	1.08
4	9	15	21.05	25.39	-22.27	-12.20	208.71	-4.33	.94
6	9	15	34.82	35.28	35.20	-2.49	355.96	-.47	.98
1	10	15	29.32	33.31	24.00	-23.10	316.10	-3.99	.94
3	10	15	36.20	36.17	-35.91	4.36	173.07	.03	1.01
0	0	16	37.05	36.14	-35.86	-4.48	187.13	.91	.98
1	1	16	45.48	44.04	-23.23	-37.41	238.16	1.44	1.15
0	2	16	18.68	16.85	16.75	1.85	6.31	1.83	.85
2	2	16	10.79	9.77	2.40	-9.47	284.22	1.02	1.28
1	3	16	36.71	34.73	33.48	9.23	15.42	1.99	.98
3	3	16	49.05	49.16	-49.16	-.42	180.49	-.11	1.22
0	4	16	36.87	38.62	38.52	2.85	4.24	-1.75	.98
2	4	16	11.11	13.89	-8.75	10.78	129.06	-2.77	1.21
4	4	16	30.63	29.62	-29.61	.91	178.24	1.01	.91
0	5	16	17.85	19.93	-19.93	-.03	180.07	-2.08	.91
3	5	16	25.87	20.40	16.93	11.38	33.91	5.47	.83
5	5	16	11.26	14.08	-3.97	-13.51	253.64	-2.82	1.28
0	6	16	52.75	48.20	-48.04	-3.97	184.72	4.55	1.30
2	6	16	27.18	27.51	25.98	9.04	19.18	-.33	.90
3	6	16	12.09	11.38	.49	11.37	87.55	.71	1.21
4	6	16	38.89	39.57	39.49	-2.55	356.31	-.69	1.02
6	6	16	44.05	41.85	-41.31	-6.69	189.20	2.20	1.12
1	7	16	14.60	21.39	-20.72	5.35	165.52	-6.80	1.08
3	7	16	44.03	41.15	40.99	-3.66	354.89	2.88	1.12
5	7	16	13.92	11.85	-7.58	9.11	129.79	2.07	1.08
0	8	16	14.48	8.62	8.60	.53	3.54	5.86	1.08
2	8	16	18.85	16.23	1.26	-16.18	274.47	2.62	.92
1	9	16	22.76	24.39	23.47	-6.63	344.23	-1.63	.90
0	1	17	16.32	13.21	-13.19	-.73	183.18	3.10	.96
1	2	17	37.46	40.22	4.20	-40.00	275.99	-2.76	.99
0	3	17	24.01	24.61	24.57	1.36	3.17	-.60	.86
2	3	17	15.66	16.02	-11.99	-10.62	221.51	-.36	1.02
1	4	17	36.22	36.94	8.05	36.05	77.41	-.72	1.01
1	5	17	11.01	7.14	-6.13	-3.67	210.93	3.87	1.28
2	5	17	38.59	36.96	6.18	36.44	80.38	1.63	1.01
4	5	17	30.25	25.61	2.15	-25.52	274.82	4.64	.90
2	6	17	11.53	6.82	-1.88	-6.55	254.03	4.72	1.28
3	6	17	19.58	19.42	17.78	7.79	23.67	.17	.92
2	7	17	25.43	25.19	11.29	-22.52	296.64	.24	.88
0	0	18	25.22	25.80	25.69	2.42	5.38	-.58	.87
1	1	18	18.18	18.70	10.82	-15.25	305.37	-.52	.98
2	2	18	27.48	25.57	19.02	-17.09	318.05	1.91	.91
3	3	18	20.05	22.13	20.71	-7.79	339.38	-2.08	.93

3.2.4 *Ir studies of bis(2-aminomethylpyridine) metal(II) complexes: assignments and structural aspects of the spectra*

As observed in Section 3.2.1 and 3.2.2, ligand bands above 700 cm^{-1} in the ir spectra of complexed 2-aminomethylpyridine do not change significantly with differing coordinated species. Their assignment is therefore not considered relevant to a discussion of structural aspects of the ir spectra, and a detailed investigation of only the region 700 - 140 cm^{-1} has been undertaken.

Differences are observed in the number of bands in the far ir spectra of the *bis*(2-aminomethylpyridine) metal(II) complexes studied, which indicates, as expected, that the ligands are arranged in varying configurations. Detailed assignment of vibrations is therefore relatively complicated as compared with that in the related *tris*(2-aminomethylpyridine) metal(II) complexes.

It has been well established [28,32,95] that in the ir spectra of complexes of metal(II) halides, complications may arise in the assignment of metal-to-pyridine ring vibrations owing to the fact that metal-to-halogen vibrations are found in the same region. In addition, it has been shown [171] that the stretching and bending modes of metal-to-pyridine ring vibrations, can occur with a separation as low as 20 cm^{-1}. For this reason, assignment of bands in the spectra of the *bis*(2-aminomethylpyridine) complexes, has frequently been based upon the metal-to-amino nitrogen stretch ($\nu M\text{-}NH_2$), which is not only in a more suitable region for assignment (with the only nearby bands being those of the ligand itself) but also shows sensitivity to *N,N*-d_2 and ^{15}N(amino) substitutions and change of metal ion.

3.2.4.1 The ir spectra of the complexes Zn amp$_2$X$_2$: X = Cl$^-$, Br$^-$, I$^-$

Ir frequencies, isotopic shifts and band assignments of these complexes are given in Table 19. The spectral region 700 - 140 cm^{-1} is depicted in Figure 5. Similarities in the spectra of these three complexes indicate that they are isostructural. In accordance with the findings of Sections 3.2.1 and 3.2.2, the band at *ca.* 630 cm^{-1} is assigned as an in-plane deformation of the pyridine ring; that at *ca.* 465 cm^{-1} is a skeletal CCN bend; and the band near 412 cm^{-1} is an out-of-plane deformation of the pyridine ring, its additional sensitivity to metal ion substitution and insensitivity to *N,N-d*$_2$ and ^{15}N(amino) labelling implying coupling to νZn-py.

Deuteration of the bromide complex shifts the bands at 589 and 560 cm^{-1} approximately 100 cm^{-1} to lower frequency which implies that they are NH_2 rocking modes. Additional sensitivity to ^{15}N amino isotopic substitution (shifts of -5 cm^{-1} for both bands) confirms this assignment. The only other band which experiences low frequency shifts on *N,N-d*$_2$ and ^{15}N(amino) labelling is that at 398 cm^{-1} (-14 and -5 cm^{-1}, respectively), and is hence νZn-NH_2.

The assignments of νZn-X and νZn-py given in Table 19 are based on the fact that for terminal halogens, a νM-Cl generally occurs at a higher frequency than a νM-py because of the mass effect, while for the same reason, νM-py occurs at a higher frequency than νM-Br and νM-I. Further, the expected ratio [172] νM-Cl:νM-Br:νM-I is approximately 1:0.7:0.5. The weak band at 187 cm^{-1} in the chloride spectrum may be δCl-Zn-Cl, although its frequency is rather high.

Table 19. Ir frequencies (4000 - 150 cm^{-1}) and band assignments for the complexes $Zn(amp)_2X_2$

X →	Cl[a]	Br[b]	I	Assignment
	3321	3270(9,812)	3283	
	3215	3188(7,813)	3220	νNH_2
	3138	3125(3,804)	3138	
	3068	3045	3044	
	2950	2928	2934	
	2919	2910	2909	
	1603	1601	1603	
	1596	1588(0,157)	1583	NH_2 scissor
	1570	1566	1568	
	1488	1486	1486	
	1438	1426	1431	
	1363	1361	1362	
	1302	1297	1294	
	1260	1254(0,74)	1256	δNH_2
	1223			
	1153	1140	1143	
	1129	1124(0,67)	1118	δNH_2
	1103			
	1092	1091	1092	
	1048	1034	1034	
	1022	1019	1018	
	980	979	975	
	941	937(0,31)	937	
	899	897(0,17)	894	δNH_2
	814	812(0,22)	809	
	776	773	771	
	727	722	721	
	638	638	638	i.p. δpy
	595	589(5,81)	583	NH_2 rock
	568	560(5,120)	558	NH_2 rock
	470	463	458	skeletal δCCN
	413	412	411	o.o.p. δpy
	398	398(5,14)	398	$\nu Zn\text{-}NH_2$
	273	188	160	νZn-X
	239	240	239	νZn-py
	212	209	201	δZn-py
	187			

a Hydrated species $[Zn(amp)_2Cl_2].1\frac{1}{2}H_2O$

b (x,y) x and y are the respective negative shifts on ^{15}N- and $N,N\text{-}d_2$-amino isotopic substitutions

Fig. 5. The ir spectra (700 - 150 cm^{-1}) of the complexes $Zn(amp)_2X_2$

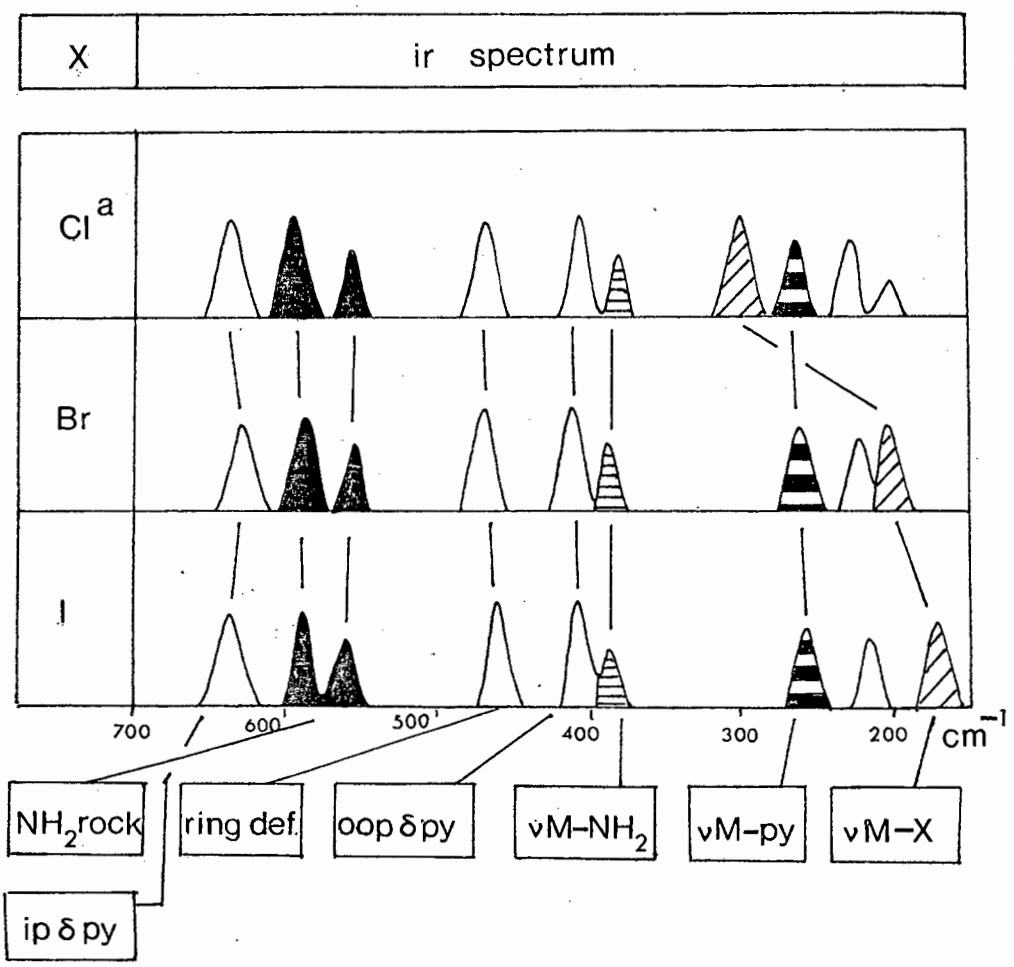

a Hydrated complex $Zn(amp)_2Cl_2.1\frac{1}{2}H_2O$

Since this complex is hydrated ($[Zn(amp)_2Cl_2].1\frac{1}{2}H_2O$), it is also possible that the band is a hydrogen bond stretch.

The insensitivity of the band near 240 cm^{-1} to either form of isotopic substitution employed implies that it is a νM-py mode. The observation of one νM-NH_2, one νM-py and one νM-X is consistent with D_{2h} point symmetry of the central metal ion which indicates that the complexes are *trans* planar octahedral (see Figure 6). On this basis the remaining absorption at 212 cm^{-1} is unlikely to be νZn-py, but may rather be associated with a Zn-N=C bend. Results of the deuteration and ^{15}N(amino) studies show that no band above 140 cm^{-1} may be assigned as δZn-NH_2.

While an earlier infrared study [71] of these complexes supports the proposal of a *trans* planar octahedral structure, the previous assignment of the band at 240 cm^{-1} to νZn-NH_2 receives no support from the investigation.

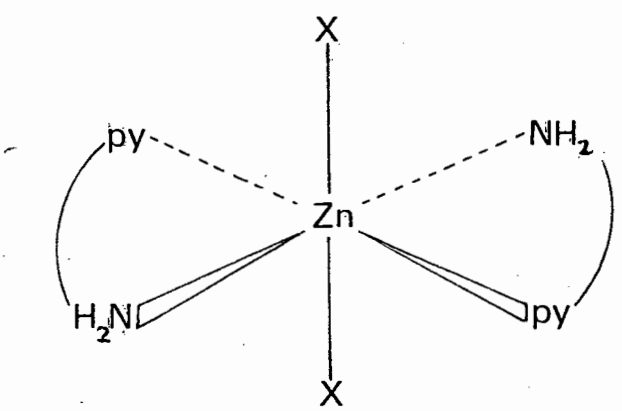

Fig. 6. Diagrammatic representation of $Zn(amp)_2X_2$

3.2.4.2 The ir spectra of the complexes $Cu(amp)_2X_2.nH_2O$: $X = Cl^-$, Br^-, I^-, ClO_4^-, BF_4^-, SCN^-; $n = 0, 2$.

The ir frequencies, shifts on deuteration of the amino group and band assignments are given in Table 20. Figure 7 depicts the spectral region 700 - 140 cm^{-1}.

The halide complexes

All, except for the $Cu(amp)_2Br_2$ prepared in ethanol, show marked similarities in their ir spectra which indicates that the complexes are isostructural.

By analogy with the spectra of 2-aminomethylpyridine and the complexes discussed previously it may be inferred that the bands in the region 700 - 500 cm^{-1} arise from NH_2 rocking modes and the in-plane pyridine ring deformation. However, on amino-deuteration of the $Cu(amp)_2Br_2$ complex prepared in water, all of these bands undergo shifts to lower frequencies with the greatest isotopic sensitivity being exhibited by the 596 cm^{-1} band (504 cm^{-1} in the *N,N-d_2* sample). This indicates that all the vibrations are coupled, the purest NH_2 rock being that at the lowest frequency.

The band at about 415 cm^{-1} is assigned to the expected out-of-plane pyridine ring deformation, while that at *ca.* 490 cm^{-1} is presumably the δCCN skeletal mode. It is about 30 cm^{-1} higher in $Cu(amp)_2X_2$ than in the analogous zinc complexes. This is most likely indicative of a change in coordination number from six in $Zn(amp)_2X_2$ to four in the copper complexes. On this basis it is proposed that all the halide complexes, except for the $Cu(amp)_2Br_2$ prepared in ethanol, are exhibiting the well noted [173] tendency of

Table 20. Ir frequencies (4000 - 150 cm^{-1}) and band assignments for the complexes $Cu(amp)_2X_2$

X →	Cl	Cl[a]	Br[b]	Br[c]	I	ClO_4	BF_4	SCN	Assignments
	3253	~3240	3220(850)	3248	3221	3326	3341	3223	}
	3216		3129(840)	3203	3208	3272	3288	3148	} νNH_2
	3120	3130	3053		3122	3163	3176		}
	3059	3061	3027(~720)		3064	3113	3091		}
	2941	2936	2937	2938	2924	2950	2968	2952	} νCH_2
	2918	2917	2912	2907	2908	2942	2950	2940	}
								2044	$\nu C\equiv N$
	1609	1608	1608	1605	1608	1612	1616	1606	
	1594	1592	1591(150)	1590	1585	1591	1599		NH_2 scissor
	1569	1569	1570	1567	1569	1574	1576	1568	
					1547	1551			
	1488	1486	1485	1487	1486	1491	1492	1485	
	1437	1440	1447(47)	1445	1442	1447	1450	1446	}
	1430	1432	1434(61)	1434	1432	1433		1437	}
	1369	1370	1375(92)	1375	1373	1382	1383	1381	} δNH_2
	1327	1328	1331(130)	1332	1329	1334	1336	1329	}
	1296	1294	1290	1292	1286	1291	1292	1288	
	1259	1255	1254	1256	1254	1256	1258	1256	
	1221	1216	1203	1221		1227	1228	1218	
	1190	1192		1191	1195	1186	1190	1191	
						1166	1169		
	1141	1144	1147	1144	1148	1145	1148	1137	
				1133	1136	1123			
	1093	1094	1100	1097	1102	1113		1108	
						1083	1085		ClO_4^- (BF_4^-)
	1055	1055	1055	1055	1056	1033	1062	1058	
	1034	1032	1029(16)	1032	1030	1021	1023	1030	δNH_2
	981	980	975	971	974	970	972	1011	
						951	953		
								965	$2\delta NCS$
	944	943	946(31)		945			944	δNH_2
				939	892	934		935	
	852	850	898(65)		892	895	897	895	δNH_2
								887	$\nu C\text{-}S$
	818	815	816(22)	816	813	817	817	815	δNH_2
	782	780	774	778	774			774	
						756	756	766	
	723	722	723(3)	722	722	729	729	726	
			668(16)		665	673	675	671	NH_2 rock
	654	653	649(24)	653	650	658	658	650	i.p. δpy
	639	633		602					NH_2 rock
						627			δClO_4^-
	586		596(92)	585	587	584	589	594	NH_2 rock
							523		δBF_4^-
	486	478	492(9)	489	490	491	493	491	skeletal ring def.
								484	δNCS
	457	466	459(16)	458	457	455	459	464	$\nu Cu\text{-}NH_2$
	421	417	414	420	416	423	424	420	o.o.p δpy
				400			355		$\nu Cu\text{-}NH_2$
	309	312	311	312	312	318	319	310	} $\nu Cu\text{-py}$
				267			272		}
	272	251	263	226	262	263	234	252	}
	198	222	235		229			235	} $\delta Cu\text{-py}$
	170	189	185	187	167	235	182	194	}
	152	154	165		154				}

a - Dihydrate $Cu(amp)_2Cl_2.2H_2O$. b - Prepared in water. c - Prepared in ethanol. d - Figures in parentheses indicate negative shift experienced on deuteration of the amino group.

Fig. 7. Ir spectra (700 - 150 cm^{-1}) for the complexes $Cu(amp)_2X_2$

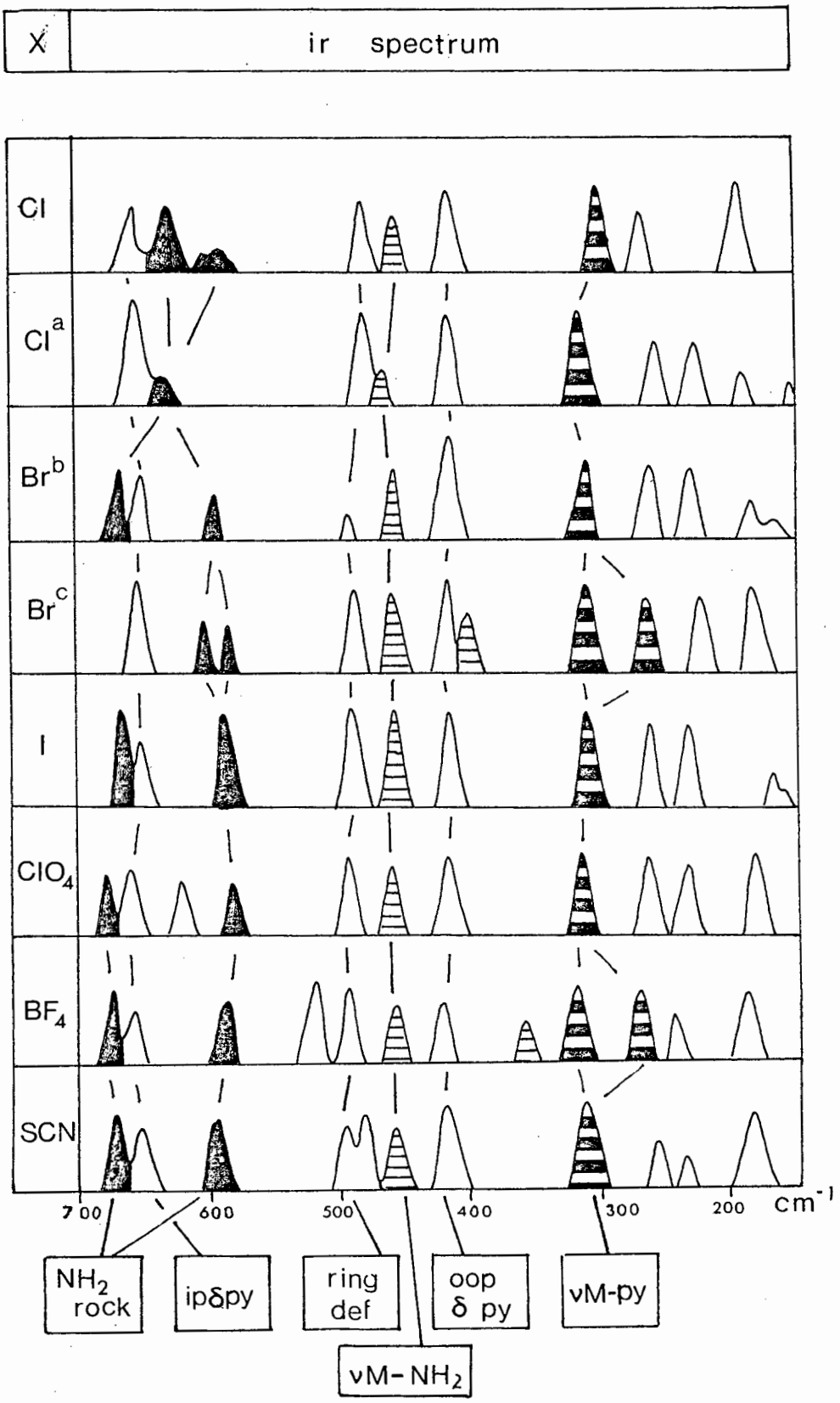

a - Dihydrate $Cu(amp)_2Cl_2.2H_2O$. b - Prepared in water. c - Prepared in ethanol

copper complexes to be square planar. Owing to the high ligand field strength of 2-aminomethylpyridine [62], the halide ions are most likely uncoordinated and no νCu-X modes are expected. On the basis of a shift of -16 cm^{-1} on *N,N*-d_2-substitution in the aqueous prepared $Cu(amp)_2Br_2$ complex, the band near 460 cm^{-1} is assigned to νCu-NH_2. The insensitivity to amino-deuteration of all bands below 350 cm^{-1} implies that they are νCu-py or δCu-py modes.

The observation of only one band attributable to νCu-NH_2 is consistent with the D_{2h} point symmetry of *trans*-square planar coordination (see Fig.8). Hence all the $Cu(amp)_2X_2$ complexes except for the bromo complex prepared in ethanol, have this structure. On this basis, the band at about 311 cm^{-1} is assigned to νCu-py, while the two absorptions immediately below it are δCu-py modes.

The ir spectrum of the remaining halide complex, $Cu(amp)_2Br_2$ prepared in ethanol differs from those discussed previously in that two bands at 458 and 400 cm^{-1} are attributable to νCu-NH_2. On the basis of group theoretical predictions, this implies that the complex has either a *trans* planar five coordinate structure or alternatively a *cis*-square planar configuration, both of which exhibit

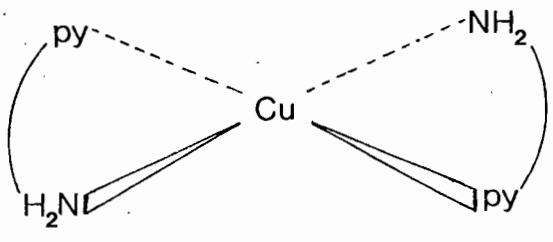

Fig. 8. Diagrammatic representation of *trans*-square planar $Cu(amp)_2X_2$

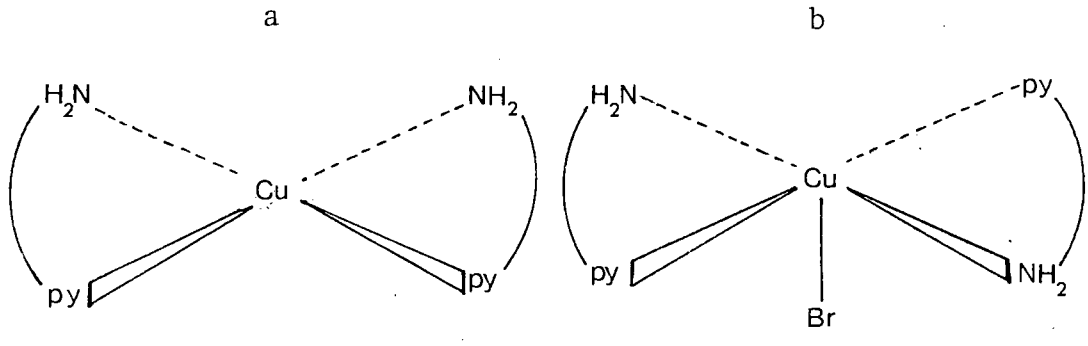

Fig. 9. Diagrammatic representation of a) *cis*-square planar and b) *trans*-planar five-coordinate $Cu(amp)_2Br_2$

localized C_{2v} point symmetry (see Figure 9). The former may be considered more likely in view of the fact that the analogous $Cu(aep)_2Br_2$ complex has been shown [79] to have a five-coordinate structure.

The perchlorate, tetrafluoroborate and thiocyanate complexes

Over and above the vibrations discussed for the previous $Cu(amp)_2X_2$ complexes additional δClO_4^-, δBF_4^-, and δNCS modes are expected for these complexes in the spectral region below 700 cm^{-1}. They are indeed observed at 627, 523 and 484 cm^{-1} respectively, and since none of the anions is expected to be coordinated, all remaining bands arise from the 2-aminomethylpyridine and its bidentate coordination to the Cu(II) ion. Assignments based upon the data discussed previously imply that the ClO_4^- and SCN^- complexes have *trans* square planar coordination (see Figure 8) while the greater complexity of the spectrum of the BF_4^- species has one of two possible sources: either the additional bands are attributable to

νCu-NH_2 and νCu-py modes (in which case the complex has a *cis*-square planar structure), or splitting of bands has occurred owing to disorder of the BF_4^- anions (as observed (Section 3.2.3.) in a related 2-aminomethylpyridine complex).

It may be noted that assignments of νM-L and consequent structural proposals made here differ significantly from those of the earlier ir study [71].

3.2.4.3 *The ir spectra of the complexes* $Ni(amp)_2X_2.nH_2O$: $X = Cl^-$, Br^-, I^-, SCN^-; $n = 0, 1, 2$

Fig. 11 depicts the ir spectra of this series of complexes in the region 700 - 150 cm^{-1}. Frequencies (cm^{-1}) and proposed assignments are listed in Table 21.

The complexes $[Ni(amp)_2(H_2O)_2]X_2$

Similarities in the band patterns of the spectra for these complexes indicate that they are isostructural. Owing to the greater ligand field strength of water as opposed to halide, the water molecules rather than the halide ions are considered to be coordinated to the nickel ion. A similar conclusion has been reached with the analogous N-methyl-2-aminomethylpyridine complex of NiI_2 on the grounds of conductance measurements in nitromethane [58]. The complex with coordinated water is preferentially precipitated for solubility reasons. Assignments are made by analogy with the $M(amp)_2X_2$ complexes discussed previously. The bands at *ca.* 645 and 420 cm^{-1} are the respective in-plane and out-of-plane pyridine ring deformations; the remaining absorptions above 500 cm^{-1} are NH_2 rocking modes; while the band at *ca.* 470 cm^{-1} is the expected skeletal δCCN mode. The

Table 21. Ir frequencies (4000 - 150 cm^{-1}) and band assignments for the complexes $Ni(amp)_2X_2H_2O_n$

X → Cl n → 2	Br 2	I 2	I 1	Cl 0	Br 0	SCN 0	Assignments
			3269	3317	3281	3302	
3240	3252	3242	3235	3258	3240	3240	
3150	3158	3151	3149	3160	3054		
2931	2926	2934	2929	2940	2938		
2917	2921	2920	2909	2923	2920		
						2104(30)[a]	νC≡N
						2085(25)	νC≡N
1608	1609	1611	1604	1606	1604	1604	
			1594			1598	
1570	1574	1571	1569	1569	1570	1570	
1482	1486	1487	1481	1480	1482	1485	
1431	1432	1435	1430	1426	1434	1437	
1372	1371	1373	1373	1371	1374	1372	
1321	1320	1323	1327	1322	1330	1322	
1280	1281	1283	1283	1284	1284	1281	
1257	1259	1255	1256	1260	1252	1251	
1218	1218	1221	1216	1220	1214	1220	
1165	1174	1178	1187	1154	1192	1170	
1145	1147	1150	1144	1142	1145	1151	
1110	1107	1112	1112	1106	1113	1105	
1091	1096	1092	1100	1090	1098	1077	
1055	1051	1052	1054		1055	1053	
1033	1031	1029	1031	1032	1035	1027	
1023	1023	1024	1022	1022	1025	1020	
972	971	970	972	971	971	968	b
937	931	934	935	930	938	930	b
886	885	890	890	888	892	885(3)	b
817		811	811	812	811	813	
774			787	778	773	786	
746				772		777	
		764	769		766	764	
						758	
722	724	723	724	723	725	731	
			653				OH_2 rock
654	651	656	639	647	654	652	NH_2 rock
642	644	648	625	631	641	642	i.p. δpy
					585	590	NH_2 rock
609	603	575	579	560		560	NH_2 rock
512							
474	475	465	482	477	483	477	skeletal ring def
						472(4)	δNCS
457	449	452	450	450	452	440	νNi-NH_2
419	421	419	422	424	423	422	o.o.p δpy
397	395	384	392	397	394	368	νNi-NH_2
299	302	300	300	291	299	286	νNi-py
				291			νNi-X
247	245	245	251	258	252	267	νNi-py
				205	235		νNi-X
					194		
						242	νNi-X
			231				
			183				νNi-I
225	219	216	153	175	173		
206	191	194				203	δL-Ni-L
159	157	152				177	δL-Ni-L
						165	δL-Ni-L

[a] Figs. in parentheses indicate negative shift on ^{15}NCS isotopic substitution.
[b] νC-S and 2δNCS expected in this region are presumably masked by ligand modes.

Fig. 11. The ir spectra (700 - 150 cm^{-1}) of the *bis* complexes $Ni(amp)_2X_2.nH_2O$

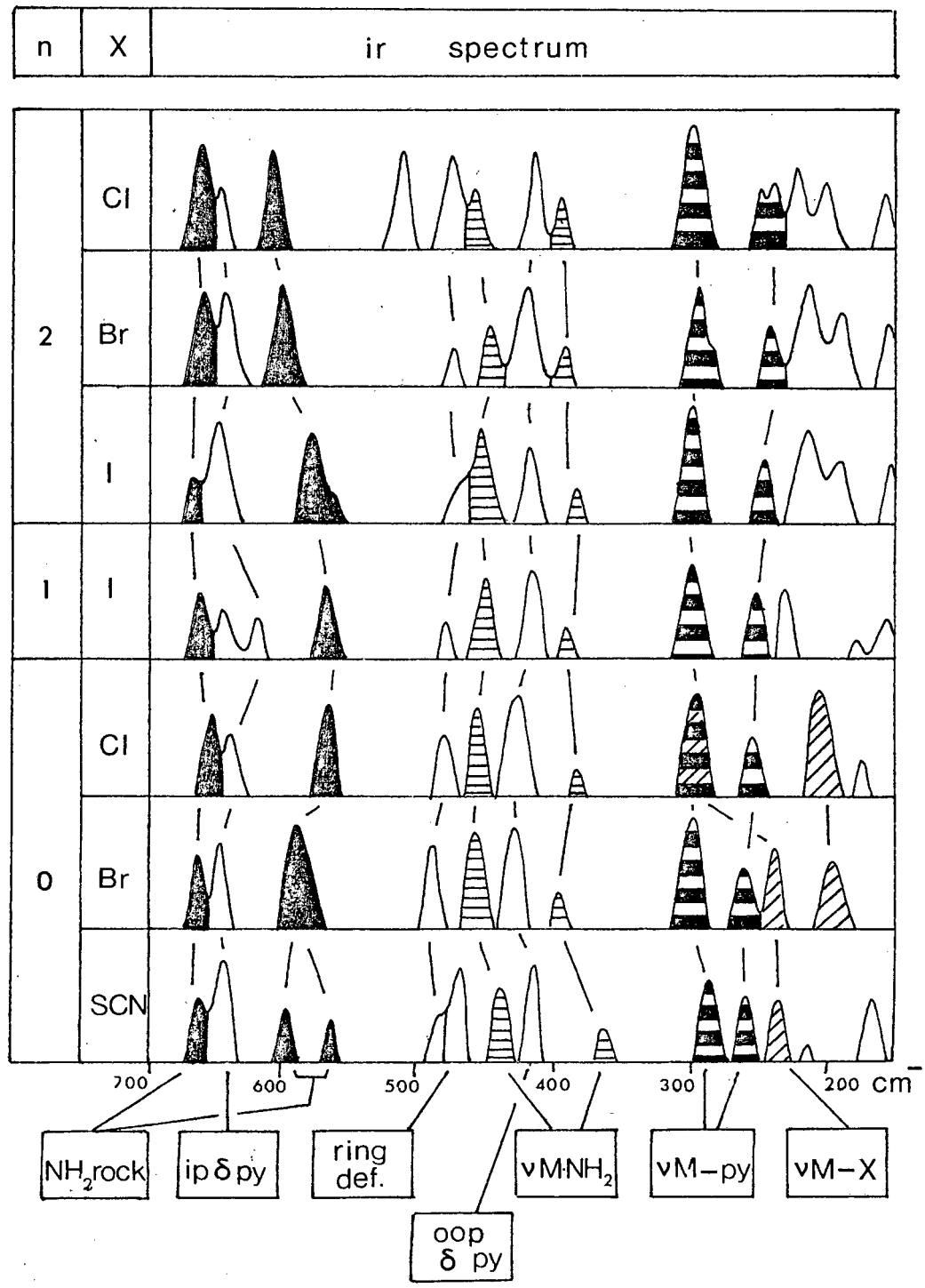

additional band at 512 cm^{-1} in the $[Ni(amp)_2(H_2O)_2]Cl_2$ complex is considered to arise from one of two sources: it is either an OH_2 rock or an additional NH_2 rock caused by hydrogen bonding between the coordinated water molecules and the amino groups. The bands near 450 and 390 cm^{-1} are assigned to νNi-NH_2 while those at *ca.* 300 and 245 cm^{-1} are νNi-py modes. These assignments are in agreement with the Group Theoretical predictions for the locallised C_{2v} point symmetry of *cis*-planar octahedral structure (Fig. 10), which is subsequently assigned.

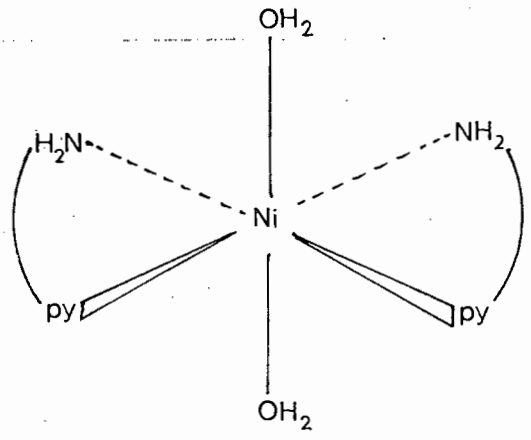

Fig. 10. Diagrammatic representation of $[Ni(amp)_2(H_2O)_2]X_2$

The complex $[Ni(amp)_2H_2O.I]I$

The ir spectrum of this complex shows marked similarity in band-pattern to that of its bis-aquo analogue indicating that no great structural change has occurred in the dehydration *i.e.* the 2-aminomethylpyridine ligands are similarly oriented about the central nickel ion. However there are two additional bands in the spectrum of the mono-hydrate which require assignment: the higher, at 653 cm^{-1} is most likely an extra OH_2 rock

of coordinated H_2O while the lower, at 183 cm^{-1} is tentatively assigned as, νNi-I, suggesting that one iodide ion is indeed coordinated.

The complexes $[Ni(amp)_2X_2]$

Similarities in the band patterns of the spectra of these complexes is again indicative of isostructurality. Assignment of bands above 350 cm^{-1}, by analogy with other $M(amp)_2X_2$ complexes is straight-forward and is therefore not discussed except to note that an expected δNCS mode at 472 cm^{-1} is observed in the spectrum of $Ni(amp)_2(SCN)_2$. Its assignment is confirmed by a -4 cm^{-1} shift on ^{15}NCS isotopic substitution. By analogy with the $[Ni(amp)_2(H_2O)_2]X_2$ complexes, the bands near 300 and 250 cm^{-1} are assigned to νNi-py. The higher frequency band in the chloride complex is of very much greater intensity than that in $Ni(amp)_2Br_2$; this indicates that another vibration, possibly νM-Cl, occurs at the same frequency. Hence the coordinated halogens give rise to νNi-Cl modes at 291 and 205 cm^{-1} and νNi-Br at 235 and 194 cm^{-1}. The ratios νNi-Br:νNi-Cl are therefore 0.81 and 0.95 for the higher and lower bands respectively. These are both somewhat higher than the expected [172] value of 0.7. However the discrepancy may arise because of coupling and interaction between νNi-Cl and νNi-py. In the spectrum of $Ni(amp)_2(SCN)_2$ no bands below 400 cm^{-1} undergo any shift on ^{15}NCS substitution. This implies that the SCN^- is bonded to the metal ion through the sulphur atom, νNi-S occurring at 242 cm^{-1} [174].

The observation in all cases of two νNi-NH_2 and two

νNi-py modes is in complete agreement with the group theoretical expectations for a *cis*-planar $Ni(amp)_2X_2$ octahedral configuration having localized symmetry C_{2v}. Hence in changing from $[Ni(amp)_2(H_2O)_2]X_2$ to $Ni(amp)_2X_2$ there is no change in the symmetry of the complex species; water molecules are merely substituted by halide ions. Again assignments and structural proposals presented here differ from those published previously [71].

3.2.4.4 *The ir spectra of the complexes $Mn(amp)_2X_2$ and $Co(amp)_2X_2$: $X = Br^-$, SCN^-.*

The ir spectra of the remaining three *bis*(2-aminomethylpyridine) complexes investigated are depicted in Fig. 12, Table 22 reports the ir frequencies (4000 - 150 cm^{-1}) and their assignments. In the thiocyanate complexes all the expected bands attributable to NCS modes above 400 cm^{-1} are observed and thus assigned. Remaining bands in all three complexes have been assigned by analogy with the other *bis*(2-aminomethylpyridine) complexes reported in Section 3.2.4. The observation of two $\nu M\text{-}NH_2$ and νM-py modes in each complex is consistent with their having *cis*-planar octahedral configurations. No bands attributable to νM-X are observed. An expected νMn-Br would be at a frequency below the range measured here, while absence of bands attributable to νM-NCS in the $M(amp)_2(SCN)_2$ complexes suggests that bonding of the thiocyanate group to the metal ions occurs through the sulphur groups giving rise to νM-S modes. The interest in the spectra of these three complexes lies predominantly in the information they yield

Table 22. Ir frequencies (4000 - 150 cm^{-1}) and band assignments for the complexes $Mn(amp)_2X_2$ and $Co(amp)_2X_2$

X	Mn Br	Mn SCN	Co SCN	Assignment
	3290	3312	3309	
	3248	3252	3251	
	3156	3163	3164	
	3054	3068	3074	
	2910	2915	2911	
	2848	2859	2858	
		2083	2097	νC≡N
		2068	2080	
	1603	1604	1606	
	1597	1591	1593	
	1567	1570	1570	
	1481	1484	1485	
	1442	1438	1439	
	1372	1375	1374	
	1325	1325	1324	
	1289	1282	1283	
	1256	1251	1258	
	1212	1221	1220	
	1181	1171	1171	
	1153	1151	1152	
	1108	1106	1112	
	1086	1070	1075	
	1052	1051	1053	
	1022	1024	1028	
	1015	1012	1020	
	971	967	967	
		951	946	2δNCS
	927	934	930	
	893	885	886	
	807	807	811	
		788	789	νC-S
	775	781	780	
		767	762	
	723	729	728	
	641	641	647	NH_2 rock
	626	626	633	i.p. δpy
	588	539	567	NH_2 rock
	521			
	497			
	471	514	536	skeletal ring def.
		472	472	δNCS
	426	423	432	o.o.p. δpy
	417	412	416	νM-NH_2
	321	339	354	
	232	234	268	νM-py
	203	203	226	
		165	172	

Fig. 12. Ir spectra (700 - 150 cm^{-1}) of the complexes $M(amp)_2X_2$: M = Mn, Co; X = Br^-, SCN^-

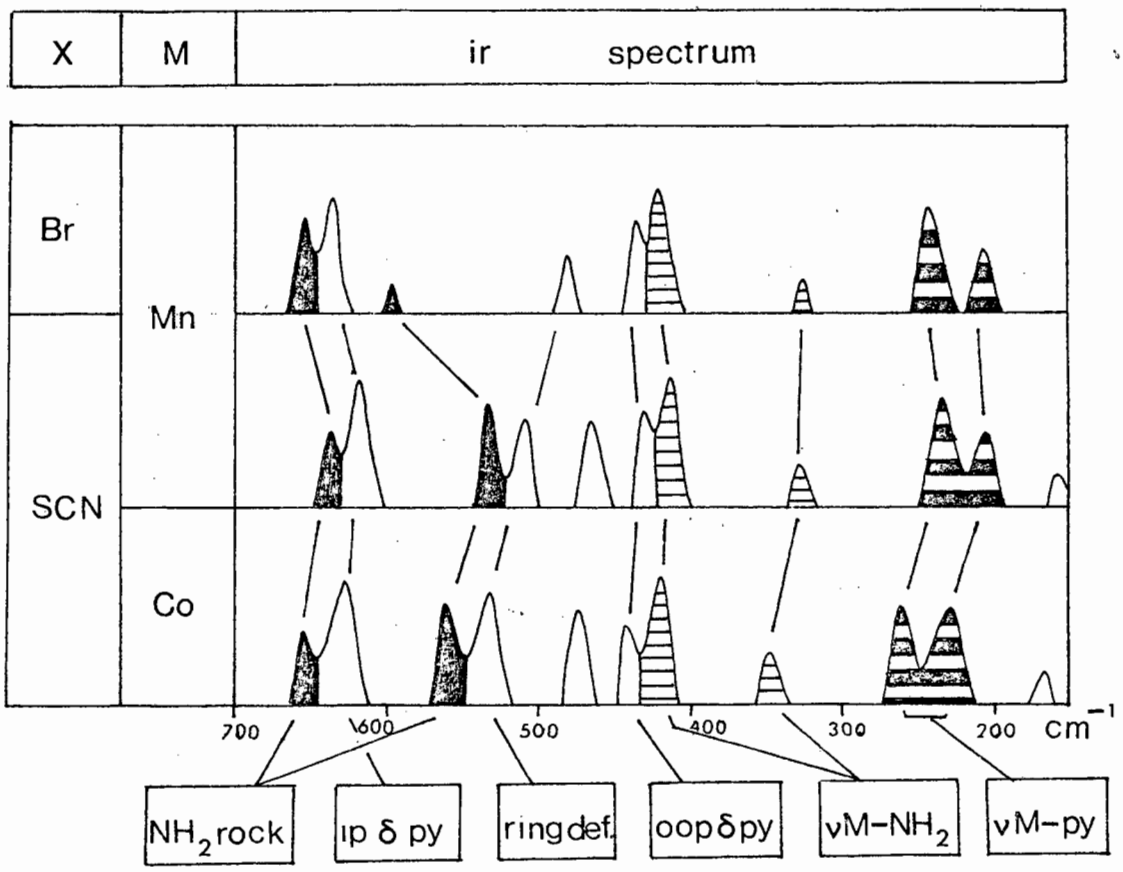

concerning frequency comparisons of series of metal complexes where only the metal-ion is varied. These data are now discussed.

The complexes $M(amp)_2X_2$: a final comparison

If structural variations are not significant in a series of metal complexes in which only the metal ion is varied, metal-ligand stretching frequencies are expected to mimic the sequence of calculated cfse values, and (if Cu(II) complexes are included) the Irving-Williams stability series. For the complexes $M(amp)_2Br_2$ the metal ion effect is most strongly exhibited by the higher frequency νM-NH_2 and the higher frequency νM-py modes giving rise to the sequence Mn < Ni < Cu > Zn. Similar bands in the complexes $M(amp)_2Cl_2.nH_2O$: M = Ni, Cu, Zn; n = 2, $1\frac{1}{2}$ again give rise to the sequence Ni < Cu > Zn as does the series $M(amp)_2I.nH_2O$: M = Ni, Cu, Zn; n = 2, 0. The only remaining relatively complete series of metal complexes with a particular anion are the *bis*(2-aminomethylpyridine) thiocyanate complexes. Again it is seen that the metal-ligand stretching frequencies are in the sequence Mn < Co < Ni < Cu. The above factors clearly support the assignments presented.

3.2.5 *Ir studies of mono(2-aminomethylpyridine) metal(II) complexes: assignments and structural aspects of the spectra*

The regions of the ir spectra which are considered significant to structural investigations of metal complexes, are those regions where metal-ligand modes are expected. Hence a detailed discussion of the bands between 700 and 150 cm^{-1} only is given. Diagrammatic representations of the spectra are given in Fig.13 while Table 23 lists the frequencies (4000 - 150 cm^{-1}) and proposed assignments.

3.2.5.1 *The complexes Pt(amp)X_2; X = Cl^-, Br^-, SCN^-*

In accordance with assignments made for the related *tris* and *bis*(2-aminomethylpyridine) complexes, the bands near 660, 420 and 470 cm^{-1} are assigned as the in-plane and out-of-plane pyridine ring deformations and a skeletal ring bend, respectively. Insensitivity of these bands to *N,N-d_2*-amino substitution supports these assignments. The somewhat high frequency of the in-plane deformation of the pyridine ring (some 50 cm^{-1} greater than is observed in spectra of analogous first transition series metal complexes) may be rationalized by considering the [Pt(amp)X_2] species to be square planar as are *cis* and *trans*[Pt(py)$_2$$Cl_2$], where the same ligand vibration is found near 670 cm^{-1} [175]. An additional band in this region at 476 cm^{-1} which is observed only in the spectrum of Pt(amp)(SCN)$_2$, is most likely a δNCS mode as evidenced by its sensitivity to ^{15}*N*CS isotopic substitution.

The band near 450 cm^{-1} is readily assigned to a νPt-NH_2

Fig. 13. The ir spectra (700 - 150 cm^{-1}) of the complexes $M(amp)X_2$

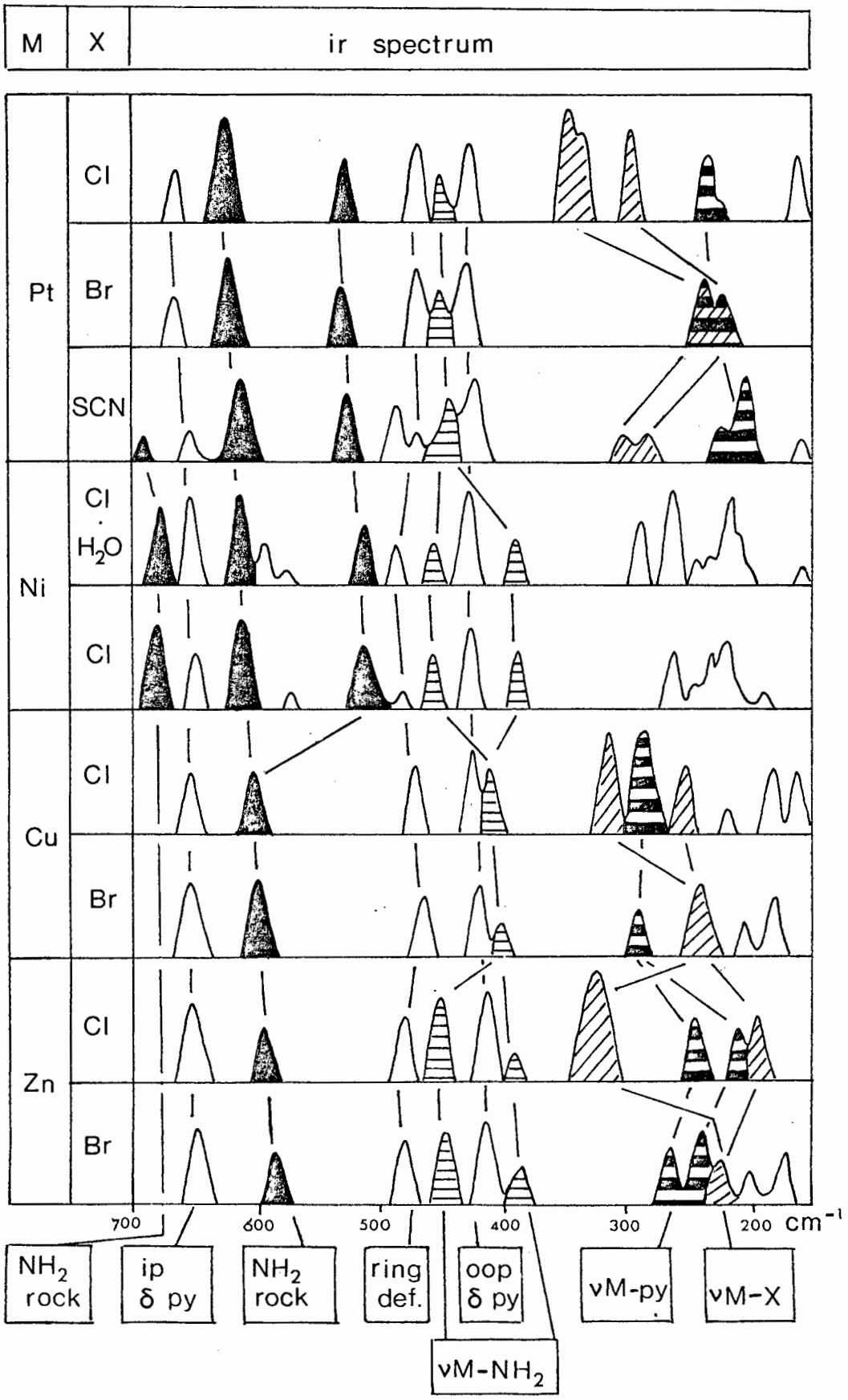

Table 23. Ir frequencies (4000 - 150 cm^{-1}) and band assignments for the complexes M(amp)X_2

M X	Ni	Ni[a]	Cu Cl	Zn	Pt	Cu	Zn Br	Pt	Pt SCN	Assignment
	3423		3291	3251	3228(806)[b]	3282(10,811)[c]	3280	3224	3244	
	3324	3300	3244	3161	3193(797)	3236(8,821)	3161	3189	3205	
	3291		3079		3115(813)	3089(12,803)		3117		
	3261		3031		3081(810)	3040(12,801)		3055		
	2990	2985	2988		2972	2981	2982	2963	2971	
	2950	2947	2948	2942	2935	2943	2940	2928	2940	
									2124(28)[d]	νC≡N
									2113(30)	νC≡N
		1631								OH_2 scissor
	1604	1603	1603	1615	1615	1603	1607	1614	1611	
	1590	1589	1582		1582(157)	1580(0,143)		1578	1598	
	1571	1570	1567	1571	1564	1563	1570	1565	1577	
	1481	1480	1480	1481	1488	1481	1482	1484	1486	
			1444	1439	1449	1451	1447	1448	1477	
	1434	1434	1430	1416	1422	1430	1436	1421	1456	
	1375	1371	1368	1383	1374	1369	1380	1376	1381	
	1321	1320		1332			1322	1321	1309	
	1283			1292	1289	1287	1287	1289	1279	
	1254	1260	1257	1255	1257(62)	1255(0,72)	1254	1257	1257	
	1220	1221	1229	1223	1226	1225	1225	1223	1225	
	1207	1206	1213	1179	1177(81)	1205(0,96)		1172	1208	
	1179	1181	1164	1157	1161	1162	1155	1161	1159	
	1151	1153	1118	1135	1115	1117	1127	1113	1152	
	1111	1110	1098	1099	1071(90)	1097(0,86)	1097	1073	1109	
	1091	1090								
	1054	1050	1056	1054	1062	1052	1053	1062	1061	
	1040	1043	1043	1031	1041	1040	1029	1041	1038	
	1027	1027	1027	1017	1014	1025	1013	1016	1009	
	979	980				975		972	974	
				968	975	965	969		947	
	932	933	931	935	943(52)	930(0,41)	933	939	927	
	893	894		889			891		896	e
					892				867	
					825			821	850	
	812	812		811	776(16)	817(0,14)	810	779	826	
	781	784	787	768	763	780	767	759	771	
								741	732	
	727	726	719	725	726	715	727		721	
	681	679							697	NH_2 rock
	649	651	654	652	668	651	648	666	661	i.p. δpy
	612	615	607	595	625(16)	599(2,f)	588	625	617	NH_2 rock
	570	591			531(12)			527	560	NH_2 rock
		576								OH_2 rock of co-ordinated water
									476(3)	δNCS
	513 g	514 g								
	480	488	472	481	471	468(2,3)	480	469	462	skeletal ring def.
	460	459		452	449(20)		449	449	442	νM-NH_2
	428	428	426	413	429	422	413	426	426	o.o.p δpy
	393	391	411	392		405(5,14)	386			νM-NH_2
					335			227	308	νM-X
			318	320	326	245	226	210	294	νM-X
	256	288	287	247		292	266		224	νM-py
	242	241		210			239		196	νM-py
	251 g	232 g	254		294	141				νM-X
	216	216			227(14)					νM-py + (δPt-NH_2)
				196	165					δL-M-L

[a] Ni(amp)Cl_2.H_2O. [b] Figs. in parentheses - $N,N\text{-}d_2$-shift. [c] Figs. in parentheses - ^{15}N(amino)- and $N,N\text{-}d_2$-shifts. [d] Figs. in parentheses - ^{15}NCS-shift. [e] The νC-S and 2δNCS modes expected in this region are most likely masked by ligand modes. [f] Disappears on amino deuteration.
[g] See text.

mode, since it experiences a shift of -20 cm^{-1} on aminodeuteration of the Pt(amp)Cl_2 complex. Also showing sensitivity to *N,N*-d_2- substitution are the bands at *ca.* 620 and 530 cm^{-1}; they may consequently be assigned to NH_2 rocking modes. The lower of the two may however contain a contribution from νPt-NH_2, since platinum-nitrogen stretches have been reported in this region [176-177].

A band near 230 cm^{-1} is found in all the Pt(amp)X_2 complexes and is therefore assigned to νPt-py. The low-frequency shoulder on νPt-py in the spectrum of Pt(amp)Cl_2 moves -14 cm^{-1} on deuteration and is therefore assigned to δPt-NH_2. In Pt(amp)Cl_2, a split band occurs near 330 cm^{-1} while in Pt(amp)Br_2 a similar split band is found at about 220 cm^{-1}, partially overlapping with νPt-py. Assignment of nearly-coincident bands is extremely difficult, but in this case has been simplified by the fact that similar overlap has been reported [178] in complexes of the form *cis*- $Ptpy_2Cl_2$. The split bands are presumably νPt-Cl and νPt-Br in the chloro- and bromo-complexes, respectively. Such an assignment yields a ratio νPt-Br:νPt-Cl of 0.67, which is entirely reasonable [172]. The analogous split bands in Pt(amp)$(SCN)_2$ occur at 308 and 294 cm^{-1}, and may be assigned to νPt-S modes, as evidenced by their ^{15}NCS insensitivity.

Remaining low frequency bands in the spectra of these complexes are most likely various deformations of the metal-ligand bonds but no more specific assignments are attempted. However the assignments which have been given are entirely consistent with the group theoretical predictions for a square-planar structure having localized symmetry C_s; *i.e.* 4*a'* ir active stretches: νPt-NH_2, νPt-py and 2νPt-X.

3.2.5.2 The complexes Ni(amp)Cl_2 and Ni(amp)$Cl_2.H_2O$

Similarities in the spectra of these two complexes indicate that they are isostructural. By analogy with the other complexes previously discussed the bands at about 650 and 428 cm^{-1} are assigned to in- and out-of-plane pyridine ring deformations respectively; similarly, the band at about 485 cm^{-1} is a skeletal ring deformation. The most likely assignments for the bands at 680, 6 0 and 570 cm^{-1} are to NH_2 rocking modes. Their number indicates that the amino groups do not always find themselves in the same environment, which situation would arise if the structures of the complexes are polymeric octahedral. This seems probable since many Ni(II) complexes have been found to be polymeric octahedral [176].

By comparison of these spectra with those of the *bis*-complexes Ni(amp)$_2X_2$ (also octahedral), the bands at about 460 and 392 cm^{-1} are assigned to νNi-NH_2, with an extra νNi-NH_2 arising at about 514 cm^{-1}, because of coupling interactions. The remaining bands which lie below 300 cm^{-1} are difficult to assign because of overlap of νNi-py and νNi-Cl (bridging).

3.2.5.3 The complexes Cu(amp)X_2: X = Cl, Br

Similarities in the spectra of these two complexes indicate that they are isostructural. The assignment of bands at about 650, 425 and 470 cm^{-1} to the two pyridine ring deformations and a skeletal ring bend respectively are confirmed by the insensitivity of these bands to ^{15}N- and N,N-d_2-amino substitutions in Cu(amp)Br_2. The band at about

600 cm^{-1} disappears on aminodeuteration of $Cu(amp)Br_2$ and is subsequently assigned to an NH_2 rocking mode. The smaller *N,N-d_2* sensitivity (-14 cm^{-1}) and concomitant ^{15}N-amino sensitivity (-5 cm^{-1}) allow the assignment of the band at about 400 cm^{-1} to $\nu Cu-NH_2$. A band unshifted by either form of isotopic substitution is found near 290 cm^{-1} in both the chloro- and bromo-complexes; it is therefore the $\nu Cu-py$ expected in that region. Significant bands still to be assigned are at 318 and 254 cm^{-1} in $Cu(amp)Cl_2$ and 245 cm^{-1} in $Cu(amp)Br_2$. These bands are most likely $\nu M-Cl$ and $\nu M-Br$ respectively.

Nicholson and Sutton [58] have shown by conductance and magnetic moment measurements that in general $Cu(amp)X_2$ complexes are most likely dimers based upon double halogen-to-copper bridging consistent with five-coordinate copper rather than monomers consistent with four-coordinate behaviour, while an x-ray investigation [73] has shown that $Cu(amp)Br_2$ has a polymeric structure, with a distorted octahedral geometry about each copper centre.

3.2.5.4 The complexes $Zn(amp)X_2$: $X = Cl^-, Br^-$

Similarities in the spectra of these two complexes are again indicative of isostructurality. Assignments are made by analogy with those of complexes discussed previously. Of greatest interest are the metal-ligand modes: two bands attributable to $\nu Zn-NH_2$ are observed near 450 and 390 cm^{-1} in in the spectra of both complexes while two bands attributable to $\nu Zn-py$ are observed at 247 and 210 cm^{-1} in the chloro complex, and 266 and 239 cm^{-1} in the bromo complex. In

$Zn(amp)Cl_2$, νZn-Cl is assigned at 320 cm^{-1}. The analogous νZn-Br mode in the bromo complex is presumably the absorption at 226 cm^{-1} giving the reasonable [172] ratio of 0.7 for νM-Br:νM-Cl. Additional νM-L modes over and above those predicted for the C_s point symmetry of a tetrahedral structure are considered to owe their existance to distortions of the chelating ligand.

The complexes $M(amp)X_2$: a final comparison

Structural differences in this series of complexes prevent any correlation between νM-L and the sequence of calculated crystal field stabilization energies. However the lower frequency of νM-Cl in the Cu(II) complex than in the related $Zn(amp)Cl_2$ supports the supposition [58] that $Cu(amp)Cl_2$ has a higher coordination number than the Zn(II) complex.

3.3 THE IR SPECTRA OF *BIS*- AND *MONO*-2-(2-AMINOETHYL)-PYRIDINE COMPLEXES OF COPPER(II) AND ZINC(II) PERCHLORATES, TETRAFLUOROBORATES, HALIDES AND PSEUDOHALIDES

An investigation of the ir spectra of metal complexes of 2-(2-aminoethyl)pyridine is of particular interest in this work in so far as a number of correlations with the data obtained for the metal complexes of 2-aminomethylpyridine can be anticipated: the structural similarity of the two ligands implies that many of the ligand modes giving rise to absorptions in the ir spectra will be virtually the same for both types of species; that chelation occurs through identical donor atoms is likely to simplify the assignment of metal-ligand modes in the spectra of the 2-(2-aminoethyl)pyridine complexes; and finally similarities in the configurations of the ligands around the metal ions can be expected. Again, in an investigation of the bonding of the ligands around the metal ions, it is the metal-ligand modes which are of greatest interest. Metal-to-amino nitrogen vibrations are designated M-NH_2, while metal-to-pyridine-nitrogen modes are termed M-py. Under all symmetry conditions, the number of νM-NH_2 bands is most likely the same as the number of νM-py modes in a given complex. Therefore since the identification of νM-py is often complicated by νM-X bands occurring in the same region [28,32,95,171] assignment of the number of νM-py modes has largely been based upon the more easily discernible νM-NH_2 bands.

3.3.1 *The spectrum of the free ligand aep (800 - 150 cm^{-1})*

As depicted in Figs. 14 and 16, only six bands are observed at 770, 750, 592, 516, 415 and 395 cm^{-1}. As in the spectrum of 2-aminomethylpyridine the band at 592 cm^{-1} is most likely the in-plane deformation of the pyridine ring [88] while that at 516 cm^{-1} is the CCN bend of the side chain [167]. The absorption at 415 cm^{-1} is therefore the out-of-plane pyridine ring deformation, with the additional peak at 395 cm^{-1} arising from a C-C bend of the ligand side chain [83]. The two remaining bands in this region at 770 and 750 cm^{-1} are somewhat high in frequency for the expected NH_2 rocking modes; an alternative assignment to out-of-plane C-H deformations is proposed, indicating that the NH_2 rocking modes are not ir active in the free ligand.

3.3.2 *The bis complexes $M(aep)_2X_2$: M = Cu(II), Zn(II); X = Br^-, I^-, SCN^-, BF_4^- and ClO_4^-*

Ir frequencies (4000 - 150 cm^{-1}) and assignments are listed in Table 24, while the spectra are depicted in Fig. 14. Only the region 800 - 150 cm^{-1} is discussed.

Without exception, all the ligand bands are easily discernible in the spectra of the complexes, and it is noted that they frequently experience a high-frequency shift. Assignments of these absorptions is therefore straightforward, the δCCN mode of the ligand taking the form of a skeletal deformation of the chelate ring. Bands arising from vibrations

Table 24. Ir frequencies (4000 - 150 cm^{-1}) and band assignments for the complexes $M(aep)_2X_2$

X / M	Br	I	SCN Cu	BF_4	ClO_4	ClO_4 Zn	Assignments
	3258	3301	3244	3340	3323	3321	
	3191	3225	3159	3293	3272	3268	νN-H
	3123	3146	3071	3189	3170	3133	
	2966	2953	2944	2980	2983	2968	
	2941	2921	2936	2988	2961	2910	νC-H
	2886	2854	2881	2901	2895	2849	
			2068				νC≡N
			2061				
	1602	1608	1609	1613	1614	1615	
	1575	1582	1595	1601	1594	1588	
	1568	1564	1568	1570	1570	1576	
	1478	1482	1481	1488	1487	1490	
	1448	1452	1449	1452	1452	1465	
	1435	1435	1441	1443	1441	1447	
	1375	1368	1364	1374	1377	1392	
	1337	1345	1345	1351	1348	1364	
		1321	1329	1330	1329	1327	
	1307	1310	1314	1320	1319	1305	
	1246		1248	1293		1263	
	1221	1207	1218	1249	1252	1248	
	1170	1173	1176	1239	1237		
	1156		1152	1225	1223	1219	
	1131	1139		1167	1166		
					1155	1148	
	1114	1097	1103		1103		
					1076	1086	ClO_4 ν_3
	1052	1066	1065				
	1030	1038	1042	1073	1043	1034	
	1020	1027	1024	1028	1028		
	1004	1011	1001	1000	1014	990	
	960	965	960	972	969	949	
					933	935	ClO_4 ν_1
					925		
			935				2δNCS
			890				δC-S
	907						
	891	895	890	904	898	885	
	832	860	860	860	857	859	
	813						
	781	786	781	787	788	787	o.o.p. δC-H
	777	771	766	777	770	774	
	758			740		750	
	732	725	726	725	730	725	NH_2 rock
						678	
	648	649	647	651	649	654	i.p. δpy
					623	626	δClO_4
	600	617	616	608	607		NH_2 rock
	572	596	600				
				523			δBF_4
	514	516	522		518	507	skeletal ring def.
	460	491	492	495	496	465	$\nu M-NH_2$
			468				δNCS
	429	434	432	435	435	433	o.o.p. δpy
	409	413	413	416	416	417	o.o.p. δC-C
	382			400			$\nu M-NH_2$
	344	347	341	353	356	323	νM-py
				344			
	307			292			νM-py
	277	288	287	253	291	298	
	236	249	240	225	252	227	νCu-Br
	212						
		224	220	193	197	205	
	173	195	200	176		184	

Fig. 14. The ir spectra (800 - 150 cm^{-1}) of the *bis* complexes $M(aep)_2X_2$

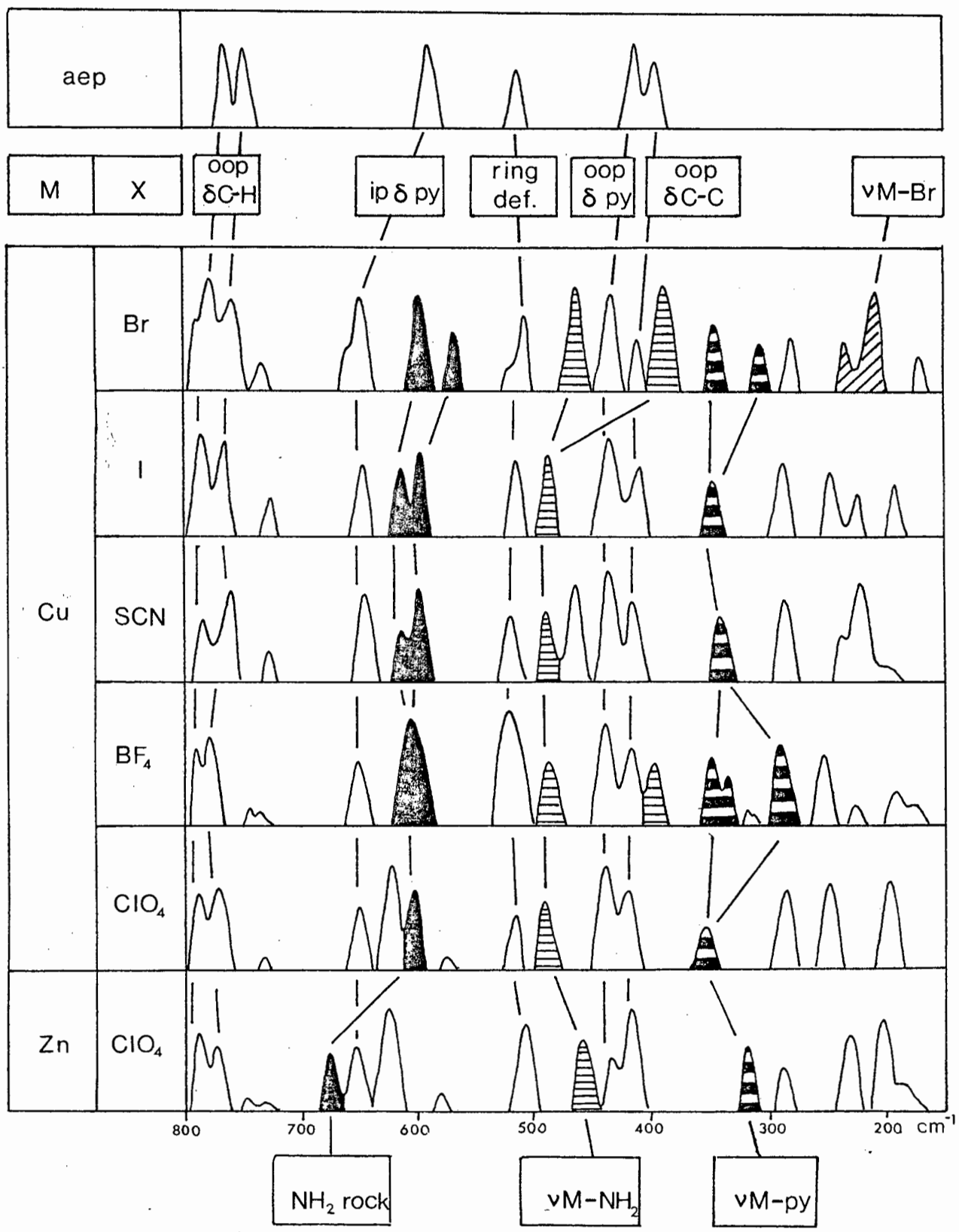

of the anionic species alone are expected for the SCN^-, ClO_4^- and BF_4^- complexes: a δNCS mode at 468 cm^{-1} is observed for $Cu(aep)_2(NCS)_2$; additional bands near 625 cm^{-1} in the spectra of both the Cu(II) and Zn(II) perchlorates are presumably [18] δClO_4 vibrations, while an analogous δBF_4 mode at 523 cm^{-1} is also observed in the spectrum of $Cu(aep)_2(BF_4)_2$ coinciding with the skeletal ring deformation of the chelated ligand, as evidenced by the enhanced intensity of this band. Bands above 500 cm^{-1} still to be assigned occur at frequency values comparable to those of the NH_2 rocking modes observed in the spectra of the 2-aminomethylpyridine complexes and they are therefore similarly assigned. All remaining bands are metal-ligand modes, and their assignment and structural implications are now discussed. By analogy with the findings of Section 3.2 $\nu M\text{-}NH_2$ modes are expected in the region 370 - 500 cm^{-1}. In the spectra of the 2-(2-aminoethyl)pyridine complexes, the bands observed in this region over and above the previously identified ligand modes are therefore assigned to $\nu M\text{-}NH_2$.

Only one such vibration at 491 cm^{-1} is observed for the complex $Cu(aep)_2I_2$. A crystallographic investigation of the iodide complex [78] has reported that the complex is four-coordinate with a *trans*-square planar geometry at the copper ion. The observation of only one $\nu Cu\text{-}NH_2$ is group theoretically consistent with the D_{2h} localized point symmetry of such a structure. The band at 347 cm^{-1} is subsequently assigned to a νCu-py mode. The relatively high frequency values of these metal-ligand stretching vibrations are ascribed to the fact that the Cu(II) exhibits a square-planar configuration, bonding power being distributed over only four coordination sites.

Virtually identical $\nu M\text{-}NH_2$ and νM-py vibrations are

observed at 492 and 341 cm^{-1} in the spectrum of $Cu(aep)_2(NCS)_2$. However a crystallographic investigation of this complex [82] reports a tetragonally distorted six-coordinate geometry at the copper, the aep ligands occupying the *trans*-planar coordination sites while NCS^- groups weakly bonded to the Cu(II) ions are in the axial positions. Such a structure still has localized D_{2h} point symmetry, in which case the number of $\nu Cu\text{-}NH_2$ and $\nu Cu\text{-}py$ modes is as predicted theoretically. An additional weak $\nu Cu\text{-}NCS$ mode is also expected and although no definite assignment is able to be made, it most likely gives rise to one of the remaining absorptions below 250 cm^{-1}. The relatively high frequencies of $\nu Cu\text{-}NH_2$ and $\nu Cu\text{-}py$ support the contention that the Cu-NCS bonding is weak, *i.e.* it employs very little of the metal-bonding power, leaving the Cu(II) ion essentially four-coordinate.

An x-ray report on the complex $Cu(aep)_2(ClO_4)_2$ [81] indicates that the molecule is a six-coordinate monomer, the two aep ligands constituting the equatorial plane, while the perchlorate groups are very weakly coordinated at the axial positions, having Cu-O bond lengths of 2.883(2) Å. The observation of one $\nu Cu\text{-}NH_2$ at 498 cm^{-1} and hence only one $\nu Cu\text{-}py$ at 356 cm^{-1} is consistent with the group theoretical predictions for the D_{2h} localized point symmetry of such a *trans*-planar tetragonal structure in which case a $\nu Cu\text{-}O$ band due to the coordinated perchlorate is expected in the very low frequency regions of the ir spectrum. However, Hathaway *et al.* [179] concluded that for perchlorate complexes, the appearance of a strong band near 1080 cm^{-1} and a weak band

near 930 cm^{-1} being assigned to the ir-allowed ν_3 and the ir-forbidden ν_1 modes, respectively, of the perchlorate ion, are consistent only with non-coordinated perchlorate. The observation of these bands in the ir spectrum of $Cu(aep)_2(ClO_4)_2$ therefore suggests that insofar as vibrational studies are concerned, the Cu-O bond length is too great for the perchlorate to be considered coordinated. Support for this proposal is received not only from the number of metal-ligand stretching modes observed (a *trans*-square planar structure is still of D_{2h} localized point symmetry, requiring one νCu-NH_2 and one νCu-py) but also from the fact that the frequency values of these modes are high, indicative of a four- rather than a six-coordinate geometry.

The ir spectrum of the complex $Zn(aep)_2(ClO_4)_2$ also reveals only one band at 465 cm^{-1} attributable to νZn-NH_2, allowing the assignment of the absorption at 323 cm^{-1} to a corresponding νZn-py. The lower frequencies of these metal-ligand stretching modes as opposed to those assigned in the $Cu(aep)_2(ClO_4)_2$ complex is entirely expected in terms of the metal-ion effect. The Zn(II) complex is presumably tetrahedral, the perchlorate groups lying outside of the coordination sphere of the metal ion.

The structure of $Cu(aep)_2(BF_4)_2$ might be expected to be the same as that of the analogous perchlorate complex, owing to the fact that the two types of anion are so similar. However the ir spectrum of the former reveals a doubling of bands which may be assigned to νM-NH_2 modes at 495 and 400 cm^{-1}. This phenomenon may be attributed to a change in structure;

or as observed in the related $M(amp)_3(BF_4)_2$ (Sections 3.2.2 and 3.2.3) and $Cu(amp)_2(BF_4)_2$ (Section 3.2.4.), the increased complexity of the ir spectrum may arise from disordering of the BF_4 anions.

The final complex to be discussed in this Section is $Cu(aep)_2Br_2$. Two νCu-NH_2 bands are observed at 460 and 382 cm^{-1} indicating that the absorptions at 344 and 307 cm^{-1} are most logically assigned to νCu-py. The observation of four metal-to-ligand stretching modes is consistent with the group theoretical calculations based upon a five-coordinate *trans*-structure having localized C_{2v} point symmetry. (see Fig. 15).

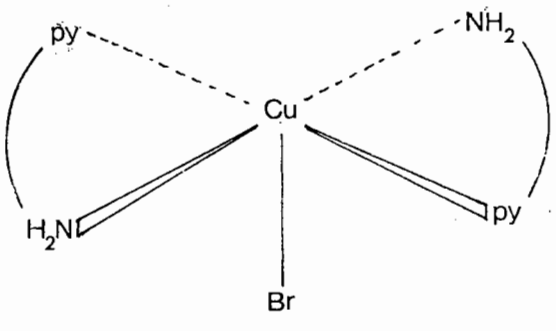

Fig. 15. Diagrammatric representation of five-coordinate *trans* structure of $Cu(aep)_2Br_2$

Such a structural proposal is confirmed by a previously-reported x-ray investigation of the complex [80]. The expected νCu-Br mode is assigned to the relatively intense band in the spectrum at 212 cm^{-1}.

Remaining low frequency vibrations in the spectra of the *bis*{2-(2-aminoethyl)pyridine} complexes are presumably metal-

ligand bending modes, but no attempt at their specific assignment is made.

3.3.3 *The mono complexes M(aep)X_2: M = Cu(II), Zn(II); X = Cl^-, Br^-, I^-*

Ir frequencies (4000 - 150 cm^{-1}) and band assignments of these complexes are listed in Table 25, while the spectra are depicted in Fig. 16. Again, only the region 800 - 150 cm^{-1} is discussed. As observed in Section 3.3.2 with reference to the spectra of the *bis*{2-(2-aminoethyl)pyridine} complexes, bands of the free ligand are all apparent in the spectra of the *mono* complexes, generally having undergone a high frequency shift on complexation. They are therefore assigned as discussed previously. Additional bands near 740 and 575 cm^{-1} are also assigned to ligand modes: NH_2 rocking vibrations, which again appear to have been activated only on the formation of the metal complexes.

In the spectral region 500 - 370 cm^{-1} where $\nu M\text{-}NH_2$ modes are expected, only one band attributable to such a vibration is observed for each of the complexes. It occurs at about 480 cm^{-1} in each of the copper complexes and at a slightly lower frequency in the spectra of the zinc analogues.

X-ray investigations [77,79] of $Cu(aep)Cl_2$ and $Cu(aep)Br_2$ show that despite very minor differences, the crystals of the two complexes are isomorphous, the halide ions acting as bridges between six-coordinate distorted octahedra around the central copper(II) ions. The fact that $\nu M\text{-}NH_2$ modes in the zinc complexes are only very slightly lower in frequency than those

Fig. 16. The ir spectra (800 - 150 cm^{-1}) of the *mono* complexes M(aep) X_2

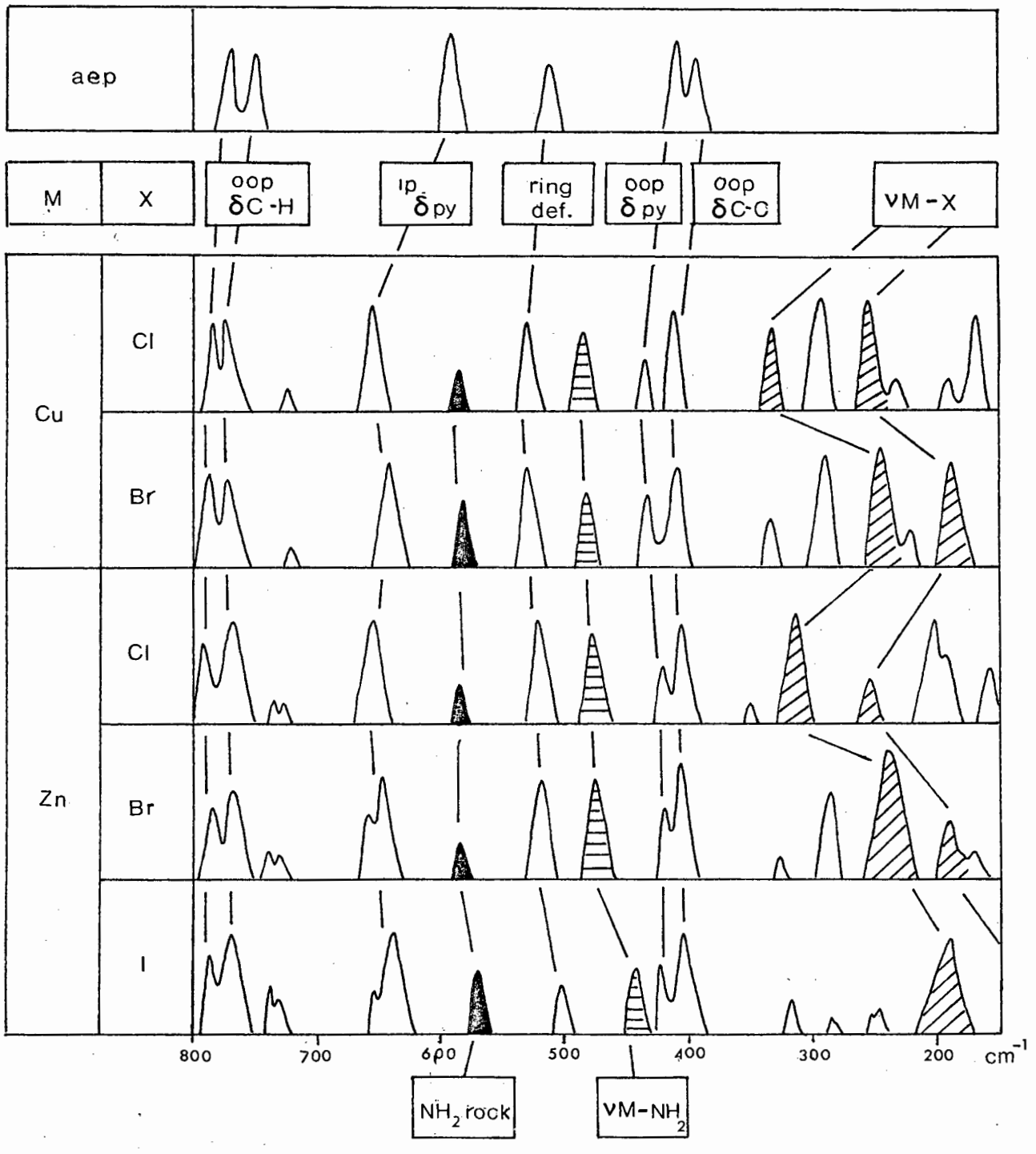

Table 25. Ir frequencies (4000 - 150 cm^{-1}) and band assignments for the complexes $M(aep)X_2$

X	Cl	Br	Cl	Br	I	Assignments
	Cu			Zn		
	3259	3246	3259	3248	3273	
	3197	3188	3222	3232	3227	νN-H
	3115	3107	3155	3149	3132	
	3055	3052	2963	2959	3074	
	2981	2970	2955	2951	2952	
	2964	2958	2913	2906		νC-H
	2942	2937	2888	2887	2893	
	2926	2918	2852	2850		
	2876	2869				
	1607	1605	1610	1610	1611	
	1575		1598	1593	1581	
	1567	1567	1571	1570	1568	
	1480	1480	1484	1484	1487	
	1446	1446	1460	1458	1458	
	1432	1432	1447	1446	1445	
	1369	1370	1384	1383	1386	
	1354	1352	1350	1349	1367	
	1313	1314	1321	1322	1311	
	1251	1249	1256	1258	1263	
	1236	1235	1239	1239	1246	
	1223	1222	1222	1223	1217	
	1206	1200				
	1159	1159	1161	1160	1157	
	1147	1142	1145	1142	1126	
	1106	1105	1103	1105	1105	
	1060	1064	1066	1066	1062	
	1050	1049	1040	1040	1046	
	1027	1025	1031	1031	1028	
	1014	1012			1018	
	999	997	990	989	989	
	964	961			971	
	952	950	947	947	949	
	892	889	897	897	898	
	875	873	860	859	860	
	786	784	783	781	781	o.o.p. δC-H
	777	774	769	768	769	
			738	743	742	NH_2 rock
	726	723	726	728	727	
	654	644	653	654	651	i.p. δpy
				641	636	
	580	577	581	579	574	NH_2 rock
	529	527	517	517	501	skeletal ring def.
	487	483	475	473	448	$\nu M\text{-}NH_2$
	430	429	421	420	419	o.o.p. δpy
	411	409	403	403	403	o.o.p. δC-C
					317	
					286	
		331	351	325	247	
		294		287	213	
	336	245	313	231	194	νM-X
	298	221				
	251	190	251	195		νM-X
	232					
	181		200			
	164		158	169		

in their copper analogues, indicates that the metal-ion effect is possibly being outweighed by the coordination number effect. Hence, the zinc complexes probably have a four-coordinate tetrahedral structure. In the region below 350 cm^{-1}, assignment of the expected νM-py vibrations is complicated by the presence of νM-X modes and has therefore not been attempted. However, on the basis of the ratios of νM-Br:νM-Cl predicted by Clark [172] the antisymmetric and symmetric metal-halogen stretching frequencies have been identified. The assignments of these bands as presented in Table 25 yield, for the copper complexes, νM-Br:νM-Cl ratios of 0.73 and 0.76 for the higher and lower bands, respectively. For the zinc complexes, νM-Br:νM-Cl ratios of 0.74 and 0.78 for the higher and lower absorptions, respectively, are obtained. In the spectrum of $Zn(aep)I_2$, the very intense peak at 194 cm^{-1} is presumably the antisymmetric νZn-I vibration, the symmetric stretching mode occurring beyond the range of measurement. The observation of one $\nu M\text{-}NH_2$ and two νM-X modes in each of the spectra of the complexes is group-theoretically consistent with the structures proposed.

3.4 QUINOLINE, QUINOLINE-d_7 AND THEIR COMPLEXES

3.4.1 Examination of ν^D/ν^H for ir bands assigned to C-H(D) and ring vibrations in quinoline, quinoline-d_7, and their metal complexes

The ir frequency data (4000 - 140 cm^{-1}) and band assignments for quinoline and quinoline-d_7 are reported in Table 26. Correlations between the spectra of the unlabelled and labelled species are complicated by the fact that some of the bands experience substantial shifts on deuteration; identification of corresponding vibrations was hence carried out in the following manner: using previous assignments [86] of quinoline modes, together with deuterated/undeuterated ratios calculated from data reported [85] for naphthalene and naphthalene-d_8 (*viz.* 0.92 ± 0.06 for ring modes and 0.79 ± 0.06 for C-H modes), expected positions for bands in the spectrum of quinoline-d_7 were deduced. These calculated frequencies were compared with those in the experimentally-determined spectrum of quinoline-d_7. Despite minor shifts, agreement between the calculated and observed spectra was found to be excellent, with the exception of the band observed in the experimentally-determined spectrum of quinoline at 866 cm^{-1} which was found to shift to 696 cm^{-1} in the spectrum of quinoline-d_7, yielding a ratio of 0.80 for ν^D/ν^H. This indicates that the previous assignment [86] of this mode to a ring vibration is possibly incorrect. Identification of this band as a δC-H(D) mode is more consistent with the data reported here.

Band assignments for the related ligands, pyridine and pyridine-d_5 have previously been established [180-184]. Based on the assignments of Kline and Turkevich [181] the ratio ν^D/ν^H falls within the ranges 0.76 ± 0.03 (C-H modes) and 0.94 ± 0.04

Table 26. Ligand bands and assignments for quinoline, quinoline-d_7 and their metal complexes[a]

Quin.			$Co(quin)_2Cl_2$			$Cu(quin)_2Cl_2$			$Zn(quin)_2Cl_2$			$Co(quin)_2Br_2$			$Ni(quin)_2Br_2$			$Cu(quin)_2Br_2$			$Zn(quin)_2Br_2$			$Zn(quin)_2I_2$			$Cu(quin)_2SCN_2$			$Zn(quin)_2SCN_2$			Assignments [85,86]	
H_7	d_7	ratio	H_7	d_7	ratio	H_7	d_7	ratio	H_7	d_7	ratio	H_7	d_7	ratio	H_7	d_7	ratio	H_7	d_7	ratio	H_7	d_7	ratio	H_7	d_7	ratio	H_7	d_7	ratio	H_7	d_7	ratio	(band number)	
3054	2275	0.74	3077			3070			3080			3077												3065									νC-H	(1,41)
3034	2256	0.74	3062	2260	0.74	3052	2274	0.75	3061	2269	0.74	3060	2278	0.74	3073	2272	0.74	3048			3077	2274	0.74	3045	2278	0.75	3063	2276	0.74	3076	2280	0.74	νC-H	(14,29)
3003	2243	0.74	3052	2254	0.74	3044	2256	0.74	3054	2257	0.74	3050	2261	0.74	3053	2260	0.74	3028	2260	0.75	3052	2266	0.74	3005	2255	0.75	3048	2256	0.74	3048	2262	0.74		
																											2111	2111	(21)[b]	2072	2072	(29)[b]	νN≡CS	
																											2082	2080	(32)[b]					
1619	1584	0.97	1620	1588	0.98	1619	1590	0.98	1620	1589	0.98	1619	1587	0.98	1619	1587	0.98	1619	1589	0.98	1620	1589	0.98	1621	1585	0.98	1619	1598[c]	0.98	1621	1590	0.98	ν ring	(16)
1594	1551	0.97	1594	1558	0.98	1592	1557	0.98	1593	1559	0.98	1593	1558	0.98	1592	1558	0.98	1592	1555	0.98	1593	1559	0.98	1590	1559	0.98	1592	1555	0.98	1595	1561	0.98	ν ring	(17,31)
1569	1542	0.98	1584	1543	0.97	1582	1544	0.98	1585	1546	0.98	1583	1543	0.97	1581	1544	0.98	1581	1543	0.98	1584	1544	0.97	1582	1543	0.98	1583	1543	0.97	1586	1545	0.97	ν ring	(3)
1549	1219	0.83		1282			1275			1283			1282		1556	1277	0.82		1264		1548				1263			1277		1551				
1533	1451	0.95	1550	1478	0.95	1550	1463	0.94	1548	1465	0.95	1550	1460	0.94	1546	1458	0.94	1552	1454	0.95	1544	1460	0.95	1544	1460	0.95	1540			1540				
1512	1224	0.81																																
1500	1438	0.96	1509	1448	0.96	1506	1448	0.96	1510	1447	0.96	1509	1448	0.96	1507	1448	0.96	1505	1444	0.96	1510	1448	0.96	1508	1449	0.96	1508	1447	0.96	1510	1450	0.96	ν ring	(44)
1468	1383	0.94	1462	1380	0.94	1464	1382	0.94	1464	1380	0.94	1463	1380	0.94	1462	1380	0.94	1462	1381	0.94	1465	1380	0.94	1462	1381	0.94	1462	1388[c]	0.95	1466[c]	1379	0.94		
1453	1366	0.94	1441	1364	0.95		1364			1365		1458	1363	0.93		1363			1364		1459	1365	0.94	1454	1366	0.94	1437	1362	0.95	1444	1367	0.95		
1430	1163	0.81	1435	1167	0.81	1439	1164	0.81	1437	1160	0.81	1435	1160	0.81	1438	1160	0.81	1438	1167	0.81	1437	1155	0.80	1437	1160	0.81	1434	1164	0.81	1439	1165	0.81	δC-H	(18)
1412	1303	0.92		1318			1316		1418	1320	0.93	1416	1336	0.94	1409	1332	0.95	1397	1315	0.94		1320			1318			1314			1318			
1391	1281	0.92	1401	1296	0.93	1392	1292	0.93	1402	1296	0.92	1400	1295	0.93	1396	1295	0.93	1391	1292	0.93	1401	1297	0.93	1398	1295	0.93	1399	1292	0.92	1400[c]	1297	0.93	ν ring	(32)
1370	1239	0.90	1376	1237	0.90	1379	1238	0.90	1375	1241	0.90	1375	1234	0.90	1375	1235	0.90	1377	1238	0.90	1376	1240	0.90	1376	1238	0.90	1375[c]	1238	0.90	1375	1241	0.90	ν ring	(4)
1336	1257	0.94		1268			1265														1351										1328	1258	0.95		
1332	1232	0.92	1328	1254	0.94				1328	1252	0.94	1327	1250	0.94	1330			1321			1328			1320	1246	0.94		1252		1317	1252	0.95		
1312	1092	0.83	1308[c]	1098	0.84	1313	1099	0.84	1310[c]	1099	0.84	1307[c]	1097	0.84	1311	1097	0.84	1311	1098	0.84	1309[c]	1098	0.84	1309	1098	0.84	1310	1099	0.84	1312	1098	0.84	δC-H	(33)
1278	1036	0.81	1282	1035	0.82		1044		1282	1044[c]	0.81	1282	1046	0.82	1280	1046	0.82	1280	1044	0.82	1282	1044[c]	0.81	1279	1046	0.82		1041		1298	1046	0.81	γC-H	(10)
1253	1015	0.81	1274	1028	0.81	1265	1017	0.80	1276	1020	0.80	1275	1015	0.80	1278	1016	0.79	1268[c]	1018	0.80	1266	1020	0.81	1263	1016	0.80	1268	1017	0.80	1266	1021	0.81	δC-H	(5)
1230	1024	0.83	1236			1232			1237			1236			1228			1230			1236			1233			1235			1240				
1215	963	0.79	1225	975	0.80	1206	972	0.81	1226	975	0.80	1227	975	0.79		962			972		1228	975	0.78	1218	976	0.80	1219	974	0.80	1221	978	0.80		
1191	915	0.78	1201			1190	929	0.78	1201			1200			1198			1205	928	0.77	1201			1200	927	0.77	1205	927	0.77		933			
			1164			1165			1164			1162						1160			1163			1156			1151			1152				
1139	891	0.78	1140	906	0.79	1137	907	0.80	1140	908[c]	0.80	1141	905	0.79	1146	906	0.79	1139	907	0.80	1141	901[c]	0.79	1141[c]	906[c]	0.79	1143	901	0.79	1143	906	0.79	γC-H	(26)
1117	876	0.78	1130	880	0.78	1131	891[c]	0.79	1131	880[c]	0.78	1129	883	0.78	1129[c]	884	0.78	1131	890[c]	0.79	1129	885[c]	0.78	1126[c]	883	0.78	1128	893	0.79	1134	880	0.78	δC-H	(19,45)
1094	860	0.79	1090	846	0.78	1092	843	0.77	1091	841	0.77	1089	846	0.78	1100	847	0.77	1089	842	0.77	1089			1083	879	0.81	1090	879	0.81	1088	875	0.80	γC-H	(37)
1031	932	0.90	1053[c]			1056[c]			1053[c]			1054			1056			1050			1054			1054			1053	947	0.90	1060	948	0.89	δ ring	(6)
1012	838	0.83	1020	832	0.82	1019			1023	832	0.81				1024			1018				831		1024	848	0.83	1020	844	0.83	1022	845	0.83	δC-H	(46)
978	825	0.84	991	825	0.83	999[c]	829	0.83	992	827	0.83	991	827	0.83	995[c]	828	0.83	998[c]	830	0.83	991	825	0.83	987	835	0.85	990	827	0.84	991	830	0.84		
952	749	0.79	967	758	0.78		757		971	760[c]	0.78	967	757	0.78	972						970				782[c]			752		975	760	0.78	γC-H	(22)
938	780	0.83	959[c]	780	0.81	959	779	0.81	958[c]	780	0.81	959[c]	780	0.81	957[c]	779	0.81	958	778	0.81	959[c]	780	0.81	953	791	0.83	955[c]	777[c]	0.81	956	782[c]	0.82	δC-H	(7)
924	712	0.77		718[c]			715[c]			719[c]			713		889	718	0.81	889	721	0.81		719			717			724[c]			718[c]			
																								889	690	0.76	862	680	0.79	864[c]	678	0.78	δ ring	(20)
866	696	0.80[e]	861	684	0.79	864	670	0.78	863	683	0.79	862			866			861			862	713	0.83					927[d]			967[d]		2δNCS	
842	806	0.96		791			801			792			791			791			787			792		845	825[c]	0.97		801			815		γ ring	(12)
																											835	835	(13)[b]	839	839	(13)[b]	νNC-S	
803	641	0.80	809	642	0.79	811	647	0.80	811	644	0.79	809	641	0.79	807	640	0.79	808	643	0.80	810	643	0.79	803	640[c]	0.80	805	638	0.79	805	638	0.79	γC-H	(23)
784	613	0.78	781	610	0.78	782	614	0.79	781[c]	609[c]	0.78	781[c]	610	0.78	779[c]	611	0.78	781	613	0.78	781	612[c]	0.78	782	608	0.78	777	614	0.79	783[c]	612	0.78	γC-H	(38)
758	674	0.90	723			723			720												773			776[c]	650	0.84				775			δ ring	(8)
742	665	0.90		667			661			665			649			647								742	660	0.89		661		740	661	0.89	δ ring	(47)
736	584	0.79	740	575	0.78	740	583	0.79	741	575	0.78	740	580	0.78	746	579	0.78	744			741	575	0.78	731	575	0.79	729	573	0.79	734	573	0.78	γC-H	(27)
627	589	0.94	637	582	0.91	636	593	0.93	634	592	0.93	634[c]	592	0.93	635	589	0.93	637	591	0.93	633	590	0.93	632	588	0.93	633[c]	591	0.93	637	591	0.93	δ ring	(35)
610	568	0.93	634			624			622			622			623						622			921	570	0.92	623			621			δ ring	(21)
521	504	0.97	528[c]	510[c]	0.97	530[c]	513	0.97	528[c]	511[c]	0.97	528[c]	511	0.97	527[c]	511	0.97	530	512	0.97	527[c]	511[c]	0.97	527[c]	509[c]	0.97	528[c]	503[c]	0.95	529[c]	512[c]	0.97	δ ring	(9)
477	417	0.87	488	432[c]	0.89	499	444	0.89	485	428	0.88	487[c]	432	0.89	486	432	0.89	498	442	0.89	485	432[c]	0.89	484	428	0.88	488	431	0.88	485[c]	428	0.88	γ ring	(24)
																												470[d]			481[d]		δNCS	
469	409	0.87	464	408	0.88	466	410[c]	0.88	464	408	0.88	465	407	0.88	464	408	0.88	464	406	0.88	464	408	0.88	463	407	0.88	465	405	0.87	463[c]	406	0.88	δ ring	(48)
390	351	0.90	397	362	0.91	404	365	0.90	397	364	0.92	399	359	0.90	396	360	0.91	404	365	0.90	397	365	0.92	397	364	0.92	402	364	0.91	398	365	0.92	γ ring	(13)
375	345	0.92	393	356	0.91	398	360	0.90	393	356	0.91	394	355	0.90	392	355	0.91	398	360	0.90	393	357	0.91		354		394	359	0.91	394	356	0.90	δ ring	(36)
178	166	0.93	186	177	0.95	187	181	0.97	186	175	0.94	188	171	0.91	186	170	0.91	185	179	0.97	191	178	0.93	194	178	0.92	195	193	(2)[b]	159	149	(1)[b]	γ ring (coupled to δNCS)	(25)

[a] The region 2000 - 1700 cm^{-1} where harmonic frequencies and combinations are expected [86] has not been reported.

[b] Figures in parentheses denote shift on ^{15}NCS labelling.

[c] Mean of doublet.

[d] Revealed only on d_7-substitution.

[e] Anomalously low value for the assignment cited.

(ring modes). Analogous studies of metal complexes of pyridine and pyridine-d_5 [84] have shown that the ν^D/ν^H ratios for complexes are remarkably consistent with those observed for the parent ligand. Likewise, ir studies of metal complexes of aniline, aniline-d_5 [84] and imidazole, imidazole-d_3 and imidazole-d_4 [185] have again illustrated that the ν^D/ν^H ratios parallel those of the free parent ligands. Considering the range of complexes studied [89] the ratio ν^D/ν^H lies within 0.76 ± 0.08 (C-H modes) and 0.92 ± 0.08 (ring modes). Absence of overlap between these ranges has suggested that the observed ratios serve to distinguish between C-H and ring modes in metal complexes as they do in the parent ligands. Distinction also, between these vibrations and metal-ligand modes or bands originating in the vibrations of other functional groups or other coordinated ligands has also been shown to be possible by this type of investigation since the latter generally yield ν^D/ν^H ratios close to unity. The application of this technique to metal complexes of quinoline is now reported.

Ligand bands in the ir spectra of metal complexes of quinoline

Table 26 also reports the assignments of ligand vibrations in the spectra of the complexes $M(quin)_2X_2$, and $M(quin\text{-}d_7)_2X_2$. While intensities of modes are very often different for the free and coordinated quinoline and quinoline-d_7, the band frequencies and hence ratios ν^D/ν^H are remarkably similar. The quinoline vibrations in the spectra of the complexes are thus relatively easily assigned.

In addition to quinoline ligand modes in the spectra of $Cu(quin)_2(NCS)_2$ and $Zn(quin)_2(NCS)_2$, internal modes of the SCN^- anion are expected. These are also shown in Table 26.

Two $\nu C{\equiv}N$ modes at 2111 and 2082 cm^{-1} are observed for the copper complex while only one such mode is found at 2072 cm^{-1} for the zinc complex. Each of these shifts about -20 and -30 cm^{-1} on ^{15}NCS isotopic substitution as expected [186]. Sharp shoulders and splittings of these bands are considered [94] to be diagnostic of either polymeric octahedral or tetrahedral structures. ν C-S modes at 835 and 839 cm^{-1} are observed in the spectra of the copper and zinc complexes, respectively, their shifts of about -10 cm^{-1} on ^{15}NCS isotopic substitution being ascribed to the fact that the vibrations of the SCN group are most likely coupled and do not occur independently.

The expected δNCS and 2δNCS modes have not been observed previously in these complexes owing to the fact that they are obscured by quinoline vibrations. However, quinoline-d_7 substitution reveals weak bands around 927 and 967 cm^{-1} for both the Cu and Zn complexes which may be assigned to 2δNCS modes. Similarly, bands at about 470 cm^{-1}, which are the δNCS modes for each of the complexes, are revealed on the quinoline-d_7 substitution.

3.4.2 *The far ir spectra of quinoline complexes of metal(II) halides and isothiocyanates: assignments by isotopic labelling and structural aspects of the spectra*

Fig. 17 depicts the spectra of the complexes $M(quin)_2X_2$ (M = Co, Ni, Cu, Zn; X = Cl^-, Br^-, I^-, NCS^-) over the range 400 - 140 cm^{-1}. The frequencies and isotopically-induced shifts and assignments are listed in Table 27.

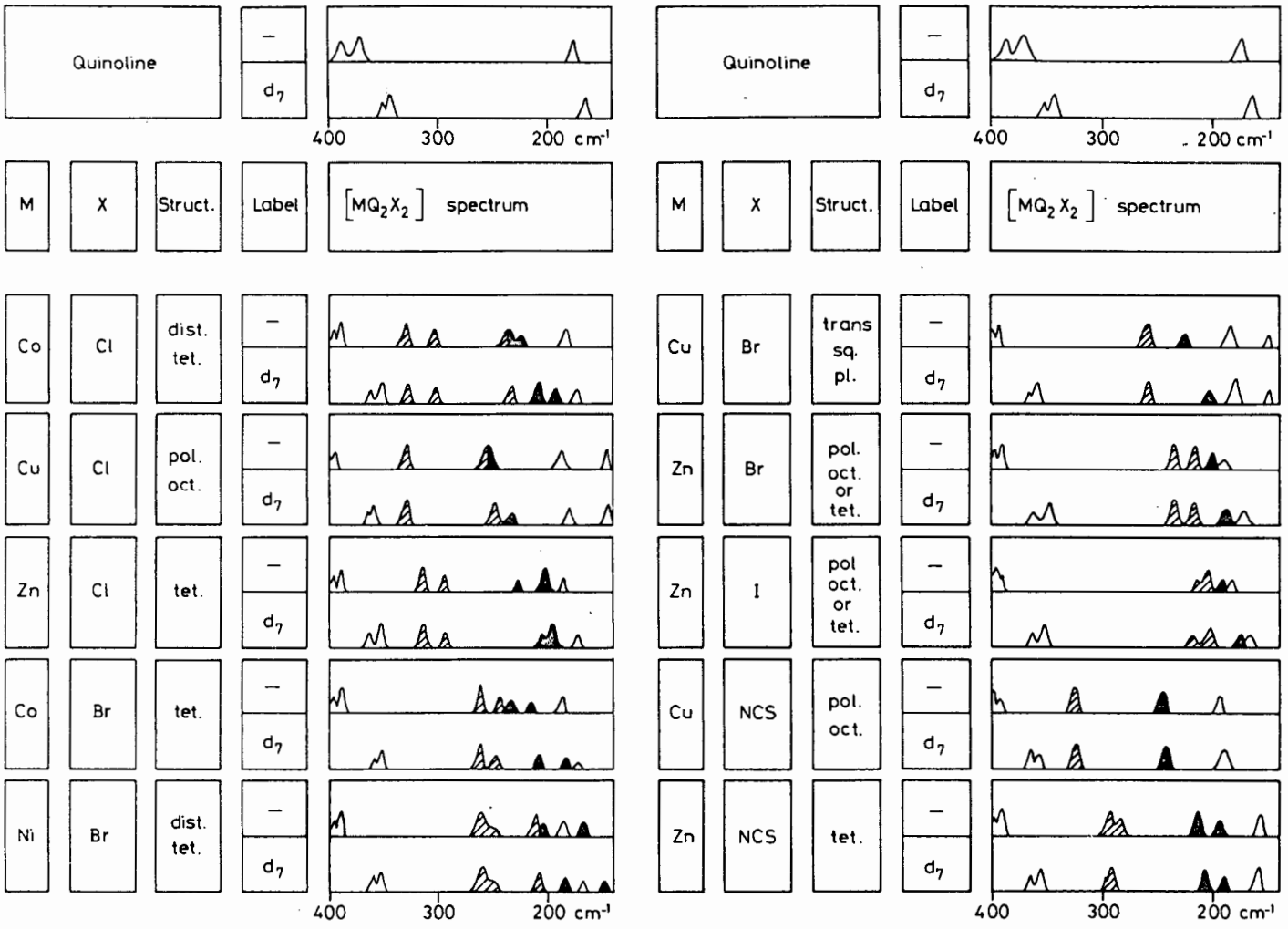

Fig. 17. Ir spectra (400 - 140 cm^{-1}) of quinoline, quinoline-d_7 and their complexes $[M(quin)_2X_2]$: solid bands are νM-N; shaded bands are νM-X

Table 27. Frequencies, isotopically induced shifts (to lower wavenumber) and assignments for ligand and metal-ligand bands in the complexes $M(quin)_2X_2$ (cm^{-1})

M	X	Mode	Present assignments[a] (cm^{-1})	Previous assignments [ref] (cm^{-1})
Co	Cl	νCo-Cl	332(2),306(0),233(4)[b]	327,310[89];333,312[90]
		νCo-N	233(24)[b], 223(29)	226[90]
		Quinoline	397(35),393(37),186(9)	
Cu	Cl	νCu-Cl	328(0),253(5)[b]	330[19];332[90]
		νCu-N	253(19)[b]	257[19];259[90]
		δCl-Cu-Cl	149(1)	151[19]
		Quinoline	404(39),398(38),187(6)	
Zn	Cl	νZn-Cl	313(0),295(0)	316,300[90]
		νZn-N	224(16),202(6)	205[90]
		Quinoline	397(33),393(37),186(11)	
Co	Br	νCo-Br	261(0),244(0)	260[89]
		νCo-N	234(27),215(30)	
		Quinoline	399[40],394(39),188(17)	
Ni	Br	νNi-Br	255(1)[c],210(2)	263,252[2];258,251[89]
		νNi-N	205(19),171(20)	212[88]
		Quinoline	396(36),392(47),186(16)	
Cu	Br	νCu-Br	259(4)	266[19]
		νCu-N	228(25)	256[19]
		δBr-Cu-Br	148(0)	110[19]
		Quinoline	404(39),398(38),185(6)	
Zn	Br	νZn-Br	236(2),218(3)	
		νZn-N	201(8)	
		Quinoline	397(32),393(36),191(13)	
Zn	I	νZn-I	220(0),205(2)	
		νZn-N	194(16)	
		Quinoline	397(33),393(39),194(16)	
Cu	NCS	νCu-NCS	325(0,9)	326[94]
		νCu-N	245(4,0)	247[94]
		Quinoline	402(38,0),394(35,0),195(2,2)	
		νN-CS	2111(0,21),2082(0,31),	2128,2080[94];2130,2080[92]
		2δNCS	927[b]	
		νC-S	835(0,12)	
		δNCS	470(2,7)	463,472[94]
Zn	NCS	νZn-NCS	293(0,4),281(0,1)	290,280[94]
		νZn-N	214(5,0),195(3,0)	215[94]
		Quinoline	298(33,0),394(38,0),159(10,1)	
		νN-CS	2072(0,29)	2070[94];2090[93]
		2δNCS	967[b]	
		νC-S	839(0,12)	840[94];810,780,735[93]
		δNCS	481(0,4)	463,467[94];488-480[93]

[a] Figures in parentheses are the shifts (cm^{-1}) caused by quinoline deuteration. For the complexes with X = NCS, the figures in parentheses are the shifts on quinoline deuteration and ^{15}NCS-labelling, respectively.

[b] Masked in unlabelled spectrum but revealed in deuterated spectrum.

[c] Mean of band at 262(1) cm^{-1} and shoulder at 247(1) cm^{-1}.

As mentioned in Section 3.4.1, the only internal quinoline vibrations to absorb within this region are the ring deformations at 390, 375 and 178 cm^{-1} in the quinoline spectrum [85,86], and the corresponding bands in the spectra of the metal halide complexes have been readily identified at 399 ± 5, 394 ± 4 and 188 ± 7 cm^{-1} by their sensitivities to quinoline deuteration which are similar to the shifts for the free ligand. The high frequency shifts which these bands have undergone on metal ion complexation is a general feature of certain of the skeletal deformations of nitrogen heterocycles [84, 187]. Remaining bands in this region are all associated with metal-ligand vibrations.

It has been established from electronic spectra [157] that the cobalt ion in $Co(quin)_2Cl_2$ is tetrahedrally coordinated; the consequent C_{2v} point symmetry requires two νM-N and two νM-X ir active modes. In previous studies [19,89,90] two νCo-Cl and only one νCo-N have been assigned. Clearly difficulties have arisen owing to the fact that in tetrahedral complexes metal-chlorine vibrations occur in a similar region to metal-nitrogen vibrations so that the latter are often obscured. Isotopic labelling has alleviated this problem. In $Co(quin)_2Cl_2$ the large shifts of bands at 233 and 223 cm^{-1} (-24 and -29 cm^{-1}, respectively) on quinoline-d_7 substitution allow their assignment to νCo-N modes while the small (-2 cm^{-1}) and zero shifts of bands at 332 and 306 cm^{-1}, respectively, indicate that these are νCo-Cl modes. Deuteration reveals a further band at 229 cm^{-1} in the labelled complex which implies that the higher of the νCo-N vibrations has a partial

contribution from an additional νCo-Cl mode. This third νCo-Cl suggests that some distortion from regular tetrahedral structure occurs in this complex.

Masking of νM-N by νM-Cl also occurs in the $CuCl_2$ complex. The 328 cm^{-1} band has zero *d*-sensitivity while the 253 cm^{-1} band is split by deuteration into a νCu-Cl component at 248 cm^{-1} and a weaker νCu-N band at 234 cm^{-1}. The existence of one νCu-N and two νCu-Cl bands is consistent with polymeric octahedral (or tetragonal) coordination (C_i symmetry). An earlier assignment [19] of the band at 149 cm^{-1} to δCl-Cu-Cl is confirmed by its insensitivity to quinoline deuteration. While zinc complexes of the form ZnL_2X_2 (where L is a neutral electron donor ligand) are very often tetrahedral, very little structural information on the complexes $Zn(quin)_2X_2$ has actually been obtained. Brown *et al.* [19] have found that the visible spectrum of $Zn(quin)_2Cl_2$ is inconclusive with respect to the stereochemistry of the complex, although a comparison with its pyridine analogue has indicated that it is most likely tetrahedral. However, two νZn-Cl but only one νZn-N modes have previously [90] been assigned; this would be consistent with the number of modes expected for a polymeric octahedral species of C_i point symmetry. The present study reveals the two νZn-Cl modes at 313 and 295 cm^{-1}, respectively, while two bands sensitive to quinoline-d_7 substitution (at 224 and 202 cm^{-1} in the unlabelled complex) may be assigned to νZn-N. Hence it may be concluded that $Zn(quin)_2Cl_2$ is definitely tetrahedral.

The spectrum of the $CoBr_2$ complex reveals two νCo-Br modes

and two νCo-N modes, only the latter showing significant d-sensitivity on quinoline-d_7 substitution. This is in perfect agreement with the tetrahedral structure suggested by its electronic spectrum [99].

Tetrahedral coordination has also been proposed [157] for the $NiBr_2$ complex on the basis of its electronic spectrum. The band at 262 cm^{-1} and its shoulder at 247 cm^{-1} have been cited [88,89] as the two νNi-Br modes while the 210 cm^{-1} band has been assigned [88] to one of the two νNi-N vibrations expected for the C_{2v} point symmetry of a tetrahedral coordination sphere; the remaining νNi-N mode was not assigned. Deuteration shows that the 210 cm^{-1} band shifts only -2 cm^{-1} and is definitely νNi-Br rather than νNi-N. The two νNi-N modes are assigned, on the basis of their substantial d-sensitivities, to the two relatively weak bands at 205 and 171 cm^{-1}.

The splitting of the 262 cm^{-1} band is consistent with the observation [188] that this complex is not isomorphous with tetrahedral $Co(quin)_2Br_2$ and with the magnetic moment [188], which suggests distortion from regular tetrahedral structure.

The spectrum of the $CuBr_2$ complex is the simplest among the complexes studied. Only one d_7-insensitive band above 200 cm^{-1} is found at 259 cm^{-1} and may hence be assigned to νCu-Br. This, together with the fact that there is also only one νCu-N found at 228 cm^{-1} and shifting -25 cm^{-1} in the deuterated complex, is consistent with a *trans*-planar arrangement of the ligands and D_{2h} point symmetry of the coordination sphere. The reduction in coordination number from six in the chloro complex to four in the bromo complex

might easily arise from the bulkiness of not only the quinoline but also the bromide anion. That the $CuBr_2$ complex differs structurally from the $CuCl_2$ complex is also suggested by the appearance of a *d*-insensitive δBr-Cu-Br band at 148 cm^{-1} *i.e.* at practically the same position as δCl-Cu-Cl in the $CuCl_2$ complex. This is understandable if the $CuBr_2$ complex has a lower coordination number.

Structural information has also been obtained from the ir spectrum of $Zn(quin)_2Br_2$ for which no previous band assignments have been made. Two bands at 236 and 218 cm^{-1} showing shifts on quinoline-d_7 substitution of only -2 and -3 cm^{-1} respectively may be assigned to νZn-Br. The band at 201 cm^{-1} which shifts -8 cm^{-1} on quinoline-d_7 substitution is νZn-N. No other bands which may be ascribed to metal-ligand modes are found in the region of the $Zn(quin)_2Br_2$ spectrum studied, nor are any additional bands revealed on quinoline-d_7 substitution. While it is possible that a second νZn-N band required for C_{2v} point symmetry and tetrahedral coordination lies beyond the limit of measurement, thermogravimetry [157] shows that thermal decomposition of the $ZnBr_2$ complex proceeds by a mechanism which differs from that of the $ZnCl_2$ complex and from that of other tetrahedral quinoline complexes of metal(II) halides. This suggests that the $ZnBr_2$ complex may differ structurally from the $ZnCl_2$ complex. The ir spectrum of the $ZnBr_2$ complex is consistent with the polymeric octahedral coordination (C_i point symmetry), which pertains to the pyrazine and pyrimidine complexes of $ZnCl_2$ [176]. Support for the νM-Br assignments proposed above is provided

by the fact that νM-Br:νM-Cl ratio for each M is 0.77 ± 0.03 which is in good agreement with the value of 0.76 quoted [172] for the tetrahalide ions $[MX_4]^{2-}$.

In the spectrum of the ZnI_2 complex, the νZn-I and νZn-N bands occur within the narrow frequency range 220-190 cm^{-1}. The shoulder at 220 cm^{-1} and the neighbouring strong band at 205 cm^{-1} are assigned to νZn-I since they have insignigicant *d*-sensitivities. The band at 194 cm^{-1} is shifted -16 cm^{-1} on deuteration and is therefore assigned to νZn-N. One νZn-N and two νZn-I bands satisfy the selection rules for polymeric octahedral coordination (C_i point symmetry) but a second νZn-N band may occur beyond the limit of determination so that the possibility of tetrahedral structure cannot be excluded.

The ir spectra of both isothiocyanate complexes investigated here have previously been studied [92-94]. Generally, the earlier assignments are consistent with those now proposed on the basis of ^{15}NCS-labelling and quinoline deuteration. In the $Cu(quin)_2(NCS)_2$ complex, the one νCu-N mode assigned on the basis of its d_7-sensitivity and the one very broad νCu-NCS assigned on the basis of its ^{15}NCS sensitivity, together with the very large separation between the two νN≡CS modes mentioned previously, seems to support the supposition [92] that the complex is binuclear with both terminal and bridging NCS. The remaining band at 195 cm^{-1} which would normally be assigned to a quinoline mode expected in that region, shows slight sensitivity to both quinoline-d_7 and ^{15}NCS substitution and is hence assigned to a quinoline + δCu-NCS mode.

For the $Zn(quin)_2(NCS)_2$ complex, isotopic shifts on the independent quinoline-d_7 and ^{15}NCS substitutions allow the identification of two νZn-NCS (at 293 and 281 cm^{-1}) and two νZn-N (at 214 and 195 cm^{-1}) which is indicative of the C_{2v} point symmetry for a tetrahedral configuration. The remaining band at 159 cm^{-1}, showing slight sensitivity to both quinoline-d_7 and ^{15}NCS isotopic substitution is considered to be a coupled quinoline and δZn-NCS mode.

The present labelling study has enabled reliable assignments to be provided for many bands previously unobserved or unassigned (Table 27).

3.5 STUDIES OF METAL(II) ACETYLACETONATES

3.5.1 *An ir study of the monohydrate of zinc(II) acetylacetonate employing metal ion and ligand atom isotopic substitutions*

As mentioned in the Introduction, despite the fact that considerable attention has been given to the ir spectra of metal acetylacetonates, assignments of (particularly) the metal ligand vibrations remain controversial. The classic example has been the spectrum of *tris*(acetylacetonato)chromium(III) for which normal coordinate treatments, ^{18}O-labelling and metal-ion isotopic substitutions have been carried out [45,100,103-105].

The variation in the resultant assignments for bands in the region 600 - 300 cm^{-1} is illustrated in Table 28.

The results of these studies have very often been used to make correlations with the spectra of metal(II) acetylacetonates [118,119]. Owing to a significant difference in bonding power between metal(III) and metal(II) ions, and in view of the tremendous variations in band assignments, any such comparative studies must necessarily be suspect. It is therefore hoped that an examination of the ir spectrum of $Zn(acac)_2.H_2O$ in conjunction with those of its ^{18}O-, ^{64}Zn- and ^{68}Zn-analogues, might clarify assignments of metal-ligand and other low-frequency modes of vibration. The ir spectrum of $Zn(acac)_2.H_2O$ is depicted in Fig. 18, the ir frequencies (4000 - 150 cm^{-1}) and isotopic shift data are given in Table 29.

The 4000 - 660 cm^{-1} region of the spectra

This is the spectral region where only bands arising from the coordinated ligands themselves are expected.

Table 28. Frequencies (cm^{-1}), isotopically-induced shifts ($\Delta\nu$, cm^{-1}) and band assignments for $[Cr(acac)_3]$[a]

Band frequency				Method	Ref
592	463	416	358		
o.o.p. ring def	ν(Cr-O)	o.o.p. ring def	ν(Cr-O)	nct	100
o.o.p. ring def	ν(Cr-O) + δ(C-CH_3)	ring def	ν(Cr-O)	nct	103
ν(Cr-O) $\Delta\nu$ = 19[b]	ν(Cr-O) + δ(C-CH_3) $\Delta\nu$ = 5[b]	δ(O-Cr-O) $\Delta\nu$ = 8[b]	na	^{18}O-labelling	45
o.o.p. ring def $\Delta\nu$ = 0.7[c]	ν(Cr-O) $\Delta\nu$ = 3.0[c]	o.o.p. ring def $\Delta\nu$ = 0[c]	ν(Cr-O) $\Delta\nu$ = 3.9[c]	$^{53,50}Cr$-labelling	104
ν(Cr-O) $\Delta\nu$ = 19[b]	ν(Cr-O) + δ(C-CH_3) $\Delta\nu$ = 10[d]	i.p. δ(O-Cr-O) $\Delta\nu$ = 5[d]	i.p. δ(C-C-C) $\Delta\nu$ = 2[d]	^{18}O-labelling	105

a Abbreviations: nct = normal coordinate treatment, na = not assigned.
b Shift in ir band on ^{18}O-labelling.
c Difference in frequencies between ^{53}Cr- and ^{50}Cr-labelled species.
d Shift in Raman band on ^{18}O-labelling.

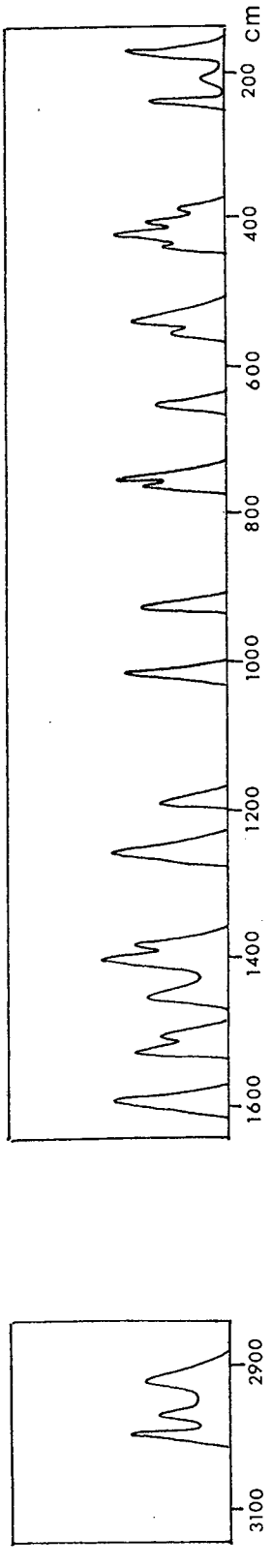

Fig. 18. The ir spectrum of $Zn(acac)_2.H_2O$

Table 29. Ir frequencies (4000 - 150 cm^{-1}) isotopic shift data ($\Delta\nu$)[a] and assignments in the spectrum of $Zn(acac)_2.H_2O$ and its isotopically substituted analogues

	$\Delta\nu$			Assignments
	^{64}Zn	^{68}Zn	^{18}O	
3300				
2966	-	-	-	νC-H
2927	-	-	-	
1599	-	-	2	νC=O
1522	-	-	1	νC=C + νC=O
1513	-	-	4	νC=O
1453	-	-	-	δC-H
1400	-	-	-	CH_3 deg. def.
1370	-	-	-	CH_3 symm. def.
1264	-	-	-	νC-C + νC-CH_3
1191	-	-	-	i.p. δC-H
1020	-	-	-	CH_3 rock
933	-	-	1	νC-CH_3 + νC=O
779	-	-	-	o.o.p. δC-H
772	-	-	-	
656	-	1	-	ring def.
570	-	1	-	ring def.
557	+1	1	3	νZn-O + δC-CH_3
439	+1	1	1	νZn-O (H_2O)
422	-	-	1	i.p. δC-C-C
413	+1	5	5	νZn-O
388	+1	-	1	i.p. δO-Zn-O
241	+2	3	6	o.o.p. δO-Zn-O
208	-	-	-	o.o.p. δC-C-C
173	+1	2	1	δO-Zn-O (H_2O)

[a] All shifts are to lower wavenumber unless preceded by a + sign.

Insensitivity of all the absorptions to the metal-ion isotopic substitutions confirms this fact. A relatively comprehensive investigation of the vibrational modes of coordinated actylacetonate has already been carried out [102]. Although based upon theoretical calculations, assignments proposed in that work are substantiated partially, if not totally, by the ^{18}O isotopic shift data obtained here. The only significant differences are as follows. The sensitivity of the bands at 1599, 1522 and 1513 cm^{-1} to ^{18}O-labelling implies that all have a contribution from the $\nu C{=}O$ vibration; the 1522 cm^{-1} absorption undergoes the smallest shift (-1 cm^{-1}) which can be attributed to its being coupled to the $\nu C{=}C$ expected in this region. The only other band above 660 cm^{-1} to experience any sensitivity to ^{18}O isotopic substitution is that at 933 cm^{-1} which supports its earlier assignment [102] to $\nu C{=}O + \nu C\text{-}CH_3$.

The 660 - 150 cm^{-1} region of the spectra

Logically, bands showing the greatest sensitivity to ^{18}O- and metal-ion labelling are those resulting from the metal-ligand vibrations. The C_{4v} localized point symmetry of the molecule dictates that there should be six ir active metal-ligand modes: $2a_1 + e$ stretches and $a_1 + 2e$ bends. Of these, two νZn-O(acac) and two δO-Zn-O(acac) are expected, the remaining modes arising from vibrations involving the Zn(II) ion and the coordinated water. In accordance with the isotopic shift data the bands at 557 and 413 cm^{-1} are assigned to the νZn-O(acac) modes, the lower of the two being considered to be the more pure as evidenced by its greater sensitivity to the isotopic substitutions.

A band attributable to νZn-O(H_2O) is observed at 439 cm^{-1}. The small shift experienced on ^{18}O-labelling possibly arises from a degree of coupling to the νZn-O(acac) vibrations.

On the basis of their metal ion- and ^{18}O-sensitivities the three expected bending modes are also able to be identified at 388, 241 and 173 cm^{-1}. All remaining bands in this region of the spectra undergo only small or insignificant shifts on isotopic labelling and have subsequently been assigned to various deformations within the acetylacetone ring itself and to those resulting from its coordination.

A comparison of the results reported here with assignments made for the related $Cr(acac)_3$ appear to support predominantly the work of Pinchas and Shamir [105] rather than that of Nakamoto *et al.* [104].

3.5.2 *The ir spectra (3500 - 140 cm^{-1}) of the 2,2'-bipyridine, 2-aminomethylpyridine and ethylenediamine adducts and the sodium tris compounds of cobalt(II) nickel(II) and zinc(II) acetylacetonates*

The ir spectra are depicted in Fig. 19 and the vibrational frequencies with their assignments are given in Table 30. The extensive degree of electron delocalization in the chelated acetylacetonate ring leads to coupling of vibrational modes so that few bands in the ir spectra represent pure vibrations. Accordingly, assignments have generally been given to those vibrations which make the most dominant contribution to each ir band.

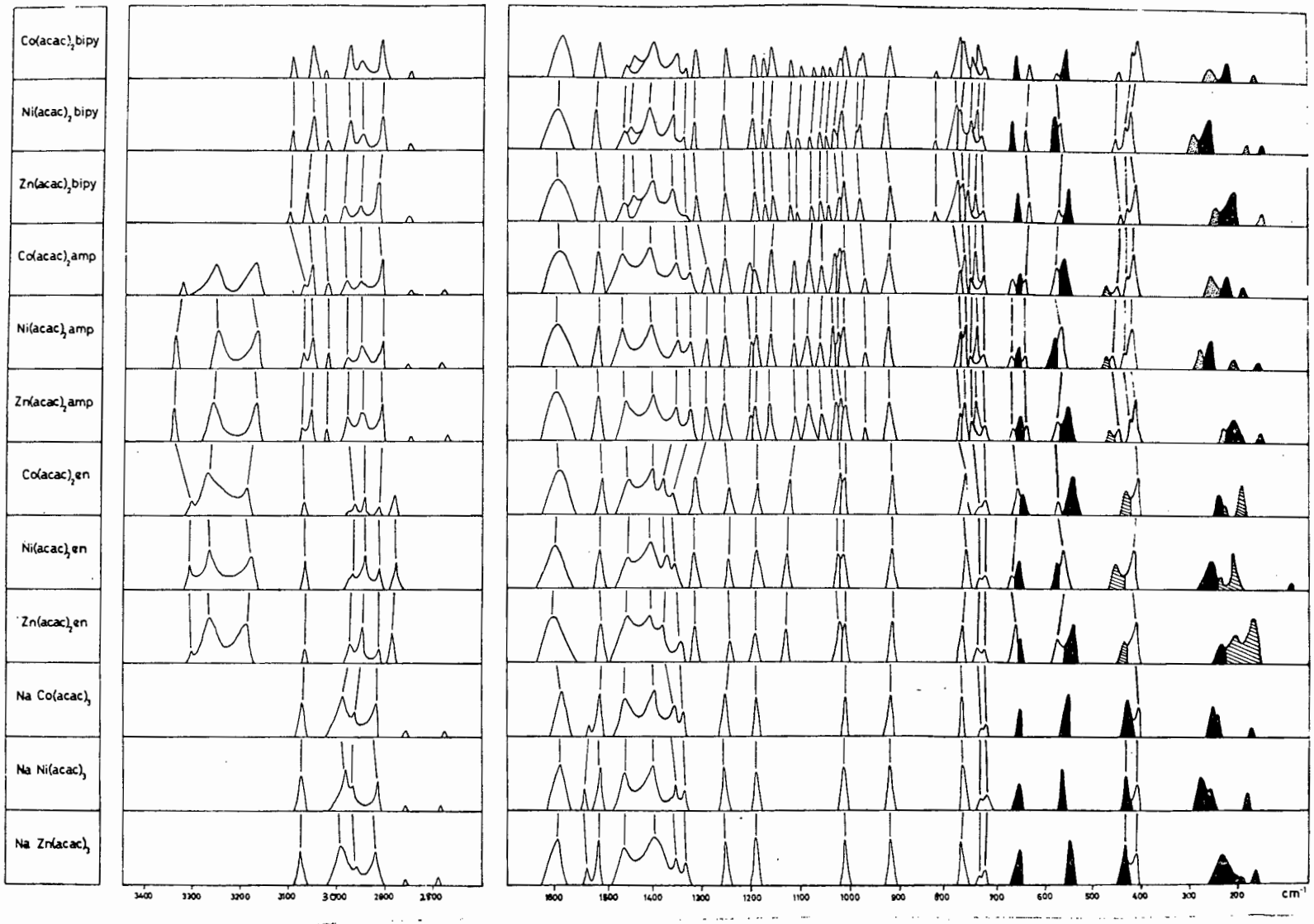

Fig. 19. The ir spectra (3400 - 140 cm^{-1}) of the base adducts of Co(II), Ni(II) and Zn(II) and the sodium *tris* complexes

Table 30. Vibrational frequencies and assignments of infrared bands in base adducts and sodium salts of metal(II) acetylacetonates (3500 cm^{-1} - 140 cm^{-1})

[M(acac)$_2$bipy]			[M(acac)$_2$amp]			[M(acac)$_2$en]			Na[M(acac)$_3$]			Assignment
Co	Ni	Zn	Co	Ni	Zn	Co	Ni	Zn	Co	Ni	Zn	
			3344	3348	3348	3310	3316	3309				antisymmetric ν(N-H)
			3268	3258	3265	3279	3273	3275				symmetric ν(N-H)
			3175	3171	3173	3195	3187	3191				ν(N-H) H-bonded to O of acac
3101	3102	3105	3077	3079	3078	3075	3075	3075	3077	3077	3078	ν(C-H) acac + ν(C-H) heterocyclic ring
3064	3062	3069	3060	3061	3058							ν(C-H) heterocyclic ring
3038	3033	3031	3028	3029	3027							
2985	2982	2991	2988	2985	2985	2967	2977	2979	2991	2987	2991	ν(C-H) acac + heterocyclic ring
2962	2960	2958	2958	2956	2956	2948	2950	2952	2963	2972	2959	
2916	2916	2917	2916	2916	2914	2919	2920	2918	2921	2921	2921	
						2887	2888	2890				ν(C-H) methylene group
2858	2853	2856	2855	2856	2854				2860	2861	2858	unassigned weak bands
			2783	2790	2775				2788	2788	2788	
1591	1595	1596	1600	1604	1605	1609	1613	1617	1590	1591	1594	ν(C-O); + ν(C-C) and ν(C-N) of heterocyclic ring; + NH_2 scissor:(broad unresolved band).
									1535	1536	1535	ν(C-C) acac + heterocyclic ring
1513	1517	1514	1514	1514	1514	1508	1510	1508	1512	1512	1514	stretch and -H bend
1459	1458	1461	1467	1466	1464	1455	1456	1454	1466	1464	1463	
1444	1445	1443										heterocyclic ring stretch +C-H bend
1404	1403	1403	1411	1405	1403	1407	1408	1409	1403	1402	1401	δCH_3 + heterocyclic ring stretch and -H bend
1354	1359	1362	1353	1351	1352	1382	1375	1385	1357	1356	1357	
1335	1337	1337	1326	1325	1325	1363	1364	1342	1341	1341	1339	
			1291	1291	1292	1317	1318	1319				NH_2 wag or twist
1315	1314	1313										inter-ring stretch in bipy (not allowed)
1255	1255	1256	1253	1253	1252	1250	1251	1246	1260	1261	1259	ν(C-CH_3) + ν(C-C) acac
			1196	1198	1197							heterocyclic ring -H bend
1194	1193	1191	1192	1192	1192	1190	1191	1194	1197	1198	1197	ν(C-CH_3)
1175	1174	1171										heterocyclic ring -H bend
1160	1159	1153	1160	1161	1159							
			1112	1115	1106	1125	1130	1130				ν(C-C) amp and en
1121	1121	1116										in plane δ(C-H) heterocyclic ring
1100	1101	1105										
1074	1076	1078	1081	1086	1081							
1052	1052	1057	1055	1057	1055							
1040	1041	1043										
1019	1023	1017	1027	1032	1026							
			1018	1021	1017	1020	1025	1021				ν(C-N) amp and en
1009	1010	1011	1014	1013	1009	1013	1017	1012	1016	1017	1015	CH_3 rock
977	977	977										out of plane δ(C-H) heterocyclic ring
972	972		968	968	968							
918	920	916	917	917	917	915	916	913	921	923	921	in plane δ(C-H) acac
818	818	822										out of plane δ(C-H) heterocyclic ring
771	771	774	767	767	774	766	764	771	773	773	773	out of plane δ(C-H) acac
766	766	765	760	759	765							ring torsion of heterocyclic ring
744	745	758	749	746	758	733	737	738	733	737	735	out of plane δ(C-H) acac
737	737	741	740	738	741							out of plane δ(C-H) heterocyclic ring
725	723	726	725	725	726	723	725	726	724	723	725	δ(C-CH_3)
			661	666	661	660	669	660				NH_2 rock
653	655	650	647	648	646	650	655	650	656	657	654	ν(M-O) + δ(C-CH_3)
628	630	627	633	638	633							in plane heterocyclic ring deformation
571		568	568		570	572		572				skeletal ring deformation -CCN bend
551	566	545	553	571	547	548	573	540	559	568	548	ν(M-O)
	559			563			561					skeletal ring deformation -CCN bend
			468	469	467	436	454	437				ν(M-NH_2)
446	448	439	447	455	445							heterocyclic ring torsion
421	423	423	423	428	421							out of plane heterocyclic ring deformation
									432	437	432	ν(M-O) + δ(C-CH_3)
408	410	406	410	415	408	410	416	409	409	410	409	δ(C-C-C) skeletal ring deformation of acac
252	282	241	251	279	224							ν(M-py)
220	250	201	228	255	207	244	258	235	255	281	235	
									248	260	190	in plane δ(O-M-O)
						230	236	208				δ(NH_2-M-NH_2)
						192	210	168				
			188	203	150							δ(NH_2-M-py)
166	173	148										δ(py-M-py)
	146			157			155		175	183	164	out of plane δ(O-M-O)

The adducts $M(acac)_2B$ (M = Co(II), Ni(II), Zn(II); B = bipy, amp, en)

A similarity in the band patterns of the ir spectra of the bipy, amp and en adducts of metal(II) acetylacetonates supports the supposition that they are isostructural. Assignment of certain of the vibrational frequencies on a comparative basis is therefore considered valid. Each of the skeletal groups undergoes particular vibrations and contributes certain peaks to the ir spectra. Hence particular note is taken of the following:

(a) Bands found in the ir spectra of only the bipy and amp adducts must be associated with the aryl ring vibrations or with metal-heterocyclic nitrogen (M-py) vibrations.

(b) Bands found in the ir spectra of only the amp and en adducts must be associated with methylene or amine vibrations (including the vibration of the C-N bond linking these two groups), or with metal-amino nitrogen ($M-NH_2$) vibrations.

(c) Bands arising in the ir spectra of all the adducts must be associated with the acetylacetonate anion vibrations or the metal-acetylacetonate (M-O) vibrations.

Using the above criteria and by analogy with previous ir studies of the nitrogeneous bases and various metal(II) acetylacetonates [102,165,166,189,190] the assignment of bands above 700 cm^{-1} is relatively straightforward. Only assignments in the 700 - 140 cm^{-1} region are therefore discussed.

A band near 666 cm^{-1} is found in the spectra of only the amp and en adducts. This absorption shows extreme metal ion

dependence. Since it has been well-established [32] that NH_2 rocking vibrations exhibit this degree of metal sensitivity, the band has been assigned to an NH_2 rocking mode.

Near 650 cm^{-1} there is a band found in the spectra of all the adducts. Owing to its strong metal ion sensitivity and in accordance with related work it has been assigned to $\nu M\text{-}O + \delta C\text{-}CH_3$ of acetylacetonate.

By analogy with assignments for pyridine [88] the two bands at *ca.* 630 cm^{-1} and 420 cm^{-1} which appear in the spectra of the bipy and amp adducts only, are considered to be the in-plane and out-of-plane heterocyclic ring deformation modes respectively.

The band at *ca.* 550 cm^{-1} found in the spectra of all the adducts exhibits high metal sensitivity and is hence a relatively pure $\nu M\text{-}O$ of the acetylacetonate ring. There is an additional band in this region between 575 and 540 cm^{-1} which again appears in the spectra of all the adducts. It exhibits metal ion dependence and is hence most likely a skeletal ring deformation of the nitrogeneous bases (CCN bend). At about 468 cm^{-1} in the amp adducts, a band expected (on the basis of the findings in Section 3.2.) for $\nu M\text{-}NH_2$ is found. The equivalent band in the en adducts, exhibiting strong metal ion dependence, is found near 440 cm^{-1}. Its lower frequency may be rationalized in terms of the lower ligand field strength of en compared with that of amp [62]. Near 450 cm^{-1}, a band found in the spectra of only the bipy and amp adducts is considered to be a heterocyclic ring torsion by analogy with an assignment previously proposed [165].

Pinchas and Shamir [105] have assigned a band at 356 cm^{-1} in the spectrum of *tris*(acetylacetonato)chromium(III) to a C-C-C in-plane bend, on the basis of ^{18}O isotopic labelling. In this work, the band near 410 cm^{-1}, which appears in the spectra of all the adducts is analogously assigned. A band near 260 cm^{-1} which shows strong metal ion dependence is found in the spectra of only the bipy and amp adducts. It is hence assigned as νM-py, which is confirmed by analogy with its occurence in related complexes of 2,2'-bipyridine, 1,10-phenanthroline [28] and pyridine [95].

The in-plane δO-M-O vibration expected for coordinated acetylacetonate is considered to be related to the band found in the spectra of all the adducts at about 230 cm^{-1}. This assignment is confirmed, not only by the observed metal-ion dependence of the band, but also by the fact that its frequency is highest in the en, intermediate in the amp and lowest in the bipy adducts as expected [62] in terms of the relative ligand field strengths of the three bases. The remaining bands found below 240 cm^{-1} in the spectra of all the adducts show metal sensitivity. Accordingly the bands in the en adducts at *ca.* 230 cm^{-1} and 200 cm^{-1} are assigned to δNH_2-M-NH_2; the band in the amp adducts at *ca.* 190 cm^{-1} is δNH_2-M-py; and the band in the bipy adducts at *ca.* 160 cm^{-1} is the δpy-M-py vibration.

One peak at *ca.* 150 cm^{-1} in the spectra of the adducts remains to be discussed. It is only observed in the spectra of the Ni(II) complexes; hence it is very likely a metal-ion dependent band, appearing in the cobalt and zinc

adducts at a frequency lower than the range of determination in this work. Accordingly it is assigned to an expected out-of-plane δO-M-O of the coordinated acetylacetonate.

The sodium tris(acetylacetonato)metal(II) compounds Na[M(acac)$_3$] (M = Co, Ni or Zn)

The spectra of these compounds have been reported previously [190]. A good correlation exists between the acetylacetonate bands in the ir spectra of the adduct complexes studied and bands arising in the ir spectra of Na[M(acac)$_3$]. This not only supports the assignments made for the M(acac)$_2$B complexes but also allows assignments to be made for the spectra of the sodium *tris* compounds. These are also indicated in Table 30. Additional bands in the spectra of the Na[M(acac)$_3$] complexes owe their existence to differing symmetry from that of the M(acac)$_2$B complexes.

3.5.3 *The ir spectra of quinoline adducts of transition metal(II) acetylacetonates*

The vibrational frequencies, (700 - 150 cm^{-1}), shifts on quinoline-d_7 substitution and band assignments for the complexes *trans*- M(acac)$_2$(quin)$_2$ for M = Mn(II), Co(II), Zn(II) and M(acac)$_2$quin for M = Cu, Zn are given in Table 31. An illustration of this spectral region appears in Fig. 20.

Fig. 20. Ir spectra of quinoline and $[M(acac)_2(quin)_n]$ complexes

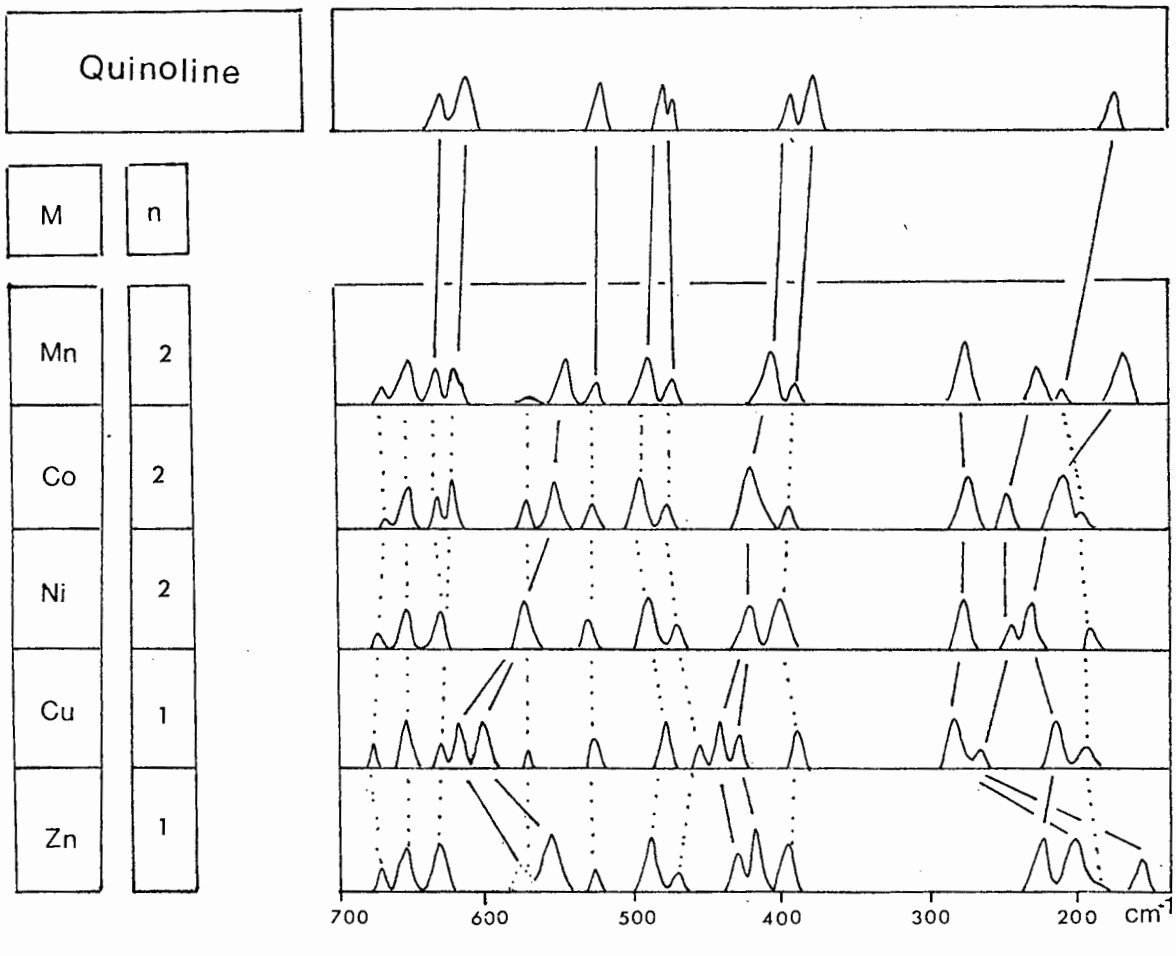

Table 31. Frequencies, quinoline-d_7 shifts (cm^{-1}) and assignments for quinoline and the adducts $[M(acac)_2(quin)_n]$[a]

Band	quin	Mn $n = 2$	Co $n = 2$	Ni $n = 2$	Cu $n = 1$	Zn $n = 1$	Assignment[b]
		670(0)	662(0)	664(0)	678(0)	670(0)	acac ring def. + ν(M-O)
		650(5)	653(10)	655(8)	656(14)	654(1)	acac ring def. + quin
	627(38)	635(36)	636(36)	627(22)	627(27)	632(22)	quin δ(ring) (35)
	610(42)	621(41)	622(41)				quin δ(ring) (21)
		568(0)	572(0)	575(0)	571(3)	~578[c]	acac ring
		543(0)	552(0)		616(2)		ν(M-O)
					600(0)	558(0)	
	521(17)	526(17)	525(16)	527(16)	525(16)	528(16)	quin δ(ring) (9)
	477(60)	488(59)	493(59)	489(57)	479(52)	489(55)	quin γ(ring) (24)
	469(60)	470(55)	472(55)	468(48)	455(43)	468(49)	quin δ(ring) (48)
		404(0)	418(1)	420(0)	441(0)	427[d]	ν(M-O) + δ(C-CH_3)
					427(0)	419(0)	
	383(35)[e]	389(26)	393(26)	399(34)	388(32)	395(32)	quin δ,γ-ring (13,36) + ν(M-N)
		274(0)	275(0)	277(0)	283(0)	204(0)	δ(O-M-O)
		227(1)	252(0)	251(0)	264(0)	158(1)	
	178(12)	206(30)	198(26)	192(15)	195(22)	188(11)	quin γ(ring) (25)
		169(2)	219(7)	238(3)	225(3)	231(3)	ν(M-N)

[a] Data in parentheses are the shifts (cm^{-1}) to lower wavenumber induced by quinoline deuteration. [b] The figures in brackets for quinoline modes are the band numbers in the notation of McClellan and Pimentel. [85] [c] Band not resolved from 558 cm^{-1} band in the unlabelled complex but observed at 578 cm^{-1} in the deuterated complex. [d] Masked by ν_9 in the labelled complex. [e] Mean of 390(39) and 375(30) cm^{-1} bands.

Internal modes of coordinated quinoline

As reported in Section 3.4.1, the ir spectrum of quinoline yields eight bands within the range 700 - 150 cm^{-1}; these modes are readily identified in the spectra of the adducts as the only bands to exhibit substantial shifts on d_7 isotopic substitution of quinoline. Each ligand band of the free quinoline spectrum recurs in the spectra of the adducts with the exception of the 390, 375 cm^{-1} doublet which occurs as a single band in that region in the adduct spectra and the 627, 610 cm^{-1} doublet which is observed as an unresolved singlet in the spectra of the Ni(II), Cu(II) and Zn(II) adducts. As expected for ligand modes the quinoline bands are relatively unshifted in the spectra of the complexes despite the substitution of the various metal ions with the exception of the band near 390 cm^{-1} which mimics the metal sensitivity of νM-N and with which it is therefore possibly coupled.

Internal modes of coordinated acetylacetonate

Bands in this category, if vibrationally pure, are expected to be relatively insensitive to both quinoline deuteration and metal ion substitution. There appears to be only one such vibrationally pure mode: that at *ca.* 578 cm^{-1}, which is assigned to a ring deformation in accordance with an ^{18}O-labelling study of $Cr(acac)_3$ [105]. Its very low intensity, except for the Ni(II) complex where it coincides with νNi-O, fits the assignment. In the Zn(II) complex it

is only observed in the deuterated spectrum. Further comparisons with the reported [105] spectrum of $Cr(acac)_3$ yield the following assignments: the band near 670 cm^{-1} is a ring deformation of the acetylacetonate ring coupled to νM-O; the coupling suggested by the slight M-sensitivity of the band; a further ring deformation of the acetylacetonate occurs as a band at *ca.* 650 cm^{-1}, with its significant *d*-sensitivity being ascribed to a coupled quinoline mode. The only remaining acetylacetonate vibration expected [105] in the region below 700 cm^{-1}, is the $C-CH_3$ deformation coupled to a νM-O; the band at about 420 cm^{-1} is accordingly assigned to this mode.

Metal-ligand modes

The metal-oxygen stretching modes are expected to be insensitive to quinoline deuteration. Two such bands are found at about 550 and 420 cm^{-1}, both of which undergo a splitting or doubling in the spectra of the Cu(II) and Zn(II) complexes. These assignments are confirmed by the fact that the frequencies are in the order Mn < Co < Ni < Cu > Zn which is the Irving-Williams stability sequence. The lower of the two bands is somewhat less metal sensitive than that at *ca.* 550 cm^{-1}; this may be ascribed to its coupling to a $C-CH_3$ deformation as mentioned earlier. In addition, the existence of two νM-O bands in the six-coordinate Mn(II), Co(II) and Ni(II) adducts satisfies the selection rules for the D_{4h} point symmetry of *trans*-octahedral coordination; their doubling in the spectra of the Cu(II) and Zn(II) adducts is consistent with

the selection rules for the C_{4v} point symmetry of the square pyramidal coordination established crystallographically [116] for the Cu(II) complex and presumed for the Zn(II) adduct. The two bands at *ca.* 270 and 250 cm^{-1} are also insensitive to substitution with quinoline-d_7 although they shift significantly on variation of the metal ion; subsequent assignment of these bands to δ O-M-O modes is therefore plausible. That these bending modes arise at frequencies about one half those of the stretches supports the assignments.

The only remaining band to be assigned occurs at *ca.* 200 cm^{-1} and is observed to undergo shifts on both quinoline-d_7 and metal ion substitution. Both observations suggest its assignment to a νM-N mode and, in terms of their point symmetries, only one νM-N band is expected for both the *trans*-octahedral and square pyramidal adducts.

The relative positions of νM-N in the spectra of the Ni(II), Cu(II) and Zn(II) adducts provides support for the assignment. The Cu-N bond length (2.36 Å) is, as a result of Jahn-Teller distortion, considerably longer than is commonly observed ($\sim$2 Å) in copper(II) complexes with nitrogen donors which are non-axially bonded [116]. The weak Cu-N bonding is expected to yield a relatively low value of νCu-N. The band at 225 cm^{-1} is at a lower frequency than νNi-N for the Ni(II) complex despite the higher coordination number of the latter. It is also at a lower frequency than the νZn-N value of the Zn(II) complex despite the equivalent coordination number and zero cfse of the latter. Both features suggest a relatively small force constant for the Cu-N bond and support the assignments of the νM-N modes as given in Table 31.

3.6 THE IR SPECTRA OF METAL COMPLEXES OF GLYCINE

It will be apparent from the ensuing discussion of the application of multiple isotopic labelling to the ir spectra of metal glycinate complexes, that many bands show shifts resulting from a number of the independent isotopic substitutions. This is indicative of extensive vibrational coupling which is to be expected [191,192] from the relative degree of complexity of the systems studied. Hence, assignments are described in terms of degrees of purity and various different modes of vibration are considered to contribute to each particular band in the ir spectra.

3.6.1 *Band assignments in the ir spectrum of cadmium glycinate monohydrate by multiple isotopic labelling*

A partial crystal structure analysis [161] of $[Cd(gly)_2].H_2O$ has revealed that the metal coordination of the complex is distorted octahedral, two glycinate ligands chelating with the metal in a *trans*-planar arrangement, while the two axial positions are occupied by the carboxyl oxygen atoms of neighbouring glycinate ligands (Fig. 21). In addition there is extensive hydrogen bonding between the amino groups, neighbouring carboxyl oxygen atoms and the uncoordinated water molecules. While the nitrogen atoms are covalently bound to the metal, the nature of the metal-oxygen bonding has yet to be established.

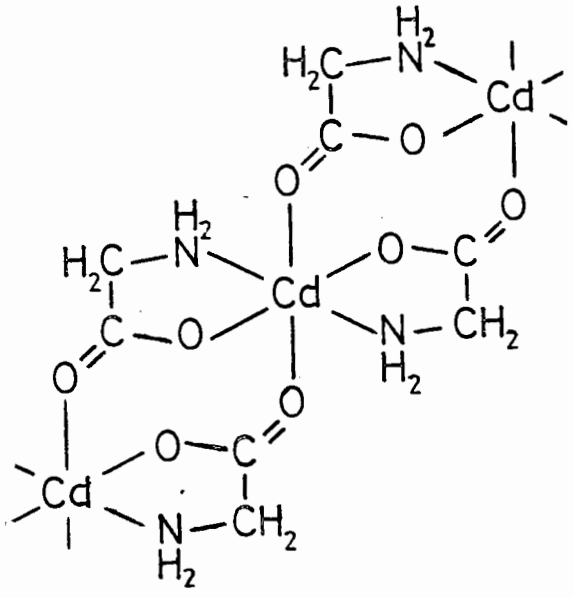

Fig. 21. Diagram showing coordination of glycinate ligands to Cd^{2+} in $[Cd(gly)_2].H_2O$

The ir spectra (4000 - 150 cm^{-1}) of $[Cd(gly)_2].H_2O$ and its isotopically-substituted analogues are depicted in Fig. 22 while the frequencies and shifts ($\Delta\nu$) are recorded in Table 32. Owing to extensive hydrogen bonding the νN-H and νO-H vibrations occur in the same region and are considered to give rise to the broad unresolved band centred at 3280 cm^{-1}. Small shifts in the peak frequencies indicate that in certain of the complexes the νN-H vibrations give rise to bands which are more intense than those of the νO-H vibrations, while in others, the reverse is true. However, the νN-H assignment is supported by a -7 cm^{-1} shift on ^{15}N-labelling and is confirmed by the appearance of new bands at 2473, 2420 and 2368 cm^{-1} on N,N-d_2-labelling, leaving a

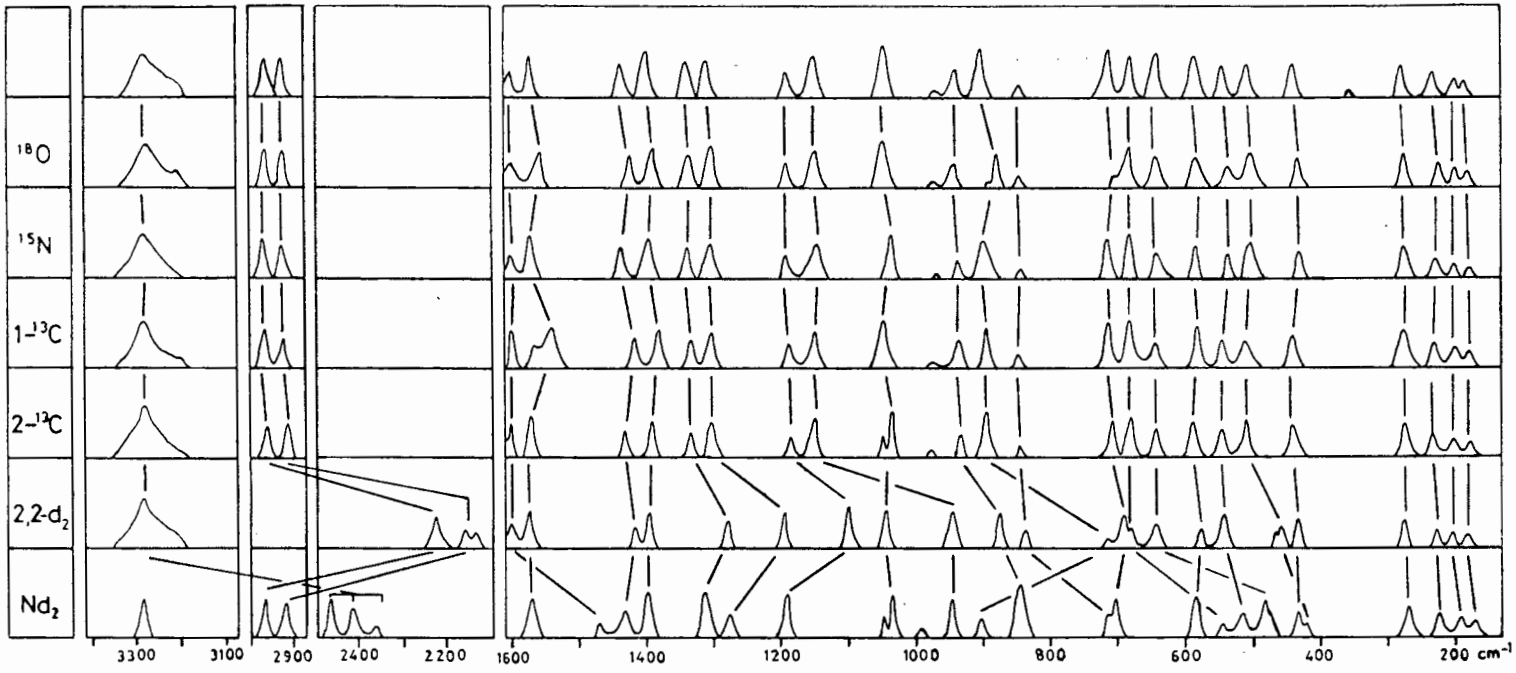

Fig. 22. The ir spectra of $[Cd(gly)_2].H_2O$ and its labelled analogues

Table 32. Frequencies, isotopically-induced shifts and ir band assignments for $[Cd(gly)_2].H_2O$ (cm^{-1})[a]

ν	Δν						Assignments
	^{18}O	^{15}N	1-^{13}C	2-^{13}C	2,2-d_2	N,N-d_2	
3280		7				∿850	νN-H + νO-H
2973				11	743		$\nu C\text{-}H_{as}$
2929				8	769		$\nu C\text{-}H_{s}$
1609		2				134	NH_2 scissor
1574	10		40[b]			1	νC=O
1438	7		12	3	10		νC-O + CH_2 scissor
1401	3		15	5			νC-O + νC-C
1344	4	2	4	4	60	20	νC-O + CH_2 wag
1316	5	1	3	6	119	43	+ NH_2 twist
1198			5	5	95		νC-C
1155		2		3	207	200	CH_2 twist + NH_2 wag
1058		13		18	10	17	νC-N
947		1	9	8	69	96	νC-C + CH_2 twist + NH_2 wag
907	26		6	7	180		CO_2 scissor + CH_2 rock
857		1			20	139	NH_2 rock
723	18		2	9	26	11	CO_2 rock + CH_2 rock
687		1				128	NH_2 rock
646		1				155	
593	4		5	1	15	4	CO_2 wag + ring def.
552	8	6			6	30	νCd-O + νCd-N
514	8	3	2	1	52	93	ring def. + νCd-O
443	8	6			7	9	νCd-O + νCd-N
280	5	2			2	4	δL-Cd-L
234	6	2			1	4	
204		1			2	8	
186	3	3	3		4	9	

a All shifts are to lower wavenumber. Absence of data implies shift <1 cm^{-1}

b When this shift occurs, a band at 1567 cm^{-1} is revealed in the spectrum of the 1-^{13}C-labelled complex

relatively sharp band in the 3280 cm^{-1} region. This feature suggests that deuteration of the amino group does not simultaneously exchange deuterium oxide for the lattice water nor does re-exchange with atmospheric water occur.

The 2-^{13}C- and 2,2-d_2-sensitivities of the bands at 2973 and 2929 cm^{-1} allow their assignment to the asymmetric and symmetric νC-H vibrations. In addition, the magnitudes of the shifts on both types of isotopic substitution are of the order of those predicted by the diatomic oscillator relationship; this fact, together with the insensitivity of these bands to the other forms of isotopic substitution, indicates that these modes are vibrationally pure.

The band at 1609 cm^{-1} is assigned to an NH_2 scissoring mode. While it is vibrationally pure showing shifts on only ^{15}N- and N,N-d_2-isotopic substitutions the magnitudes of the shifts are somewhat less than those predicted using the diatomic oscillator analogy. This is easily rationalised when the hydrogen-bonding effects are taken into consideration. The band at 1574 cm^{-1} is uniquely sensitive to ^{18}O- and 1-^{13}C-labelling, suggesting its assignment to νC=O. Again, hydrogen bonding causes the ^{18}O shift to be smaller than that predicted theoretically while the 1-^{13}C shift is of the calculated order of magnitude for a vibrationally-pure νC=O band. Of all the modes of isotopic labelling employed, only the 1-^{13}C substitution shifts this band sufficiently to reveal an additional band at 1567 cm^{-1} which is assigned to the δH-O-H mode of the lattice water. In *trans*-$[Ni(gly)_2(H_2O)_2]$, in which the water molecules are coordinated, the analogous band occurs [54] at 1610 cm^{-1}.

On the grounds of their sensitivities towards ^{18}O-, 1-^{13}C-, 2-^{13}C- and 2,2-d_2-labelling the bands at 1438 and 1401 cm^{-1} are assigned to the coupled vibrations, νC-O + CH_2 scissor and νC-O + νC-C, respectively. The small 2,2-d_2-shift compared with that observed for the vibrationally-pure CH_2 scissoring mode in $[Ni(gly)_2(H_2O)_2]$ [54] is consistent with the coupled nature of the vibration in the cadmium complex. The region 1350 - 1300 cm^{-1} is characterized by two bands at 1344 and 1316 cm^{-1}, both of which show sensitivity to all the forms of isotopic substitution employed. Hence it is likely that a form of multiple coupling is occurring. The proposed assignment of these bands to coupled νC-O + CH_2 wag + NH_2 twist modes is reasonably indicated by the nature of the shifts and the region in which the bands occur.

The band at 1198 cm^{-1} is firmly assigned to νC-C on the basis of the equivalent shifts observed for ^{13}C-labelling of both carbon atoms and the substantial shift which occurs on 2-2-d_2 substitution. The band at 1155 cm^{-1} is assigned to a CH_2 twist + NH_2 wag on the grounds of the ^{15}N and 2-^{13}C shifts observed; the assignment is confirmed by the large 2,2-d_2 and N,N-d_2 sensitivities observed for the band.

Again using the diatomic oscillator analogy, with reference to ^{15}N and 2-^{13}C shifts, the band at 1058 cm^{-1} is a relatively pure νC-N vibration - seemingly uncoupled and uninfluenced by intermolecular interactions. The band at 947 cm^{-1} shows sensitivity to all forms of isotopic substitution employed except for the ^{18}O-labelling and is subsequently assigned to a coupled νC-C + CH_2 twist + NH_2 wag.

It has been noted [122] that while all the CH_2 and NH_2 deformation vibrations are coupled in glycinate complexes, this is particularly true for the CH_2 and NH_2 rocking vibrations. A number of bands associated with these vibrations in the region 900 - 600 cm^{-1} are therefore expected. Shifts on 2,2-d_2 and 2-^{13}C isotopic substitutions for the band at 907 cm^{-1} allow its assignment to a CH_2 rock, while additional sensitivities to ^{18}O- and 1-^{13}C-labelling indicate that this vibration is coupled to a CO_2 scissoring mode expected [54] in this region.

On the basis of its ^{15}N and N,N-d_2 sensitivities the band at 857 cm^{-1} is assigned to an NH_2 rocking mode. Absence of a 2-^{13}C shift indicates that there is no contribution to this band from a CH_2 mode. Hence the 2,2-d_2 sensitivity must arise from some other effect.

A similar situation arises for the band at 723 cm^{-1}; its insensitivity to ^{15}N substitution indicates that no NH_2 mode is contributing to the band, and leaves the assignment to a CO_2 rock + CH_2 rock on the grounds of the ^{18}O-, 1-^{13}C, 2-^{13}C and 2,2-d_2 isotopic shifts. The sensitivity to N,N-d_2 substitution must therefore be supposed to arise from some other effect.

An explanation of both the 2,2-d_2 sensitivity of the 857 cm^{-1} band and N,N-d_2 sensitivity of the 723 cm^{-1} band is proposed on the basis of accidental degeneracy. This phenomenon [195] describes how two bands, very close together but arising from different fundamental modes, may undergo resonance and energy exchange in such a way that the higher is raised in frequency and the lower is depressed. (This is known as Fermi resonance when a fundamental and an overtone

are involved).

In the 2,2-d_2 spectrum, resonance between the NH_2 rock (857 cm^{-1} in the unlabelled complex) and the CD_2 twist now in this region (947 cm^{-1} in the unlabelled complex) would account for the observed shift. Likewise the shift on *N,N*-d_2 substitution of the band at 723 cm^{-1} in the unlabelled complex may arise from resonance with the ND_2 rock now in this region (857 cm^{-1} in the unlabelled complex). However, it is acknowledged that the validation of such a rationalization of observed shifts is virtually impossible. While it is plausible that, in the spectrum of a complex molecule exhibiting many fundamentals, there is a good chance of accidental degeneracy, not all such degeneracies lead to resonance: certain conditions of symmetry and the type of degeneracy must be satisfied. Hence occurrence of resonance is infrequent. In addition, observation of the physical manifestations of the phenomenon have, in the past, been extremely limited, owing to the necessary approximations which must be made for theoretical calculations of a single ir spectrum of a relatively complicated molecule.

The clear illustration of accidental degeneracy as revealed here by the various forms of isotopic substitution is believed to be the first of its kind reported.

Bands at 687 and 646 cm^{-1} which are only sensitive to ^{15}N- and *N,N*-d_2-labelling are assigned to NH_2 rocking modes. The 646 cm^{-1} band probably corresponds to the 626 cm^{-1} band in $[Ni(gly)_2(H_2O)_2]$ where it was assigned [54] to an OH_2 rock. Had that study included *N,N*-d_2-labelling it is

possible that a shift would have been observed and have led to its assignment to an NH_2 rock. Owing to the shifts observed for the band at 593 cm^{-1} on all forms of isotopic substitution except ^{15}N, it is assigned to the coupled CO_2 wag + ring deformation ($\delta OCCH_2$). The bands at 552 and 443 cm^{-1} are particularly sensitive to ^{15}N- and ^{18}O-labelling. They are assigned to coupled νCd-O and νCd-N modes. No bands in this region are uniquely sensitive to only ^{18}O- or only ^{15}N-labelling. Hence there are no vibrationally pure νCd-O nor νCd-N bands. The relatively high frequencies of these metal-ligand modes suggests that there is considerable covalency in both the Cd-O and Cd-N bonds. This contradicts an earlier suggestion [196] that the M-O bonds in glycinate complexes are ionic, a suggestion which is also contrary to the crystallographically-determined [161] Cd-O bond lengths in $[Cd(gly)_2].H_2O$.

The band at 514 cm^{-1} shows sensitivity to all forms of isotopic substitution; it is therefore assigned to a ring deformation involving all the ligand atoms. The enhanced sensitivity of the band to ^{18}O-labelling indicates coupling to an additional νCd-O mode. The remaining bands below 300 cm^{-1} exhibit sensitivity to both ^{15}N- and ^{18}O-labelling which suggests their assignment to coupled Cd-ligand bending modes.

3.6.2 Band assignments in the ir spectrum of anhydrous cadmium glycinate, by multiple isotopic labelling: a comparison with the hydrated analogue

The ir spectrum (4000 - 150 cm^{-1}) of $Cd(gly)_2$ is depicted in Fig. 23, while the frequencies and shifts ($\Delta\nu$) are recorded in Table 33.

The procedure adopted for the interpretation of the spectra was similar to that described in detail for the hydrated complex $[Cd(gly)_2].H_2O$: the isotopic shift data were rationalized in terms of the various modes expected for each particular region of the spectrum, and definite assignments were then able to be carried out. Examination of the data presented in Table 33, together with the discussion of the spectrum of the $[Cd(gly)_2].H_2O$ complex makes a detailed account of the assignments of bands in the spectrum of $Cd(gly)_2$ superfluous. However, of far greater interest is a comparison of the spectrum of $Cd(gly)_2$ with that of its hydrated analogue with special reference to the degree of complexity and vibrational coupling, and differences in frequency of specific modes of vibration.

An initial examination of the spectra of the two complexes reveals that, despite the absence of any bands attributable to H_2O vibrations, the spectrum of $Cd(gly)_2$ is very much more complicated than that of the hydrate, implying that the former species is of lower symmetry. If the coordination of the glycinate ligands around the central metal ion is the same in both the Cd(II) complexes, removal of only the lattice water would be unlikely to affect the

Table 33. Frequencies, isotopically induced shifts and ir band assignments for $Cd(gly)_2$ (cm^{-1})

ν	$\Delta\nu^{18}O$	$\Delta\nu^{15}N$	$\Delta\nu1\text{-}^{13}C$	$\Delta\nu2\text{-}^{13}C$	Assignment
3351	-	9	-	-	νN-H H bonded
3322	2	8	2	3	antisym νN-H
3273	-	5	4	1	sym νN-H
3169	n.o.	n.o.	2	5	
2946	-	-	-	10	antisym νC-H
2926	-	-	-	8	sym νC-H
1635	21	2	29	5	νC=O + NH_2 scissor + CH_2 scissor
1589	18	-	30	-	νC=O
1549	9	-	27	-	νC=O
1431	6	-	9	3	νC-O + CH_2 wag
1414	27	-	32	6	
1397	-	3	2	9	CH_2 wag + NH_2 twist
1347	15	1	18	4	νC-O + CH_2wag + NH_2twist
1339	7	4	10	3	
1309	-	2	2	5	CH_2 wag + NH_2 twist
1182	2	-	4	2	νC-C + CO_2 scissor
1175	-	-	3	1	νC-C
1094	-	4	-	7	νC-N
1073	-	4	-	5	
1027	-	10	-	10	
951	-	-	5	6	νC-C
934	-	-	5	5	
911	13	-	7	7	CO_2 scissor + CH_2 rock
901	17	-	6	6	
722	17	1	5	7	
619	3	4	2	-	NH_2 rock + CO_2 rock
596	8	-	7	2	CO_2 rock + νCd-O
542	11	3	3	-	CO_2 rock + νCd-N
532	10	3	3	-	
481	9	2	2	1	ring def
412	9	10	-	-	νCd-O + νCd-N
396	8	6	4	4	ring def
254	-	4	-	-	δN-Cd-N
239	4	2	-	-	δN-Cd-O
214	5	3	4	4	
184	8	-	-	-	δO-Cd-O
152	5	-	-	2	

n.o. not observed

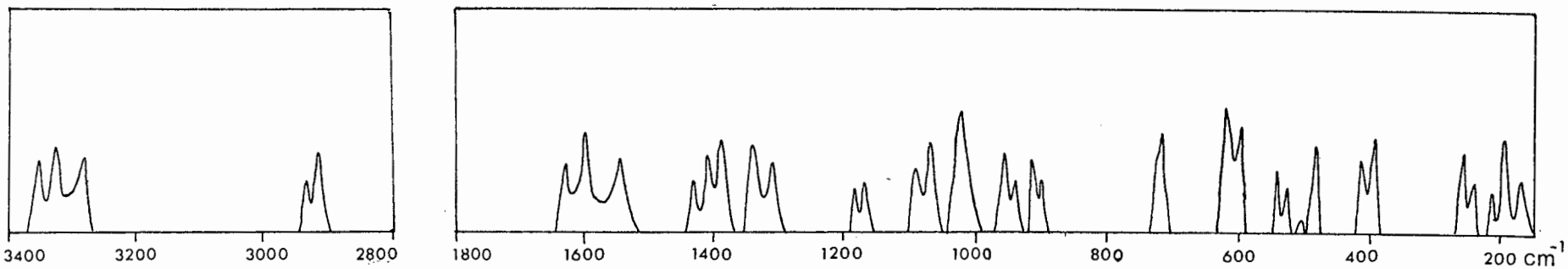

Fig. 23. The ir spectrum of the anhydrous complex $Cd(gly)_2$

crystallographic symmetry of the complex. Hence, it is postulated that the lower symmetry of the anhydrous species arises from a change in the localized point symmetry around the Cd(II) ion with subsequent changes to the site and space group.

The glycinate ligands in the anhydrous $Cd(gly)_2$ complex are therefore most probably arranged so as to give a four-coordinate tetrahedral configuration. This reduction in coordination number from six to four would manifest itself in the appearance of metal-ligand stetching vibrations at higher frequencies than those found in $[Cd(gly)_2].H_2O$. This is indeed observed, with νCd-O and νCd-N modes providing contributions to bands as high as 596 and 542 cm^{-1} in the spectrum of the anhydrous complex. Bands above 1300 cm^{-1} are generally much sharper in the spectrum of $Cd(gly)_2$ as opposed to those in the hydrate spectrum. This is indicative of less hydrogen bonding occurring in the former species. This factor may also be contributing to a lowering of the symmetry and increased complexity of the ir spectrum.

The purity of absorption bands and hence the degree of vibrational coupling appears to be similar in both of the Cd(II) complexes. νN-H, νC-H, νC=O, νC-C and νC-N modes are observed as pure vibrations in each of the two species while nearly all other bands exhibit some degree of coupling, the greatest being observed for the NH_2 and CH_2 deformation vibrations.

From the isotopic shift data for $Cd(gly)_2$, it is again apparent that there are no vibrationally pure νCd-O nor νCd-N

modes and while their high frequency may be attributed to the distribution of the metal bonding power over fewer atoms, it is also indicative of considerable covalency in both the Cd-O and Cd-N bonds.

3.6.3 *Band assignments in the ir spectrum of zinc glycinate monohydrate by multiple isotopic labelling*

Results of the x-ray crystallographic investigation by Low *et al.* [161] indicate that the structure of zinc glycinate monohydrate is essentially similar to that of the $[Cd(gly)_2].H_2O$ complex discussed earlier with the coordination of the zinc complex showing considerably greater distortion from a regular octahedral environment.

Although a large quantity of ir data for various metal(II) glycinate complexes has been accumulated, the spectrum of $[Zn(gly)_2].H_2O$ has been given only limited attention. Again, disagreement on the nature of the metal-oxygen bonding has arisen [121,176,197]. It has been suggested [196] that the position of $\nu C{=}O$ near 1600 cm^{-1} is indicative of low covalency in the Zn-O bonds. In fact, this frequency is very close to the $\nu C{=}O$ value of *trans*-$[Ni(gly)_2(H_2O)_2]$ [54], for which crystallographic analysis has revealed [198] no abnormally low covalency in the Ni-O bonds. It is therefore considered worthwhile to apply the technique of multiple isotopic labelling of ligand atoms to an ir study of this complex. However, owing to the fact that extensive vibrational coupling has been found in related metal glycinate complexes, contribution of

metal-ligand modes to ligand vibrations in the region below 600 cm^{-1} is expected. The isotopic substitution of ligand atoms (only) is hence not really sufficient for a complete band assignment to be made. For this reason it has been considered useful to include metal isotope shift data together with the independent labelling of ligand atoms.

The ir spectra of $[Zn(gly)_2].H_2O$ and its ^{18}O, ^{15}N, 1-^{13}C, 2-^{13}C, 2,2-d_2, N,N-d_2, ^{64}Zn and ^{68}Zn substituted analogues are depicted in Fig. 24. Frequencies, shifts ($\Delta\nu$) and assignments are given in Table 34.

The 4000 - 1500 cm^{-1} region

The bands at 3450 and 3306 cm^{-1} originate in the uncoordinated water molecule. The weak residual bands at these frequencies in the N,N-d_2-labelled complex indicate some H-D exchange while the D_2O bands occur, as expected [191] near 2600 cm^{-1} where they form part of a band envelope which also comprises the N-D stretching modes. Some degree of ^{15}N-sensitivity of the O-H bands is evidence of hydrogen bonding with amino groups, as indicated by the crystallographic study [161]. The two νN-H bands are readily identified by their ^{15}N- and N,N-d_2-sensitivities as the bands at 3268 and 3160 cm^{-1}, while the absorptions at 2982 and 2939 cm^{-1} are clearly νC-H bands in view of their sensitivities to 2-^{13}C- and 2,2-d_2-labelling only. All the νN-H and νC-H modes are relatively pure, their observed shifts being approximately those calculated [191] for isolated N-H(D) or C-H(D) diatomic species from the ratio $\nu^D/\nu^H = 0.73$.

Table 34. Frequencies (cm^{-1}), isotopically induced shifts (cm^{-1}) and ir assignments for *trans*-$[Zn(gly)_2].H_2O$ and its labelled analogues[a]

ν	Δν $^{68,64}Zn$[b]	^{18}O	^{15}N	1-^{13}C	2-^{13}C	2,2-d_2	N,N-d_2	Assignment
3450			2				16	νO—H---N
3306			10				11	νO—H---N
3268			8				14,∿800[c]	νN-H
3160			7				∿800	νN-H
2982					10	743		νC-H
2939					9	783		νC-H
1594		28		44				νC=O
1578		-[d]	2		-[d]		137	NH_2 scissor
1439		5	2	12	4	19	118	νC-O + NH_2 scissor + CH_2 scissor
1407		9		12	4	12		νC-O + CH_2 scissor
1393		-[d]	8	-[d]	-[d]	119	202	NH_2 scissor + CH_2 wag
1387		18	-[d]	12		170		νC-O + CH_2 wag
1343		6	2	10	4	145	29	νC-O + CH_2 wag + NH_2 twist
1307		5		3	5	197	45	νC-O + CH_2 wag + NH_2 twist
1188		2				16	4	CH_2 twist
1167						85	195	CH_2 twist + NH_2 wag
1146		6	3			194	189	CO_2 twist + NH_2 wag
1092			2			151	37	NH_2 wag + CH_2 twist
1061			14		19	19	19	νC-N
1057		7	13		24	16	22	νC-N + CO_2 scissor
952		2		8	7	77	14	coupled νC-C
915		4		16	9	25	48	coupled νC-C
904		22[e]		17	7	63	67[e]	CH_2 rock + NH_2 rock + CO_2 scissor
721		33		12[e]	7	19	15	CO_2 rock + CH_2 rock
648		13	6			3	51	CO_2 rock + NH_2 rock
602		12	5	4		24	59	ring def.
588	>2[d]	-[d]	3	8		10		CO_2 wag + νZn-N (?)
567	-[d]	17	5	-[d]	-[d]	24	-[d]	NH_2 rock + CH_2 wag (?)
533		11	6			50	63	NH_2 rock + CH_2 rock
512	2		4	2		29	22	νZn-N + ring def.
473	2	3	8			6	-[d]	νZn-N + νZn-O
458	6	11	10			11	25	νZn-N + νZn-O
327	3		3			3	5	νZn-N
249	4	8		2				νZn-O
212	4	8	7	2		4	-[d]	δO-Zn-N
168	2	7				-[d]	-[d]	δO-Zn-O

[a] Absence of data implies shifts ≤ 1 cm^{-1}. [b] Shift to lower wavenumber from $[^{64}Zn(gly)_2].H_2O$ to $[^{68}Zn(gly)_2].H_2O$. [c] Two shift values indicate incomplete deuterium exchange.

[d] Shift undeterminable owing to masking by neighbouring band or because band is too broad.

[e] Mean of doublet

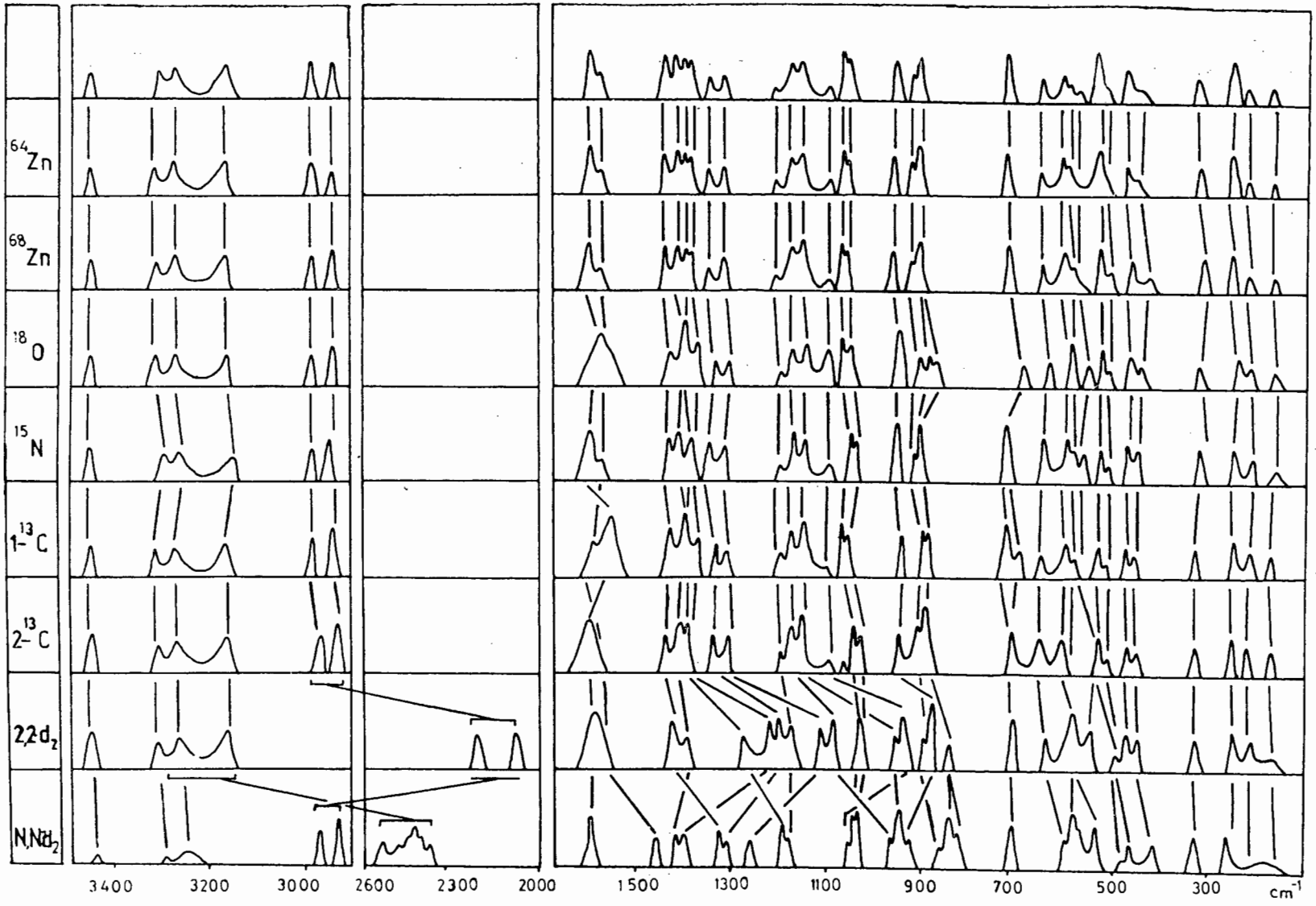

Fig. 24. The ir spectrum of $[Zn(gly)_2].H_2O$ and its labelled analogues

The intense absorption at 1594 cm^{-1} shows significant sensitivities to only ^{18}O- and 1-^{13}C-labelling. In addition, the magnitude of its 1-^{13}C shift (-44 cm^{-1}) is of the order expected for νC=O - on the basis of the diatomic oscillator analogy. These factors indicate that this vibrational mode is a pure νC=O, its reduced -^{18}O-sensitivity being ascribed to the hydrogen bonding to the carbonyl group. The NH_2 scissoring mode which is also expected in this region appears as a shoulder at 1578 cm^{-1} in the unlabelled complex, its assignment being supported by the negative shifts of -2 and -137 cm^{-1} on ^{15}N and N,N-d_2 isotopic substitutions, respectively.

The 1500 - 600 cm^{-1} region

Many bands in this region show shifts on a number of ligand atom isotopic substitutions, which is indicative of extensive vibrational coupling. The five bands at 1439, 1407, 1387, 1343 and 1307 cm^{-1} all show ^{18}O- and 1-^{13}C-sensitivities and are therefore considered to be coupled νC-O modes. The remaining contributions to these bands from the various CH_2 and NH_2 bending vibrations expected in this region are easily deduced from the shift values obtained and are not discussed further.

The peak at 1393 cm^{-1} in the unlabelled complex is unfortunately masked in the spectra of the ^{18}O, 1-^{13}C and 2-^{13}C complexes as a result of the negative shift of the band occurring immediately above it. However, the sensitivity of the 1393 cm^{-1} band to the 2,2-d_2 and N,N-d_2 isotopic substitutions allow tentative assignment to a coupled NH_2 scissor + CH_2 wag.

The four peaks between 1190 and 1090 cm^{-1} also show significant sensitivities to (predominantly) the 2,2-d_2 and N,N-d_2 isotopic substitutions and may therefore also be assigned to variously coupled -CH_2 and -NH_2 wagging and twisting vibrations. The additional ^{18}O shift experienced by the band at 1146 cm^{-1} in the spectrum of the unlabelled complex is surprising since the frequency is too low for a νC-O mode and too high for a CO_2 scissoring vibration. The νC-N vibration is easily identifiable as a relatively intense doublet at 1061, 1057 cm^{-1}, showing significant sensitivities to ^{15}N and 2-^{13}C isotopic substitutions. In further support of this assignment, their 2,2-d_2 and N,N-d_2 shift values are smaller than those observed for CH_2 and NH_2 bending modes respectively. The additional shift of the lower component of the doublet in the spectrum of the ^{18}O-labelled complex indicates that some contribution from a CO_2 scissoring mode is likely.

The similar shifts of the 952 and 915 cm^{-1} bands on 1-^{13}C, 2-^{13}C and 2,2-d_2 substitutions indicate that a νC-C mode makes a substantial contribution to the absorptions; additional small shifts in the ^{18}O and N,N-d_2 spectra indicate that the bands are not pure and are experiencing coupling to CO_2 and NH_2 bending modes.

The remaining peaks in this region all show considerable ^{18}O- and some 1-^{13}C-sensitivity which supports their assignment to CO_2 rocking and scissoring modes. The two higher bands at 904 and 721 cm^{-1} are also shifted significantly on 2-^{13}C isotopic substitution indicating additional CH_2 rocking character. Sensitivity of the 648 cm^{-1} absorption to ^{15}N-

and *N,N-d*$_2$-labelling implies coupling of the CO_2 rock to an NH_2 rock while the shifts of the remaining band at 602 cm^{-1} allow its assignment to a ring deformation.

The 600 - 140 cm^{-1} region

This is the region where metal-ligand vibrations are usually found, and hence shifts due to metal isotope labelling are expected to occur.

The two weak shoulders at 588 and 567 cm^{-1} in the spectrum of the unlabelled complex are unfortunately not observed in some of the labelled spectra. Hence, no definite assignments can be made. However, negative shifts of the higher band on ^{68}Zn, ^{15}N and 1-^{13}C substitutions permit its assignment to a coupled νZn-N + CO_2 wag while the ^{18}O- and ^{15}N-sensitivities of the lower band indicate that it is a CO_2 rock coupled to an NH_2 rock, both vibrations being expected in this region. The band at 533 cm^{-1}, exhibiting similar ^{15}N- and ^{18}O-sensitivities but again, no metal ion isotope shifts, must be similarly assigned. All remaining bands show sensitivity to ^{64}Zn and ^{68}Zn substitution and hence must comprise some metal-ligand character. Comparable ^{15}N sensitivities of the absorptions at 512 and 327 cm^{-1} indicate that they are most likely νZn-N modes with the sensitivities of the higher band to other forms of labelling indicating coupling to a ring deformation. Sensitivity of the bands at 249 and 168 cm^{-1} to metal isotope and ^{18}O substitutions only, allow their assignment to νZn-O and δO-Zn-O

vibrations, respectively. The remaining peaks at 473, 458 and 212 cm^{-1} undergo frequency shifts on both ^{18}O- and ^{15}N-labelling. Subsequent assignments to coupled Zn-O and Zn-N stretching and bending modes are therefore plausible.

3.6.4 *Band assignments in the ir spectra of the β-forms (cis-cis) of tris(glycinato)chromium(III) and cobalt(III) complexes*

To date, very much less information has been accumulated for metal(III) glycinate complexes as compared with their metal(II) analogues.

Studies of the cobalt(III) complexes have largely involved investigation of the nature of the coordination about the metal ion, since two geometric isomers are possible. A violet dihydrate and rose-red monohydrate have been prepared [163,199-201] and absorption spectra [163,199,201] and thermal stabilities [163] have been determined, establishing differences between the *cis-trans* α- and *cis-cis* β-isomers.

Thermochemical properties of a *tris* (glycinato) chromium(III) complex have also been investigated [162] and an x-ray crystal structure analysis [204] has shown that a red $[Cr(gly)_3].H_2O$ has the *cis-cis* configuration.

Previous studies of the ir spectra of these complexes [197,205] have not been extended below 700 cm^{-1} and only limited attempts to assign vibrations to specific absorptions have been made.

The ir spectra of the *cis-cis* complexes $Cr(gly)_3$ and $[Co(gly)_3]2H_2O$ are depicted in Fig. 25. A list of recorded

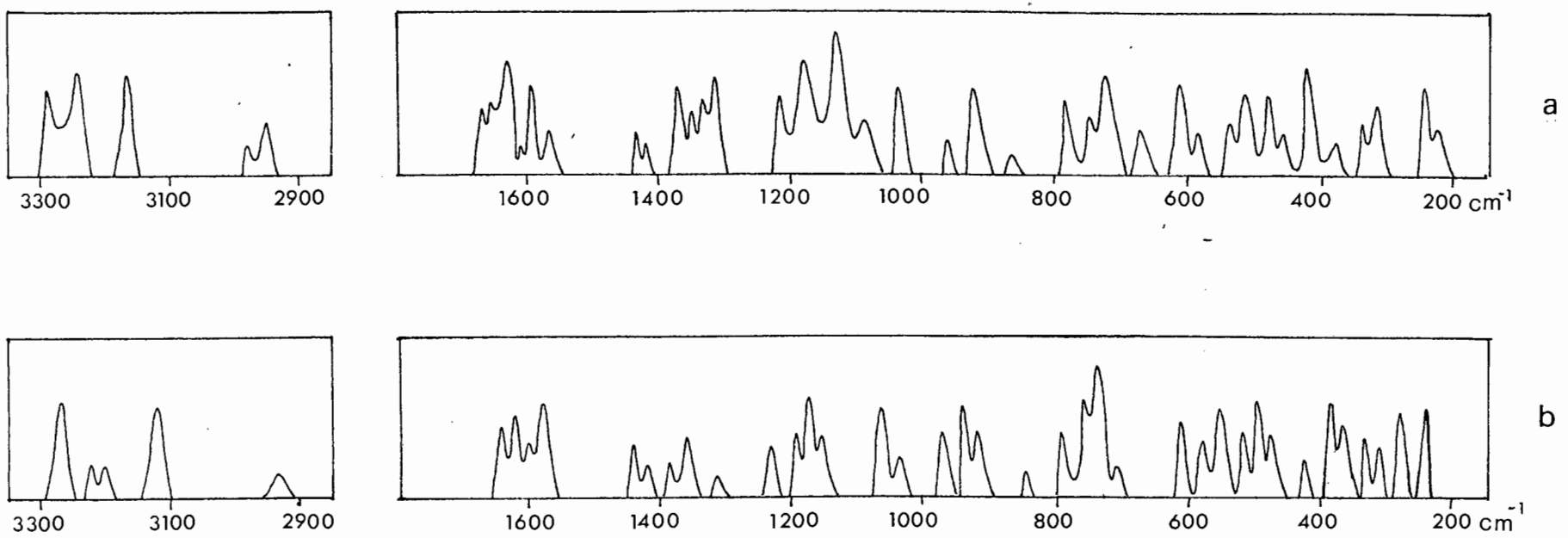

Fig. 25. The ir spectra (4000 - 150 cm^{-1}) of a - $Cr(gly)_3$ and b - $[Co(gly)_3].2H_2O$

frequencies, isotopic shift data ($\Delta\nu$) and band assignments is given in Tables 35 and 36.

The 4000 - 550 cm^{-1} region

Examination of the isotopic shift data and comparisons with the results of Sections 3.6.1, 3.6.2 and 3.6.3, allow the relatively straightforward assignment of vibrations in the spectra of the two *tris* complexes. The following aspects of the spectra are of interest:

For the $Cr(gly)_3$ complex, the five bands above 2000 cm^{-1} undergo shifts which allow their assignment to pure vibrations. The bands are all relatively sharp, indicating that the H-bonding which is occurring is less extensive than that of the $[Co(gly)_3].2H_2O$ complex, for which the analogous bands are broader and less well resolved. This is most likely a consequence of the uncoordinated water molecules of the Co(III) complex; the absence of additional absorptions attributable to νO-H modes implies that the νN-H bands have partial νO-H character.

In the spectra of both complexes, the 1700 - 1300 cm^{-1} regions are characterized by two pure νC=O modes which undergo shifts on only ^{18}O and 1-^{13}C isotopic substitutions, and two pure CH_2 bending modes which undergo significant shifts on 2-^{13}C- and 2,2-d_2-labelling which allow their subsequent assignment to scissoring and wagging vibrations. A pure NH_2 scissor mode is observed only in the spectrum of $Cr(gly)_3$ at 1668 cm^{-1}. The analogous vibration in the Co(III) complex occurs as a doublet (1614, 1600 cm^{-1}) with its concomitant

Table 35. Frequencies, isotopically induced shifts (Δν) and assignments for ir bands in the spectrum of *cis,cis*- $Cr(gly)_3$ (cm^{-1})

ν	$\Delta\nu^{18}O$	$\Delta\nu^{15}N$	$\Delta\nu 1\text{-}^{13}C$	$\Delta\nu 2\text{-}^{13}C$	$\Delta\nu 2,2\text{-}d_2$	Assignment
3293	-	9	-	-	-	H-bonded νN-H
3241	-	10	-	-	-	antisym νN-H
3138	-	8	-	-	-	sym νN-H
2979	-	-	-	12	817	antisym νC-H
2947	-	-	-	15	792	sym νC-H
1668	-	4	-	-	-	NH_2 scissor
1657	15	-	7	-	-	νC=O
1638	13	-	14	-	-	νC=O
1608	7	5	6	6	6	νC=O + NH_2 scissor + CH_2 scissor
1591	6	-	5	-	8	νC=O + CH_2 scissor
1570	-	-	-	2	113	CH_2 scissor
1435	-	-	-	4	63	CH_2 scissor
1425	3	-	3	4	53	νC-O + CH_2 scissor
1367	11	4	7	-	22	νC-O + NH_2 twist
1345	5	-	a	4	114	νC-O + CH_2 wag
1330	21	-	22	3	111	νC-O + CH_2 wag
1309	21	-	25	5	202	νC-O + CH_2 wag
1210	-	2	-	2	20	NH_2 twist + CH_2 twist
1173	-	2	-	3	104	NH_2 twist + CH_2 twist
1125	4	-	2	4	163	CO_2 scissor + CH_2 twist
1083	2	-	3	n.o.	-	CO_2 scissor
1036	1	12	-	18	-	νC-N
958	-	-	9	4	27	νC-C
908	9	-	5	9	21	CO_2 scissor + CH_2 rock
863	20	8	8	-	28	CO_2 scissor + NH_2 rock
776	-	4	-	5	24	CH_2 rock + NH_2 rock
745	4	-	-	7	120	CH_2 rock
733	7	4	4	-	12	NH_2 rock + CO_2 rock
684	4	-	2	-	5	CO_2 rock
603	9	3	6	-	32	CO_2 rock + NH_2 rock
589	6	4	6	-	3	CO_2 rock + NH_2 rock
535	5	5	3	1	38	ring def.
514	5	4	2	1	41	ring def.
485	3	6	-	-	31	νCr-O + νCr-N
470	10	7	-	-	21	νCr-O + νCr-N
412	3	-	-	-	-	δO-Cr-O
379	2	-	-	-	5	δO-Cr-O
336	3	3	-	-	-	δO-Cr-N
326	4	3	-	-	-	δO-Cr-N
248	-	5	-	-	4	δN-Cr-N
236	9	8	-	-	8	δO-Cr-N

a Masked
n.o. not observed

Table 36. Frequencies, isotopically induced shifts ($\Delta\nu$) and assignments for ir bands in the spectrum of *cis,cis*-$[Co(gly)_3].2H_2O$ (cm^{-1})

ν	$\Delta\nu^{18}O$	$\Delta\nu^{15}N$	$\Delta\nu1\text{-}^{13}C$	$\Delta\nu2\text{-}^{13}C$	$\Delta\nu2,2\text{-}d_2$	Assignment
3286	-	6	-	-	-	H-bonded νN-H + νO-H
3221	-	7	-	-	-	antisym νN-H + νO-H
3200	-	18	-	-	-	
3122	-	12	-	-	-	sym νN-H
~2940	-	-	-	10	710 752	νC-H (poor resolution)
1645	17	-	10	-	-	νC=O
1614	11	3	3	2	2	νC=O + NH_2 scissor + νO-H
1600	a	2	3	2	2	
1578	9	-	24	-	-	νC=O
1430	3	-	11	4	80	νC-O + CH_2 scissor
1422	2	-	a	2	83	CH_2 scissor
1391	18	2	16	7	-	νC-O + NH_2 twist + νC-C
			b	b	b	
1357	16	-	26	27	185	νC-O + CH_2 wag
1309	-	-	-	-	119	CH_2 wag
1233	-	4	-	-	4	NH_2 twist
1196	-	-	2	2	67	νC-CH_2
1173	-	2	2	5	96	CH_2 twist + NH_2 twist
1157	-	-	4	-	89	CH_2 twist
1064	-	-	-	-	121	νC-N + CH_2 rock
1038	-	3	-	2	108	
967	1	-	7	8	-	νC-C
932	27	-	5	8	37	CO_2 scissor + CH_2 rock
917	28	-	5	8	31	
844	4	-	-	7	11	CH_2 rock
786	3	4	-	4	18	CO_2 rock + NH_2 rock + CH_2 rock
757	a	-	4	a	30	
745	5	3	-	3	18	
717	-	3	-	2	11	NH_2 rock + CH_2 rock
607	9	7	2	2	5	CO_2 rock + NH_2 rock
582	9	9	-	-	5	
557	2	-	2	-	5	CO_2 rock
531	4	2	3	1	n.o.	ring def.
499	7	4	-	-	7	νCo-O + νCo-N
487	7	6	-	-	15	
428	6	-	-	-	3	νCo-O
384	9	-	-	-	3	δO-Co-O
363	6	-	-	-	-	
323	3	-	-	-	-	
309	7	-	-	n.o.	2	
274	2	4	-	-	2	δO-Co-N
231	6	6	-	-	2	

a Masked or split

b Revealed on 1-^{13}C and 2-^{13}C isotopic labelling at 1361 and 1353 cm^{-1} respectively and shifting to 1246 on 2,2-d_2 substitution

n.o. not observed.

^{18}O- and 1-^{13}C-sensitivities indicating coupling to an additional νC=O mode. The δO-H vibration expected [54] in this region is presumed to contribute to this band as well. Remaining bands in this region undergo shifts on at least four of the independent isotopic substitutions indicating extensive vibrational coupling, which is entirely expected [191,192]. Again, assignments given are those most logically deduced from the magnitudes of the shift data and the postions of the ir bands.

Further vibrations of the glycinate ligand are both expected and found for both complexes in the spectral region 1300 - 550 cm^{-1}. The νC-N vibration in the $Cr(gly)_3$ spectrum is easily identifiable at 1036 cm^{-1} from its ^{15}N and 2-^{13}C shift values; a split of the equivalent mode into two bands at 1064 and 1038 cm^{-1} is apparent in the spectrum of the $[Co(gly)_3].2H_2O$ complex with an additional strong sensitivity to 2,2-d_2 substitution indicating coupling to a CH_2 rocking mode. In the spectra of both complexes, bands attributable to νC-C and CH_2 rocking modes appear to comprise relatively pure vibrations with no significant sensitivity to isotopic substitutions other than 1-^{13}C, 2-^{13}C and 2,2-d_2 being observed. The only other bands which may be assigned to uncoupled ligand modes in the spectrum of the Co(III) complex are an NH_2 twist at 1233 cm^{-1}, a CH_2 twist at 1157 cm^{-1}, a CH_2 rock at 844 cm^{-1} and a CO_2 rock at 557 cm^{-1}. By comparison, a CO_2 scissor at 1083 cm^{-1}, a CH_2 rock at 745 cm^{-1} and a CO_2 rock at 684 cm^{-1} are pure vibrations in the spectrum of $Cr(gly)_3$. Once again, the multiple isotopic sensitivities of remaining bands necessitates assignment of each absorption to more than one mode which is evidence of significant vibrational coupling.

The 550 - 200 cm^{-1} region

In this spectral region of both the complexes, bands above 500 cm^{-1} undergo shifts on all the isotopic substitutions employed allowing their assignment to deformations of the coordinated glycinate ring. All the other absorptions show significant sensitivities to ^{18}O- and ^{15}N-labelling only, which implies that they arise from metal ligand vibrations. Assignments of these bands to stretching and bending modes, respectively, have been based upon the relative frequencies and shifts observed: stretches generally occur at a higher frequency and often undergo more significant isotopic shifts owing to their greater effect on dipole moment change and participation of individual atoms in the vibration.

The sensitivity of some of these modes to 2,2-d_2-labelling cannot logically be explained as this region of the spectrum is well below that in which any CH mode is expected.

Finally, it is interesting to note that the assignments for metal-to-ligand stretching frequencies proposed here yield the sequences Co(III) > Cr(III) > M(II). This is entirely expected in terms of metal bonding power and cfse values, cogniscance being taken of the fact that the Co(III) complex is $3d_6$ low-spin while its Cr(III) analogue is $3d_3$ high-spin.

3.7 METAL COMPLEXES OF UREA

3.7.1 *The crystal and molecular structure of hexakis(urea) chromium-(III) chloride trihydrate*

Results

Crystal data and experimental details of the data collection are listed in Table 37. The crystals were found to be hexagonal having cell parameters a = 1756.3(9) pm, c = 1412.9(7) pm. Their density was measured in a *meta*-xylene (d = 0.86 Mg m^{-3}) / methyl iodide (d = 2.26 Mg m^{-3}) flotation mixture, and found to be 1.48 Mg m^{-3}. Substitution in the Equation given in Section 3.2.3 yielded a value of six "molecules" per unit cell, and a calculated density of 1.51 Mg m^{-3}.

The diffractometer intensity data were consistent with the requirements for five possible space groups. The condition limiting the possible reflections was

$$hkil : \quad -h + k + l = 3n$$

which allows R3 (No. 146), $R\bar{3}$ (No. 148), R32 (No. 155), R3m (No. 160) and $R\bar{3}m$ (No. 166). Hence an initial postulate that the chromium(III) chloride complex is isomorphous with its titanium and vanadium iodide analogues [137,139], both of $R\bar{3}c$ (No. 167) crystal symmetry had to be discounted at this stage since the reflections $hh0l$ for $Cr(ur)_6Cl_3.3H_2O$ are not limited by the condition $l = 2n$.

Of the possible space groups, $R\bar{3}$ (No. 148) was selected primarily as it is the only one having the $\bar{3}$ symmetry, which

Table 37. Crystal data, experimental and refinement parameters

Molecular formula	$[Cr(CON_2H_4)_6]Cl_3.3H_2O$
M_r	572.76
Space group	$R\bar{3}$
a	1756.3(9) pm
c	1412.9(7) pm
D_m	1.48 Mg m^{-3}
D_c	1.51 Mg m^{-3}
μ(Mo$K\alpha$)	7.67 mm^{-1}
F(000)	1782
Crystal dimensions	0.2 x 0.15 x 0.15 mm
Scan mode	ω-2θ
Scan width	1.00$^{o}\theta$
Scan speed	0.03$^{o}\theta$ s^{-1}
Range scanned (2θ)	3-20^{o}
Stability of standard reflections	2.0%
Number of reflections collected	1256
Number of observed reflections	574 with>I(rel)>2σI(rel)
Number of variables	51
$R = \Sigma\|\|F_o\|-\|F_c\|\|/\Sigma\|F_o\|$	0.0809
$R_w = \Sigma w^{\frac{1}{2}}\|\|F_o\|-\|F_c\|\|/\Sigma w^{\frac{1}{2}}\|F_o\|$	0.0721
Weighting scheme w	$(\sigma^2F)^{-1}$

would most easily accommodate an octahedral environment of the Cr(III). The subsequent refinement of the structure has vindicated this choice. The chromium(III) ions were located in a Patterson map, at the *3a* and *3b* positions, with $\bar{3}$ symmetry obtaining for all of them. Subsequent weighted difference syntheses yielded the positions of the remaining non-hydrogen atoms of the coordinated species - in two sets of the general positions *f*: one as listed in the space group table and another shifted by $\frac{1}{2}$ in *z*. The locations of chloride ions and the oxygens of the uncoordinated water molecules were similarly established to be at the general *f* positions.

In the final refinement the chromium and chloride ions were treated anisotropically, the other atoms isotropically and hydrogens were not included in the model.

Fractional atomic coordinates and thermal parameters are listed in Table 38. Bond lengths and angles are quoted in Table 39, while the complex cation is depicted in Fig. 26. A final listing of Miller indices and the observed and calculated structure factors for each reflection is given in Table 40.

Discussion

Examination of the data presented for the *A* and *B* sets of complex ion species shows as expected, that the various particular bond lengths in each grouping are entirely comparable in so far as their magnitudes and e.s.d.'s, while

Table 38. Fractional atomic coordinates ($x10^4$) and thermal parameters ($pm^2 \times 10^{-1}$) for $[Cr(ur)_6]Cl_3.3H_2O$

Atom	x	y	z	U_{11}	U_{22}	U_{33}	U_{23}	U_{13}	U_{12}
Cr A	0.0(0)	0.0(0)	0.0(0)	23(2)	23(2)	51(4)	0.0(0)	0.0(0)	12(1)
Cr B	0.0(0)	0.0(0)	5000(0)	32(2)	32(2)	42(4)	0.0(0)	0.0(0)	16(1)
Cl	2976(2)	277(2)	1440(3)	44(2)	58(2)	100(3)	-15(2)	-19(2)	21(2)
OA	478(5)	1063(4)	782(5)	34(2)					
CA	1271(8)	1593(8)	1092(8)	42(4)					
N1A	1463(6)	2414(6)	1308(6)	47(3)					
N2A	1862(6)	1348(6)	1173(7)	47(3)					
OB	496(5)	1072(5)	5777(5)	44(2)					
CB	1237(8)	1556(8)	6220(9)	47(4)					
N1B	1356(7)	2331(7)	6545(7)	62(3)					
N2B	1835(7)	1322(6)	6328(7)	60(3)					
O	2477(6)	2826(6)	3578(7)	99(4)					

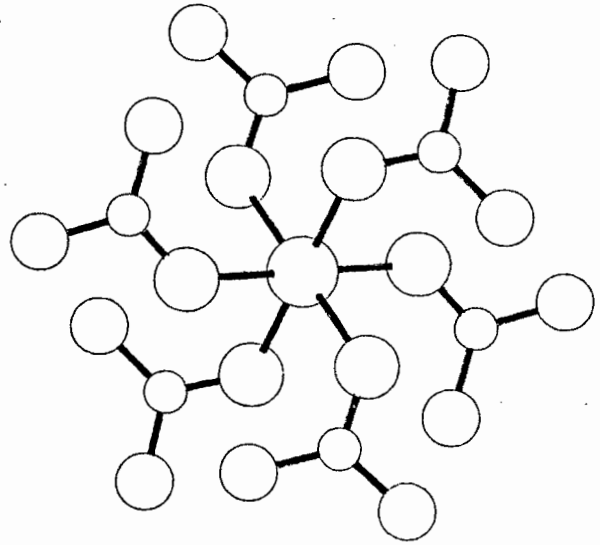

Fig. 26. Coordination around the cation

Table 39. Interatomic distances (pm) and bond angles (deg.) in $[Cr(ur)_6]Cl_3.3H_2O$ [a]

(a) Coordination polyhedron

CrA – OA	196(1)	CrB – OB	197(1)
OA – CrA – $OA^{(i)}$	91.3(3)	OB – CrB – $OB^{(i)}$	91.9(3)
OA – CrA – $OA^{(ii)}$	88.7(3)	OB – Cr(B) – $OB^{(ii)}$	88.1(3)

(i) $-y, x-y, z$

(ii) $y, y-x, -z$

(b) Urea molecule

OA – CA	130(1)	OB – CB	131(1)
CA – N1A	134(1)	CB – N1B	135(1)
CA – N2A	131(1)	CB – N2B	131(1)
OA – CA – N1A	116.6(1.0)	OB – CB – N1B	114.9(1.0)
OA – CA – N2A	122.2(1.1)	OB – CB – N2B	123.0(1.2)
N1A – CA – N2A	121.2(1.1)	N1B – CB – N2B	122.1(1.1)

(c) Hydrogen bonding

Cl – $O^{(iii)}$	308(2)	Cl – $N2A^{(iii)}$	327(3)
Cl – $O^{(iii)}$	307(2)		

(iii) $\frac{2}{3} - x, \quad \frac{1}{3} - y, \quad \frac{1}{3} - z$

[a] Standard deviations in least significant figures given in parentheses

definite though not as marked similarities in the bond angles are also observed. The ensuing discussion therefore refers to both the A and B $[Cr(ur)_6]^{3+}$ identities.

The O-Cr-O bond angles indicate that there are significant distortions of the CrO_6 coordination polyhedron from O_h symmetry. The symmetry of the polyhedron and of the whole complex ion must be S_6 from the space group requirements and this is the maximum observed point symmetry. Hence the structure is somewhat different from that reported [206] for $[Cr(ur)_6](ClO_4)_3$. Dingle [207] has quoted that crystals of $[Cr(ur)_6]X_3$ where X = Cl^-, I^-, NO_3^- and ClO_4^- are isomorphous and isostructural. Therefore it would appear that the presence of water molecules in the crystal lattice of the chromium(III) chloride complex investigated here, have a significant effect upon the crystal symmetry. This could logically be rationalized in terms of additional hydrogen bonding and subsequent distortion factors. That hydrogen bonding is likely to be occurring between the amide groups, the $O(H_2O)$ and the Cl atoms outside the complex cation, is evidenced by the fact that N2A-Cl, and O1-Cl distances are less than the sums of the relevant Van der Waals' radii for the atoms as calculated by Pauling (209) (see Table 39).

A further comparison between the data reported here and those for the titanium(III) and vanadium(III) iodide analogues [137,139], indicates that the main difference in the structures lies only in the orientation of the polyhedra which are different (seen down c) in $R\bar{3}c$ and the same in $R\bar{3}$. The reason for the variation in space group of the two species

may be attributed to the very much larger size of the iodide anions as opposed to the chlorides, as well as the inclusion of the water molecules in the crystal lattice of $[Cr(ur)_6]Cl_3.3H_2O$.

The O-C-N and N-C-N bond angles in $[Cr(ur)_6]Cl_3.3H_2O$ are very similar to those reported [208] in an x-ray study of free crystalline urea: slight deviations of the angles around the carbon atoms from the 120^o expected for sp^2 hybridization are observed in both cases.

The carbonyl bond distance might be expected to be longer in coordinated urea than in the free molecule, but compared with the x-ray data for the latter [208], there is no significant change.

The geometry of the urea molecules in this investigation differs from that of free urea in that the two C-N distances differ by 5(1) pm. This may be attributed to a redistribution of electron density on coordination of the ligand to the chromium(III) ion, the two C-N distances no longer being equivalent in any bonding scheme.

OBSERVED AND CALCULATED STRUCTURE FACTORS FOR $[Cr(ur)_6]Cl_3.3H_2O$

H	K	L	FO	FC	H	K	L	FO	FC	H	K	L	FO	FC	H	K	L	FO	FC	H	K	L	FO	FC
0	3	0	170	183	-6	15	0	59	53	-11	9	1	32	30	-2	2	2	240	242	-13	9	2	128	123
-2	4	0	95	-84	-3	15	0	19	20	-8	9	1	38	41	1	2	2	295	287	-10	9	2	101	106
-4	5	0	76	-84	-11	16	0	35	34	-5	9	1	35	32	-4	3	2	135	131	-7	9	2	22	32
-1	5	0	87	99	-5	16	0	21	13	1	9	1	23	-21	-1	3	2	230	225	-4	9	2	79	71
-3	6	0	226	205	-3	2	1	27	-34	4	9	1	41	-35	2	3	2	507	510	-1	9	2	131	128
0	6	0	14	15	0	2	1	48	-53	7	9	1	63	-58	-6	4	2	204	-191	2	9	2	86	93
-5	7	0	171	167	1	3	1	26	33	-16	10	1	26	-24	-3	4	2	245	-241	5	9	2	79	79
-2	7	0	29	-17	-7	4	1	25	27	-13	10	1	32	-32	0	4	2	106	124	-15	10	2	24	20
-7	8	0	44	53	-4	4	1	64	67	-7	10	1	63	59	3	4	2	56	50	-12	10	2	66	70
-4	8	0	98	102	-1	4	1	33	43	-4	10	1	55	64	-8	5	2	74	80	-9	10	2	120	119
-1	8	0	186	188	-9	5	1	15	-10	-1	10	1	16	15	-5	5	2	192	175	-6	10	2	183	189
-3	9	0	29	12	-6	5	1	81	-82	2	10	1	29	22	-2	5	2	127	-113	-3	10	2	163	163
0	9	0	47	-39	-3	5	1	69	-83	5	10	1	35	29	1	5	2	91	-69	3	10	2	29	21
-8	10	0	169	171	0	5	1	73	-78	-15	11	1	21	21	4	5	2	76	65	6	10	2	47	52
-5	10	0	88	91	-11	6	1	48	43	-9	11	1	53	-52	-10	6	2	107	105	-14	11	2	25	34
-10	11	0	58	-57	-8	6	1	26	31	-6	11	1	62	-62	-7	6	2	216	-195	-8	11	2	122	126
-7	11	0	76	79	-5	6	1	38	47	-3	11	1	37	-32	-1	6	2	333	322	-5	11	2	20	5
-4	11	0	277	271	-2	6	1	62	61	0	11	1	17	11	2	6	2	245	237	1	11	2	118	119
-1	11	0	86	107	1	6	1	43	40	3	11	1	27	31	5	6	2	189	199	4	11	2	78	84
-9	12	0	105	107	4	6	1	47	-47	-5	12	1	21	16	-12	7	2	111	98	-16	12	2	125	124
-6	12	0	114	119	-13	7	1	70	-68	1	12	1	30	-27	-9	7	2	132	-120	-13	12	2	68	66
-3	12	0	48	42	-7	7	1	40	36	4	12	1	34	-34	-6	7	2	27	34	-10	12	2	21	10
0	12	0	33	-39	-4	7	1	61	69	-13	13	1	25	22	-3	7	2	167	171	-7	12	2	49	41
-11	13	0	100	95	-1	7	1	73	71	-10	13	1	38	36	0	7	2	158	144	-4	12	2	32	-13
-8	13	0	173	177	2	7	1	31	35	-7	13	1	25	21	3	7	2	28	22	-1	12	2	23	17
-5	13	0	61	50	5	7	1	27	27	-15	14	1	25	14	6	7	2	123	126	-15	13	2	60	58
-2	13	0	18	26	-15	8	1	19	24	-12	14	1	26	23	-14	8	2	51	48	-12	13	2	71	71
-13	14	0	21	-21	-9	8	1	57	-54	0	14	1	21	25	-11	8	2	139	129	-9	13	2	169	170
-10	14	0	159	154	-6	8	1	95	-97	-14	15	1	45	-45	-8	8	2	39	42	-6	13	2	137	144
-7	14	0	72	73	-3	8	1	120	-125	-11	15	1	35	-35	-2	8	2	295	274	-3	13	2	47	49
-4	14	0	87	85	0	8	1	51	-51	-5	15	1	22	24	1	8	2	33	-25	0	13	2	26	-22
-1	14	0	82	83	3	8	1	34	39	-7	16	1	21	-18	4	8	2	80	72	-14	14	2	43	37
-12	15	0	27	26	6	8	1	52	48	-4	16	1	55	-48	7	8	2	45	46	-11	14	2	48	50
-9	15	0	129	121	-14	9	1	30	33	0	1	2	221	231	-16	9	2	29	22	-8	14	2	66	62

Table 40. Individual reflection data for the crystal $[Cr(ur)_6]Cl_3.3H_2O$

OBSERVED AND CALCULATED STRUCTURE FACTORS FOR $[Cr(ur)_6]Cl_3.3H_2O$

H	K	L	FO	FC	H	K	L	FO	FC	H	K	L	FO	FC	H	K	L	FO	FC	H	K	L	FO	FC
-5	14	2	65	67	-3	9	3	17	17	2	4	4	100	103	-7	10	4	29	22	-5	5	5	23	-26
-2	14	2	28	24	0	9	3	16	13	-9	5	4	96	90	-4	10	4	19	-6	-2	5	5	25	-29
-13	15	2	95	86	-14	10	3	46	-45	-6	5	4	74	71	-1	10	4	109	101	1	5	5	75	72
-7	15	2	58	55	-11	10	3	68	-67	-3	5	4	234	250	2	10	4	32	25	4	5	5	95	93
-12	16	2	28	38	-8	10	3	44	-45	0	5	4	389	382	5	10	4	18	-8	-10	6	5	29	-23
-9	16	2	109	110	-2	10	3	51	47	3	5	4	37	35	-15	11	4	60	57	-4	6	5	55	-55
-6	16	2	87	91	1	10	3	67	71	-11	6	4	46	-52	-12	11	4	83	87	-1	6	5	58	-55
0	0	3	62	-67	4	10	3	31	30	-5	6	4	56	-48	-9	11	4	86	90	2	6	5	71	-70
1	1	3	46	43	-16	11	3	22	21	-2	6	4	142	126	-6	11	4	108	109	5	6	5	27	-26
-1	2	3	87	96	-4	11	3	63	-60	1	6	4	224	206	-3	11	4	36	44	-12	7	5	36	31
2	2	3	89	88	-1	11	3	79	-74	4	6	4	192	193	0	11	4	66	56	-9	7	5	50	49
-3	3	3	135	-134	2	11	3	40	-39	-13	7	4	117	115	3	11	4	41	-33	-6	7	5	38	38
0	3	3	89	-93	5	11	3	29	23	-10	7	4	57	48	-14	12	4	72	69	0	7	5	21	-23
3	3	3	33	-30	-15	12	3	50	50	-7	7	4	115	-120	-11	12	4	161	176	-14	8	5	19	8
-2	4	3	35	-36	-12	12	3	45	40	-4	7	4	113	-112	-8	12	4	38	29	-11	8	5	20	-23
4	4	3	15	15	-9	12	3	38	43	-1	7	4	101	92	1	12	4	38	50	-8	8	5	34	-31
-7	5	3	15	10	-6	12	3	26	31	2	7	4	69	68	-13	13	4	94	93	-5	8	5	18	17
-4	5	3	77	69	-14	13	3	27	-31	5	7	4	66	61	-7	13	4	44	44	-2	8	5	60	68
-1	5	3	31	31	-11	13	3	38	-36	-15	8	4	53	55	-4	13	4	33	40	1	8	5	37	30
-3	6	3	19	-17	-5	13	3	43	42	-12	8	4	41	48	-1	13	4	25	19	4	8	5	23	18
0	6	3	36	-33	-2	13	3	55	53	-9	8	4	94	89	-12	14	4	47	41	-13	9	5	16	-6
6	6	3	41	41	1	13	3	26	22	-6	8	4	123	121	-9	14	4	64	-62	-4	9	5	24	23
-11	7	3	40	-40	-4	14	3	34	-33	-3	8	4	256	264	-6	14	4	76	79	2	9	5	39	-33
-8	7	3	60	-60	-1	14	3	39	-32	0	8	4	123	124	-11	15	4	22	29	5	9	5	32	-31
-2	7	3	49	51	-12	15	3	29	33	6	8	4	53	-51	-8	15	4	59	59	-15	10	5	19	3
1	7	3	30	30	-8	16	3	24	24	-14	9	4	35	36	-7	16	4	78	85	-3	10	5	29	-28
7	7	3	22	-12	-1	1	4	354	-327	-11	9	4	58	45	0	1	5	50	-52	3	10	5	23	2
-10	8	3	19	20	-3	2	4	262	252	-8	9	4	44	43	1	2	5	76	80	-14	11	5	34	30
2	8	3	52	-54	0	2	4	174	172	-5	9	4	162	165	2	3	5	49	-49	-10	12	5	34	31
5	8	3	24	-24	-5	3	4	49	59	-2	9	4	90	108	-6	4	5	55	50	-7	12	5	51	44
8	8	3	20	13	-2	3	4	251	235	1	9	4	144	135	-3	4	5	45	44	-4	12	5	22	17
-12	9	3	58	52	1	3	4	216	230	7	9	4	93	97	0	4	5	27	28	-12	13	5	26	-29
-9	9	3	76	76	-4	4	4	32	-31	-13	10	4	96	92	3	4	5	28	-23	-9	13	5	59	-59
-6	9	3	21	27	-1	4	4	66	69	-10	10	4	113	106	-8	5	5	64	-63	-6	13	5	37	-30

Table 40 continued/

OBSERVED AND CALCULATED STRUCTURE FACTORS FOR $[Cr(ur)_6]Cl_3.3H_2O$

H	K	L	FO	FC	H	K	L	FO	FC	H	K	L	FO	FC	H	K	L	FO	FC	H	K	L	FO	FC
0	13	5	25	25	-1	8	6	85	88	-4	4	7	50	48	2	10	7	23	-22	-7	9	8	22	25
-2	14	5	33	-23	2	8	6	149	142	-1	4	7	64	65	0	11	7	19	9	-4	9	8	22	-28
-10	15	5	36	31	5	8	6	34	-23	2	4	7	21	18	-8	12	7	26	-33	-1	9	8	49	46
-7	15	5	52	54	-15	9	6	37	39	-9	5	7	26	-18	0	1	8	123	129	2	9	8	43	51
-4	15	5	26	30	-3	9	6	18	23	-6	5	7	30	-26	-2	2	8	17	-2	-12	10	8	60	58
0	0	6	107	99	0	9	6	154	158	-3	5	7	20	-12	1	2	8	76	-83	-9	10	8	55	39
1	1	6	25	-27	6	9	6	42	37	-11	6	7	30	29	-4	3	8	88	87	-3	10	8	87	79
-1	2	6	155	-159	-14	10	6	70	64	-8	6	7	26	36	-1	3	8	51	43	3	10	8	57	56
2	2	6	123	-135	-11	10	6	130	124	-5	6	7	55	-59	2	3	8	93	91	-8	11	8	34	41
-3	3	6	120	120	-8	10	6	63	57	-2	6	7	30	-26	-6	4	8	49	48	-5	11	8	47	41
0	3	6	101	99	-5	10	6	23	32	4	6	7	19	-21	0	4	8	46	36	-2	11	8	48	58
3	3	6	117	119	-2	10	6	20	-11	-13	7	7	26	-26	3	4	8	146	160	1	11	8	58	57
-5	4	6	122	130	1	10	6	31	-37	-10	7	7	21	18	-8	5	8	108	101	-7	12	8	37	-43
-2	4	6	246	262	4	10	6	22	14	-7	7	7	42	45	-5	5	8	181	188	-4	12	8	20	27
1	4	6	102	99	-13	11	6	106	105	-4	7	7	60	55	-2	5	8	39	38	-1	12	8	60	66
4	4	6	73	71	-10	11	6	116	118	-1	7	7	25	15	1	5	8	59	-60	-9	13	8	90	91
-7	5	6	163	162	-4	11	6	119	123	2	7	7	23	29	-10	6	8	69	73	-3	13	8	61	67
-4	5	6	72	73	-1	11	6	91	106	5	7	7	18	-17	-7	6	8	171	167	0	0	9	37	55
-1	5	6	181	182	2	11	6	35	40	-12	8	7	26	-24	-4	6	8	155	168	1	1	9	31	-31
2	5	6	149	147	-12	12	6	78	73	-9	8	7	28	-35	-1	6	8	59	61	-1	2	9	46	44
-9	6	6	20	21	-9	12	6	38	-28	-6	8	7	29	-34	2	6	8	96	104	-3	3	9	33	-51
-3	6	6	211	222	-6	12	6	32	30	-3	8	7	54	-52	-9	7	8	43	39	0	3	9	26	-31
0	6	6	163	172	-3	12	6	70	67	3	8	7	38	37	-6	7	8	138	148	3	3	9	21	16
3	6	6	74	68	0	12	6	39	36	6	8	7	41	35	-3	7	8	82	89	-5	4	9	24	-18
6	6	6	37	-46	-11	13	6	79	80	-14	9	7	40	41	0	7	8	82	86	1	4	9	34	-38
-11	7	6	42	52	-8	13	6	22	-18	-8	9	7	22	-15	3	7	8	27	15	-4	5	9	30	32
-8	7	6	193	192	-10	14	6	29	29	-5	9	7	20	-2	6	7	8	20	11	-1	5	9	28	30
-5	7	6	105	96	-4	14	6	45	48	-2	9	7	53	-53	-11	8	8	43	44	-9	6	9	23	15
-2	7	6	27	-22	-6	15	6	32	29	1	9	7	24	-17	-8	8	8	112	113	-3	6	9	28	36
1	7	6	87	93	0	2	7	45	-50	4	9	7	29	-27	-5	8	8	46	52	0	6	9	27	-25
4	7	6	18	-13	-5	3	7	17	-15	-10	10	7	22	22	-2	8	8	50	43	1	7	9	37	36
-10	8	6	65	68	-2	3	7	20	36	-7	10	7	52	46	1	8	8	23	12	-10	8	9	32	-11
-7	8	6	98	89	1	3	7	23	-17	-4	10	7	56	60	-13	9	8	29	27	-4	8	9	30	-36
-4	8	6	107	109	-7	4	7	17	12	-1	10	7	31	34	-10	9	8	66	71	-12	9	9	29	26

Table 40 continued/

OBSERVED AND CALCULATED STRUCTURE FACTORS FOR $[Cr(ur)_6]Cl_3.3H_2O$

H	K	L	FO	FC	H	K	L	FO	FC	H	K	L	FO	FC	H	K	L	FO	FC	H	K	L	FO	FC
-9	9	9	37	37	-2	3	10	73	69	-10	7	10	47	38	-3	11	10	30	29	1	1	12	101	99
0	9	9	27	-23	1	3	10	71	72	-7	7	10	50	52	1	2	11	30	36	-1	2	12	25	29
3	9	9	20	-9	-7	4	10	44	38	-9	8	10	67	66	-4	3	11	28	-27	2	2	12	44	50
-2	10	9	32	21	-4	4	10	40	45	-6	8	10	72	83	-6	4	11	19	8	-3	3	12	66	75
1	10	9	23	22	-1	4	10	54	-76	-3	8	10	53	59	0	4	11	26	-24	0	3	12	50	51
-10	11	9	37	-38	2	4	10	29	16	0	8	10	19	-21	3	4	11	25	-16	3	3	12	26	17
-7	11	9	28	-26	-9	5	10	82	83	-8	9	10	63	72	-5	5	11	21	26	-5	4	12	47	49
-1	11	9	35	-24	-6	5	10	103	103	-5	9	10	70	71	1	5	11	22	13	-2	4	12	58	63
-9	12	9	26	18	-11	6	10	21	16	-2	9	10	66	70	4	5	11	33	41	1	4	12	45	40
-1	1	10	62	54	-8	6	10	61	62	1	9	10	29	21	-7	6	11	18	-20	-7	5	12	35	39
-3	2	10	88	99	-5	6	10	127	143	-7	10	10	33	39	-5	8	11	23	-4	0	6	12	26	11
0	2	10	86	83	-2	6	10	45	30	-1	10	10	26	23	-2	8	11	36	45	-5	7	12	26	8
-5	3	10	91	90	4	6	10	33	44	-6	11	10	25	23	0	0	12	33	18					

Table 40 continued/

3.7.2 *A vibrational analysis of hexakis(urea) chromium(III) chloride trihydrate*

As reported in Section 3.7.1, $[Cr(ur)_6]Cl_3.3H_2O$ crystallizes in the hexagonal system with space group No. 148 - $R\bar{3}$ with six formula units in the crystallographic unit cell. The Wyckoff site occupancy of the various atoms in the unit cell are as follows: the Cr atoms occupy the *3a* and *3b* positions while all other atoms are at general *f* positions. Distortions of the polyhedra are such that the maximum observed point symmetry of the complex ion (*i.e.* around the Cr atom) is S_6.

Derivation of the selection rules for the factor group is readily achieved by making use of tables for Factor Group and Point Group Analysis derived by Adams and Newton [17]. The number of atoms in each formula unit (n) is 61 and the number of formula units in the primitive unit cell (z') is 2. Analysis is therefore carried out using one third the number of sites quoted for the non-primitive cell.

Using group No. 148 in the tables, and choosing the relevant rows corresponding to the site occupancy of the various atoms the total number of vibrational modes N_{total} is obtained (Table 41).

Taking into account that E represents doubly-degenerate modes, a total of 366 modes is obtained, corresponding to $3 \times z' \times n$. Contributions from the external or lattice modes may now be separated out from N_{total} (Table 41), leaving the internal modes of all the molecular species, Table 42.

Table 41.

		S_6	A_g	E_g	A_u	E_u
Cr	1	*a*	0	0	1	1
Cr	1	*b*	0	0	1	1
O(ur)	2x6	*f*	6	6	6	6
C(ur)	2x6	*f*	6	6	6	6
N(ur)	4x6	*f*	12	12	12	12
H(ur)	8x6	*f*	24	24	24	24
Cl	6	*f*	3	3	3	3
O(H_2O)	6	*f*	3	3	3	3
H(H_2O)	2x6	*f*	6	6	6	6
N_{total}			60	60	62	62

Table 42.

	S_6	A_g	E_g	A_u	E_u
N_{total}[a]		60	60	62	62
$T' + R$[b]		13	13	9	9
Cl [c]		1	1	1	1
N_{int} [d]		46	46	52	52

a From Table 41

b $T' + R$ corresponds to translatory, acoustic and rotatory modes which are read directly from the S_6 character table.

c Contribution of the unbonded Cl^- anions to the lattice modes.

d Row 1 less rows 2 and 3.

A partial check on the correctness of the factor group analysis may be carried out at this stage using the method described by Ross [210]:

if z = number of molecules in primitive unit cell = 2

s = number of structural groups = 14

m = number of monoatomic groups = 6

q = number of polyatomic groups having p atoms

i.e. $q = 2$, $p = 49$ for $[Cr(ur)_6]^{3+}$

$q = 6$, $p = 3$ for H_2O

Then, N_{total} is given by the sum of the following:

Acoustic modes	= 3
Translatory modes = $3(s-1)$	= 39
Rotatory modes = $3q$:	
for $[Cr(ur)_6]^{3+}$ 3 x 2	= 6
for H_2O 3 x 6	= 18
Internal modes = $(3p - 6)q$:	
for $[Cr(ur)_6]^{3+}$ (3 x 49 - 6)2	=282
for H_2O (3 x 3 - 6)6	= 18
N_{total}	366

Agreement between the above values and those reported in Tables 41 and 42 indicate that the procedures adopted thus far are correct.

A factorization of modes arising from the CrO_6 skeleton is now possible. Ideally, the symmetry around the metal ion is O_h, but as shown by the x-ray investigation (Section 3.7.1), it has been lowered to S_6 by the disposition of the ligands.

However the CrO_6 vibrations should show little departure from predictions on the basis of O_h symmetry [211] and a correlation of $O_h \rightarrow S_6$ should give the Cr-O normal vibrations in the crystal.

An O_h point group analysis yields six normal vibrations *viz.* $A_{1g} + E_g + 2T_{1u} + T_{2g} + T_{2u}$, and a correlation [210] of these to S_6 *via* T_h is given in Table 43.

Table 43.

O_h	T_h	S_6
A_{1g}	A_g	A_g
E_g	E_g	E_g
T_{1u}	T_u	$A_u + E_u$
T_{1u}	T_u	$A_u + E_u$
T_{2g}	T_g	$A_g + E_g$
T_{2g}	T_u	$A_u + E_u$

Four modes, $2A_g + 2E_g$ are Raman active vibrations while six, $3A_u + 3E_u$, are ir active modes.

These vibrations may now be subtracted from N_{int} (Table 42), to leave only the internal vibrations of the coordinated urea and uncoordinated water molecules, *i.e.* N_{int} (ur + H_2O) = $44A_g + 44E_g + 49A_u + 49E_u$. Further factorization of the internal modes into specific vibrations of the ligands is regretably not possible since both the urea and water molecules are located on general positions (f) in the crystal lattice. Hence, despite the high symmetry of the crystal very little

information has been able to be obtained from the factor group analysis of the complex, and the inclusion of experimental isotopic shift data is vital if any attempt at band assignment in the vibrational spectra of $[Cr(ur)_6]Cl_3.3H_2O$ is to be made. The ir and Raman spectra (4000 - 80 cm^{-1}) of the complex are depicted in Fig. 27, while the frequencies isotopic shifts ($\Delta\nu$) on ^{18}O, ^{13}C and ^{15}N labelling and assignments are given in Table 44.

An initial examination of the spectra (which were determined at 25°C), shows that the number of bands observed is considerably less than that predicted by the factor group analysis. This indicates that many of the splittings are very small, requiring low temperature studies for their detection.

Attempted correlations between the isotopic shift data and assignments in a previously published [131] ir investigation of the anhydrous complex which was based upon a comparison with the ir spectra of urea and urea-d_4, discount the supposition [131] that the formation of oxygen-to-metal bonds between urea molecules and a metal ion should bring about only minor changes in many of the urea vibrations. Data obtained here for the ^{18}O-, ^{15}N- and ^{13}C-isotopic substitutions imply that many of the vibrations are coupled and distributed over more than one band, in both ir and Raman spectra.

The 4000 - 550 cm^{-1} region of the spectra

Three bands above 3000 cm^{-1} attributable to νN-H modes are observed in both the ir and Raman spectra; their broadness

Table 44. Ir and Raman data obtained for the complex $[Cr(ur)_6]Cl_3.3H_2O$, the isotopic shift values ($\Delta\nu$) for its ^{18}O, ^{13}C and ^{15}N substituted analogues, and band assignments

Ir				Raman				Assignments
ν	$\Delta\nu^{18}O$	$\Delta\nu^{13}C$	$\Delta\nu^{15}N$	ν	$\Delta\nu^{18}O$	$\Delta\nu^{13}C$	$\Delta\nu^{15}N$	
				3453^{vw}_{br}	a	a	20	νN-H + νO-H
3449	-	-	6					
				3348^{vw}_{br}	-	-	5	
3335	-	-	b					
				3200^{w}_{br}	-	-	-	
3184	-	-	4					
				1648^{w}	-	-	7	NH_2 scissor
1625	2	9	-					νC=O
				1618^{w}	-	10	15	NH_2 scissor + νC=O
1574	5	32	-					
				1563^{m}	10	32	-	νC=O
1553	7	27	2					νC-N + νC=O
				1498^{m}	-	25	-	?
1487	2	26	3					νC-N + νC=O
1307	5	-	-					?
1168	15	-	6	1165^{w}	20	-	10	νC-N + νC=O
1033	15	-	20	1036^{vs}	12	-	22	
				998sh	-	-	10	NH_2 twist
763	4	21	2					
634	18	2	3					
				628^{m}	18	-	5	δN-C-O
555	6	2	7	553^{m}	5	-	10	
535	2	-	5	533^{m}	5	-	5	νCr-O + NH_2 rock
470	-	2	2					δN-C-N
387	2	-	2					δN-C-O
				308^{m}	5	-	4	νCr-O + δN-C-O
284	2	2	2					δN-C-O
247	7	-	-					δO-Cr-O
226	7	-	-	223^{w}	b	b	b	
				203^{vw}	-	5	5	δN-C-O
191	6	-	-					δO-Cr-O
177	-	-	-					lattice mode
158	-	-	-	155^{m}	-	-	-	H-bond stretch
148	6	-	-					δO-Cr-O
141	6	-	-					
106	-	-	-					lattice mode

v - very; w - weak; br - broad; s - strong; sh - shoulder; m - medium

a Too broad for determination of shift value

b Undergoes high frequency shift - not explained

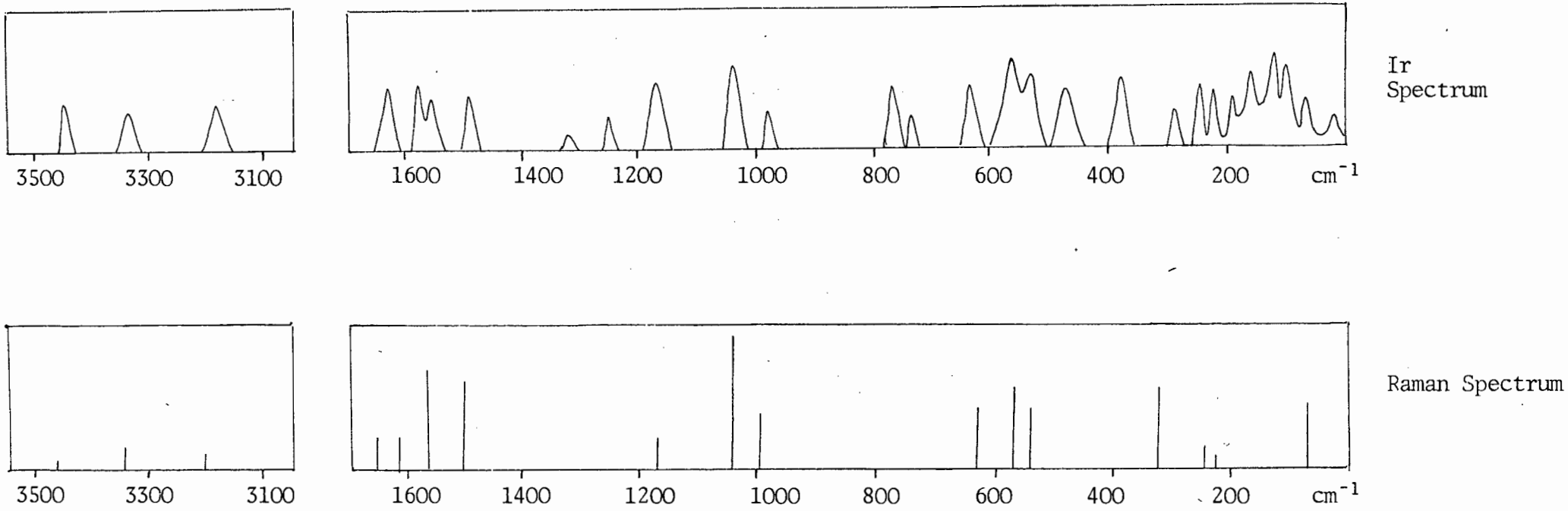

Fig. 27. Ir and Raman spectra of $Cr(ur)_6Cl_3.3H_2O$

may be ascribed to either coupling to νO-H modes of the uncoordinated water molecules, or to hydrogen-bonding with the chloride ions. The next highest frequency vibrations expected, involving the amide groups are NH_2 scissoring modes. The ^{15}N sensitivity of the Raman active bands at 1648 and 1618 cm^{-1} allow their assignment to these vibrations, the additional ^{18}O-shift of the lower of the two being ascribed to coupling to a νC=O mode.

On the basis of their ^{18}O- and ^{13}C-sensitivities, and ^{15}N-insensitivity, the bands at 1625, 1574 (ir) and 1563 (Raman) have been assigned to νC=O modes. The absence of any band totally insensitive to isotopic labelling of the urea indicates that no pure δH-O-H mode of the lattice water is occurring; coupling of a water deformation to urea vibrations in this region is therefore likely, although the data presented preclude its observation. Coordination of urea to the metal ion increases the single bond character of the CO group and coupling between CO and CN modes is expected [131]. Four such coupled vibrations are observed in the ir spectrum of the complex, the lower two showing coincidence with Raman bands which are hence similarly assigned.

An ir absorption at 1307 cm^{-1} and a Raman band at 1498 cm^{-1} show sensitivity to only ^{18}O- and ^{13}C-isotopic substitutions respectively. No rationalization of these individual shifts is possible and no assignment is therefore given.

Aside from the 998 cm^{-1} shoulder in the Raman spectrum

which is shifted only on ^{15}N labelling and is therefore an NH_2 twisting mode, remaining bands in this spectral region, are assigned to various δN-C-O modes of the urea skeleton. The absence of any ^{13}C shift for some of these bands implies that the carbon atom does not move sufficiently to cause any great dipole-moment change. This is entirely expected for any i.p. δN-C-O in view of the structure of the urea skeleton.

The 550 - 80 cm^{-1} region of the spectra

By analogy with assignments made for $Cr(gly)_3$ (Section 3.6.) whose Cr-O bond lengths [204] are very similar to those for $[Cr(ur)_6]Cl_3.3H_2O$ the highest νCr-O is expected near 500 cm^{-1}. On the basis of their ^{18}O sensitivities in both the ir and Raman spectra the bands near 530 cm^{-1} are accordingly assigned with their concomitant ^{15}N shifts implying coupling to an NH_2 rocking mode. An additional ^{18}O sensitive band at 308 cm^{-1} in the Raman spectrum is also assigned to a νCr-O mode which on the basis of its ^{15}N shift is considered to be coupled to a δN-C-O mode expected [131] in this region. Further δN-C-O modes of the urea skeleton as well as δN-C-N vibrations have been assigned to bands in both the ir and Raman on the basis of ^{18}O, ^{15}N and sometimes ^{13}C shifts (see Table 44). Remaining bands showing sensitivity to ^{18}O isotopic substitution only have been assigned to δO-Cr-O modes.

The isotopic labelling has allowed the identification of 6 ir and 2 Raman active metal-ligand modes. Once again

it is apparent, at least for the Raman spectrum, that not all the factor group splittings are discernable.

Finally, low frequency bands insensitive to all forms of isotopic substitution employed are either lattice or possible H-bonding stretching modes.

3.7.3 *Isotopic labelling applied to the ir spectra of urea complexes of platinum(II) and palladium(II) chloride*

In a previous ir investigation of these complexes [131] band assignments of some of the ligand modes only were carried out by a comparison with the ir spectra of urea and urea-d_4. From the data reported it was postulated that in each complex the chlorine atoms and only one nitrogen atom of each urea molecule are coordinated to the central metal ion. This being the case, the C_{2v} symmetry of the ligand is destroyed on coordination, and hence the coupling among the ligand vibrations in the metal complexes is expected to differ markedly from that in the free urea molecule. Assignments on a comparative basis are therefore suspect and a reinvestigation of the spectra has been carried out.

The ir spectra (4000 - 140 cm^{-1}) of the complexes $Pt(ur)_2Cl_2$ and $Pd(ur)_2Cl_2$ are depicted in Fig. 28 while the band frequencies and isotopically-induced shifts ($\Delta\nu$) on ^{18}O, ^{13}C and ^{15}N labelling of the urea molecules are listed in Table 45. A similarity in band pattern of the spectra of the two unlabelled complexes indicates that they are

Table 45. Ir frequencies and band assignments for the complexes $Pt(ur)_2Cl_2$ and $Pd(ur)_2Cl_2$ and the shift data ($\Delta\nu$) for their ^{18}O-, ^{13}C- and ^{15}N-substituted analogues

$Pt(ur)_2Cl_2$				$Pt(ur)_2Cl_2$				Assignments
ν	^{18}O	^{13}C	^{15}N	ν	^{18}O	^{13}C	^{15}N	
3408				3411				νN-H uncoodinated
3322	a			3324				
3278				3278	a			νN-H coordinated
3172				3172				
3054				3057				
1739	16	~20	6	1733	22	18	5	νC=O + NH_2 scissor
1719	13	34	8	1714	12	33	8	
				1653	6	12	8	
1612	3	14	4	1607	3	10	4	
1584	-	3	5	1577	-	5	6	
				1448	54	41	15	
1395	10[b]	33	10[b]	1398	22	29	5	νC-N + νC=O
1212	10	3	6	1219	11	4	7	
1184	-	-	4	1142	-	-	4	NH_2 twist
1148	10	13	23					νC-N + δC=O
1086	12	-	13	1079	9	-	9	NH_2 twist + δC=O
898	6	5	19	908	4	3	20	νC-N + δC=O
				833	-	-	7	NH_2 rock
763			3	765	-		6	
757	4	21	4	759	3	20	2	NH_2 rock + δC=O
734	3	11	-					δC=O
719	-		23	721	-	-	6	NH_2 rock
613	2	-	2	612	3	-	5	
591	14	-	7	591	12	-	7	δN-C-O
539	4	-	6	542	3	-	7	
451	-	-	8	438	-	-	8	νM-N
331	-	-	-	336	-	-	-	νM-Cl
261	6	-	6	255	4	-	4	δN-C-O
224	-	-	4	222	-	-	5	δM-N
193	4	-	2	198	4	-	2	δN-C-O

a Too broad for determination of shift

b Mean of doublet

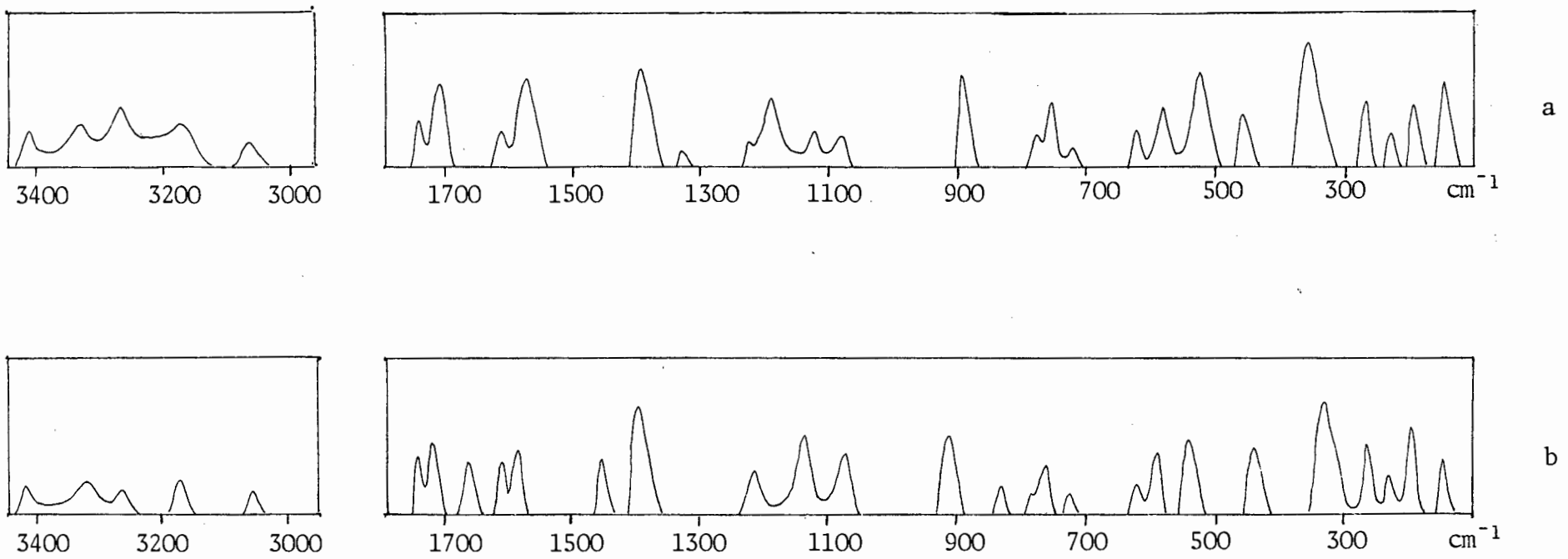

Fig. 28. The ir spectra (4000 - 140 cm^{-1}) of the complexes a) $Pt(ur)_2Cl_2$
b) $Pd(ur)_2Cl_2$

isostructural. This is supported by the fact that for most of the bands, the frequency shifts experienced on the various isotopic substitutions, are comparable.

The 4000 - 500 cm^{-1} region of the spectra

The only bands expected above 3000 cm^{-1} are those attributable to N-H stretching modes. Five such absorptions are observed and assigned as such, despite the fact that their broadness (most likely due to hydrogen bonding) precludes the determination of any isotopic shift values. As postulated previously [131] the number of νN-H modes implies that both coordinated and uncoordinated amide groups are present.

An examination of the isotopic shift data obtained in the region 1800 - 900 cm^{-1} shows that concomitant sensitivity to all forms of labelling employed occurs for a considerable number of the absorptions. Previous assignments [131] of individual bands to specific modes of vibration must therefore be discounted, except in the case of the absorption at 1184 cm^{-1} in the $Pt(ur)_2Cl_2$ (1142 cm^{-1} in the Pd complex) whose sensitivity to ^{15}N-substitution alone allows its assignment to an NH_2 twisting mode. Extensive coupling is observed between νC=O and NH_2-scissoring modes, and νC=O and νC-N modes, the vibrations forming contributions to about four absorptions in each case. Similarly the band at 1148 cm^{-1} in the Pt complex arises from a coupled vibration showing significant shifts on ^{18}O, ^{13}C and ^{15}N isotopic substitutions; it is

therefore assigned to νC-N + δC=O, as is the absorption at *ca.* 900 cm^{-1} in the spectra of both complexes.

Only one band below 800 cm^{-1}, that at *ca.* 758 cm^{-1} in each complex shows sensitivity to all forms of labelling, and is subsequently assigned to an NH_2 rock + a C=O deformation. Remaining ligand vibrations in this region appear to be relatively pure, showing shifts on, at most, two forms of isotopic substitution. One δC=O is observed at 734 cm^{-1} in the spectrum of $Pt(ur)_2Cl_2$, while NH_2 rocking modes are assigned to the bands undergoing isotopic shifts on ^{15}N substitution alone. Three bands at *ca.* 612, 591 and 540 cm^{-1} show sensitivity to ^{18}O and ^{15}N isotopic labelling. Only δNCO modes are expected [131] in this region, and the absorptions are thus assigned. The absence of any shift on ^{13}C-substitution is not entirely unexpected since the carbon atom is unlikely to move significantly during the vibration, and hence does not contribute to the dipole moment change.

The 500 - 140 cm^{-1} region of the spectra

In addition to further deformations of the urea skeleton, metal-ligand modes are expected in this region.

An intense absorption at *ca.* 330 cm^{-1} in the spectra of both complexes does not undergo a shift on any of the ligand-atom isotopic substitutions and is hence most likely a νM-Cl mode. Support for this assignment is received from the observation of a similar band in the spectrum of $Pt(amp)Cl_2$

(Section 3.2.5.1). Bands at *ca.* 440 and 220 cm^{-1} are sensitive to ^{15}N labelling only; they are therefore νM-N and δN-M-N (or δN-M-Cl) modes respectively. Remaining absorptions are assigned to the expected [131] δN-C-O vibrations, on the basis of their ^{18}O and ^{15}N sensitivities; the absence of ^{13}C shifts for these vibrations has been explained previously.

REFERENCES

1. K. Nakamoto, *Instrument News, 20* (1970) 1.

2. G.T. Behnke and K. Nakamoto, *Inorg. Chem., 6* (1967) 433.

3. I.M. Mills, *Spectrochim. Acta, 16* (1960) 35.

4. J. Aldous and I.M. Mills, *Spectrochim. Acta, 18* (1962) 173, *19* (1963) 1567.

5. J.L. Duncan and I.M. Mills, *Spectrochim. Acta, 20* (1964) 523.

6. G. Herzberg, *Molecular Spectra and Molecular Structure II: Infrared and Raman Spectra of Polyatomic Molecules;* Van Nostrand, Reinhold, (1945).

7. N. Mohan, S.J. Cyvin and A. Müller, *Coord. Chem. Rev., 21* (1976) 221.

8. S. Pinchas and I. Laulicht, *Infrared Spectra of Labelled Compounds,* Academic Press, London (1971).

9. F.A. Cotton, *Chemical Applications of Group Theory,* Second Edition, Wiley-Interscience, New York (1971).

10. E.B. Wilson Jr., J.C. Decius and P.C. Cross, *Molecular Vibrations,* McGraw-Hill, New York (1955).

11. J.R. Ferraro and J.S. Ziomek, *Introductory Group Theory and its Applications to Molecular Structure,* Plenum, New York (1969).

12. D.C. Harris and M.D. Bertolucci, *Symmetry and Spectroscopy,* Oxford University Press, New York (1978).

13. A. Vincent, *Molecular Symmetry and Group Theory,* Wiley, New York (1977).

14. R.S. Halford, *J. Chem. Phys., 14* (1946) 8.

15. S. Bhagavantam and T. Venkatarayudu, *Proc. Ind. Acad. Sci., 9A* (1939) 224.

16. D.M. Adams, *Coord. Chem. Rev., 10* (1974) 183.

17. D.M. Adams and D.C. Newton, *Tables for Factor Group and Point Group Analysis,* Beckman-RIIC Ltd., Croydon (1970).

18. K. Nakamoto, *Infrared Spectra of Inorganic and Coordination Compounds,* second edition, Wiley-Interscience, New York (1970).

19. M. Goldstein, E.F. Mooney, A. Anderson and H.A. Gebbie, *Spectrochim. Acta, 21* (1965) 105.

20. J.M. Haigh, N.P. Slabbert and D.A. Thornton, *J. Mol. Struct., 7* (1971) 199.

21. R.D. Hancock and D.A. Thornton, *J. Mol. Struct., 4* (1969) 377.

22. B.N. Figgis, *Introduction to Ligand Fields*, Interscience, New York (1966).

23. C.K. Jørgensen, *Absorption Spectra and Chemical Bonding in Complexes*, Pergamon Press, London (1962).

24. P. George and D.S. McClure, *Progr. Inorg. Chem., 1* (1959) 381.

25. R.D. Hancock and D.A. Thornton, *J. Mol. Struct., 4* (1969) 361.

26. L.G. Hulett and D.A. Thornton, *Spectrochim. Acta, 27A* (1971) 2089.

27. R.D. Hancock and D.A. Thornton, *J. S. Afr. Chem. Inst., 23* (1970) 71.

28. G.C. Percy and D.A. Thornton, *J. Mol. Struct., 10* (1971) 39.

29. G.S. Shephard and D.A. Thornton, *Helv. Chim. Acta, 54* (1971) 2212.

30. G.S. Shephard and D.A. Thornton, *J. Mol. Struct., 16* (1973) 321.

31. C.A. Fleming and D.A. Thornton, *J. Mol. Struct., 17* (1973) 79.

32. J.M. Haigh, R.D. Hancock, L.G. Hulett and D.A. Thornton, *J. Mol. Struct., 4* (1969) 369.

33. R.D. Hancock and D.A. Thornton, *J. Mol. Struct., 6* (1970) 441.

34. L.G. Hulett and D.A. Thornton, *J. Mol. Struct., 13* (1972) 115.

35. L.G. Hulett and D.A. Thornton, *Chimia, 26* (1972) 72.

36. G.C. Percy and D.A. Thornton, *J. Inorg. Nucl. Chem., 34* (1972) 3357.

37. G.C. Percy and D.A. Thornton, *J. Inorg. Nucl. Chem., 34* (1972) 3369.

38. G.C. Percy and D.A. Thornton, *J. Inorg. Nucl. Chem., 35* (1975) 2319.

39. K. Nakamoto, *Angew. Chem. Internat. Ed., 11* (1972) 666.

40. G.N. Rayner Canham and A.B.P. Lever, *Canad. J. Chem., 50* (1972) 3866.

41. A.B.P. Lever and E. Mantovani, *Canad. J. Chem., 51* (1973) 514.

42. B. Hutchinson, D. Eversdyk and S. Olbricht, *Spectrochim. Acta, 30A* (1974) 1605.

43. H. Musso and H. Junge, *Tetrahedron Lett.,* (1966) 4003.

44. H. Junge and H. Musso, *Spectrochim. Acta, 24A* (1968) 1219.

45. S. Pinchas, B.L. Silver and I. Laulicht, *J. Chem. Phys., 46* (1967) 1506.

46. H. Junge, *Spectrochim. Acta, 24A* (1968) 1957.

47. C.A. Fleming and D.A. Thornton, *Spectrosc. Lett., 6* (1973) 245.

48. C.A. Fleming and D.A. Thornton, *J. Mol. Struct., 27* (1975) 335.

49. J.B. Hodgson and G.C. Percy, *Spectrosc. Lett., 8* (1975) 975.

50. J.B. Hodgson and G.C. Percy, *Spectrochim. Acta, 32A* (1976) 1291.

51. G.C. Percy, *J. Inorg. Nucl. Chem., 37* (1975) 2071.

52. G.C. Percy and H.S. Stenton, *J. Inorg. Nucl. Chem., 38* (1976) 1255.

53. G.C. Percy, *Spectrochim Acta, 32A* (1976) 1287.

54. G.C. Percy and H.S. Stenton, *J. Chem. Soc. (Dalton)* (1976) 1466.

55. G.C. Percy and H.S. Stenton, *J. Chem. Soc. (Dalton)* (1976) 2429.

56. G.J. Sutton, *Austral. J. Chem., 13* (1960) 74,222,473; *14* (1961) 37,545,550; *13* (1962) 232,563.

57. S. Utsuno and K. Sone, *J. Chem. Soc. Japan, 37* (1964) 1038.

58. A.R. Nicholson and G.J. Sutton, *Austral. J. Chem., 22* (1969) 59,373,1543.

59. L. El-Sayed and R.O. Ragsdale, *Inorg. Chem., 6* (1967) 1640.

60. A. Syamal, *J. Ind. Chem. Soc., 45* (1968) 343.

61. A. Earnshaw, L.F. Larkworthy and K.C. Patel, *J. Chem. Soc. A*, (1970), 1840.

62. R.D. Hancock and E.J. McDougall, *J. Chem. Soc. Dalton*, (1977), 67.

63. K. Michelson, *Acta Chem. Scand.*, *24* (1970) 2003; *26* (1972), 769, 1517.

64. K. Michelson, *Acta Chem. Scand.*, *27* (1973) 5.

65. D.E. Goldberg and W.C. Fernelius, *J. Phys. Chem.*, *63* (1959) 1246.

66. F. Holmes and F. Jones, *J. Chem. Soc.*, (1960) 2398.

67. R.G. Lacoste and A.E. Martell, *Inorg. Chem.*, *3* (1964) 881.

68. J.L. Walter and S.M. Rosalie, *J. Inorg. Nucl. Chem.*, *28* (1966) 2969.

69. T.M. Hseu and Y.H. Tsai, *J. Chinese Chem. Soc.*, *21* (1974) 211.

70. T.M. Hseu, Y.H. Tsai and C.W. Cheng, *J. Chinese Chem. Soc.*, *22* (1975) 299.

71. M. Noji, Y. Kidani and H. Koike, *Bull. Chem. Soc. Japan*, *48* (1975) 245.

72. A.A. Amaro and K. Seff, *Acta Cryst.*, *B28* (1972) 2298.

73. H.M. Helis, W.H. Goodman, R.B. Wilson, J.A. Morgan and D.J. Hodgson, *Inorg. Chem.*, *16* (1977) 2412.

74. E. Uhlig and M.Z. Masser, *Z. anorg. allg. Chem.*, *25* (1963) 322.

75. E. Uhlig and M.Z. Masser, *Z. anorg. allg. Chem.*, *127* (1964) 328.

76. E. Uhlig, H-J. Bergmann and U. Schneider, *Z. anorg. allg. Chem.*, *354* (1967) 130.

77. V.C. Copeland, W.E. Hatfield and D.J. Hodgson, *Inorg. Chem.*, *12* (1973) 1340.

78. V.C. Copeland and D.J. Hodgson, *Inorg. Chem.*, *12* (1973) 2157.

79. V.C. Copeland, P. Singh, W.E. Hatfield and D.J. Hodgson, *Inorg. Chem.*, *11* (1972) 1826.

80. P. Singh, V.C. Copeland, W.E. Hatfield and D.J. Hodgson, *J. Phys. Chem.*, *76* (1972) 2887.

81. O.L. Lewis and D.J. Hodgson, *Inorg. Chem., 13* (1974) 143.

82. D.L. Kozlowski and D.J. Hodgson, *J. Chem. Soc. Dalton,* (1975) 55.

83. D.K. Rastogi and K.C. Sharma, *J. Inorg. Nucl. Chem., 36* (1974) 2219.

84. A.T. Hutton and D.A. Thornton, *Spectrochim. Acta, 34A* (1978) 645.

85. A.L. McCellan and G.C. Pimentel, *J. Chem. Phys., 23* (1954) 245.

86. P. Chiorboli and A. Bertoluzza, *Ann. Chim. (Italy), 49* (1959) 245.

87. N.S. Kolodina, *Opt. Spectrosc., Akad. Nauk. SSSR, Otd. Fiz.-Mat. Nauk, Sb Statei, 3* (1967) 274.

88. R.J.H. Clark and C.S. Williams, *Inorg. Chem., 4* (1965) 350.

89. J.R. Allan, D.H. Brown, R.H. Nuttall and D.W.A. Sharp, *J. Inorg. Nucl. Chem., 27* (1965) 1305.

90. C.W. Frank and L.B. Rogers, *Inorg. Chem., 5* (1966) 615.

91. M. Goldstein and W.D. Unsworth, *Inorg. Chim. Acta, 4* (1970) 342.

92. C.S. Williams and K.F. Fouché, *Z. Naturforschg., 19a* (1964) 363.

93. M. Aslam and W.H.S. Massie, *Inorg. Nucl. Chem. Lett., 7* (1971) 961.

94. R.J.H. Clark and C.S. Williams, *Spectrochim. Acta, 22* (1966) 1081.

95. J.E. Rüede and D.A. Thornton, *J. Mol. Struct., 34* (1976) 75.

96. C. Engelter and D.A. Thornton, *J. Mol. Struct., 42* (1977) 51.

97. A. Werner, *Ber. dtsch. chem. Ges., 34* (1901) 2584.

98. J.P. Fackler, *Prog. Inorg. Chem., 7* (1966) 361.

99. D.P. Graddon, *Coord. Chem. Rev., 4* (1969) 1.

100. K. Nakamoto, P.J. McCarthy, A. Ruby and A.E. Martell, *J. Amer. Chem. Soc., 83* (1961) 1066; 1272.

101. R.D. Gillard, H.G. Silver and J.L. Wood, *Spectrochim. Acta, 20* (1964) 63.

102. K. Nakamoto, P.J. McCarthy and A.E. Martell, *J. Amer. Chem. Soc., 83* (1960) 1272.

103. M. Mikami, I. Nakagawa and T. Shimanouchi, *Spectrochim. Acta, 23A* (1967) 1037.

104. K. Nakamoto, C. Udovich and J. Takemoto, *J. Amer. Chem. Soc.*, 92 (1970) 3973.

105. S. Pinchas and J. Shamir, *J. Chem. Soc. Perkin II,* (1974) 1098.

106. K. Nakamoto and A.E. Martell, *J. Chem. Phys., 32* (1960) 588.

107. K.E. Lawson, *Spectrochim. Acta, 17* (1961) 248.

108. C. Djardjevic, *Spectrochim. Acta, 17* (1961) 448.

109. H. Musso and H. Junge, *Tetrahedron Lett., 33* (1966) 4003, 4009.

110. D.P. Graddon and E.C. Walton, *J. Inorg. Nucl. Chem., 21* (1961) 49.

111. P.E. Rakita, S.J. Kopperl and J.P. Fackler, *J. Inorg. Nucl. Chem., 30* (1968) 2139.

112. S. Ambe and F. Ambe, *J. Inorg. Nucl. Chem., 35* (1973) 1109.

113. F. Cariati, D. Galizzioli, F. Morazzoni and L. Naldini, *Inorg. Nucl. Chem. Lett., 9* (1973) 743.

114. J.T. Hashagen and J.P. Fackler, *J. Amer. Chem. Soc., 87* (1965) 2821.

115. H. Montgomery and E.C. Lingafelter, *Acta Cryst., 17* (1964) 1481.

116. P. Jose, S. Ooi and Q. Fernando, *J. Inorg. Nucl. Chem., 31* (1969) 1971.

117. F.P. Dwyer and A.M. Sargeson, *J. Proc. Roy. Soc. N.S.W., 90* (1956) 29.

118. C. Engelter and D.A. Thornton, *J. Mol. Struct., 39* (1977) 25.

119. J.B. Hodgson, G.C. Percy and D.A. Thornton, *Transition Metal Chem., 3* (1978) 302.

120. R.A. Condrate and K. Nakamoto, *J. Chem. Phys., 42* (1965) 2590.

121. T.J. Lane, J.A. Durkin and R.J. Hooper, *Spectrochim. Acta, 20* (1964) 1013.

122. J.L. Walter and R.J. Hooper, *Spectrochim. Acta, 25A* (1969) 647.

123. J.A. Kieft and K. Nakamoto, *J. Inorg. Nucl. Chem., 29* (1967) 2561.

124. M. Tsuboi, T. Onishi, I. Nakagawa, T. Simanouchi and S. Mizushima, *Spectrochim. Acta, 12* (1958) 253.

125. I. Laulicht, S. Pinchas, D. Samuel and I. Wasserman, *J. Phys. Chem., 70* (1966) 2719.

126. S. Suzuki and T. Shimanouchi, *Spectrochim. Acta,* 19 (1963) 1195.

127. J.B. Hodgson, G.C. Percy and D.A. Thornton, *Transition Metal Chem., 3* (1978) 302.

128. J.B. Hodgson, G.C. Percy and D.A. Thornton, *Spectrochim. Acta, 35A* (1979) 949.

129. J.B. Hodgson, G.C. Percy and D.A. Thornton, *Trans. Roy. Soc. S. Afr.,* (1980) in press.

130. G.A. Foulds, G.C. Percy and D.A. Thornton, *Spectrochim. Acta, 34A* (1978) 1231.

131. R.B. Penland, S. Mizushima, C. Curran and J.V. Quagliano, *J. Amer. Chem. Soc., 79* (1957) 1575.

132. R. Rivest, *Canad. J. Chem., 40* (1962) 2234.

133. P.S. Gentile and L.S. Campisi, *J. Inorg. Nucl. Chem., 27* (1965) 2291.

134. M. Kishita, M. Inoue and M. Kubo, *Inorg. Chem., 3* (1964) 237.

135. A. Merjanian and H.M. Neumann, *Inorg. Chem., 6* (1967) 165.

136. B.N. Figgis and L.G. Wadley, *Austr. J. Chem., 25* (1972) 223.

137. P.H. Davis and J.S. Wood, *Inorg. Chem., 9* (1970) 1111.

138. W. van de Giesen and C.H. Stam, *Cryst. Struct. Comm., 1* (1972) 257.

139. B.N. Figgis and L.G. Wadley, *J. Chem. Soc. Dalton* (1972) 2182.

140. A. Zalkin, H. Ruben and D.H. Templeton, *Inorg. Chem., 18* (1979) 519.

141. J.E. Stewart, *J. Chem. Phys., 26* (1957) 248 and references cited therein.

142. P.H.H. Fisher and C.A. McDowell, *Canad. J. Chem., 38* (1960) 187.

143. L. Kellner, *Proc. Roy. Soc. A177* (1941) 456.

144. R.D. Waldron, R.M. Badger, *J. Chem. Phys., 18* (1950) 566.

145. E.R. Andrew and D. Hyndman, *Proc. Phys. Soc., A66* (1953) 1187.

146. A. Yamaguchi, T. Miyazawa, T. Shimanouchi and S. Mizushima, *Spectrochim. Acta, 10* (1957) 170.

147. I. Laulicht, S. Pinchas, E. Petreanu and D. Samuel, *Spectrochim. Acta, 21* (1965) 1487.

148. G.H. Stout and L.H. Jensen, *X-ray Structure Determination*, Macmillan, London (1968).

149. G.M. Shelrick, *The SHELX Program System*, University Chemical Laboratory, Cambridge (1976).

150. W.D.S. Motherwell, Cambridge, *To be published.*

151. D.T. Cromer and J.B. Mann, *Acta Cryst., A24* (1968) 321.

152. W.W. Brandt, F.B. Dwyer and E.C. Gyarfas, *Chem. Rev., 54* (1954) 959.

153. L.G. Hulett, *Ph.D. Thesis*, University of Cape Town, 1972.

154. C. Engelter and D.A. Thornton, *J. Mol. Struct., 33* (1976) 119.

155. A. Syamal, *J. Indian Chem. Soc., 45* (1968) 343.

156. E. Borsbach, *Chem. Ber., 23* (1890) 434.

157. D.H. Brown, R.H. Nuttall and D.W.A. Sharp, *J. Inorg. Nucl. Chem., 26* (1964) 1151.

158. G. Rudolph and M.C. Henry, *Inorg. Synth., 10* (1967) 74.

159. J.B. Ellern and R.O. Ragsdale, *Inorg. Synth., 11* (1968) 82.

160. Y. Nishikawa, Y. Nakamura and S. Kawaguchi, *Bull. Chem. Soc. Japan, 45* (1972) 155.

161. B.W. Low, F.L. Hirshfeld and F.M. Richards, *J. Amer. Chem. Soc., 81* (1959) 4412.

162. C.E. Skinner and M.M. Jones, *Inorg. Nucl. Chem. Lett., 3* (1967) 185.

163. M. Mori, M. Shibata, E. Kyuno and M. Kanaya, *Bull Chem. Soc. Japan, 34* (1961) 1837.

164. P. Pfeiffer, *Chem. Ber., 36* (1903) 1927.

165. J.S. Strukl and J.L. Walter, *Spectrochim. Acta, 27A* (1971) 209.

166. T. Iwamoto and D.F. Shriver, *Inorg. Chem., 10* (1971) 2428.

167. A.B.P. Lever and E. Mantovani, *Inorg. Chim. Acta, 5* (1971) 429; *Inorg. Chem., 10* (1971) 817.

168. G.W. Rayner Canham and A.B.P. Lever, *Canad. J. Chem.,* (1972) 3866.

169. G.C. Percy, *Ph.D. Thesis,* University of Cape Town, 1972.

170. *International Tables for X-ray Crystallography, Vol. 1,* Kynoch Press, England (1969)

171. M.D. Child and G.C. Percy, *Spectrosc. Lett., 10* (1977) 71.

172. R.J.H. Clark, *Spectrochim. Acta, 21* (1965) 955.

173. F.A. Cotton and G. Wilkinson, *Advanced Inorganic Chemistry,* 3rd Edition, Wiley, New York, (1972).

174. S.M. Nelson and T.M. Shepherd, *J. Inorg. Nucl. Chem., 27* (1965) 2123.

175. N.S. Gill, R.H. Nuttall, D.E. Scaife and D.W.A. Sharp, *J. Inorg. Nucl. Chem., 18* (1961) 79.

176. J.R. Ferraro, *Low Frequency Vibrations of Inorganic and Coordination Compounds,* Plenum, New York, (1971).

177. D.B. Purrell and N. Sheppard, *Spectrochim. Acta, 17* (1971) 68.

178. C. Engelter, A.T. Hutton and D.A. Thornton, *J. Mol. Struct., 44* (1978) 23.

179. B.J. Hathaway, R.C. Slade, I.M. Procter and A.A.G. Tomlinson, *J. Chem. Soc. A,* (1969) 2219.

180. L. Corrsin, B.J. Fox and R.C. Lord, *J. Chem. Phys., 21* (1952) 1170.

181. C.H. Kline and J. Turkevich, *J. Chem. Phys., 12* (1944) 300.

182. J.K. Wilmhurst and H.J. Bernstein, *Canad. J. Chem., 18* (1957) 1183.

183. D.A. Long, F.S. Murfin and E.L. Thomas, *Trans. Faraday Soc., 59* (1963) 12.

184. D.B. Cunliffe-Jones, *Spectrochim. Acta, 21* (1965) 747.

185. J.B. Hodgson, *Ph.D. Thesis*, University of Cape Town, (1979).

186. C. Engelter and D.A. Thornton, *J. Mol. Struct., 33* (1976) 119.

187. S. Akyüz, A.B. Dempster, R.L. Morehouse and S. Suzuki, *J. Mol. Struct., 17* (1973) 105.

188. D.M.L. Goodgame and M. Goodgame, *J. Chem. Soc.*, (1963) 207.

189. K. Shobatake and K. Nakamoto, *J. Chem. Phys., 49* (1968) 4792.

190. R.D. Hancock and D.A. Thornton, *J. S. Afr. Chem. Inst., 23* (1971) 71 and references cited therein.

191. S. Pinchas and I. Laulicht, *Infrared Spectra of Labelled Compounds*, Academic Press, London and New York (1971)

192. W. Rayner-Canham and A.B.P. Lever, *Spectrosc. Lett., 6* (1973) 109.

193. G.W. Watt and J.F. Knifton, *Inorg. Chem., 6* (1967) 1010.

194. A.W. Herlinger, S.L. Wenhold and T. Veach Long, *J. Amer. Chem. Soc., 92* (1970) 6474.

195. C.N. Banwell, *Fundamentals of Molecular Spectroscopy*, McGraw Hill, London (1966)

196. D.M. Sweeny, C. Curran and J.V. Quagliano, *J. Amer. Chem. Soc.*, 77 (1955) 5508.

197. A.J. Saraceno, I. Nakagawa, S. Mizushima, C. Curran and J.V. Quagliano, *J. Amer. Chem. Soc.*, 80 (1958) 5018.

198. H.C. Freeman and J.M. Guss, *Acta Cryst., 24B* (1968) 1133.

199. H. Lay and H. Winkler, *Chem. Ber., 42* (1909) 3894.

200. H. Krebs and R. Rasche, *Z. Anorg. Chem., 276* (1954) 236.

201. R.G. Neville and G. Gorin, *J. Amer. Chem. Soc., 78* (1956) 4893.

202. M. Mori, M. Shibata, E. Kyuno and M. Kanaya, *Bull. Chem. Soc. Japan, 34* (1961) 1837.

203. C.E. Skinner and M.M. Jones, *Inorg. Nucl. Chem. Lett., 3* (1967) 185.

204. R.F. Bryan, P.T. Greene, P.F. Stokely and E.W. Wilson, *Inorg. Chem., 10* (1971) 1468.

205. K. Nakamoto, Y. Morimoto and A.E. Martell, *J. Amer. Chem. Soc., 83* (1961) 4528.

206. J.H.M. Mooy, H.J. de Jong, M. Glasbeek and J.D.W. Van Voorst, *Chem. Phys. Lett.*, *18* (1973) 51.

207. R. Dingle, *J. Chem. Phys.*, *50* (1969) 1952.

208. A. Caron and J. Donohue, *Acta Cryst.*, *17* (1964) 544.

209. L. Pauling, *The Nature of the Chemical Bond*, 3rd Edition, Cornell Univ. Press.

210. S.D. Ross, *Inorganic Infrared and Raman Spectra*, McGraw-Hill (London).

211. D.M. Adams and W.R. Trumble, *J.C.S. Dalton* (1975) 30.